

Synthesis and Electrical Conductivity Measurements on Semiconducting Organic Polymers Derived from Nitriles

B. S. WILDI* and J. E. KATON,† *Research and Engineering Division,
Monsanto Chemical Company, Dayton, Ohio*

Synopsis

A number of polymeric organic semiconductive materials derived from low molecular weight nitriles are described. These infusible, insoluble materials possess electrical resistivity values which are remarkably low for organic materials. The synthesis and resistivity-temperature behavior of these materials is described and their probable structures discussed.

INTRODUCTION

The area of semiconductive organic materials has recently received a good deal of attention. The major effort, to this time, has been devoted to molecular complexes, polycyclic hydrocarbons, and polymeric carbons, however, with only a minor effort devoted to the direct synthesis of semiconducting polymers. The investigations in these laboratories have been directed toward the latter class of compounds, and Epstein and Wildi¹ have published the results of some of these investigations.

Of the materials developed to date, those with the lowest resistivity generally have been derived from organic nitriles. Although a good deal of effort has been devoted by other authors to the development of a semiconductor from polyacrylonitrile,^{2,3} little previous work has been reported in which monomeric nitriles were used to synthesize semiconductive materials. The synthesis and electrical conductivity of several of these latter polymers is here reported. Investigations of thermal conductivities and thermoelectric powers of these materials are reported elsewhere.⁴

EXPERIMENTAL

Synthesis

Poly(copper Phthalocyanine) and Pyromellitonitrile. The synthesis of these two materials has been described by Epstein and Wildi.¹

* Present address: Central Research Department, Monsanto Chemical Company, St. Louis, Mo.

† Present address: Monsanto Research Corporation, Dayton, Ohio.

Pyrolyzed Pyromellitonitrile-Methanol Reaction Product (Oxidized Polyphthalocyanine). A mixture of 50.0 g. of pyromellitonitrile and 3 liters of absolute methanol was refluxed for 24 hr. and then filtered hot. The filtrate was concentrated to one-half volume, cooled, and filtered to yield 32.4 g. of colorless solid. On further concentration of the mother liquors, 11.5 g. of additional, less pure solid was obtained. Upon slow heating this material became green at 157°C. and dark purple at 195°C., without melting or crumbling. The material did not melt below 300°C. A portion of the solid was heated at 250°C./0.07 mm. pressure for 72 hr. to yield a purple solid.

Analysis of this polymer gave the following results.

ANAL. Calcd. for $C_{46}H_{20}N_{17}O_4$: C, 63.16%; H, 2.30%; N, 27.22%. Found: C, 63.24%; H, 2.34%; N, 27.23, 27.01%.

Pyromellitonitrile-Hydrogen Sulfide Reaction Product. A solution of 27 g. of pyromellitonitrile and 5 ml. of pyridine in 500 ml. of chlorobenzene was saturated with hydrogen sulfide at 40°C. The temperature was then raised to 110–115°C., and hydrogen sulfide was bubbled into the solution at this temperature for 4 hr. The solution was cooled, filtered, and the residue washed successively with 3 liters of hot acetone, 200 ml. of ether, and 200 ml. of chlorobenzene. The residue was dried at 200°C./0.2–0.5 mm. pressure for 2 days to yield 26.7 g. of brownish-black product.

ANAL. Found: C, 56.55, 56.60%; H, 2.30, 2.20%; N, 23.16, 23.61%; S, 10.77, 10.94%.

Pyrolyzed Pyromellitonitrile-Ammonia Reaction Product. A stream of anhydrous ammonia was passed into a refluxing solution of 10 g. of pyromellitonitrile and a trace of sodium methoxide in 500 ml. of anhydrous methanol for 1 hr. The mixture was filtered, cooled, and the filtrate concentrated to yield a yellow solid. This solid was heated at 250°C./0.5 mm. pressure for 24 hr. and at 350°C./0.05 mm. pressure for 24 hr. to yield a black solid. Analysis of this material gave the following results.

ANAL. Calcd. for $C_{46}H_{19}N_{19}O_2$: C, 63.52%; H, 2.20%; N, 30.60%. Found: C, 63.64, 63.36%; H, 2.14, 2.28%; N, 30.53, 30.71%.

Polyphenyltriazine. A mixture of 8 g. of pyromellitonitrile and 125 ml. of freshly distilled quinoline was refluxed for 18 hr. The resulting mixture was filtered and the residue washed with hexane and dried at 200°C./0.5 mm. The resulting black solid gave the following analytical results.

ANAL. Calcd. for $C_{78}H_{43}N_{23}O_4$: C, 67.18%; H, 3.10%; N, 25.11%. Found: C, 67.53, 67.23%; H, 3.14, 3.10%; N, 24.80, 24.88%.

Polyvinyltriazine. A 300 ml. glasslined autoclave was charged with 10 g. of fumaronitrile and heated at 300°C. for 18 hr. under 1000 psi of nitrogen. The resulting black solid was heated at 300–320°C./0.1–0.3 mm. pressure

for 15 hr., during which time some yellowish-brown material was removed. The resulting black solid gave the following analytical results.

ANAL. Calcd. for $C_{44}H_{16}N_{16}O_2$: C, 66.00%; H, 1.89%; N, 28.02%. Found: C, 66.33, 66.02%; H, 1.90, 1.84%; N, 28.02, 27.99%.

Poly(copper tetracyanoethylene). A 300 ml. glass lined autoclave was charged with a mixture of 12.8 g. of tetracyanoethylene, 5 g. of cuprous chloride and one gram of urea under 1000 psi of nitrogen. The bomb was heated at 250°C. for 2 hr. and subsequently for 18 hr. at 300°C. The crude black product was extracted with pyridine in a Soxhlet extractor for 5 days and then dried at 300°C./0.5 mm. pressure for 1 hr.

ANAL. Found: C, 46.23, 45.98%; H, 1.05, 0.86%; N, 19.21, 19.11%.

Electrical Measurements

The temperature-resistivity measurements were made in a $3/4$ -in. diameter cylindrical quartz cell, the thickness of which could be varied from 0.7 to 5 mm. The quartz cell was fitted with a heater, platinum electrodes and a thermocouple. The cell was covered by a bell jar connected to a gas inlet and vacuum system.

The sample in the form of a powder was placed in the cell holder, and the electrodes attached under a constant spring tension. The bell jar system containing the sample in the cell was evacuated and then flushed with anhydrous nitrogen. The sample was then heated for several hours at a point slightly below its melting or decomposition temperature under vacuum and then measurements were taken.

The resistances of the samples were taken at various temperatures by use of a vibrating reed electrometer (resistance $> 10^{12}$ ohm), a megohm bridge (10^7 – 10^{12} ohm), or an RCA vacuum tube voltmeter ($< 10^7$ ohm). The resistance at the range limit of each instrument was checked carefully with the second instrument to insure correct readings.

Since some of the samples showed hysteresis effects, all measurements were taken as the temperature decreased.

RESULTS

The temperature-resistivity behavior of the samples are shown in Figures 1–8. The "energy gaps" and extrapolated ρ_0 values of the compounds are listed in Table I. These were calculated from the observed slope with the aid of the relationship $\rho = \rho_0 e^{\Delta E/2KT}$. In the case of pyrolyzed fumaronitrile, the high temperature portion of the curve was utilized for these calculations. The figures which contain two curves represent the cases where the material was measured as obtained and was then subjected to a pyrolysis treatment and the resulting product measured. In all cases, the curve labeled *A* represents the original material and that labeled *B* represents the pyrolyzed product.

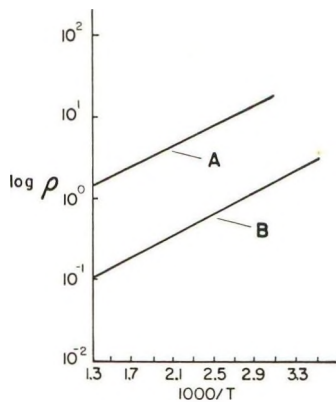


Fig. 1. Temperature-resistivity behavior of poly(copper phthalocyanine): (A) original material; (B) pyrolyzed product.

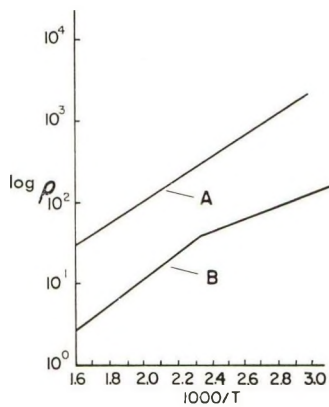


Fig. 2. Temperature-resistivity behavior of pyromellitonitrile-methanol reaction product: (A) original material; (B) pyrolyzed product.

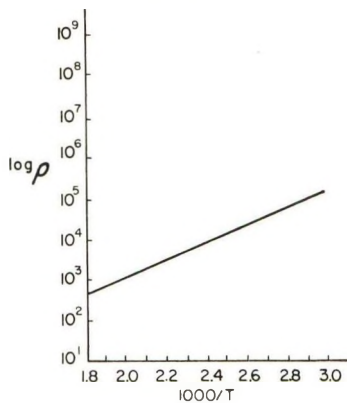


Fig. 3. Temperature-resistivity behavior of pyromellitonitrile-methanol reaction product.

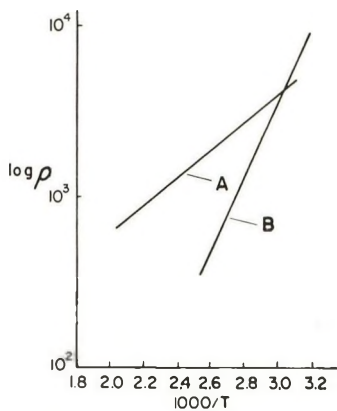


Fig. 4. Temperature-resistivity behavior of pyromellitonitrile-ammonia reaction product: (A) original material; (B) pyrolyzed product.

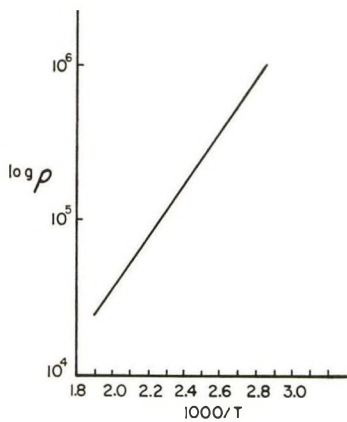


Fig. 5. Temperature-resistivity behavior of pyromellitonitrile-H₂S reaction product.

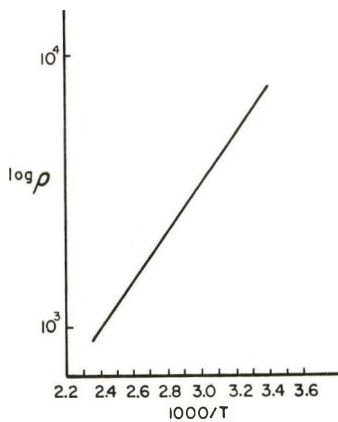


Fig. 6. Temperature-resistivity behavior of polyphenyltriazine.

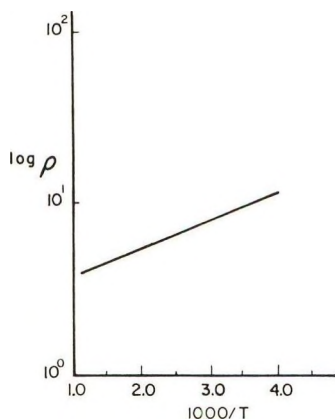


Fig. 7. Temperature-resistivity behavior of poly(copper tetracyanoethylene).

TABLE I
Electrical Properties of Polymers Derived from Nitriles

Material	ΔE , e.v.	ρ_0 , ohm-cm.	Figure
Poly(copper phthalocyanine)	0.24	3.8×10^{-1}	1A
Poly(copper phthalocyanine), heated at 820°C./- 0.1 mm. (37% wt. loss)	0.26	1.35×10^{-2}	1B
Pyromellitonitrile-methanol reaction product	0.98	3.3×10^1	2A
Pyromellitonitrile-methanol, heated at 320°C./- 0.1-0.7 mm., 3 days	0.79	6.9×10^{-1}	2B
Pyromellitonitrile-methanol reaction product, heated at 476-560°C. for 44 hr.	0.50	2.8×10^{-3}	3
Pyromellitonitrile-ammonia reaction product (heating curve)	0.32	14	4A
Pyromellitonitrile-ammonia reaction product (cooling curve)	0.84	1.5×10^{-3}	4B
Pyromellitonitrile-H ₂ S reaction product	0.72	8.0	5
Polyphenyltriazine	0.36	6.2	6
Poly(copper tetracyanoethylene)	0.06	3.0	7
Pyrolyzed fumaronitrile	0.22	6.3×10^1	8

Discussion

The polymers obtained are all similar in physical appearance and behavior. They are generally darkly colored and are insoluble or only very slightly soluble in the usual solvents. They do not melt or soften when heated.

The probable structure of poly(copper phthalocyanine) has been discussed by Epstein and Wildi.¹ It is likely that the pyrolyzed pyromellitonitrile-methanol and pyromellitonitrile-ammonia reaction products are similar in structure, having an oxidized phthalocyanine nucleus as the recurring unit. In the literature are shown reactions in which phthalonitrile was used instead of pyromellitonitrile.⁵

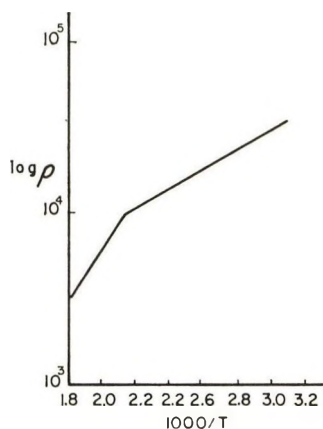
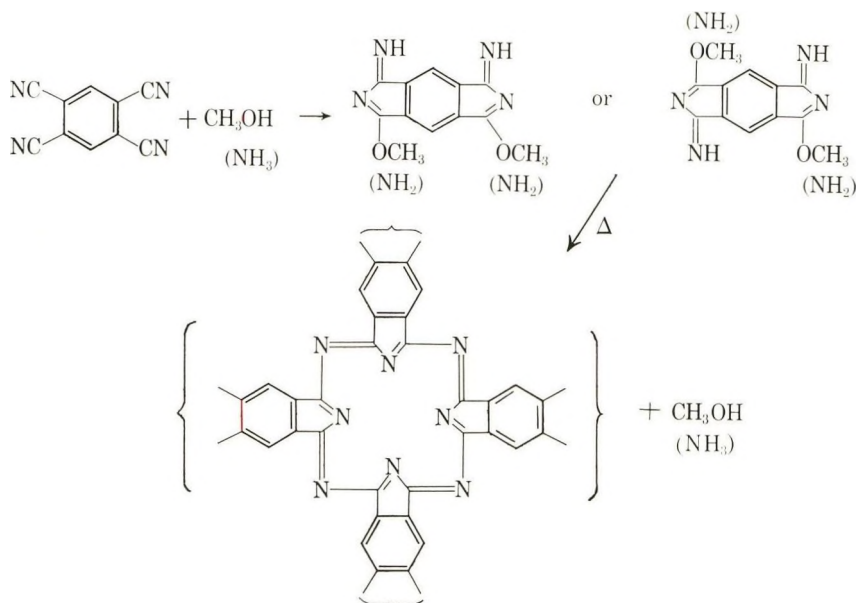
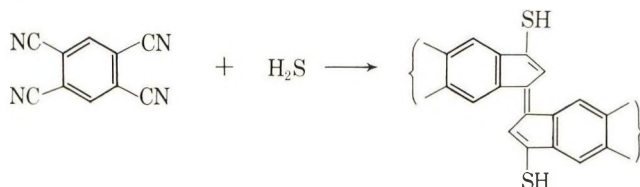


Fig. 8. Temperature-resistivity behavior of pyrolyzed fumaronitrile.



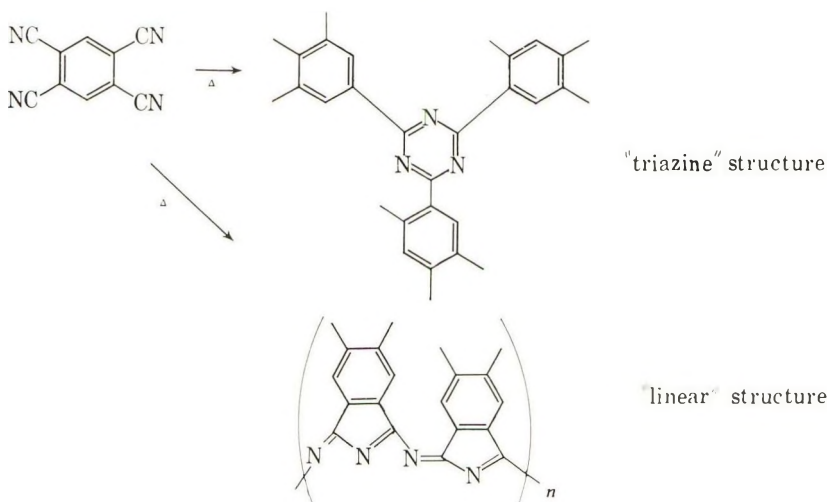
The reaction of pyromellitonitrile with hydrogen sulfide probably gives linear polymer, however. In the literature are shown reactions of phthalonitrile with hydrogen sulfide.^{6,7}



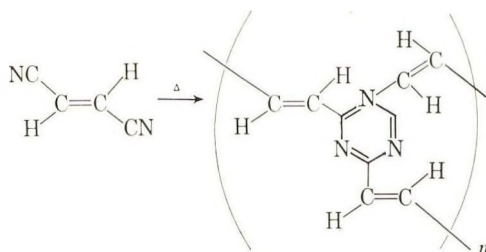
Since these materials are noncrystalline, infusible and insoluble, direct structure proof would be nearly impossible.

Ethanol and ethylene glycol also react with pyromellitonitrile, but these reactions appear to follow a somewhat different course. Although a semi-conducting polymer can be obtained by pyrolysis of the products, the pyrolysis must be carried out at a considerably higher temperature and the structures of the products are not known. It is likely that they are partial graphites of the type commonly observed upon high temperature pyrolysis of organic compounds.

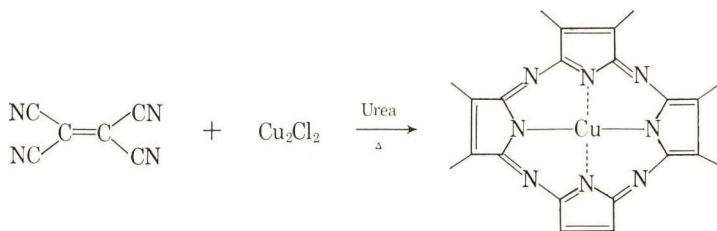
The pyrolysis of nitriles in presence of alkalis to yield 1,3,5-triazines is a well-known reaction with simple aryl nitriles.^{8,9} In the case of pyromellitonitrile, the major portion of the polymer should be formed by this same reaction, although a certain amount of linear condensation, such as that proposed to occur in the pyrolysis of polyacrylonitrile may also occur.



Fumaronitrile, on the other hand, is quite unlikely to form a linear polymer to any significant extent, and the polymer is probably nearly exclusively in the "triazine" form.



Tetracyanoethylene probably forms a ring structure similar to that of phthalocyanine.



This compound has also been reported by Berlin and co-workers.¹⁰

It is likely that the structure of poly(copper tetracyanoethylene) is not as regular as that of poly(copper phthalocyanine), however, since tetracyanoethylene is a much more reactive entity than pyromellitonitrile and would be prone to undergo side reactions to a greater extent.

The polymers all show a definite increase in conductivity upon pyrolysis, however, those derived from pyromellitonitrile show this behavior at pyrolysis temperatures which are rather low for significant carbonization or graphitization. It is likely in these cases that the heat treatment merely promotes the polymerization reaction, leading to a polymer with higher molecular weight. This, of course, increases the conjugated path which the charge carrier may follow and would lead to greater conductivity.

Hall effect measurements on poly(copper phthalocyanine) have been previously reported.¹ No Hall measurements could be made on the other polymers. Measurements of the thermoelectric power of two of these polymers are reported elsewhere.⁴

References

1. Epstein, A., and B. S. Wildi, *J. Chem. Phys.*, **32**, 324 (1960).
2. Topchiev, A. V., M. A. Gelderikh, B. E. Davydov, V. A. Kargin, B. A. Krentsel, I. M. Kustanovich, and L. S. Polak, *Dokl. Akad. Nauk SSSR*, **128**, 312 (1959).
3. Brennan, W. D., J. J. Brophy, and H. Schonkorn, paper presented at Armour Research Foundation Conference on Organic Semiconductors, Chicago, Illinois, April 18-19, 1961.
4. Katon, J. E., and B. S. Wildi, *J. Chem. Phys.*, **40**, 2977 (1964).
5. Elvidge, J. A., and R. P. Linstead, *J. Chem. Soc.*, **1952**, 3536; *ibid.*, **1952**, 5000.
6. Elvidge, J. A., and J. N. Golden, *J. Chem. Soc.*, **1956**, 4144.
7. Drew, H. D. K., and D. B. Kelley, *J. Chem. Soc.*, **1941**, 631.
8. Smolin, E. M., and L. Rapoport, *S-Triazines and Derivatives*, Interscience, New York, 1959, p. 151.
9. Migrdichian, *The Chemistry of Organic Cyanogen Compounds*, Reinhold, New York, 1947, pp. 349-369.
10. Berlin, A. A., N. G. Matveeva, and A. I. Sherle, *Izv. Akad. Nauk SSSR, Otd. Khim. Nauk*, **1959**, 2261.

Résumé

On décrit un certain nombre des polymères organiques semiconducteurs, dérivés de nitriles de bas poids moléculaires. Ces matériaux infusibles et insolubles ont des valeurs de résistance électrique remarquablement basses pour des matériaux organiques. La synthèse et le comportement résistance-température de ces matériaux sont décrits et leurs structures probables sont discutées.

Zusammenfassung

Eine Anzahl polymerer, organischer von niedermolekularen Nitrilen abgeleiteter halbleitender Stoffe wird beschrieben. Diese nicht schmelzbaren, unlöslichen Stoffe besitzen Werte des elektrischen Widerstands, die für organische Stoffe bemerkenswert niedrig sind. Synthese und Widerstands-Temperaturabhängigkeit dieser Stoffe wird beschrieben und ihre wahrscheinliche Struktur diskutiert.

Received February 16, 1964

Chemically Heterogeneous Populations of Copolymer Latex Particles. Preparation, Fractionation, and Characterization

J. B. YANNAS* and I. E. ISGUR, *W. R. Grace and Company, Cambridge, Massachusetts*

Synopsis

The chemical homogeneity of copolymer latex particle populations was studied as a function of polymerization conditions. The comonomer system chosen was styrene-butadiene, and the polymerization variables included the comonomer addition rate and the amount of emulsifier introduced during the reaction. It was found that under conditions of variable comonomer addition rate and with introduction of excess emulsifier during the reaction, a bidisperse latex is produced which contains two chemically distinct particle populations. These populations were separated from one another using a centrifugation technique reported recently and were characterized by electron microscopy and chemical analysis. Each particle population was relatively monodisperse with respect to particle size and differed from its counterpart with respect to average particle size and comonomer ratio. Other combinations of the polymerization variables mentioned above yielded latices with chemically homogeneous particle populations.

INTRODUCTION

The synthesis of most polymers in emulsion form has now reached a stage where the critical problem of particle size and its distribution can be said to be near its solution. In our opinion, this development started with the realization that emulsion polymerization could be understood quantitatively by application of the concepts of nucleation and growth of nuclei. As a result, several modifications of the original batch-type polymerization technique have been successfully introduced. The nucleation step, for example, has been controlled by deliberate introduction of "seed" into the original reaction mixture;¹ any further nucleation during the course of the reaction has been suppressed by judicious apportionment of emulsifier.² Aspects of the growth step have also been tampered with: for example, monomers have been added continuously or intermittently throughout the reaction.³

With the above basis for solving problems of physical (size) homogeneity, the problem of chemical homogeneity of copolymer latices assumes in-

* Present address: Frick Chemical Laboratory, Princeton University, Princeton, New Jersey.

creased importance. In discussing chemical heterogeneity in a copolymer latex system, it is necessary to distinguish clearly among three cases. The first case might be labeled chain-chain heterogeneity and includes some carefully studied examples of variation in comonomer ratio from one polymer chain to another.⁴ The second case might be referred to as shell-shell heterogeneity; it involves production of particles whose comonomer composition varies, continuously or discretely, from the center of the particle to its periphery. Particles exhibiting shell-shell heterogeneity have been prepared by Bradford and Vanderhoff and have been tentatively characterized as such by means of electron microscopy.⁵ Finally, there exists a third case, that of particle-particle heterogeneity. In this instance, particles differing in overall comonomer composition from one another comprise the members of the particle population.

A latex characterized by particle-particle heterogeneity can be prepared in several ways. In a physicochemically trivial but commercially important instance, two chemically different latices are simply mixed together to give a blend. Alternately, it should be possible to achieve the same goal by initiation of new particles during polymerization with a simultaneous drastic change in the addition schedule of monomers, as mentioned by Hughes and Brown.⁶ Other variants of such a procedure might conceivably be already in use in different laboratories as judged by the fact that a number of commercially available latices have been recently found to exhibit unmistakable particle-particle heterogeneity.⁷

In a recent paper,⁸ a simple centrifugation method for the clean fractionation of latex particles differing by 0.005 g./ml. in density was outlined in some detail. The present work demonstrates the applicability of this separation method to the problem of preparation of copolymer latices with the desired degree of particle-particle heterogeneity.

EXPERIMENTAL

Preparation of Emulsion Copolymers

The comonomer system chosen for the study of particle-particle heterogeneity was styrene-butadiene. This system has been studied extensively in several laboratories over a wide range of reaction conditions.

All polymerizations were carried out in a 5-gal. stainless steel autoclave at 77°C. In all cases, a certain amount of "seed" latex, of an average particle diameter 600 Å. and a styrene/butadiene ratio of 60/40, was initially introduced in the autoclave. Other components of the initial aqueous phase included potassium persulfate initiator and emulsifier. The comonomers and emulsifier were added continuously throughout the reaction, the precise addition schedule being one of the variables as explained below. Reactions were carried to higher than 99% conversion of monomers as determined by conventional analytical techniques.

Four distinct classes of latices are prepared. They are denoted below as I, II, III, and IV. For brevity, the discussion will center on only one example from each of the four classes of latices.

Latex I was prepared by adding the comonomers at a constant rate and at the constant styrene/butadiene ratio of 67/33. The emulsifier was also added at a constant rate, the magnitude of the rate being such that no new particles were initiated during reaction. Preliminary surface titration work performed in the conventional manner⁹ had indicated the amount of emulsifier required to achieve this condition.

Latex II was prepared by adding the comonomers at a constant rate and at a constant styrene/butadiene ratio of 67/33 throughout the reaction. However, at an intermediate conversion stage, the rate of emulsifier addition was suddenly increased to a new constant level which ensured initiation of new polymer particles.

Latex III was prepared by adding the comonomers initially at a constant rate and at a constant styrene/butadiene ratio of 67/33. At an intermediate conversion stage, addition of butadiene was discontinued and only styrene was added at a constant rate for the remainder of the reaction. Emulsifier addition throughout the reaction was such that no new particles were initiated.

Latex IV was prepared by adding the comonomers initially at a constant rate and at a constant butadiene/styrene ratio of 67/33. At an intermediate conversion state, addition of butadiene was discontinued and, at the same time, the rate of emulsifier addition was increased to a new level such that new particles would be initiated.

A summary of reaction conditions for latices I-IV is given in Table I.

TABLE I
Preparation of Latices

Latex	Reaction temp., °C.	Total comonomer addition rate	Comonomer ratio	Emulsifier excess
I	77	Constant	Constant	No
II	77	Constant	Constant	Yes
III	77	Constant	Variable	No
IV	77	Constant	Variable	Yes

Fractionation

Brief, preliminary centrifugation in a Servall SS-3 model equipped with an SM-24 rotor indicated that the particles of latices I-IV could be made buoyant by addition of distilled water (cf. case 1, ref. 8).

Each of the latices was then diluted to several levels and samples of every preparation were centrifuged at 20,000 *g* for 10 hr. At the end of the run, the transparent cellulose nitrate tubes were observed briefly in front of a suitably masked lamp. If separation of particles in distinct semisolid fractions at the top or bottom of the tube had taken place, the tube was sliced open and the liquid portion was drained out. If no separation was

evident, small portions from the top and bottom of the tubes were carefully removed by gentle pipet suction as recommended by Schneider.¹⁰

Semisolid fractions removed in this manner were slurried in a small quantity of water and mixed for a prolonged period of time with a Vibro Mixer until they reverted to the dispersed latex state.

Characterization

Whole latices as well as fractions produced by centrifugation were analyzed for weight per cent bound butadiene using an infrared absorption method standardized against copolymers of known composition. Samples of the above were also subjected to electron microscopy following dilution and bromination¹¹ and particle size distribution data were obtained from the electron micrographs. Due to slight personal bias involved in measurements of this sort,¹² our size distribution data are presented with reservation. Calibration factors used to correct for diameter changes due to bromination are those reported in the literature,¹³ these factors are open to doubt following a recent investigation.¹⁴ Finally, determinations of the buoyant density of the polymer particles were carried out with the use of a highly precise centrifugation procedure that has been developed recently in this laboratory.¹⁵

RESULTS

Latices I-IV had the characteristics summarized in Table II. The designation "monodisperse" in this table refers to a latex for which the ratio of weight-average to number-average particle diameter, D_w/D_n , was of the order 1.00. D_n was calculated as $\Sigma n_i D_i / \Sigma n_i$, where n_i is the number of particles with diameter D_i . For D_w , the pertinent expression was $(\Sigma n_i D_i^6 / \Sigma n_i D_i^3)^{1/3}$, which has been used by Maron et al.¹¹ The designation "bidisperse" in Table II refers to a distribution with two distinct peaks, an example of which is shown in Figure 1. Comparison with Table I shows that bidispersity resulted in each case where an excess of emulsifier was introduced during the polymerization (latices II and IV).

Latices I, II, and III failed to yield any fractions when centrifuged for a prolonged period of time at polymer weight concentrations corresponding to particle buoyancy.⁸ When centrifuged at several polymer weight con-

TABLE II
Characteristics of Latices I-IV

Latex	Butadiene, wt.-%	Size dispersity	Fractions separated
I	33.0 ± 0.5	Monodisperse	None
II	33.6 ± 0.5	Bidisperse	None
III	32.5 ± 0.5	Monodisperse	None
IV	33.2 ± 0.5	Bidisperse	Top and bottom

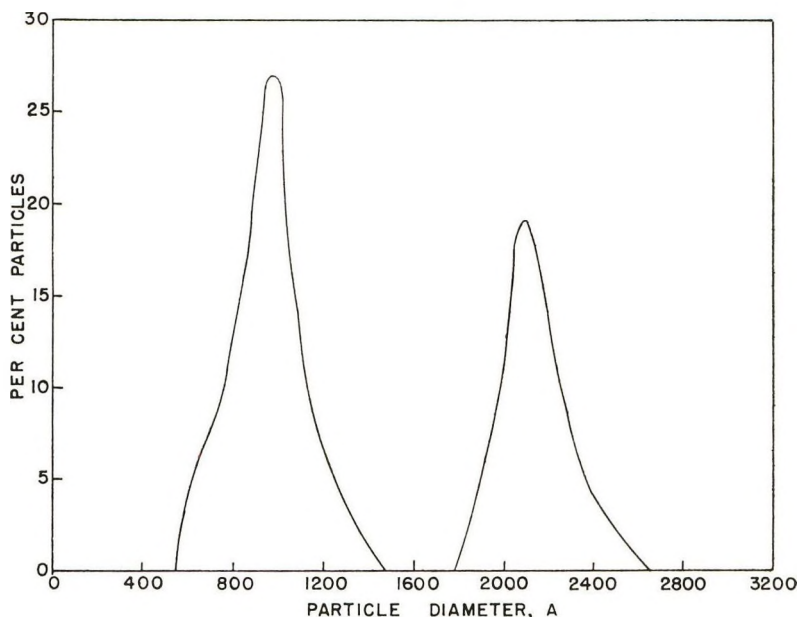


Fig. 1. Particle size distribution of latex IV. The left node represents the size distribution of the smaller, heavier particles which were grown at the second stage of the reaction and sedimented in the centrifuge. The right node is the size distribution of the larger, lighter particles grown continuously throughout the reaction; the latter floated in the centrifuge.

concentrations slightly exceeding the buoyancy concentration, semisolid particle fractions were easily collected from the top of the tube. These fractions were analyzed for butadiene content and characterized with respect to particle size distribution by electron microscopy. In all cases, these physicochemical characteristics were identical within experimental error with the characteristics of the original, uncentrifuged latex. Centrifugation at several concentrations slightly below the buoyancy concentration yielded sediments all of which were also identical with the original, uncentrifuged latex. Previous experience with this fractionation procedure⁸ has shown that the centrifugation conditions used in the present work were quite favorable for the isolation of a chemically heterogeneous fraction of particles if, indeed, such a fraction was present. Chemical homogeneity for latices I, II, and III appears, therefore, to have been established beyond doubt.

On the contrary, latex IV readily yielded top and bottom semisolid fractions upon centrifugation. These fractions were redispersed in water and characterized. Particle size distributions for the two fractions were consistent with the expectation that the bimodal population of the uncentrifuged latex (Fig. 1) would be split cleanly into two parts. The size distribution curve of the top fraction superposed within experimental error on the right node of the distribution curve for latex IV (Fig. 1) and the size

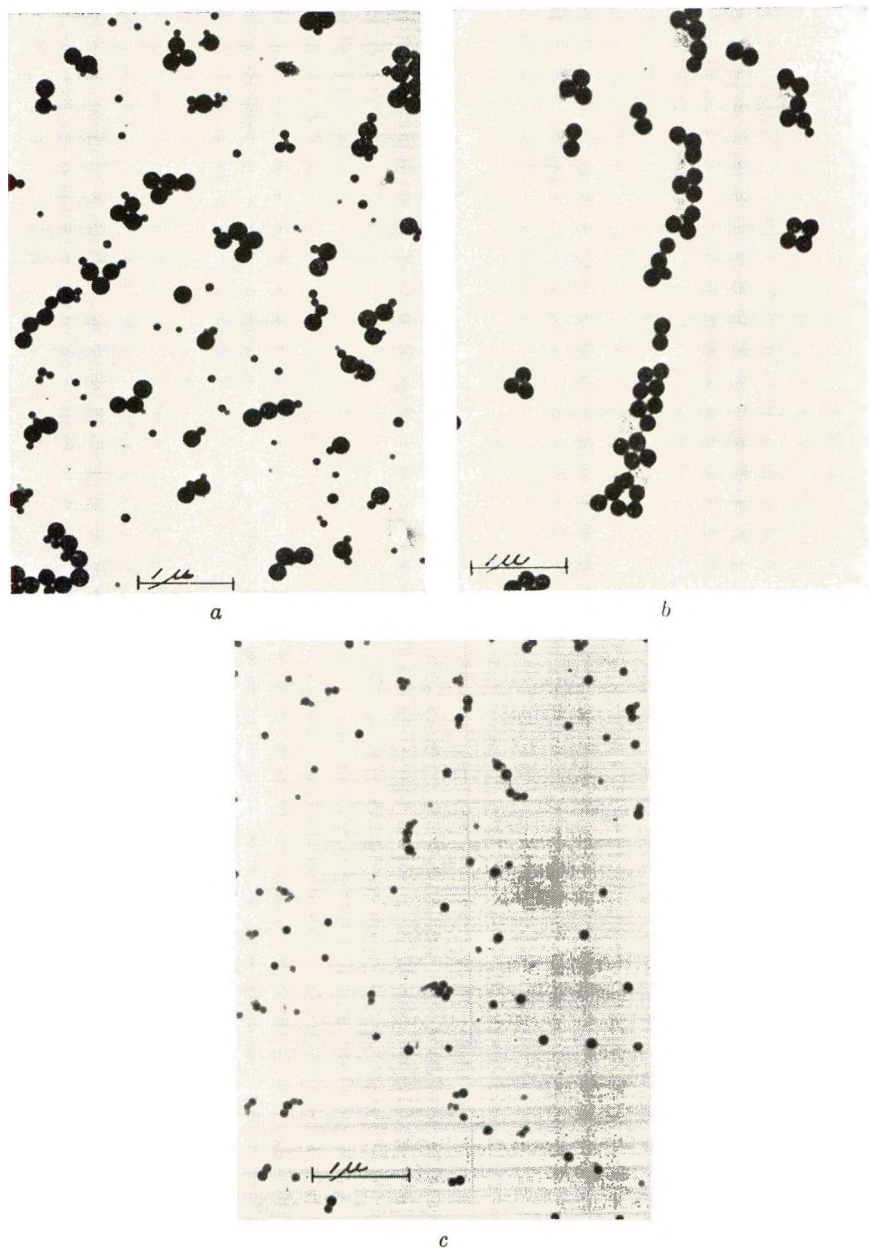


Fig. 2. Electron micrographs of latex IV particles: (a) original, uncentrifuged latex illustrating the size dispersity of the particle population; (b) top fraction obtained by centrifugation; (c) bottom fraction obtained by centrifugation. 16,000 \times .

distribution curve of the bottom fraction superposed on the left node. Representative electron micrographs of the uncentrifuged latex and of the top and bottom fractions (Fig. 2) illustrate the above and give an indication of the quality of separation obtained. Further information on the two

fractions is available in Table III. It is thus quite conclusively shown that latex IV contains two distinct populations of particles: the first comprises large, light particles, relatively rich in butadiene; the second comprises small, heavier particles, relatively rich in styrene.

TABLE III
Characteristics of Fractions Obtained From Latex IV

Fraction	Butadiene, wt.-%	Avg. particle size, A	Size distribution	Buoyant density at 25°C., g./ml.
Top	37.1 ± 0.5	2100	cf. right node Fig. 1	1.00591 ± 0.00003
Bottom	30.5 ± 0.5	940	cf. left node Fig. 1	1.01810 ± 0.00004

As observed earlier,⁸ the best separation could be effected when the density of the aqueous phase of latex IV was adjusted to a level intermediate between the densities of the two particle species (flotation-sedimentation). This procedure yielded two fractions each of which contained a negligible number of heterogeneous members. Other procedures (buoyancy-sedimentation and buoyancy-flotation) yielded fractions which, although quite pure, did not match the standards of homogeneity met by using the first procedure.

DISCUSSION

Although the results presented here pertain specifically to the styrene-butadiene copolymer system, there is no reason to believe that the fractionation and characterization procedures described would not be applicable to a greater variety of other latices. In fact, particle-particle heterogeneity has already been observed in other, quite dissimilar systems.⁷ It should now be possible, therefore, to study systematically the effect polymerization conditions have on particle-particle heterogeneity of the resulting latex. The preparation of copolymer latices with almost any degree of heterogeneity would then become feasible. In fact, as suggested previously,⁸ the study of particle-particle heterogeneous latices where the heterogeneity is due to differences in gel content, crystallinity, and other features might provide another fruitful area for experimentation.

References

1. Smith, W. V., *J. Am. Chem. Soc.*, **70**, 3695 (1948).
2. Vanderhoff, J. W., J. F. Vitkuske, E. B. Bradford, and T. Alfrey, Jr., *J. Polymer Sci.*, **20**, 225 (1956).
3. Wall, F. T., C. J. Delbecq, and R. E. Florin, *J. Polymer Sci.*, **9**, 177 (1952); P. Fram, G. T. Stewart and A. J. Szlachetun, *Ind. Eng. Chem.*, **47**, 1000 (1955); H. F. Fikentscher, H. Gerrens, and H. Schuller, *Angew. Chem.*, **72**, 856 (1960).

4. Stockmayer, W. H., L. D. Moore, M. Fixman, and B. N. Epstein, *J. Polymer Sci.*, **16**, 517 (1955); W. Bushuk and H. Benoit, *Can. J. Chem.*, **36**, 1616 (1958); M. Leng and H. Benoit, *J. Polymer Sci.*, **57**, 263 (1962).
5. Bradford, E. B., and J. W. Vanderhoff, paper presented at the 144th Meeting of the American Chemical Society, Los Angeles, April 1963.
6. Hughes, L. J., and G. L. Brown, *J. Polymer Sci.*, **5**, 580 (1961).
7. Yannas, J. B., unpublished data.
8. Yannas, J. B., *J. Polymer Sci.*, **A2**, 1633 (1964).
9. Maron, S. H., *J. Colloid Sci.*, **9**, 89 (1954); R. J. Orr and I. Breitman, *Can. J. Chem.*, **38**, 668 (1960).
10. Schneider, N., *J. Polymer Sci.*, **32**, 255 (1958).
11. Maron, S. H., C. Moore, and A. S. Powell, *J. Appl. Phys.*, **23**, 900 (1952).
12. Maclay, W. N., and E. M. Gindler, *J. Colloid Sci.*, **18**, 343 (1963).
13. Bradford, E. B., and J. W. Vanderhoff, *J. Colloid Sci.*, **14**, 543 (1959).
14. Bradford, E. B., and J. W. Vanderhoff, *J. Colloid Sci.*, **17**, 668 (1962).
15. Yannas, J. B., to be published.

Résumé

On a étudié l'homogénéité chimique des populations des particules d'un latex de copolymère en fonction des conditions de polymérisation. Le système choisi étant le styrène-butadiène et les variables de polymérisation incluaient la vitesse d'addition du comonomère et la quantité d'émulsifiant introduite durant la réaction. On a trouvé que lorsqu'on changeait la vitesse d'addition du comonomère et lorsqu'on introduisait un excès d'émulsifiant durant la réaction, on produisait un latex bidispersé qui contenait deux populations de particules chimiquement distinctes. Ces populations étaient séparées l'un de l'autre par une technique de centrifugation récemment rapportée et caractérisée par microscopie électronique et par analyse chimique. Chaque population des particules était relativement monodispersée par rapport à la dimension des particules et différait de son homonyme par la dimension moyenne des particules et par la proportion de comonomère. D'autres combinaisons des variables de polymérisation susmentionnées fournissent du latex avec des populations de particules chimiquement homogènes.

Zusammenfassung

Die chemische Homogenität von Copolymerlatexpartikelpopulationen wurde als Funktion der Polymerisationsbedingungen untersucht. Das ausgewählte Comonomersystem war Styrol-Butadien und die Polymerisationsvariablen waren die Zusatzgeschwindigkeit des Comonomeren und die Menge des während der Reaktion zugefügten Emulgators. Es stellte sich heraus, dass bei variabler Zusatzgeschwindigkeit des Comonomeren und bei Einführung eines Emulgatorüberschusses während der Reaktion ein bidisperser Latex mit zwei chemisch verschiedenen Teilchenpopulationen erhalten wird. Diese Populationen wurden mit einer kürzlich beschriebenen Zentrifugierungsmethode voneinander getrennt und elektronenmikroskopisch und mit chemischer Analyse charakterisiert. Jede Teilchenpopulation war in bezug auf Teilchengröße relativ monodispers und unterschied sich von der anderen in bezug auf mittlere Teilchengröße und Comonomerverhältnis. Andere Kombinationen der oben erwähnten Polymerisationsvariablen ergaben Latizes mit chemisch homogenen Teilchenpopulationen.

Received July 29, 1963

cis-Polychloroprene

C. A. AUFDERMARSH, JR. and R. PARISER, *Elastomer Chemicals Department, Experimental Station, E. I. du Pont de Nemours and Company, Inc., Wilmington, Delaware*

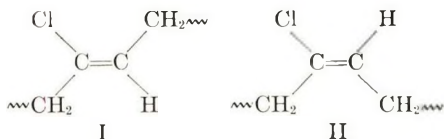
Synopsis

cis-Polychloroprene was synthesized by chlorinolysis of 1,4-poly-2-(tri-*n*-butyltin)-1,3-butadiene. The latter was obtained by free radical polymerization of 2-(tri-*n*-butyltin)-1,3-butadiene. The structure of *cis*-polychloroprene was established by ozonolysis, and by infrared and NMR spectroscopy.

INTRODUCTION

The polymer chemistry of conjugated dienes, particularly butadiene and its derivatives, isoprene and chloroprene (2-chloro-1,3-butadiene) has been widely investigated. In recent years some degree of control of the microstructures of their polymers has been achieved by the use of stereoselective catalyst systems. The most outstanding examples are the preparation of *cis*-polybutadiene and synthetic *cis*-polyisoprene,¹ which indeed appear to be assuming importance as commercial elastomers. However, to the best of our knowledge *cis*-polychloroprene has not been prepared prior to this work.

It is well known, of course, that chloroprene readily undergoes free radical-catalyzed polymerization, and it has previously been shown that the polymer produced under these conditions consists predominately of *trans*-2-chloro-2-butenylidene-1,4 units (I).² A small percentage, the order of 10%, of the corresponding *cis*-units (II) and traces of 1,2 and 3,4 units

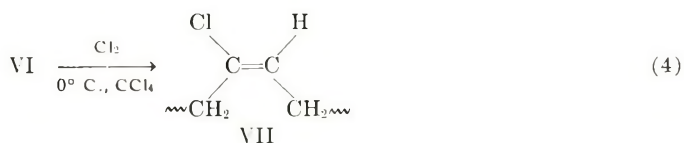
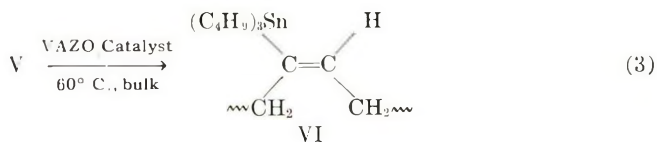
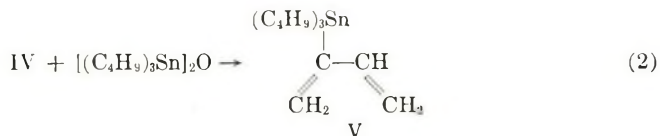
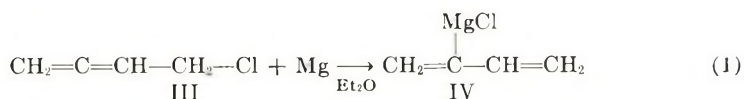


are also present.² Efforts to alter the composition in favor of II by raising the polymerization temperature produced demonstrable, but minor effects.²

RESULTS

Apparent lack of success in producing *cis*-polychloroprene by direct polymerization of chloroprene caused us to undertake a less direct syn-

thetic approach. The formal synthesis of *cis*-polychloroprene VII was achieved in four steps as indicated in eqs. (1)–(4).



Conformation of Monomer V

The first two steps [eqs. (1) and (2)] will be described in another place.³ The product V, 2-(tri-*n*-butyltin)-1,3-butadiene, is constrained by the presence of the bulky substituent in the 2-position to assume the indicated *S-cis* conformation. This assignment of conformation was indicated by an interpretation of its infrared and Raman spectra.

Theoretical symmetry arguments based on the mutual exclusion rule⁴ require that *S-trans*-1,3-butadiene, with a perfect center of symmetry, possess a single infrared absorption and a single Raman absorption in the C=C stretch region near 1600 cm.⁻¹.⁵ In fact, a strong infrared absorption assigned to the antisymmetrical stretching of the diene unit occurs at 1599 cm.⁻¹, and in the Raman spectrum, a strong symmetrical stretching band occurs at 1630 cm.⁻¹.^{6,7} In the case of a 2-substituted butadiene the mutual exclusion rule is obeyed somewhat less perfectly because the substituent perturbs the symmetry of the diene unit. As a consequence a substance of this type, although *S-trans* in conformation, possesses a pair of infrared bands and a corresponding pair of Raman bands in the pertinent region.⁶⁻⁸ In partial obedience to the mutual exclusion rule, the lower frequency antisymmetrical C=C stretching band is strong in the infrared and weak in the Raman; conversely, the higher frequency symmetrical stretching band is weak in the infrared and strong in the Raman spectrum.

However, if the substituent in the 2-position is sufficiently bulky, the diene unit assumes an *S-cis* conformation and the mutual exclusion rule be-

comes invalid. Thus, in the case of 2-*tert*-butyl-1,3-butadiene both the stronger infrared band and the stronger Raman band occur at 1610 cm.^{-1} .⁹ This was attributed to a lack of a center of symmetry with respect to the double bonds and led to the inference that this diene exists as a mixture of planar and nonplanar *S-cis* conformations.⁹ This conclusion was supported by consideration of the steric interactions of the *tert*-butyl group with the vinyl unit.

A completely analogous situation exists in the case of V, which has a bulky tri-*n*-butyltin substituent. In agreement with the above cited work, the stronger of the infrared bands and the stronger of the Raman bands of V coincided at 1620 cm.^{-1} . It is therefore concluded that V, like 2-*tert*-butyl-1,3-butadiene, exists in the nearly-planar *S-cis* form.

Polymerization of Monomer V

The monomer V was polymerized in bulk [eq. (3)] with azo bis isobutyronitrile initiator at about 60°C. Under these conditions the polymerization was relatively slow; the polymer produced had a fairly low molecular weight. Reasonably high molecular weight samples were obtained by incremental addition of catalyst followed by polymer fractionation. The polymers obtained were clear, colorless, viscous liquids soluble in hexane, benzene, carbon tetrachloride, chloroform, ether, and tetrahydrofuran but insoluble in methanol, ethanol, and acetone. Inherent viscosities (0.1% solution in benzene at 25°C.) ranged from 0.2 to 0.8. The glass transition temperature was between -80 and -90°C.

The structure was established by analysis and by infrared spectroscopy. The polymer is predominately 1,4, as shown by the absence of appreciable absorption in the regions near 980 and 910 cm.^{-1} where vinyl and terminal methylene units normally absorb. The steric factors which lead to the *S-cis* monomer conformation will induce butadienyl radicals on the ends of growing chains to retain the same conformation. Propagation of the latter *cis* radical thereby produces a polymer with the *cis* configuration.

Chlorinolysis of *cis*-1,4-Poly-2-(tri-*n*-butyltin)-1,3-butadiene

Reaction of the tin-containing polymer VI with chlorine [eq. (4)] removed the tributyltin groups and replaced them with chlorines to yield the desired product, *cis*-polychloroprene (VII). This reaction is characterized by selective cleavage of the tin-olefinic carbon linkage¹⁰ with retention of geometrical configuration.¹¹ The reaction proceeded rapidly and with high specificity at 0°C. in dilute carbon tetrachloride solutions. A slight excess of chlorine was necessary to remove essentially all of the tin substituents. Overchlorination of the polymer chain resulted if the excess of chlorine was too large. The experience gained from a number of runs showed that 5% excess chlorine was the optimum level under these conditions. We believe that, at this level, nearly all of the excess chlorine is consumed in converting tributyltin chloride to dibutyltin dichloride and butyl chloride.

cis-Polychloroprene was isolated in quantitative yield by precipitation in methanol. It was purified by reprecipitation from its benzene solution. The highest molecular weight sample, which had an osmometric molecular weight of 150,000, was a pale amber amorphous gum with elastomeric properties.

Evidence for the structure of *cis*-polychloroprene is provided by analytical, chemical, spectroscopic, and other physical data. The product analyzed as follows: Calc. for $(C_4H_5Cl)_x$: C, 54.26%; H, 5.69%; Cl, 40.05%. Found: C, 53.4, 53.2%; H, 5.9, 6.0%; Cl, 40.3, 40.4%. If one assumes that the ca. 0.4% unaccounted for is present as residual tin units, the calculated purity of the polymer is greater than 97% polychloroprene.

Ozonolysis of *cis*-Polychloroprene

Ozonization provided evidence for the high content of 2-chloro-2-butenylidene units. *cis*-Polychloroprene yielded succinic acid in 62% yield on ozonolysis (ordinary *trans*-polychloroprene yields about 90% succinic acid). Since every mole per cent of extraneous units must reduce the yield of succinic acid by at least 2 mole-% (assuming random distribution) then structure I and/or II must account for greater than 80 mole-% of the polymer backbone.

DISCUSSION

The above data indicate that the polymer contains 80–97% 1,4-polychloroprene. The polymer is believed to be *cis* by method of synthesis and from its observed differences relative to ordinary polychloroprene which is generally accepted as being largely *trans*.¹ Expected differences were demonstrated by means of infrared and NMR spectroscopy. Characteristic shifts in the =CH out-of-plane deformation and stretching frequencies and the C=C stretching frequencies in the infrared spectra and a characteristic shift of the olefinic proton resonances in the NMR spectra confirmed the *cis* structure.

The sequence distribution of the polymer also has been estimated from NMR data. The polymer contains about 50–60% of the head-to-tail and 25–20% each of the head-to-head and tail-to-tail sequence isomers. The spectra and detailed interpretations are given in the succeeding paper.¹²

cis-Polychloroprene has been obtained with an osmometric molecular weight as high as 150,000 and an inherent viscosity (0.1% in benzene at 25°C.) of 0.71. *trans*-Polychloroprene with the same inherent viscosity has a molecular weight of about 130,000.¹³ A sample of *cis*-polychloroprene with an intrinsic viscosity (benzene) of 0.55 had a k' value of 0.50. This value is consistent for a linear polymer without extensive branching. The k' values reported for *trans*-polychloroprene are mostly in the range 0.35–0.40.¹³

Some physical properties of *cis*-polychloroprene and 95% *trans*-polychloroprene are compared in Table I.

TABLE I
 Physical Properties of Polychloroprenes

1,4-Polychloroprene	Density at 25°C., g./ml.	T_m , °C.	T_g , °C.
95% <i>trans</i>	1.243 ^a	70–80 ^b	–45 ^c
<i>cis</i>	1.283	70 ^d	–20 ^e

^a Density of the amorphous (liquid) phase.

^b Data of Maynard and Mochel.¹⁴

^c Data of Garrett.¹⁵

^d Determined by differential thermal analysis (DTA).

^e Determined by DTA and length/temperature measurements.

EXPERIMENTAL

cis-1,4-Poly-2-(tri-*n*-butyltin)-1,3-butadiene

The monomer V (375 g.), b.p. 86–87°C./0.05 mm., was placed in a one-liter round-bottomed flask equipped with mechanical agitator, thermometer, and nitrogen atmosphere. It was polymerized for 24 days at 55–60°C. In order to attain the highest possible molecular weight VAZO initiator (du Pont trademark for its azobisisobutyronitrile catalyst) was added incrementally at 2–3 day intervals. A total of 0.039 g. of catalyst was added. The resulting clear, colorless solution was diluted with 200 ml. benzene and poured slowly into 2.8 liters methanol with good agitation.

The polymer, which separated, was washed twice with fresh methanol, dried, redissolved in 500 ml. benzene, and reprecipitated in 2.5 liters methanol. After two methanol washes, the polymer was dried by heating at 55–60°C. under 0.1 mm. pressure overnight. The clear, colorless polymer was obtained as a very viscous liquid (108 g., 29% conversion). Inherent viscosity (0.1% in benzene at 25°C.) was 0.47, 0.46.

ANAL. Calc. for $(C_{16}H_{32}Sn)_x$: C, 56.01%; H, 9.44%; Sn, 34.60%. Found: C, 56.0, 56.2%; H, 9.9, 10.1%; Sn, 34.7, 34.8%.

The polymer was dissolved in 2.0 liters benzene and precipitated by dropwise addition of 483 ml. methanol. The polymer phase which separated (395 ml.) was made up to 2.5 liters with fresh benzene and reprecipitated with 480 ml. methanol, which yielded 190 ml. of new polymer phase. The polymer was isolated by precipitation in 2.5 liters methanol, washed and dried at 0.1 mm. The fraction weighed 43.7 g. and had an inherent viscosity (0.1% in benzene at 25°C.) equal to 0.70.

ANAL. Found: C, 56.0, 55.8%; H, 9.5, 9.7%; Sn, 34.8%.

A 25 g. portion was further fractionated by dropwise addition of 106.5 ml. methanol to its solution in 550 ml. benzene. After isolation and drying, there remained 13.4 g. clear, colorless polymer with an inherent viscosity (0.1% in benzene at 25°C.) of 0.82–0.81.

ANAL. Found: C, 56.3, 56.1%; H, 9.7, 9.6%; Sn, 34.6%.

cis-1,4-Polychloroprene

A one-liter round-bottomed flask was equipped with mechanical agitator, 500 ml. dropping funnel, thermometer, and nitrogen atmosphere. It was charged with a solution of 12.3 g. (0.0359 mole) *cis*-1,4-poly-2-(tri-*n*-butyltin)-1,3-butadiene (described above, inherent viscosity 0.82) in 400 ml. carbon tetrachloride protected from light and cooled to 1°C. A chlorine solution was prepared by bubbling chlorine gas into 500 ml. carbon tetrachloride. (The CCl₄ had previously been stored for two days over silica gel in order to remove alcohol stabilizer.) It analyzed 0.1536*M* by titration with 0.1023*N* sodium thiosulfate. The solution was placed in the dropping funnel and added dropwise to the moderately agitated polymer solution while the temperature was maintained at 1–3°C. A total of 250 ml. (0.0384 mole chlorine) was added over a period of 4.5 hr. The chlorine appeared to react instantly as shown by the disappearance of the yellow color. The polymer was precipitated by pouring the reaction mixture into 2.5 liters methanol containing 2.0 g. NaCl and 1.0 g. Calco 2246 anti-oxidant. *cis*-Polychloroprene separated as a soft, white, elastomeric solid. It was rinsed with methanol, dissolved in 50 ml. benzene, and reprecipitated by spinning through a small capillary into 1.9 l. methanol magnetically stirred in a 2-liter graduated cylinder. The purified polymer, after being evacuated for 3 days at 0.1 mm, was an amorphous amber solid weighing 3.2 g. (theory, 3.2 g.).

ANAL. Calcd. for (C₄H₅Cl)_{*x*}: C, 54.26%; H, 5.69%; Cl, 40.05%. Found: C, 53.4, 53.2%; H, 5.9, 6.0%; Cl, 40.3, 40.4%.

The inherent viscosity (0.1% in benzene, 25°C.) was 0.71–0.70. The osmometric molecular weight measured in benzene was 150,000 ± 20,000.

Ozonolysis of *cis*-Polychloroprene

A solution of 1.60 g. *cis*-polychloroprene in 100 ml. chloroform was cooled to 2°C. in a 500-ml. round-bottomed flask equipped with a mechanical agitator, reflux condenser, thermometer, and a gas inlet tube. Water (50 ml.) was added, and the mixture was ozonized using the output of a T-19 Welsbach ozone generator. Ozonolysis was continued for three hours at 0–5°C. with an estimated O₃ output of 0.5–1.0 g./hr. The mixture was stirred overnight at 25°C., then refluxed at 57°C. for 3 hr. After cooling, the layers were separated. The chloroform layer was concentrated under a nitrogen stream to leave 0.6 g. oil which appeared to be undecomposed ozonide. After being warmed with 10 ml. water for 2 hr. at 85°C., all except 0.08 g. of the oil had dissolved. The aqueous solution was added by the original aqueous layer and concentrated by freeze drying. There remained ca. 1.9 g. off-white crystals of crude succinic acid with a HCl odor. The acid was chromatographed on silicic acid by the method of Marvel, et al.¹⁶ A total of 1.32 g. (62% yield) of succinic acid, m.p. 187–188°C., was obtained. A mixed melting point with authentic succinic acid

was 188–189°C. The infrared spectrum (KBr) of the product was identical with that of succinic acid.

The authors wish to thank R. C. Ferguson whose spectroscopic work made possible the assignment of structure. We also express our appreciation to R. R. Garrett, G. T. Perkins, and T. P. Yin without whose contributions this work could not have been completed. We are grateful to J. Fisher for technical assistance and to A. L. Barney for helpful discussions.

References

1. Madge, E. W., *Chem. Ind. (London)*, **1962**, No. 42, 1806.
2. Maynard, J. T., and W. E. Mochel, *J. Polymer Sci.*, **13**, 251 (1954).
3. Aufdermarsh, C. A., *J. Org. Chem.* in press.
4. Herzberg, G., *Infrared and Raman Spectra*, Van Nostrand, New York, 1945, p. 256.
5. Batuev, M. I., A. S. Onishchenko, A. D. Matveeva, and N. I. Aronova, *Proc. Acad. Sci. USSR (Chem. Sect.)* (Engl. transl.), **132**, 543 (1960).
6. Richards, C. M., and J. R. Nielsen, *J. Opt. Soc. Am.*, **40**, 438 (1950).
7. Rasmussen, R. S., and R. R. Brattain, *J. Chem. Phys.*, **15**, 131 (1947).
8. Szasz, G. J., and N. Sheppard, *Trans. Faraday Soc.*, **49**, 358 (1953).
9. Craig, D., J. J. Shipman, and R. B. Fowler, *J. Am. Chem. Soc.*, **83**, 2885 (1961).
10. Seyferth, D., *J. Am. Chem. Soc.*, **79**, 2133 (1957); S. D. Rosenberg and A. J. Gibbons, Jr., *ibid.*, **79**, 2137.
11. Nesmayanov, A. N., and A. E. Borisov, *Tetrahedron*, **1**, 158 (1957).
12. Ferguson, R. C., *J. Polymer Sci.*, **A2**, 4735 (1964).
13. Mochel, W. E., and J. B. Nichols, *Ind. Eng. Chem.*, **43**, 154 (1951).
14. Maynard, J. T., and W. E. Mochel, *J. Polymer Sci.*, **13**, 235 (1954).
15. Garrett, R. R., this laboratory, unpublished results.
16. Marvel, C. S., and R. B. Light, Jr., *J. Am. Chem. Soc.*, **72**, 3889 (1950).

Résumé

On a synthétisé le *cis*-polychloroprène par chlorolyse du 1,4-poly-2-(tri-*n*-butylétain)-1,3-butadiène. Ce dernier a été obtenu par polymérisation radicalaire du 2-(tri-*n*-butylétain)-1,3-butadiène. La structure du *cis*-polychloroprène a été établie par ozonolyse, par spectroscopie infrarouge et RMN.

Zusammenfassung

cis-Polychloropren wurde durch Spaltung von 1,4-Poly-2-(tri-*n*-butyl)-1,3-butadien mit Chlor synthetisiert. Letzteres wurde durch radikalische Polymerisation von 2-(Tri-*n*-butylzinn)-1,3-butadien erhalten. Die Struktur von *cis*-Polychloropren wurde durch Ozonolyse und Infrarot- und NMR-Spektroskopie ermittelt.

Received December 6, 1963

Revised January 31, 1964

Infrared and Nuclear Magnetic Resonance Studies of the Microstructures of Polychloroprenes

RAYMOND C. FERGUSON, *Elastomer Chemicals Department,
Experimental Station, E. I. du Pont de Nemours and Company, Inc.,
Wilmington, Delaware*

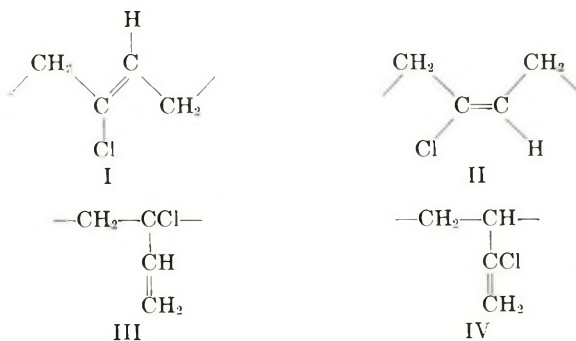
Synopsis

High resolution infrared and nuclear magnetic resonance spectra confirm the structure of *cis*-polychloroprene prepared by a stereospecific route. Head-to-tail, head-to-head, and tail-to-tail sequence isomerism in both *cis*- and *trans*-polychloroprenes has been discovered and measured quantitatively by high resolution NMR spectroscopy. The irregularity in the microstructure of neoprenes proves to be more extensive than was previously suspected.

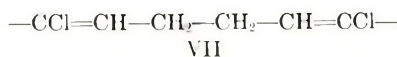
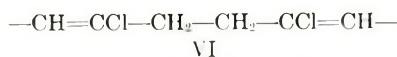
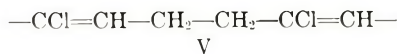
INTRODUCTION

Earlier papers from our laboratories^{1,2} have presented evidence for isomers in typical free radical-initiated chloroprene polymers (neoprenes). The stereospecific synthesis of *cis*-polychloroprene³ prompted high resolution infrared and nuclear magnetic resonance studies to confirm the microstructure of this new polymer and to elucidate additional structural information on typical *trans*-polychloroprenes.

The four structural isomers previously identified by infrared spectroscopy² were the *trans*-2-chloro-2-butenylidene-1,4 (I), *cis*-2-chloro-2-butenylidene-1,4 (II), arising from 1,4 polymerization, and also III and IV, arising from 1,2 and 3,4 polymerization.



NMR evidence has been found for sequence isomerism in the 1,4-polychloroprene units, as a consequence of "head-to-tail" (V), "head-to-head" (VI), and "tail-to-tail" (VII) addition of successive monomer units.



EXPERIMENTAL

The spectrometers employed in this work were a Cary Model 14 spectrophotometer, a Perkin-Elmer Model 221 infrared spectrophotometer equipped with a prism-grating interchange and a KBr prism interchange, a Varian A-60 NMR spectrometer, and a Varian HR-100 NMR spectrometer.

Matheson-Coleman and Bell spectroscopic grade chloroform, carbon tetrachloride, and carbon disulfide were employed as solvents. Infrared spectra of the polymer samples were run in solutions at ca. 10% concentration, and also as cast or pressed films. Cell pathlengths and solvents were selected for optimum band intensities and freedom from interference in the spectral regions being scanned. The NMR spectra of the polymers were run on 10% carbon disulfide solutions.

2-Chloro-2-butene (Columbia Organic Chemicals Co.) was partially separated by distillation into *trans*-rich (b.p. 61–66°C.) and *cis*-rich (b.p. 66–68°C.) fractions. Further purification to ca. 99% pure isomers was accomplished by vapor phase chromatography, by employing a tricresylphosphate column at 68°C.

The model compounds were run as pure liquids and in appropriate solvents. The NMR measurements on the model compounds were extrapolated to infinite dilution by standard techniques. Tetramethylsilane was employed as the internal reference standard for NMR.

The free radical-initiated, emulsion-polymerized polychloroprenes were purified by repeated precipitation from benzene with methanol, followed by vacuum drying to constant weight at room temperature.

RESULTS AND DISCUSSION

Structure of *cis*-1,4-Polychloroprene

Infrared spectra of the supposed *cis*-polychloroprenes and predominantly *trans*-polychloroprenes were obtained, covering the range from 0.6 μ to 25 μ (16,667–400 cm.^{-1}). Spectral differences throughout most of this range indicated definite structural differences between the two polymer types.

The 3500–600 cm.^{-1} range was most useful for microstructure identification and analysis. Portions of this region are reproduced in Figure 1. The infrared identification of the *cis* and *trans* structures is based on vibrational assignments which can be made from related model compound studies (Table I). The directions and magnitudes of the frequency differences are perhaps more significant than the absolute frequencies. The

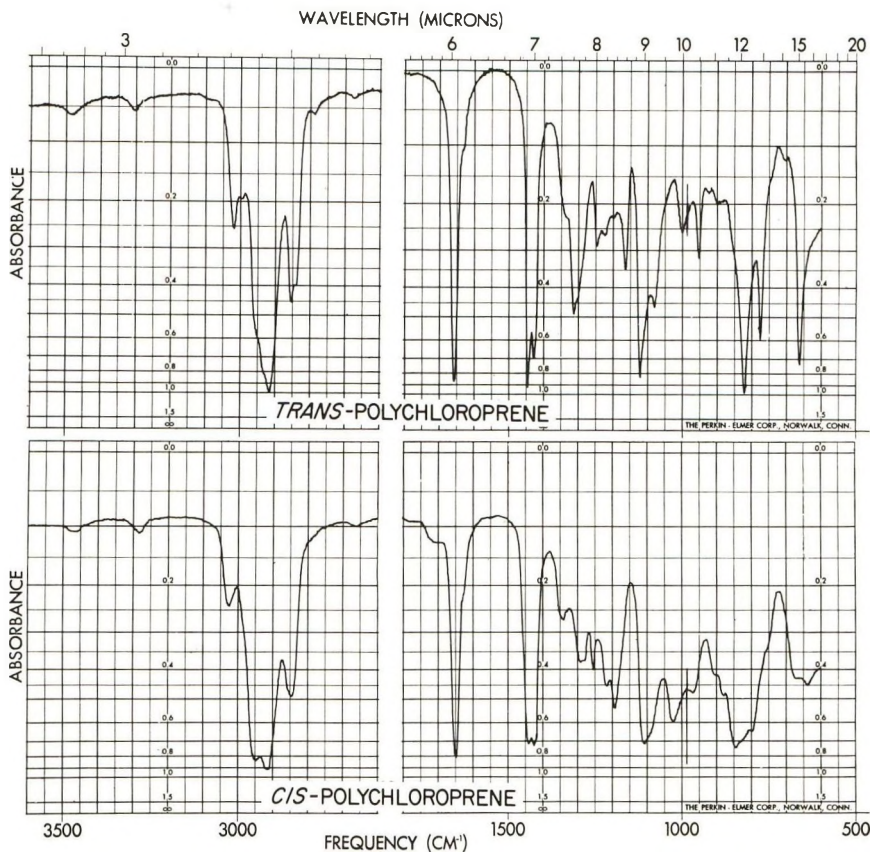


Fig. 1. Infrared spectra of polymer films. Prism-grating resolution; spectral slit width ca. 2 cm^{-1} .

absolute intensities of these vibrational modes were estimated, and the intensities of the polymer bands were consistent with those of the model compounds.

Quantitative comparison of the characteristic bands in the *cis*- and *trans*-polychloroprenes indicated a maximum possible concentration of *trans* in the *cis*-polychloroprene of 5%. As there is no independent evidence for the presence of the *trans* isomer, it appears reasonably certain that the supposed stereospecific synthesis³ produced negligible *trans*-1,4-isomer.

Weak bands at 925 and 883 cm^{-1} are due to the $=\text{CH}-$ out-of-plane deformations of the 1,2 (III) and 3,4 (IV) structures, which are present at low concentrations. In the *trans*-polychloroprene, the weak band at 1200 cm^{-1} is due to about 6% *cis*-isomer.

A revised infrared method for the microstructure analysis of polychloroprenes, based on quantitative data developed in this work, will be published elsewhere.⁴ The best estimates of the compositions of the two polymers of Figure 1 are summarized in Table II.

TABLE I
 Infrared Vibrational Frequencies of Polychloroprenes and Model Compounds

Vibrational mode	Isomer	Frequency, cm. ⁻¹		
		C ₄ H ₇ Cl ^a	C ₈ H ₁₃ Cl ^b	Polychloroprene
=CH— out-of-plane deformation	<i>trans</i>	798	811	822
	<i>cis</i>	823	826	847
C=C stretch, fundamental	<i>trans</i>	1674	1662	1660
	<i>cis</i>	1665	1653	1653
C=C stretch, first overtone	<i>trans</i>	3322		3295
	<i>cis</i>	3305		3282
=CH— stretch	<i>trans</i>	3024		3018
	<i>cis</i>	3020, 3052		3025 ^c

^a 2-Chloro-2-butene.

^b 4-Chloro-4-octene. Data from Maynard and Mochel.¹

^c Broad, possibly two unresolved bands.

 TABLE II
 Microstructures of *cis*- and *trans*-Polychloroprenes
 Examples of Figures 1 and 2

	<i>trans</i> -1,4 (I), %	<i>cis</i> -1,4 (II), %	1,2-(III), %	3,4-(IV), %
<i>cis</i> -Polychloroprene ^a	0	99	<0.1	1.0
<i>trans</i> -Polychloroprene	93	6	0.6	0.4

^a Normalized to 100% polychloroprene. The presence of approximately 3% of 1,4-poly(tributyltinbutadiene) cannot be excluded.³

Proton resonance spectra of carbon disulfide solutions of the *cis* and predominantly *trans*-polychloroprenes further substantiate the structures of the polymers. The 60 and 100 mcycle (Fig. 2) spectra show a shift of ca. 0.1 ppm between the olefinic proton resonances for the *cis* and *trans* internal olefinic proton. The olefinic chemical shifts at infinite dilution for the *cis* and *trans* polymers were 5.51 and 5.35 ppm, in good agreement with the infinite dilution values (5.52 and 5.42 ppm) of *cis* and *trans*-2-chloro-2-butene.

The incompletely resolved fine structure of the olefinic lines in the NMR spectra (Fig. 2) is due to spin-spin coupling of $J = 5-6$ cps. between the olefinic proton and the adjacent methylene protons.

Sequence Isomers

The methylene group region of the proton resonance spectra (Fig. 2) shows more nonequivalent types than predicted for regular head-to-tail 1,4 polymerization. The line separations are too great to be due to spin-spin coupling, and in addition are magnetic field-dependent; thus, they are due to chemical shift effects. The high field and low field lines are too intense to be produced by the relatively minor amounts of 1,2 and 3,4 polymerization isomers present.

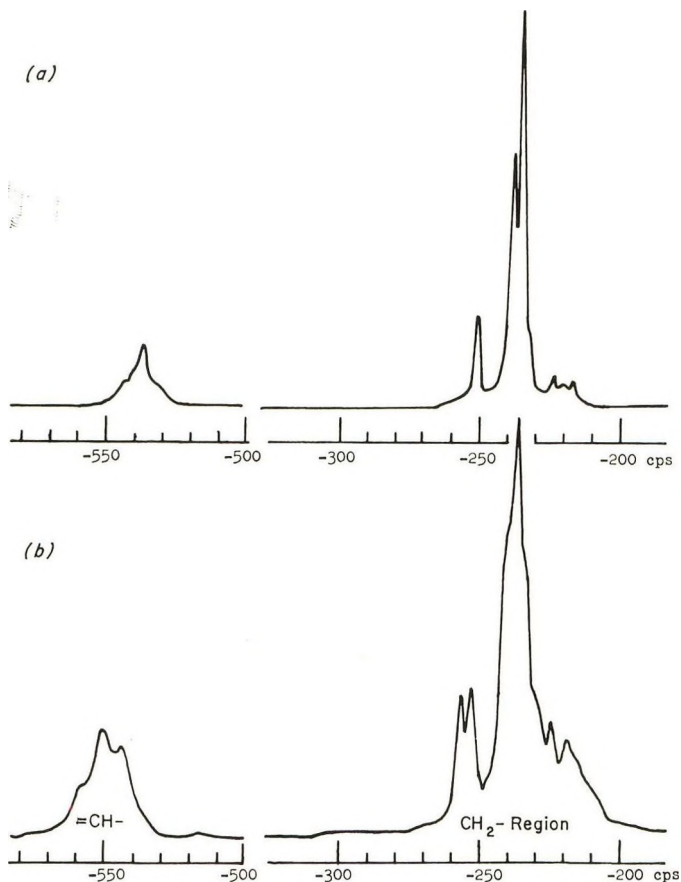


Fig. 2. Proton resonance spectra (100 mcycle) of (a) *trans*-polychloroprene and (b) *cis*-polychloroprene. Frequency in cps., the minus signs indicating positions downfield from tetramethylsilane. The chemicals shift in ppm = shift in cps./100.

The major features of the methylene resonance patterns can be accounted for satisfactorily only by postulating a distribution of sequence isomers V, VI, and VII. Model compounds for these structures have not been available. However, a complete analysis of the 2-chloro-2-butene spectra (Table III) aided the interpretation, and tentative assignments have been made on the basis of the effect of neighboring substituents on methylene proton resonances. The stronger two resonances at 2.37 and 2.33 ppm in the *trans*-polychloroprene are undoubtedly due to the slightly nonequivalent methylene groups in the head-to-tail (H-T) sequence (V). If the principal effect of a chlorine atom on the doubly bonded carbon adjacent to a methylene group is electron withdrawal (deshielding) as is the case for the methyl resonances of the chlorobutenes, the low field line at 2.50 ppm can be attributed to the two equivalent methylene groups of the head-to-head (H-H) sequence (VI). This assignment also appears most reasonable, because the line is a singlet in *trans*-polychloroprene, where the

TABLE III
 NMR Parameters of 2-Chloro-2-Butene Isomers

Isomer	Chemical shift, ppm ^a			Coupling constants, cps.		
	CH ₃ (1)	CH ₃ (4)	=CH	J ₁₃	J ₁₄	J ₃₄
<i>cis</i>	2.02	1.65	5.60	1.3	1.2	7.2
<i>trans</i>	2.07	1.70	5.47	1.2	1.6	6.7

^a Shift downfield from tetramethylsilane (internal). Neat samples.

largest expected spin-spin coupling with the methylene group would be from the olefinic proton across the double bond. This coupling is known to be less than the observed line width (ca. 1 cps).

Similarly, the high field resonances centered at ca. 2.18 ppm would be attributed to the two equivalent methylene groups of the tail-to-tail (T-T) sequence (VII). In this case a doublet methylene resonance with a splitting of 5–7 cps. due to spin-spin coupling between the methylene and adjacent olefinic protons would be expected. An apparent doublet with $J_{\text{CH}_2\text{CH}} = 6.5$ cps. is observed. The central line of the high field multiplet pattern appears to be anomalous, and, in fact, may be due to the methylene groups of the 1,2- or 3,4-isomer.

The methylene resonance pattern of *cis*-polychloroprene has not been as satisfactorily interpreted, although the presence of H-T, H-H, and T-T sequences is also apparent. The separation of the pair of low field lines at 2.56 and 2.52 ppm is magnetic field-dependent, and, therefore, is a chemical shift effect. It is possible that steric effects in the H-H *cis* configuration produce a slight magnetic nonequivalence of the methylene group protons. The two methylene resonances of the H-T sequence are not resolved, but the shape of the band centered at 2.35 ppm is consistent with a pair of overlapping doublets with predicted spacings of $J_{\text{CH}_2\text{CH}} = 6$ cps. and <1 cps. The high field methylene resonances were too poorly resolved to establish whether the two or more lines seen were due to chemical shifts or spin-spin splitting.

Quantitative estimates of the relative intensities of the H-T, H-H, and T-T methylene resonances were made by planimeter integration. The assignments of the H-H and T-T resonances could be reversed without affecting the conclusions, since the areas of the low field and high field multiplets were equal within experimental error. Essentially equal probabilities for H-H and T-T sequences are in fact required to produce the observed concentration of sequence isomers in these high molecular weight polymers.

The sequence isomer concentrations found were on the order of 70–80% H-T and 15–10% each H-H and T-T in typical free radical-initiated polychloroprenes. The *cis*-polychloroprenes were found to have on the order of 50–60% H-T and 25–20% each of H-H and T-T sequence isomers.

CONCLUSIONS

The infrared and NMR spectra obtained in this work clearly demonstrate that the supposed stereospecific route of the preceding paper³ pro-

duced a structurally unique polychloroprene. Interpretation of the spectral data in the light of the related chemical evidence confirms that the product is indeed *cis*-1,4-polychloroprene.

The NMR evidence for sequence isomers in 1,4-polychloroprene confirms the existence of an additional type of structural irregularity in the polychloroprene chain.²

Analyses of typical polychloroprenes have confirmed that all types of structural isomerism increase with polymerization temperature.^{1,2} Polychloroprenes prepared in our laboratories have been found to have the composition ranges: 78–96% I, 4–18% II, 0.3–2% III, and 0.2–2% IV. The 1,4-polychloroprene sequences are predominantly H-T (VI) in all cases, but with 10–15% each of V and VII.

It appears reasonable to conclude that the elastomeric properties of the neoprenes are largely a consequence of the irregularity in the polymer chain microstructure, which is even more extensive than previously suspected. Physical properties of neoprenes, such as hardness, crystallinity, and crystallization rate are known to be strongly dependent on the extent of structural irregularity;¹ thus, the control and knowledge of microstructure is an important aspect of neoprene technology.

The assistance of several members of the staff of this laboratory, particularly Drs. C. A. Aufdermarsh, J. W. Crary, W. J. Keller, R. M. Tabibian, and J. T. Maynard, who provided samples and much helpful discussion, is gratefully acknowledged. In addition, the contribution of Dr. N. S. Bhacca of Varian Associates, who ran the 100-mc. NMR spectra is greatly appreciated.

References

1. Maynard, J. T., and W. E. Mochel, *J. Polymer Sci.*, **13**, 235 (1954).
2. Maynard, J. T., and W. E. Mochel, *J. Polymer Sci.*, **13**, 251 (1954).
3. Aufdermarsh, C. A., Jr., and R. Pariser, *J. Polymer Sci.*, **A2**, 4727 (1964).
4. Ferguson, R. C., submitted to *Analytical Chemistry*.

Résumé

Les spectres infra-rouges et de résonance magnétique nucléaire à haute résolution confirment la structure du *cis*-polychloroprène préparé par le procédé stéréospécifique. L'isomérisation des séquences tête-à-tête, tête-à-queue et queue-à-queue a été mise en évidence et mesurée quantitativement à la fois dans le *cis* et *trans*-polychloroprènes par spectroscopie RMN à haute résolution. L'irrégularité de la microstructure des néoprènes apparaît comme étant plus importante qu'on ne l'a supposée précédemment.

Zusammenfassung

Hochauflösungsinfra- und kernmagnetische Resonanzspektren bestätigen die Struktur von mit einer stereospezifischen Methode dargestelltem *cis*-Polychloropren. "Kopf-Schwanz-", "Kopf-Kopf-" und "Schwanz-Schwanz"-Sequenzisomerie wurde sowohl bei *cis*-als auch bei *trans*-Polychloropren festgestellt und mittels Hochauflösungs-NMR-Spektroskopie gemessen. Die Irregularität in der Mikrostruktur von Neopren erweist sich als stärker als früher vermutet.

Received December 6, 1963

Anionic Polymerization and Oligomerization of Methacrylonitrile by Alkali Metal Alkoxides

BEN-AMI FEIT, JOSEPH WALLACH, and ALBERT ZILKHA,
Department of Organic Chemistry, The Hebrew University, Jerusalem, Israel

Synopsis

The anionic homogeneous polymerization of methacrylonitrile by alcoholic solutions of alkali metal alkoxides in dimethylformamide was studied. The molecular weight was found to be directly proportional to monomer concentration and inversely proportional to methanol concentration in accordance with the equation $\overline{DP} = (K_p/K_t)[MAN]/[CH_3OH]$, as consistent with termination by methanol. The average K_p/K_t value obtained was 2.1-2.2. This low value enabled the formation of low oligomers at relatively high methanol concentrations. This is in contrast with the previous results of a parallel polymerization system with acrylonitrile, where only the cyanoethylation product together with relatively high polymers, and no intermediate oligomers, were formed. The physical properties of the oligomers ($n = 2-5$) are given.

INTRODUCTION

In continuation of previous work¹⁻³ on the anionic polymerization of acrylonitrile by alcoholic solutions of alkali metal alkoxides and of acrylonitrile and methacrylonitrile by quaternary ammonium hydroxides,⁴ we have studied the homogeneous polymerization of methacrylonitrile in dimethylformamide by methanolic solutions of alkali metal alkoxides. Methacrylonitrile behaves differently from acrylonitrile, as it has no acidic α -hydrogen atom for chain transfer to monomer, and its double bond is less acidic,⁵ due to the +I effect of the methyl group. Kinetic rate studies of the cyanoethylation reaction of methanol in dimethylformamide catalyzed by alkali metal methoxides⁶ and that of the anionic homogeneous polymerization of acrylonitrile, have shown that the methanol was completely consumed in a very fast cyanoethylation reaction before propagation took place.^{3,7} On the other hand, the methoxide-catalyzed addition of methanol to methacrylonitrile was found to be much slower than its addition to acrylonitrile.⁸ Thus it was expected that in the polymerization of methacrylonitrile by alcoholic solutions of alkali metal alkoxides, the alcohol present might not be consumed before the start of the propagation so that polymerization would occur in the presence of alcohol which would act as acidic terminator. At relatively high alcohol concentration, oligomers of methacrylonitrile might be formed. The anionic oligomerization of methyl methacrylate catalyzed by sodium methoxide in methanol was reported recently.⁹

EXPERIMENTAL

Materials

Methacrylonitrile (MAN)(Fluka) was purified as previously described.⁴ Dimethylformamide (B.D.H.) was dried by azeotropic distillation with benzene, followed by fractional distillation *in vacuo* from alumina under nitrogen. The fraction boiling at 65–66°C./35 mm. was used. Methanol, analar grade, was dried over magnesium and distilled. Oxygen-free nitrogen was used. Alkali methoxide solutions were prepared by reacting the alkali metal with methanol under reflux. Liquid reagents and solutions were kept under nitrogen and transferred with hypodermic syringes, applying positive nitrogen pressure.

Polymerization and Isolation of Polymers

All manipulations were carried out under nitrogen. The polymerization was carried out in a three-necked flask, connected to vacuum and nitrogen lines, and fitted with a self-sealing rubber cap through which the reagents were added by syringes. Magnetic stirring was employed. The reaction flask was dried by flaming *in vacuo* and cooled under nitrogen. Dimethylformamide and monomer were introduced, cooled to the required temperature, and the catalyst solution subsequently added. Polymerization occurred after a certain induction period, during which the reaction mixture remained colorless, and was accompanied by the development of a yellow color. The color of the clear homogeneous polymerization mixture became brown-red in the course of the polymerization. The overall volume of the polymerization mixture was kept constant (50 ml.), temperature $0 \pm 1^\circ\text{C}$., and the polymerization time was 60 min. unless otherwise indicated.

At the end of the polymerization a 5-ml. sample of the homogeneous polymerization mixture was transferred into a 50-ml. volumetric flask containing 5 ml. of a solution of hydrochloric acid in isopropanol (1*M*) to stop the polymerization. The solution was diluted to 50 ml. by isopropanol, and aliquot portions were analyzed volumetrically for unreacted methacrylonitrile by the *n*-dodecyl mercaptan method¹⁰ described below.

The rest of the polymerization mixture was poured into dilute hydrochloric acid (2%). The polymer separated as a white fine powder, a sticky solid, or an oil, depending on its molecular weight. Potassium chloride (5–10 g.) was added, and the mixture shaken to cause coagulation and solidification of the polymer. The product was filtered, washed copiously with distilled water until it gave a negative test for chloride ion and dried *in vacuo* over phosphorus pentoxide. The previously reported purification procedure¹¹ could not be used in our case, as the polymers obtained were relatively very low and were soluble partially or completely in methanol.

Oligomerization and Isolation of Oligomers

The above polymerization procedure was used for the oligomerization. At the end of the reaction, the mixture was poured into dilute hydrochloric

acid (2%), potassium chloride (10 g.) was added, and the upper oily layer was separated. The aqueous solution was extracted several times with chloroform, and the chloroform extract was combined with the oily layer and dried over sodium sulfate. The chloroform was driven off and the oligomer was separated by fractional distillation *in vacuo*. A nondistillable residue remained which consisted of higher oligomers.

Volumetric Determination of Methacrylonitrile

The quantitative determination of acrylonitrile^{10,12} and other substances having electrophilic double bonds¹² by the *n*-dodecyl mercaptan method was modified to suit the determination of methacrylonitrile. The method consisted of the base catalyzed addition of *n*-dodecylmercaptan to the double bond, followed by a back titration of excess mercaptan with KI-KBrO₃ solution, under acidic conditions (HCl/isopropanol). Whereas the addition of the mercaptan to acrylonitrile was quantitative within 2 min. at 25°C., we found that 30 min. at 35°C. were required in the case of methacrylonitrile. The accuracy of the determination was $\pm 3\%$ for methacrylonitrile samples of 20–200 mg. The presence of large amounts of dimethylformamide did not affect the accuracy of the determination.

Viscosities and Viscosity–Molecular Weight Relationship for Polymethacrylonitrile

Overberger, Pearce, and Mayes¹¹ found the following relationship between intrinsic viscosity measured in dimethylformamide and molecular weight of polymethacrylonitrile

$$[\eta] = 3.06 \times 10^{-3} \bar{M}^{0.503} \quad (1)$$

They used this equation for determining the molecular weight of polymers having intrinsic viscosities in the range of 0.2–0.9 dl./g.

TABLE I
Viscosity–Molecular Weight Relationship for Polymethacrylonitrile

Run no.	Methoxyl, %	\bar{M}_n (from % methoxyl)	$[\eta]$, dl./g.	\bar{M}_n (from viscosity) ^a
K15	4.20	740	0.0371	690
D15	3.70	840	0.0412	850
B7	3.65	850	0.0409	840
A12	3.50	890	0.0414	860
A20	2.92	1060	0.0482	1160
A26	2.65	1170	0.0482	1160
H8	2.13	1450	0.0527	1380
L13	1.77	1750	0.0580	1660
K5	1.03	3010	0.0805	3160
D10	0.80	3870	0.0863	3630
L16	0.58	5340	0.1040	5230

^a Calculated from the derived equation, $[\eta] = 1.32 \times 10^{-3} \bar{M}_n^{0.51}$.

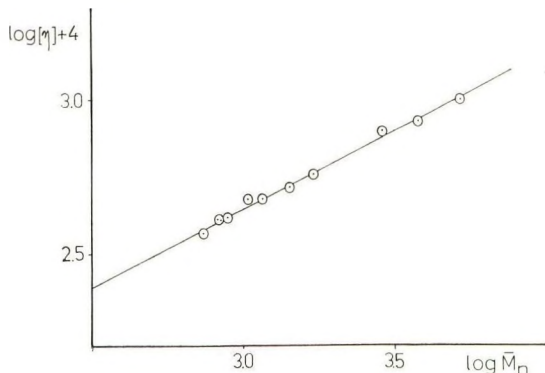


Fig. 1. Viscosity-molecular weight relationship for polymethacrylonitrile.

In the present study very low polymers having intrinsic viscosities in the range of 0.03–0.1 dl./g. were obtained. Their number-average degrees of polymerization, calculated from methoxyl endgroup analyses, assuming that each polymer molecule has one methoxyl endgroup (see Discussion), were in the range of 12–80. The above equation¹¹ was found to be unsuitable for these low polymers, as it gave too low molecular weight values. Thus for example, a solid polymethacrylonitrile sample having 4.2% methoxyl groups ($\bar{M}_n = 740$) and $[\eta] = 0.0371$ dl./g. gave a molecular weight of 176 ($n = \sim 3$) by use of eq. (1), while we have prepared the trimer which was a liquid.

Therefore we found it necessary to derive a new viscosity-molecular weight relationship which would be suitable for very low methacrylonitrile polymers. Intrinsic viscosities, methoxyl content, and calculated number-average molecular weights of some low polymers of methacrylonitrile are given in Table I. These results are illustrated in Figure 1, where $\log [\eta]$ is plotted against $\log \bar{M}_n$. From the straight line the following equation was obtained:

$$[\eta] = 1.32 \times 10^{-3} \bar{M}_n^{0.51} \quad (2)$$

This equation was used to calculate the number-average molecular weights from intrinsic viscosities measured with an Ubbelohde viscometer in dimethylformamide at 29.2°C.

RESULTS

Dependence of Molecular Weight on Monomer Concentration

This was investigated with the use of methanolic solutions of sodium and of potassium methoxide as initiators, in the presence of two different concentrations of methanol (Table II). The molecular weights increased linearly with increasing monomer concentration (Fig. 2). Accordingly linear plots were also obtained on plotting $\log [\eta]$ against $\log [\text{MAN}]$.

TABLE II
Dependence of Molecular Weight on Monomer Concentration

Run no.	Induction period, min.	[MAN], mole/l.	Polymer yield, %	MAN reacted, % ^a	$[\eta]$, dl./g.	\bar{M}_n (calc.) ^b	DP (calc.) ^b	$K = \frac{\overline{DP}[\text{CH}_3\text{OH}]}{[\text{MAN}]}$
Series A ^c								
K15		0.24	88	—	0.0371	690	10.3	2.14
K18		0.24	75	—	0.0417	870	13.0	2.70
K12		0.48	90	96	0.0522	1350	20.2	2.10
K10		0.72	80	85	0.0638	2010	29.9	2.07
K5		1.19	88	97	0.0805	3160	47.2	1.98
K7		1.19	87	95	0.0781	2980	44.5	1.86
K6		2.39	84	—	0.1080	5630	84.0	1.75
K9		2.39	85	94	0.1171	6600	98.5	2.05
K8		2.39	90	96	0.1203	6950	103.8	2.16
Series B ^d								
D15	0.75	1.19	—	99	0.0409	850	12.6	1.58
D13	0.50	1.79	—	99	0.0616	1870	28.0	2.33
D12	0.40	2.39	—	—	0.0753	2780	41.4	2.59
D8		3.58	—	99	0.0790	3050	45.5	1.90
D10	0.25	3.58	—	99	0.0863	3630	54.1	2.26

^a The per cent reacted MAN as determined volumetrically is, as seen, about 10% higher than the per cent conversion of collected polymer, which may be due to losses in the isolation of polymer.

^b Calculated from the derived equation, $[\eta] = 1.32 \times 10^{-3} \bar{M}_n^{0.51}$.

^c Potassium methoxide, 5.16 mole/l. and methanol, 49.8 mmole/l., were used.

^d Sodium methoxide, 14.4 mmole/l., and methanol, 149.7 mmole/l., were used.

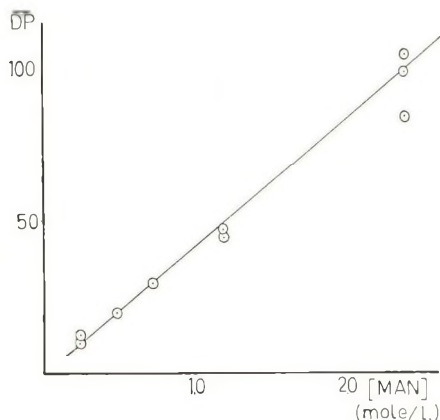


Fig. 2. Dependence of molecular weight on monomer concentration.

Dependence of Molecular Weight on Methanol Concentration

The methanol concentration had a profound influence on the molecular weights and on the physical properties of the polymers. At low methanol concentrations ($[\text{MAN}]/[\text{CH}_3\text{OH}] = 10\text{--}50$) polymers that were solid at room temperature were obtained. Polymers that were semisolid at room temperature but could be isolated as a fine powder at low temperature ($0\text{--}5^\circ\text{C}.$) were obtained at $[\text{MAN}]/[\text{CH}_3\text{OH}] = 3.5\text{--}6.0$. At still higher methanol concentrations ($[\text{MAN}]/[\text{CH}_3\text{OH}] = 1\text{--}2$), liquid polymers of various viscosities were obtained. The semisolid and liquid polymers could not be purified sufficiently from traces of inorganic salts for viscosity measurements. Therefore the dependence of the molecular weight on methanol concentration was studied at low methanol concentrations only.

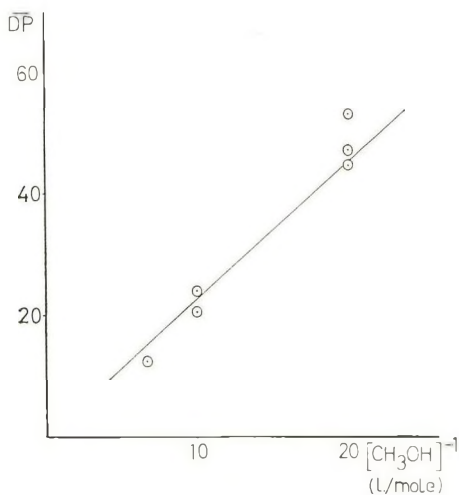


Fig. 3. Dependence of molecular weight on methanol concentration.

TABLE III
Dependence of Molecular Weight of Methanol Concentration^a

Run no.	[CH ₃ OH], mmole/l.	[Catalyst], mmole/l. ^b	Polymer yield, %	MAN reacted, %	[η], dl./g.	\bar{M}_n	\bar{DP}	$K = \frac{\bar{DP}[\text{CH}_3\text{OH}]}{[\text{MAN}]}$
D15 ^c	149.7	14.40	—	99	0.0409	850	12.6	1.58
K4	99.6	10.32	86	—	0.0570	1610	24.0	2.01
H8	99.6	4.10	—	—	0.0527	1380	20.6	1.72
K5	49.8	5.16	88	97	0.0805	3160	47.2	1.98
K7	49.8	5.16	87	95	0.0781	2980	44.5	1.86
M12	49.8	5.00	—	99	0.0854	3550	53.0	2.22

^a Methacrylonitrile, 1.19 mole/l., and potassium methoxide catalyst were used.

^b Comparable experimental conditions are being kept, since the molecular weight is independent of catalyst concentration.

^c Sodium methoxide was used.

The molecular weight was inversely proportional to the methanol concentration (Table III and Fig. 3). Accordingly straight lines were also obtained on plotting $\log [\eta]$ against $\log [\text{CH}_3\text{OH}]^{-1}$. The dependence of molecular weight on monomer and methanol concentrations could be thus expressed by the equation:

$$\overline{\text{DP}}_n = K[\text{MAN}]/[\text{CH}_3\text{OH}] \quad (3)$$

The constant, K , was determined from the slopes of the straight lines in Figures 2 and 3, and was about 2.1–2.2.

In cases where intrinsic viscosities were not measured, $\overline{\text{DP}}_n$ values, were determined from methoxyl endgroup analyses, and K values were calculated from eq. (3).

In the polymerization experiments carried out in the presence of high methanol concentrations, the K values obtained were of the same order (2–2.8)(Table V), although the experimental conditions, such as temperature and polymerization time, were not kept strictly constant. This indicates that the degree of polymerization is inversely proportional to the concentration of methanol over the whole range of monomer and methanol concentrations investigated.

Dependence of Molecular Weight on Catalyst Concentration

It was found that the molecular weights of the polymers obtained were independent of catalyst concentration (Table IV). An average value of $K = 2.0 \pm 0.25$ was obtained by calculation using the above $\overline{\text{DP}}_n$ relationship.

TABLE IV
Dependence of Molecular Weight on Catalyst Concentration^a

Run no.	[Catalyst], mmole/l.	MAN reacted, %	$[\eta]$, dl./g.	\bar{M}_n	$\overline{\text{DP}}$	$K = \frac{\overline{\text{DP}}[\text{CH}_3\text{OH}]^b}{[\text{MAN}]}$
M1	1.00	97	0.0908	4010	59.8	2.50
M6	2.00	97	0.0787	3030	45.2	1.89
M11	4.00	—	0.0743	2710	40.4	1.69
M12	5.00	99	0.0854	3550	53.0	2.22
K5	5.16	97	0.0805	3160	47.2	1.98
K7	5.16	95	0.0781	2980	44.5	1.86

^a Methacrylonitrile, 1.19 mole/l., methanol, 49.8 mmole/l., and potassium methoxide catalyst were used.

^b The average value of K is 2.07 ± 0.24 .

Oligomerization of Methacrylonitrile

Mixtures of liquid oligomers were obtained on using $[\text{MAN}]/[\text{CH}_3\text{OH}]$ ratios of 1–2 (Table V). Their general structure is

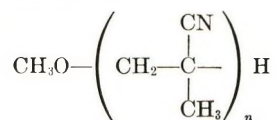


TABLE V
 Oligomerization of Methacrylonitrile

Run no.	[MAN], mole/l.	[CH ₂ OH], mole/l.	10 ³ [CH ₂ OK], mole/l.	$\frac{[\text{MAN}]}{[\text{CH}_3\text{OH}]}$	Reaction time, min.	Reaction temp., °C.	MAN reacted, %	Methoxy, %	DP	$K = \frac{\text{DP}[\text{CH}_3\text{OH}]}{[\text{MAN}]}$
115	3.57	3.59	18.06	0.99	135 ^a	0	70	16.1	2.41	2.42
116	3.57	3.59	18.06	0.99	120	22	71	17.6	2.17	2.17
118	3.57	2.57	11.60	1.39	120	0	100	11.1	3.71	2.67
114	3.57	2.49	12.90	1.43	120	0	92	14.2	2.80	1.95
112	1.79	1.25	7.20	1.43	90	5	83	10.6	3.90	2.72
112	3.57	1.99	12.90	1.79	120	0	95	10.7	3.86	2.15
111	2.39	1.25	10.32	1.91	130	0	99	7.8	5.47	2.85

^a The reaction mixture was heated for another 15 min. at 60°.

 TABLE VI
 Oligomers of Methacrylonitrile

<i>n</i>	B.p. at 0.5 mm., °C.	η_D	OCH ₃ , %		C, %		H, %		N, %	
			Calcd.	Found	Calcd.	Found	Calcd.	Found	Calcd.	Found
2	92	1.438	18.7	18.1	65.0	65.0	8.5	8.7	16.8	16.6
3	165	1.464	13.3	13.7	66.9	67.2	8.2	8.2	18.0	17.6
4	235	1.478	10.3	10.1	68.0	67.7	8.1	8.0	18.6	18.2
5	300-305	1.488	8.4	8.4	68.6	68.6	8.0	7.9	19.1	19.3

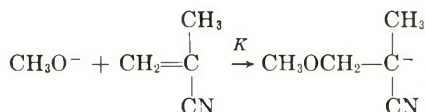
β -Methoxy isobutyronitrile ($n = 1$) was also obtained. Oligomers of $n > 5$ could not be distilled and remained as a colored residue. The average degree of oligomerization obtained was determined from methoxyl endgroup analyses carried out on the mixture of oligomers before fractionation. It increased with increasing $[\text{MAN}]/[\text{CH}_3\text{OH}]$ ratio (Table V).

Infrared spectra of the oligomers showed the absorption bands for nitrile (2225 cm.^{-1}) and for ether (1100 cm.^{-1} , $920\text{--}990 \text{ cm.}^{-1}$) bonds. Analyses and some physical properties of the oligomers are given in Table VI.

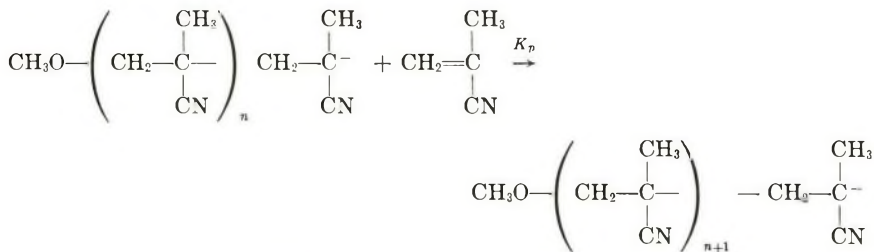
DISCUSSION

The experimentally found linear dependence of the degree of polymerization on the ratio $[\text{MAN}]/[\text{CH}_3\text{OH}]$, and its independence of the catalyst concentration are in accordance with the following scheme of polymerization.

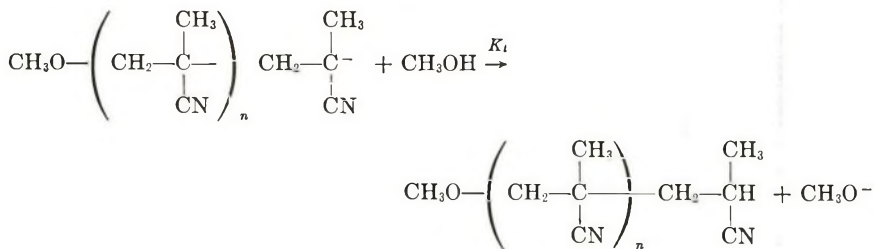
Initiation:



Propagation:



Termination (by chain transfer to methanol):

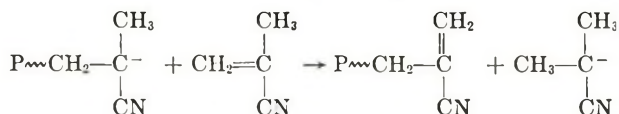


Based on these steps the following $\overline{\text{DP}}$ relationship is derived:

$$\overline{\text{DP}} = R_p/R_t = (K_p/K_t)[\text{MAN}]/[\text{CH}_3\text{OH}] \quad (4)$$

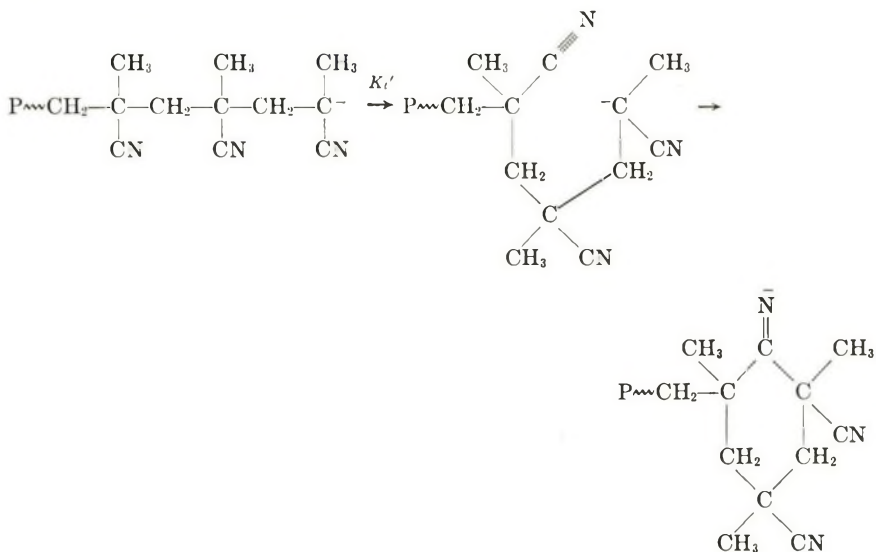
The experimentally found constant K is equal to K_p/K_t . The relatively small value of K_p/K_t (about 2) permitted in this case the formation of low oligomers under the investigated experimental conditions.

Other modes of termination may also be considered. Methacrylonitrile contains no α -hydrogen atom, so that transfer to monomer, involving such a hydrogen atom as was found in the case of acrylonitrile¹⁻³ does not exist. Overberger, Yuki, and Urakawa¹³ have proposed a transfer reaction to monomer which involves hydride ion transfer as follows:



Although this transfer reaction cannot be excluded, in our case it did not take place, as it should have resulted in a constant degree of polymerization independent of both monomer and methanol concentrations. Also, from energy considerations, termination of the carbanion growing end is much easier by the acidic methanol ($\text{p}K_a$ 16.7) than by hydride transfer.

Monomolecular termination by cyclization has been proposed for acrylonitrile¹⁴ and methyl methacrylate.^{15,16} In the case of methacrylonitrile such a termination may be possible as follows:



However, such a monomolecular termination requires that the degree of polymerization should be dependent on the monomer concentration only, $\overline{\text{DP}} = K_p/K_t'[\text{M}]$, which is contrary to the experimental results and may therefore be excluded.

From the above discussion it is seen that the only termination reaction existing is that by transfer to methanol, and that no other transfer reaction leading to new initiation centers is occurring. It follows that initiation of polymerization is by methoxide anions only and consequently every polymer chain has a methoxyl endgroup. This fact permitted the calcu-

lation of the number-average molecular weights from methoxyl endgroup determinations.

For the sake of comparison, it should be stressed that contrary to the present polymerization of methacrylonitrile, no oligomers were formed in the parallel homogeneous polymerization of acrylonitrile, where only β -methoxypropionitrile together with relatively high polymers were obtained.³ The following facts might be responsible for this difference. Due to the much greater electrophilic reactivity of the double bond of acrylonitrile,^{5,8} methanol was completely consumed in a very fast cyanoethylation reaction, leading to polymerization of acrylonitrile in the absence of methanol, and a subsequent termination by transfer to monomer. In addition, the K_p/K_t values in the case of acrylonitrile (where K_t is the transfer constant to monomer) were relatively high (13–20) compared to that of methacrylonitrile ($K_p/K_t = 2.1$ – 2.2). Since \overline{DP} for acrylonitrile was given by $\overline{DP} = K_p/K_t$, only polyacrylonitriles of $\overline{DP} \geq 13$ together with β -methoxypropionitrile formed by the complete cyanoethylation of methanol could be obtained, excluding the formation of other intermediate oligomers.

References

1. Zilkha, A., B. A. Feit, and M. Frankel, *J. Chem. Soc.*, **1959**, 928.
2. Zilkha, A., and B. A. Feit, *J. Appl. Polymer Sci.*, **5**, 251 (1961).
3. Feit, B. A., and A. Zilkha, *J. Appl. Polymer Sci.*, **7**, 287 (1963).
4. Zilkha, A., B. A. Feit, and M. Frankel, *J. Polymer Sci.*, **49**, 231 (1961).
5. Morton, M., and H. Landfield, *J. Am. Chem. Soc.*, **74**, 3523 (1952).
6. Feit, B. A., J. Sinnreich, and A. Zilkha, *J. Org. Chem.*, **28**, 3245 (1964).
7. Feit, B. A., Ph.D. Thesis submitted to the Hebrew University of Jerusalem, 1962.
8. Feit, B. A., and A. Zilkha, *J. Org. Chem.*, **28**, 406 (1963).
9. Volker, Th., A. Neumann, and U. Baumann, *Makromol. Chem.*, **63**, 182 (1963).
10. *The Chemistry of Acrylonitrile*, American Cyanamid Company, 1951, p. 69.
11. Overberger, C. G., E. M. Pearce, and N. Mayes, *J. Polymer Sci.*, **34**, 109 (1959).
12. Beeing, D. W., W. P. Tyler, D. M. Kurtz, and S. A. Harrison, *Anal. Chem.*, **21**, 1073 (1949).
13. Overberger, C. G., H. Yuki, and N. Urakawa, *J. Polymer Sci.*, **45**, 127 (1960).
14. Szwarc, M., *Fortschr. Hochpolymer. Forsch.*, **2**, 281 (1960).
15. Goode, W. E., F. H. Owens, and H. L. Myers, *J. Polymer Sci.*, **47**, 75 (1960).
16. Glusker, D. L., I. Lystoff, and E. Stiles, *J. Polymer Sci.*, **49**, 315 (1961).

Résumé

On a étudié la polymérisation anionique homogène du méthacrylonitrile dans le diméthylformamide par des solutions alcooliques d'alcoolates de métaux alcalins. On trouve que le poids moléculaire est directement proportionnel à la concentration monomérique et inversement proportionnel à la concentration en méthanol. Ceci est en accord avec l'équation $\overline{DP} = (K_p/K_t)[MAN]/[CH_3OH]$ et en même temps avec la terminaison par le méthanol. La valeur moyenne K_p/K_t obtenue est de 2.1 à 2.2. Cette valeur faible donne lieu à la formation d'oligomères à faible poids moléculaire pour des concentrations élevées en méthanol, contrairement à des résultats obtenus antérieurement pour la polymérisation de l'acrylonitrile dans de circonstances pareille. Dans le cas de l'acrylonitrile, uniquement le produit de cyanoéthylation est formé ainsi que des polymères relativement élevés et pas d'oligomères intermédiaires. On donne les propriétés physiques d'oligomères ($n = 2$ – 5).

Zusammenfassung

Die anionische homogene Polymerisation von Methacrylnitril in Dimethylformamid durch alkoholische Lösungen von Alkalimetallalkoxiden wurde untersucht. Das Molekulargewicht war der Monomerkonzentration direkt und der Methanolkonzentration umgekehrt proportional, in Übereinstimmung mit der einem Abbruch durch Methanol entsprechenden Gleichung $DP = K_p/K_t \cdot [MAN]/[CH_3OH]$. Als Mittelwert für K_p/K_t wurde 2,1-2,2 erhalten. Dieser niedrige Wert ermöglichte die Bildung niedriger Oligomerer bei verhältnismässig hoher Methanolkonzentration. Dies steht im Gegensatz zu früheren Ergebnissen an dem analogen Polymerisationssystem mit Acrylnitril, wo nur das Cyanäthylierungsprodukt zusammen mit verhältnismässig hochmolekularen Polymeren und keine oligomeren Zwischenprodukte gebildet wurden. Die physikalischen Eigenschaften der Oligomeren ($n = 2-5$) werden beschrieben.

Received December 14, 1963

Revised February 2, 1964

Amylose V Complexes from Dimethyl Sulfoxide Solutions

F. J. GERMINO* and R. M. VALLETTA,† *Research and Development Division, American Machine & Foundry Company, Springdale, Connecticut*

Synopsis

This investigation has shown that it is possible to prepare V complexes of amylose from dimethyl sulfoxide solutions. Methanol, *n*-propanol, acetone, and methyl ethyl ketone complexes have been prepared and their unit cell dimensions calculated from their x-ray powder patterns. The small unit cell, with a helix diameter of 13.0 Å, observed with a wet methanol complex from aqueous system, is also observed here. However, the wet and thoroughly dried ketone complexes prepared from DMSO have the larger helix diameter of 13.7 Å. The results indicate that factors other than the size or type of complexing agent are important in determining the helix diameter of the amylose V complex. They also indicate that these factors are complex and probably interdependent. The effect of temperature on the helix diameter was explored.

INTRODUCTION

Valletta et al.¹ reported the presence of a small unit cell in the wet methanol and ethanol amylose complexes which had previously been associated only with anhydrous V complexes.² The methanol complex of amylose containing one mole of water per mole of glucose had a 13.0 Å helix diameter while the *n*-propanol amylose complex with the same mole ratio had a helix diameter of 13.7 Å. This was the first report of an effect of the size of the complexing agent on the helix diameter of amylose V complexes. Recently, Zaslow³ has reported the existence of an amylose V complex having a helix diameter of 14.95 Å, which was obtained from a partially dried *tert*-butyl alcohol complex. This helix diameter corresponds to seven glucose residues per turn rather than the usual six.

The part that various polar solvents play in determining the diameter of the amylose helices has been the subject of some recent investigation.⁴⁻⁶ Germino et al.⁴ reported the existence on anhydrous amylose V complexes of acetone and methyl ethyl ketone with a 13.7 Å helix diameter. They also found that water had very little effect on these complexes, since the x-ray diffraction pattern was unchanged for samples having water:glucose mole ratios varying from 12:1 to 0.65:1. It has been found in the recent study conducted with low molecular weight fatty acid complexes⁵ that the varia-

* Present address: Moffett Research Center, Corn Products Company, Argo, Ill.

† Present Address: I.B.M. Components Division, Poughkeepsie, N. Y.

tion in the helix diameters of the complexes cannot be explained solely on the basis of the presence or absence of water or size of the complexing agent. Rather, there seems to be an interdependence of several factors, including the size of the organic molecule, the water content, and the method of preparation.

It was now considered desirable to examine the size effect of the complexing agent on V complexes prepared from nonaqueous solutions. The use of nonaqueous solution could eliminate one variable present in all previous studies; i.e., the influence of water molecules on the complexation and crystallization phenomena. In addition, in nonaqueous systems, the effect of complexing agent could be observed over a broader temperature range.

The studies by Foster et al.⁷ and Cowie⁸ have indicated that amylose, which is soluble in dimethylsulfoxide (DMSO), has a random coil configuration in this solvent. Studies by both workers would suggest that, possibly, the behavior of amylose in DMSO can be correlated with its structure in the solid state. Thus, a study of amylose complexes prepared from DMSO was selected.

EXPERIMENTAL

Materials

The DMSO used in the study was reagent grade. It was further purified by refluxing over CaO and distilling in a closed system.⁷

Preparation of Complexes

The V complexes of this study were prepared as follows. The appropriate weight of amylose (as Superlose, Stein Hall & Company) was added to the required volume of DMSO. The mixtures were stirred at room temperature for periods of 1, 4, 18, or 24 hr. The particular amylose complex was precipitated by rapid addition of two volumes of the corresponding solvent. After waiting 5 min. for the crystals to form, the precipitate was filtered through a Büchner funnel, washed by dispersing the filter cake in the solvent for 1 min. in a Waring Blendor, and then filtering. The washing step was repeated twice, and the final precipitate was used as the corresponding "wet" V complex. The "dry" (solvent-free) complex was obtained by heating the material at 113°C. over P₂O₅ under a vacuum of less than 1 mm. Hg.

The V complexes prepared at 95°C. were prepared in an identical manner except that the precipitating solvent was added to the DMSO solution immediately after the temperature reached 95°C.

X-Ray Analysis

The powder patterns of the complexes were obtained with a Norelco x-ray diffraction unit using Ca K α radiation and a 114.6 mm. powder camera. Exposure times were approximately 9 hr. at 45 kv. and 18 ma. The samples

were prepared by packing the various complexes into 0.3 mm. I.D. Pyrex capillaries.

RESULTS

All of the patterns obtained, except for the benzene complex, could be indexed either with the 13.0 Å. helix diameter orthorhombic unit cell ($a = 13.0$ Å., $b = 22.8$ Å., $c = 7.91$ Å.) or the 13.7 Å. helix diameter orthorhombic unit cell ($a = 13.7$ Å., $b = 23.8$ Å., $c = 8.05$ Å.). Table I summarizes the results at 25°C. while Table II contains these at 95°C.

TABLE I
Crystal Structure of Complexes Prepared at 25°C.

Complex	Time, hr.	State	Helix diameter, Å.
Methanol	1	Wet	13.7
Methanol ^a	4	Wet	—
Methanol	4	Dry	13.0
Methanol	18	Wet	13.7
Methanol	18	Dry	13.0
<i>n</i> -Propanol	4	Wet	Amorphous
<i>n</i> -Propanol	24	Wet	Amorphous
Acetone	18	Wet	13.7
Acetone	18	Dry	13.7
Methyl ethyl ketone	18	Wet	13.7
Methyl ethyl ketone	18	Dry	13.7
Benzene ^b	18	Wet	—

^a Pattern not clearly indexable.

^b Pattern similar to that observed by Zaslow³ with wet and dry *tert*-butyl alcohol complexes.

TABLE II
Crystal Structure of Complexes Prepared at 95°C.

Complex	State	Helix diameter, Å.
Methanol	Wet	13.0
Methanol	Dry	13.0
<i>n</i> -Propanol	Wet	13.7
<i>n</i> -Propanol	Dry	13.0

The patterns obtained with complexes prepared at 95°C. were characteristic of highly crystalline material. At 25°C. the complexes varied from essentially amorphous for the *n*-propanol complexes to highly crystalline in the case of some of the methanol complexes and the methyl ethyl ketone (MEK) complexes. The crystal size, with the exception of the "amorphous" *n*-propanol complexes, varied from 250 Å. to 750 Å. as estimated

TABLE III
Indexing of the Dry MEK Complex

Intensity	$\text{Sin}^2 \theta$ (obs.)	hkl	$\text{Sin}^2 \theta$ (calc.)
w	0.0044	110	0.0042
		020	0.0042
w	0.0100	030	0.0094
		001	0.0092
		011	0.0102
s	0.0126	130	0.0126
		200	0.0127
		101	0.0123
		021	0.0134
		111	0.0134
w	0.0161	040	0.0168
		220	0.0168
		121	0.0166
m	0.0213	230	0.0221
		131	0.0218
		201	0.0218
m	0.0253	050	0.0262
		041	0.0260
		221	0.0260
s	0.0292	150	0.0294
		240	0.0294
		310	0.0295
		300	0.0285
		141	0.0291
vw	0.0332	320	0.0327
m	0.0373	060	0.0378
		330	0.0379
		002	0.0366
		251	0.0380
		301	0.0376
vw	0.0419	321	0.0419
vw	0.0468	032	0.0460
		061	0.0470
		331	0.0471
vw	0.0542	170	0.0546
		350	0.0547
		420	0.0548
		042	0.0534
		222	0.0534
		341	0.0544
vw	0.0636	270	0.0641
		052	0.0628
		171	0.0638
		351	0.0638
		421	0.0639
vw	0.0737	062	0.0744
		332	0.0745
		271	0.0733

from the Scherrer formula. Table III presents the data and indexing of the dry MEK complex having a 13.7 Å helix diameter.

The powder pattern obtained for the benzene complex is similar to the pattern reported for the wet and dry *tert*-butyl alcohol complex.³ The values of $\sin^2 \theta$ and intensities observed for the benzene precipitate were 0.0038 m, 0.0055 s, 0.0079 w, 0.0119 m, 0.0168 vw, 0.0245 s, 0.0295, s, 0.0367 m, 0.0457 w, 0.0561 w, 0.0662 w, 0.0745 vw, 0.085 vw, 0.1060 vw.

The wet and dry complexes were analyzed for residual sulfur content. The residual sulfur content in all cases was less than 0.05%. The amount of residual precipitating solvent was not determined, since it was always present in excess in the wet complexes.

DISCUSSION

This investigation shows clearly that it is possible to prepare V complexes of amylose from other than aqueous solutions. The DMSO must serve to open the structure of the amylose and allow the complexing molecules to associate with the random coils and form a regular close-packed array of helices.

The effect of complexing agent is also evident in these studies. Since the residual DMSO content is very small in the wet complexes, any variation of helix diameter must be attributed to the effect of the complexing solvent, particularly when the samples have been prepared at the same temperature. For example, the wet methanol and propanol complexes prepared at 95°C. have helix diameters of 13.0 and 13.7 Å., respectively. Since the DMSO content is negligible, the primary effect must be due to the size of the *n*-propanol molecule. This role of the complexing agent is also evident with the ketone complexes prepared at 25°C. The ketone complexes have a 13.7 Å helix diameter in both the wet and dry states. Further, the powder pattern here is very crystalline, and the retention of the 13.7 Å helix cannot be attributed to the irreversibility of the retrogradation process as has been postulated for the 13.7 Å helix observed in the dry ketone complexes from aqueous solutions.⁴

In addition, the studies conducted at 95°C. indicate that one of the variables affecting the helix diameter is the temperature at which the complex has been prepared. The increase in temperature probably results in an opening of the coils of amylose the extension of the coils appears to be necessary since the *n*-propanol complex forms a crystalline V complex at 95°C. and not at 25°C. The wet methanol complex prepared at 95°C. has the unit cell with 13.0 Å helices, while that prepared at 25°C. has either the 13.7 Å helix diameter structure or a mixture of the 13.0 Å. and the 13.7 Å helix diameter phases.

A third variable which appears to be important in this study is the time of contact of amylose with the solvent. This is readily observed in the methanol complexes prepared at 25°C. This effect could be explained by one or more of the following: (1) there are changes in the conformation of the molecule during the first 24 hr. of solution contact; (2) the formation of

a true solution requires longer periods of time at 25°C.; (3) the amylose molecule is completely opened at high temperatures and more of a collapsed helix at room temperature.

The powder pattern which was observed for the benzene complex is similar to that of previously reported *tert*-butyl alcohol complex.³ It has been concluded by Zaslow that this complex has a structure based on a close packing of amylose helices with a diameter of 15 Å. This description, by analogy, could apply to the benzene complex. The benzene molecule is probably retained in the structure by a dipole-induced dipole interaction of the type suggested by Stein and Rundle.⁹

DMSO was almost completely removed from the complexes during the washings and its residual level contrasts with the large amounts of residual water remaining from the aqueous preparations. The major difference between DMSO and water is the lack of hydrogen bonding in DMSO and possibly the difference of residual amounts can be attributed to this phenomena. If this conclusion is valid, large residual amounts of hydrogen-bonding solvents should be present in V complexes prepared from any one of this type.

This study has shown that the structure of amylose V complexes is influenced by factors other than the size of the precipitating solvent and the residual solvent content. Two other factors are the temperature of the solution and, at 25°C., the solution time.

The authors wish to thank Miss Patricia Beckman for her assistance in packing the x-ray samples and reading the powder patterns reported in this paper.

The sulfur analysis were performed by Schwartzkopf Microanalytical Laboratory, Woodside, N. Y.

References

1. Valletta, R. M., F. J. Germino, R. E. Lang, and R. J. Moshy, *J. Polymer Sci.*, **A2**, 1085 (1964).
2. Rundle, R. E., *J. Am. Chem. Soc.*, **69**, 1769 (1947).
3. Zaslow, B., *Biopolymers*, **1**, 165 (1963).
4. Germino, F. J., R. J. Moshy, and R. M. Valletta, *J. Polymer Sci.*, **A2**, 2705 (1964).
5. Valletta, R. M., R. J. Moshy, and F. J. Germino, paper presented at 145th American Chemical Society, New York, N. Y., September 1963.
6. Pulley, A. O., Ph.D. Thesis, Iowa State University, 1962.
7. Everett, W. W., and J. F. Foster, *J. Am. Chem. Soc.*, **81**, 3459 (1959).
8. Cowie, J. M. G., *Makromol. Chem.*, **42**, 230 (1961).
9. Stein, R. S., and R. E. Rundle, *J. Chem. Phys.*, **16**, 195 (1948).

Résumé

Cette étude montre qu'il est possible de préparer des complexes d'amylose V à partir de solutions de diméthylsulfoxyde. Des complexes avec le méthanol, le *n*-propanol, l'acétone et la méthyl-éthyl-cétone ont été préparés et les dimensions de leur maille sont calculées à partir de spectres de rayons-X par la méthode des poudres. La maille dont le diamètre hélicoïdal est de 13.0 Å et qui est observée dans un complexe humide avec le méthanol provenant d'un système aqueux, est également observée ici. Pourtant, les complexes avec la cétone humide et séchée soigneusement, préparés à partir de DMSO ont un diamètre hélicoïdal de 13.7 Å. Les résultats indiquent que d'autres facteurs que

la dimension ou le type d'agent complexant sont importants pour déterminer le diamètre hélicoïdal du complexe d'amylose V. Les résultats indiquent aussi que ces facteurs sont complexes e qu'ils dépendent probablement l'un de l'autre. On a étudié l'effet de la température sur le diamètre hélicoïdal.

Zusammenfassung

Aus Dimethylsulfoxidlösungen können V-Komplexe von Amylose dargestellt werden. Methanol-, *n*-Propanol-, Aceton- und Methyläthylketonkomplexe wurden hergestellt und ihre Elementarzeldimensionen aus den Röntgenpulverdiagrammen berechnet. Die an einem feuchten Methanolkomplex aus wässrigem System beobachtete kleine Elementarzelle mit einem Helixdurchmesser von 13,0 Å. tritt auch hier auf. Die aus DMSO dargestellten feuchten und völlig getrockneten Ketonkomplexe besitzen dagegen einen grösseren Helixdurchmesser von 13,7 Å. Die Ergebnisse sprechen dafür, dass andere Faktoren als Grösse oder Typ des Komplexmittels bei der Festlegung des Helixdurchmessers der Amylose-V-Komplexe Bedeutung haben. Sie zeigen weiters, dass diese Faktoren komplexer Natur und wahrscheinlich voneinander abhängig sind. Die Rolle der Temperatur bei der Beeinflussung des Helixdurchmessers wurde untersucht.

Received January 22, 1964

Amylose V Complexes from 2-Aminoethanol Solutions

R. M. VALLETTA* and F. J. GERMINO,† *Research and Development Laboratory, American Machine & Foundry Company, Springdale, Connecticut*

Synopsis

The amylose V complexes with methanol, 1-propanol, 1-butanol, and acetone have been prepared from 2-aminoethanol solutions at 95°C. and their unit cell dimensions calculated from their x-ray powder patterns. The study shows that amylose V complexes having helix diameters of 13.0 Å., 13.7 Å., and a mixture of 13.7 Å. and 13.0 Å. can be produced in systems devoid of water. Further, the results indicate that the helix diameter in this system is affected by the temperature of the amylose solution prior to the formation of the V complex. In addition, there seems to be correlation between crystal structure of the amylose, size of its helical diameter, and its conformation in solution.

INTRODUCTION

The crystal structure of amylose V complexes has been the subject of numerous investigations.¹⁻⁹ These studies have established the importance of the effect of the size of the complexing agent in complexes prepared from aqueous solutions. In a recent study of amylose complexes prepared from dimethyl sulfoxide,¹⁰ further evidence was presented showing the role of the complexing agent. The latter study also found that the method of preparation had an effect on the structure of the V complex. A similar effect had previously been reported in a study of fatty acid V complexes⁵ and had also been found in a study of the preparation and properties of water-soluble amylose.¹¹ Further, the data on V complexes prepared from dimethyl sulfoxide seem to indicate that there is some correlation between the crystal structure of amylose and its conformation in solution.

The present study was initiated to determine whether or not: (a) the effect of the complexing agent in this system is similar to that previously observed; (b) the method of solubilization and preparation of complexing is important for V complex formation; and (c) there is any correlation between the previous systems evaluated and this one.

* Present address: I.B.M. Components Division, Poughkeepsie, N. Y.

† Present address: Moffett Research Center, Corn Products Company, Argo, Ill.

EXPERIMENTAL

Solvent Purification

Reagent grade 2-aminoethanol was redistilled at reduced pressure to remove the last traces of water. The middle fraction of the distillate was retained for all the studies.

Preparation of the Complexes

The amylose V complexes of methanol, *n*-propanol, *n*-butanol, and acetone were prepared as follows. A 10-g. portion of Superlose dried potato amylose (Stein Hall & Company) was dispersed in 250 ml. of 2-aminoethanol and heated to 95°C. The particular amylose complex was precipitated with 500 ml. of the corresponding solvent. After 5 min., the precipitate was filtered, washed by dispersing the cake in the corresponding solvent, blended in a Waring Blendor, and filtered. The washing cycle was repeated twice and the corresponding precipitate is designated our wet (solvent-rich) complex. This complex, when dried at 113°C. over P₂O₅ at less than 1 mm. Hg for 24 hr., was designated our dry complex.

This procedure was duplicated for complexes prepared at 110°C. For complexes prepared at 25°C., the procedure is identical to above, except that the sample was blended for 15 min. with a Waring Blendor before precipitation with the complexing solvent.

Preparation of the Exchange Complexes

The methanol-amylose complex was dispersed in 400 ml. of acetone, blended for 1 min. in a Waring Blendor, and filtered. This washing step was repeated two more times and then taken as the corresponding exchange complex. This procedure was utilized for all exchange complexes.

X-Ray Analysis

The powder patterns of the complexes were obtained with a Norelco x-ray diffraction unit using Cu K α radiation and a 114.6 mm. powder camera. Exposure times were approximately 7 hr. at 45 kv. and 18 ma. The samples were prepared by packing the various complexes into 0.3 mm. I.D. Pyrex capillaries and sealed.

Results

Table I summarizes the results obtained with methanol, *n*-propanol, *n*-butanol, and acetone complexes prepared at 95°C. All patterns had numerous lines and could be indexed using the previously reported lattice constants. Each sample was crystalline and had an average particle size ranging from 250 to 750 Å. using the Scherrer formula. The wet alcohol complexes, containing sizable amounts of residual solvent, consisted of a mixture of two helical diameters, 13.0 and 13.7 Å. Since the patterns obtained were sharp, the presence of the two species was unequivocal. In

contrast, the acetone complex was the most crystalline of all and had a helical diameter of 13.7 Å. These wet complexes, when dried at 113°C. over P₂O₅ for 24 hr., produced a reduction in volume and a contraction of the helix diameter to 13.0 Å.

TABLE I
Unit Cells of Amylose V Complexes Prepared at 95°C.

Complexing agent	State	Helix diameter, Å.
Methanol	Wet	13.0 + 13.7
Methanol	Dry	13.0
<i>n</i> -Propanol	Wet	13.0 + 13.7
<i>n</i> -Propanol	Dry	13.0 + trace of 13.7
Acetone	Wet	13.7
Acetone	Dry	13.0
<i>n</i> -Butanol	Wet	13.0 + 13.7

The observed and calculated $\sin^2\theta$ of the wet acetone complex is presented in Table II. As can be seen from this table, there is excellent agreement between the observed and the calculated values of $\sin^2\theta$.

In order to obtain an indication of what part the complexing agent plays in determining the helix diameter of an amylose V complex from nonaqueous systems, a series of exchange experiments were conducted. The data in Table III summarize the results of these experiments.

The methanol complex, which had two distinct helix diameter species of 13.7 and 13.0 Å., became one species with a helix diameter of 13.7 Å. when washed with *n*-propanol or acetone. This phenomenon was also observed

TABLE II
Indexing of Wet Acetone Complex Prepared at 95°C.

Intensity	$\sin^2\theta$ (obs.)	<i>hkl</i>	$\sin^2\theta$ (calc.)
m	0.0042	110	0.0041
		020	0.0039
w	0.0085	030	0.0094
		001	0.0092
		011	0.0103
s	0.0128	200	0.0127
		210	0.0137
		130	0.0126
		021	0.0134
		111	0.0134
		101	0.0124
		040	0.0168
4	0.0166	220	0.0169
		121	0.0163
m	0.0215	230	0.0221
		131	0.0218
		201	0.0219

(continued)

TABLE II (continued)

Intensity	$\text{Sin}^2\theta$ (obs.)	hkl	$\text{Sin}^2\theta$ (calc.)	
m	0.0250	041	0.0260	
		221	0.0261	
s	0.0292	150	0.0294	
		240	0.0294	
		310	0.0295	
		300	0.0285	
		141	0.0291	
vw	0.0331	320	0.0327	
w	0.0375	060	0.0378	
		330	0.0379	
		012	0.0376	
vw	0.0456	301	0.0377	
		340	0.0453	
		032	0.0460	
w	0.0558	420	0.0548	
		142	0.0565	
w	0.0723	271	0.0733	
		190	0.0881	
w	0.0887	460	0.0884	
		530	0.0885	
		072	0.0880	
		412	0.0883	
		281	0.0890	
		371	0.0889	
		501	0.0882	
		511	0.0893	
		0-10-0	0.1049	0.1049
		550	0.1053	
w	0.1121	233	0.1046	
		442	0.1041	
		381	0.1055	
		541	0.1058	
		153	0.1119	
w	0.1386	243	0.1119	
		313	0.1120	
		471	0.1112	
		2-11-0	0.1396	
w	0.1519	472	0.1386	
		1-11-1	0.1392	
		0-12-0	0.1511	
w	0.1582	660	0.1516	
		183	0.1528	
		612	0.1515	
		720	0.1592	
w	0.1692	134	0.1592	
		234	0.1687	
w	0.1750	3-10-2	0.1699	
		721	0.1684	
		154	0.1760	
		244	0.1760	
w	0.1750	304	0.1751	
		671	0.1745	

TABLE III
Helix Diameters of the Complexes after Exchange

Complex	Temperature of preparation, °C.	Exchange solvent	Helix diameter, A.
Methanol	95	<i>n</i> -Propanol	13.7
Methanol	95	Acetone	13.7
<i>n</i> -Propanol	95	Acetone	13.7
<i>n</i> -Butanol	95	Acetone	13.7

with the *n*-propanol and *n*-butanol complexes when exchanged with acetone.

Table IV summarizes the studies on what, if any, effect residual 2-aminoethanol might have on wet complexes as prepared and after exchange. These data show that a significantly different amount of 2-aminoethanol can be present, as in the methanol and *n*-propanol complex, without producing any change in the helix diameter. Also, the methanol complex, after being washed with either *n*-propanol or acetone, still contained equal quantities of 2-aminoethanol but showed an enlargement of the helix diameter to 13.7 A.

TABLE IV
Solvent Content of Amylose V Complexes Prepared at 95°C.

Amylose complex	State	Mole ratio of 2-aminoethanol to glucose	Helix A.
Methanol	Wet	1/8.5	13.0 + 13.7
Methanol washed with <i>n</i> -propanol	Wet	1/7.5	13.7
Methanol washed with acetone	Wet	1/7.4	13.7
<i>n</i> -Propanol	Wet	1/2.1	13.0 + 13.7

Previous studies have indicated that, in addition to type and size of complexing agent,¹² the method of preparation affects the complex formation. Methanol complexes were prepared at three temperatures, 25, 95, and 110°C. and subjected to x-ray analysis. The data, summarized in Table V, confirm that in addition to the complexing agent, the temperature of solubilization is likewise important. The methanol complex prepared at 25°C. has essentially a helix diameter of 13.7 A. An amylose solution heated to

TABLE V
Complexes Prepared at Various Temperatures of Solubilization

Complexing agent	Temperature, °C.	State	Helix diameter, A.
Methanol	25	Wet	13.7 + trace 13.0
Methanol	95	Wet	13.7 + 13.0
Methanol	110	Wet	13.0
Methanol	110	Dry	13.0

110°C. and precipitated with methanol produces a complex with a helix diameter of 13.0 Å. A similar complex prepared at 95°C. seems to be an intermediate since it consisted of a mixture of two species having helix diameters of 13.7 and 13.0 Å.

DISCUSSION

The present study continues to show that the complexing agent does affect the helix diameter of an amylose V complex. However, this study indicates that the helix diameter is also affected by the manner of preparation of the amylose solution as well as the temperature of solution.

Previous studies in the aqueous system suggested that the organic complexing agent played some role in determining the size of the amylose V complex.¹² However, varying amounts of water had an effect, and it was impossible to separate out the role of the complexing agent alone. The paper by Germino and Valletta¹⁰ on the DMSO system demonstrated the effect of the organic complexing agent alone on amylose helical diameter. The role of the complexing agent alone was further defined in these studies. For example, the exchange studies showed that the diameter of the amylose helix could be expanded by exchange of propanol or acetone molecules for methanol. Also, the residual 2-aminoethanol content of a methanol complex was essentially unchanged after three washings with *n*-propanol or acetone. The diameter change, then, must have been a direct result of a replacement of methanol by the larger molecules. This agrees with the results of other investigations concerning the effect of the precipitating solvent.⁷ However, this was the first example of an increase in helix diameter by exchange.

The data reported in this paper indicate that there is some correlation between crystal structure of amylose, size of its helical diameter, and its conformation in solution. In the previous study on the formation of amylose complex from DMSO,¹⁰ the patterns produced were distinct and different from those of comparable samples observed in this study under identical conditions. This could suggest that the conformation of amylose in 2-aminoethanol solution is different from that in dimethyl sulfoxide. Further, these data, in conjunction with previous data, would suggest that, although the complexing agent can play an important role, other preparative factors are also important. Evaluation of the methanol complexes prepared from 2-aminoethanol at 25, 95, and 110°C. suggests that there is a change of conformation of amylose in solution with progressive change in temperature. The addition of thermal energy would be expected to open the coils and make the molecules more linear. Also, the temperature at which the coils are linearized enough to allow penetration of the helix can differ from solvent to solvent depending on its interaction with the amylose and also on the size of the precipitating solvent which must penetrate the coil. Thus, one would expect to find the solvent effect on the complexing agent quite vague and ill-defined below the above described temperature.

This phenomenon was likewise observed in complexes produced with acetic and propionic acids from water.¹² There it was noted that a complex having a helix diameter of 13.7 Å, or one showing a mixture of 13.7 and 13.0 Å helix diameters could be obtained with acetic acid, depending upon method of solubilization in water. However, the amount of water present in the complex and its role in determining the size of the helix diameter somewhat obscured a complete evaluation of this effect.

It had been suggested in an earlier paper that the explanation for the difference in the retention of solvent by aqueous and DMSO system complexes could be explained by the expected difference in hydrogen bonding of water and DMSO. If this correlation is valid, the retention of 2-amino-ethanol by the amylose complexes should be intermediate to the retention of DMSO and water. Comparison of the residual solvent analyses of these complexes completely supports this correlation. This suggests that the solvent molecules are retained in the complexes by hydrogen bonds.

The authors wish to thank Miss Patricia Beckman for her assistance in packing the x-ray samples and reading the powder patterns reported in this paper.

The nitrogen analyses were performed by Schwartzkopf Microanalytical Laboratory, Woodside, N. Y.

References

1. Bear, R. S., *J. Am. Chem. Soc.*, **64**, 1388 (1952).
2. Rundle, R. E., and D. French, *J. Am. Chem. Soc.*, **65**, 1707 (1943).
3. Rundle, R. E., and F. C. Edwards, *J. Am. Chem. Soc.*, **65**, 2200 (1943).
4. Rundle, R. E., *J. Am. Chem. Soc.*, **69**, 1769 (1947).
5. Mikus, F. F., R. M. Hixon, and R. E. Rundle, *J. Am. Chem. Soc.*, **68**, 1115 (1946).
6. Zaslow, B., and R. L. Miller, *J. Am. Chem. Soc.*, **83**, 4318 (1961).
7. Zaslow, B., *Biopolymers*, **1**, 165 (1963).
8. Valletta, R. M., F. J. Germino, R. E. Lang, and R. J. Moshy, *J. Polymer Sci.*, **A2**, 1085 (1964).
9. Germino, F. J., R. J. Moshy, and R. M. Valletta, *J. Polymer Sci.*, **A2**, 2705 (1964).
10. Germino, F. J., and R. M. Valletta, *J. Polymer Sci.*, **A2**, 4757 (1964).
11. Sarko, A., F. J. Germino, and B. Zeitlin, *J. Appl. Polymer Sci.*, **8**, 1343 (1964).
12. Valletta, R. M., R. J. Moshy, and F. J. Germino, paper presented at 145th American Chemical Society Meeting, New York, N. Y., September, 1963.

Résumé

Les complexes V de l'amylose avec le méthanol, le propanol-1, le butanol-1 et l'acétone, ont été préparés à partir des solutions de 2-amino-éthanol à 95°C et les dimensions de leurs cellules unitaires ont été calculées à partir des diagrammes des rayons-X obtenus par la méthode des poudres. Cette étude montre que les complexes V d'amylose possédant des diamètres d'hélice de 13.0 Å, 13.7 Å. et d'un mélange de 13.7 Å. et 13.0 Å. peuvent être produits dans des systèmes dépourvus d'eau. De plus, les résultats indiquent que le diamètre d'hélice dans ce système est affecté par la température de la solution d'amylose avant la formation du complexe V. De plus, il semble y avoir une corrélation entre la structure cristalline de l'amylose, la dimension du diamètre de l'hélice et sa conformation en solution.

Zusammenfassung

Methanol-, 1-Propanol-, 1-Butanol- und Acetonamylose-V-Komplexe wurden aus 2-Aminoäthanollösungen bei 95°C dargestellt und die Elementarzeldimensionen aus den Röntgenpulverdiagrammen berechnet. Es zeigt sich, dass in wasserfreien Systemen Amylose-V-Komplexe mit Helixdurchmessern von 13,0 Å, 13,7 Å und ein Gemisch von 13,7 Å und 13,0 Å hergestellt werden können. Weiters lassen die Ergebnisse erkennen, dass der Helixdurchmesser in diesen Systemen von der Temperatur der Amylozelösung vor der Bildung des V-Komplexes beeinflusst wird. Ausserdem scheint eine Beziehung zwischen der Kristallstruktur der Amylose, der Grösse ihres Helixdurchmessers und ihrer Konformation in Lösung zu bestehen.

Received January 22, 1964

Thermal Degradation of Ethylene Bis(*N*-phenylcarbamate)*

H. C. BEACHELL and C. P. NGOC SON, *Department of Chemistry,
University of Delaware, Newark, Delaware*

Synopsis

The pyrolysis of ethylene bis(*N*-phenylcarbamate) was studied as the simplest model of a polyurethane. The degradation occurs by a double process of decomposition involving the simultaneous formation of 3-phenyl-2-oxazolidone, carbon dioxide, and aniline and a partial dissociation into monocarbamate and phenyl isocyanate. Further reaction produces ethylene oxide, *N,N'*-diphenylethylenediamine, *N,N'*-diphenyl-2-imidazolidone, and *N,N'*-diphenylurea.

INTRODUCTION

Extensive investigations have been carried out on the thermal degradation of urethanes,¹⁻¹⁰ as polyurethanes have become more and more important in various fields of application. In general, the first step of degradation appears to be a dissociation of the urethane into the corresponding alcohol and isocyanate or the formation of amine, olefin, and carbon dioxide by a cyclic intramolecular process. Further side reactions can occur, such as the formation of disubstituted urea from isocyanate and amine, the polymerization of isocyanate, the formation of allophanate from the reaction of isocyanate with urethane, the formation of polycarbodiimide and its derivative products.

This research was undertaken to investigate the pyrolysis of ethylene bis(*N*-phenylcarbamate) (EBPC) in order to determine to what extent the previous mechanisms could be applied to this case. This compound has not been investigated to date. It proved to be of unusual interest as the results obtained were considerably different from those reported in the past.

EXPERIMENTAL RESULTS AND DISCUSSION

Degradation of EBPC

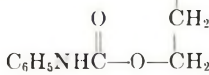
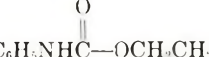
The thermal degradation of EBPC (I) under nitrogen at 200-215°C. gave as products aniline (II), 3-phenyl-2-oxazolidone (III), ethylene oxide (IV).

* Abstracted from the Ph.D. dissertation of C. P. Ngoc Son, University of Delaware. June 1962.

carbon dioxide (V), symmetrical diphenylurea SDPU (VI), *N,N'*-diphenylethylenediamine (VII), and *N,N'*-diphenyl-2-imidazolidone (VIII). These compounds were identified by elemental analysis and comparison with authentic samples (infrared spectra, mixed melting point). Ethylene oxide was detected by its infrared spectrum or by the very sensitive reaction with potassium thiocyanate in the presence of phenolphthalein.¹¹

The results are summarized in Table I.

TABLE I
Thermal Degradation of EBPC^a

	Expt. 1	Expt. 2	Expt. 3	Expt. 4	Expt. 5	Expt. 6
Time, min.	60	140	67	360	440	420
Amt. dicarbamate used, mmole	30	30	10	22	15	30
Products, mmole						
Carbon dioxide	26.61	27.4	8.45	31.9	19.6	38.18
Aniline	^b	13.33 ^c	6.50	15.17 ^d	11.24 ^d	11.61 ^e
<i>N,N'</i> -Diphenylethylenediamine	^b	^b	0.57	5.18	3.42	5.94
Oxazolidone	^b	17.65	5.34 ^f	10.6	8.23	14.25
SDPU	^b	6.56	1.65	0	0.1	0.37
Imidazolidone	^b		0	1.2	0.44	2.14
<i>p</i> -CH ₃ C ₆ H ₄ NHCOO						
	5.43					
		2.63				
Recovery, %			84 ^g	90	91	80

^a Temperature 210 ± 5°C.; N₂ = 20–22 cc./min.

^b Not determined.

^c Titration of the total basic amine by HClO₄ in glacial acetic acid (approximate quantity only due to the loss during chromatography and recrystallization).

^d Based on the weight of aniline hydrochloride obtained by difference after subtraction of the *N,N'*-diphenylethylenediamine dihydrochloride.

^e Approximate quantity obtained from recovery from the mixture of amine hydrochlorides treated with 3*N* NaOH.

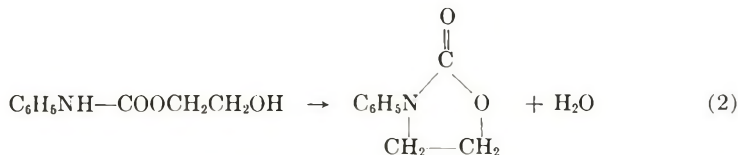
^f Excluding another mixture of oxazolidone and unidentified product (checked by infrared); m.p. 85–90°C., weight 0.251 g.

^g Including 0.251 g. oxazolidone mixture.

In experiment 1, after pyrolysis, *p*-tolyl isocyanate (2.5 cc.) was added and allowed to react with the amine liberated during the degradation; 3-phenyl-2-oxazolidone and the disubstituted ureas were then separated and the remainder was chromatographed on alumina. In experiment 2, no isocyanate was added. After separation of the oxazolidone and SDPU the rest was chromatographed. Ethylene-(*N*-phenyl-*N'*-*p*-tolyl)-dicarbamate or β -hydroxyethyl-*N*-phenylcarbamate respectively, were isolated.

It appears that the first step in the degradation process is a partial dissociation of EBPC into phenyl isocyanate and β -hydroxyethyl-*N*-phenylcarbamate.

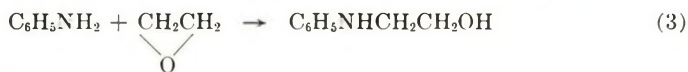
The formation of ethylene oxide, aniline, CO_2 , and 3-phenyl-2-oxazolidone may be explained by the reactions (1) and (2).



As a result it seemed desirable to study the pyrolysis of β -hydroxyethyl-*N*-phenylcarbamate. This compound was synthesized by the reaction of an excess of ethylene glycol with phenyl isocyanate. Impure monocarbamate containing less than 5% EBPC was obtained after distillation of the excess of ethylene glycol.

Degradation of β -Hydroxyethyl-*N*-phenylcarbamate

The degradation was performed at several temperatures from 180 to 205°C. In every case 3-phenyl-2-oxazolidone was obtained with small amount of SDPU, probably some 2-anilinoethanol, and large quantities of carbon dioxide and aniline. The rate of evolution of CO_2 was found to increase with an increase in temperature or in the presence of triethylenediamine (DABCO) as catalyst. The quantity of oxazolidone also increased on increasing the amount of catalyst. The quantity of amines, as estimated by the titration with perchloric acid in glacial acetic acid, was approximately equal to the quantity of carbon dioxide evolved. The experimental results fitted eqs. (1) and (2). The presence of 2-anilinoethanol could result from the reaction of aniline with ethylene oxide as shown in eq. (3) or by loss of CO_2 from the monocarbamate [eq. (4)], as shown by Read⁴ to occur in the degradation of *O*-1-hexadecyl-*N*-1-naphthylcarbamate.



2-Anilinoethanol was isolated as the phenylurethane of the corresponding urea, *N*-(β -hydroxyethyl)-*N,N'*-diphenylurea in one experiment where 17 mmoles of monocarbamate was degraded at 196–197°C., in a yield 75.9%. Table II summarizes the data obtained in the pyrolysis of β -hydroxyethyl-*N*-phenylcarbamate.

The small amount of SDPU isolated suggests a very slight dissociation of the carbamate into phenyl isocyanate and glycol; thus the formation of

3-phenyl-2-oxazolidone could not be due to the reaction of phenyl isocyanate and ethylene oxide.¹² Without catalyst the ratio of carbon dioxide to oxazolidone was much larger for the β -hydroxyethyl-*N*-phenylcarbamate than for EBPC as shown in Table I. This difference was more pronounced when later on the formation of *N,N'*-diphenylethylenediamine and *N,N'*-diphenyl-2-imidazolidone was explained. Corrections could then be made to determine the initial ratio of carbon dioxide/oxazolidone for the EBPC degradation. By comparison of these ratios of CO₂ to oxazolidone, it became apparent that other processes must be taking place in the degradation

TABLE II
Pyrolysis of β -Hydroxyethyl-*N*-phenylcarbamate

	Expt. 1	Expt. 2	Expt. 3	Expt. 4
Amount carbamate, g. ^a	5.104	5.833	5.025	3.900
Amount carbamate, mmole	28.2	32.2	27.7	21.5
Time, min.	300	210	60	35
Temperature, °C.	183 ± 1	202 ± 2	182 ± 1	183 ± 1
DABCO, mole-%	0	0	1	3
Product, mmoles				
Carbon dioxide	11.57	17.75	10.60	10.67
Amines ^b	10.70	16.36	°	8.75
3-Phenyl-2-oxazolidone	2.46	2.80	4.55	6.01
<i>N,N'</i> -Diphenylurea	0.37	°	0.52	0.38
Ratio carbon dioxide/ oxazolidone (uncorrected)	4.7	6.3	2.4	1.8

^a Purity not checked.

^b From titration using perchloric acid in glacial acetic acid.

^c Not determined.

of EBPC. In order to understand the first step in the degradation of EBPC better, the pyrolysis must be carried in such a way so as to have a faster rate of degradation and at the same time to avoid the occurrence of side reactions which complicate the analysis. Use of DABCO as catalyst and lower temperature of pyrolysis fulfills this requirement.

Degradation of EBPC in the Presence of DABCO as Catalyst

The degradation reaction was carried under nitrogen at 181–184°C. At 170°C., bubbles started to be evolved from the reaction mixture. The evolution of carbon dioxide in the presence of DABCO was very fast and followed first-order kinetics with respect to EBPC up to 50–60% degradation. At a concentration of 3 mole-% of DABCO, the amounts of CO₂, oxazolidone, and aniline (including free aniline and aniline used to form SDPU) were approximately equal (Table III). The rate constant of CO₂ formation increased as the amount of DABCO increased. The proportionality was approximately linear under the experimental conditions used here. At 3, 2, and 1 mole-% of DABCO, the initial rate constants were 4.27, 3.00, and 1.88×10^{-2} sec.⁻¹, respectively (Fig. 1).

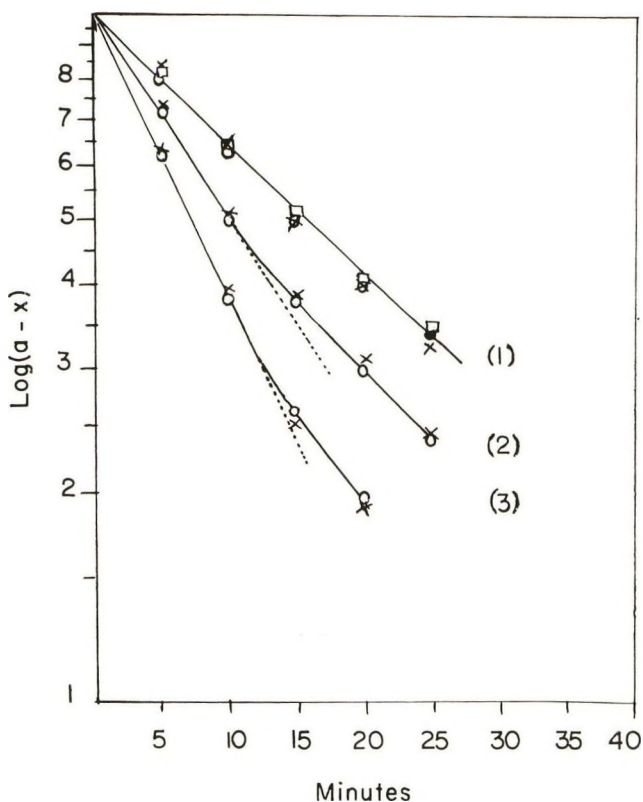


Fig. 1. Rate of loss of CO_2 in the degradation of EBPC in the presence of DABCO: (1) 1% DABCO; (2) 2% DABCO; (3) 3% DABCO.

In comparison the degradation of the bisurethane without catalyst was very slow at 210–212°C. It took 5 hr. at 183°C. or 1 hr. at 212°C. to produce the same amount of CO_2 .

TABLE III
Degradation of EBPC with 3-mole-% DABCO

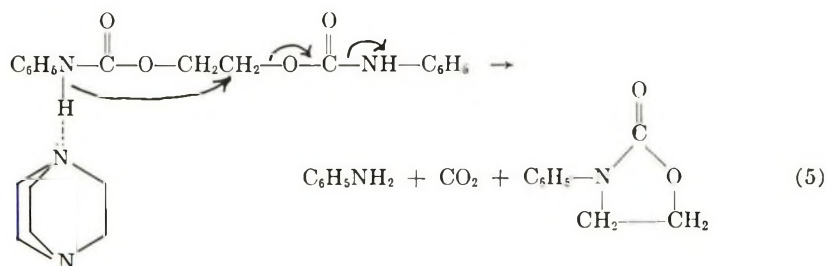
	Expt. 1	Expt. 2	Expt. 3
Time, min.	20	21	25
Temperature, °C.	183 ± 1	182 ± 1	182 ± 1
Amount EBPC, mmoles	10	10	10
Products, mmoles			
Carbon dioxide	8.21	8.50	8.72
Aniline	7 ^a	6.0 ^b	6.64 ^a
Oxazolidone	7.60	^c	7.90
SDPU	1.02	1.44	0.95
Ratio carbon dioxide/oxazolidone	1.08		1.10
Total recovery, %	82		83

^a Weight as $\text{C}_6\text{H}_5\text{NH}_2 \cdot \text{HCl}$, total aniline = aniline found + aniline from SDPU.

^b Titration with HClO_4 .

^c Not determined.

Evidently DABCO also catalyzes another process of decomposition which simultaneously produces carbon dioxide, aniline, and oxazolidone. DABCO probably helps to pull out the proton, making the nitrogen more nucleophilic [eq. (5)].



The aqueous solution of KSCN remains colorless for the first 10 min. of degradation (about 60% degradation). In another experiment, in order to show that dissociation did not take place at the beginning, and that the bubbles coming off from the reaction mixture were CO_2 , a solution of saturated barium hydroxide was used instead of Ascarite. Barium carbonate precipitated simultaneously with the formation of the bubbles. Aniline was detected but not isocyanate after 3 min. of reaction.

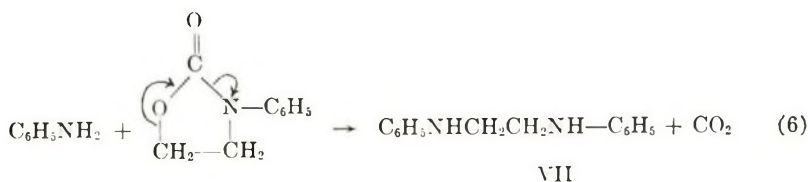
The small amount of SDPU suggests that part of the dicarbamate dissociated into phenyl isocyanate and monocarbamate and the isocyanate reacted with aniline to give *N,N'*-diphenylurea.

At 1 mole-% DABCO, dissociation into monocarbamate and isocyanate appeared to be more important, for a larger amount of SDPU was isolated (450 mg. compared to 240–300 mg. isolated when 3% of DABCO was used).

From this study it would appear that the first step in the degradation of EBPC without catalyst was a double process as shown above, with a larger amount of dissociation than in the case of the degradation with catalyst.

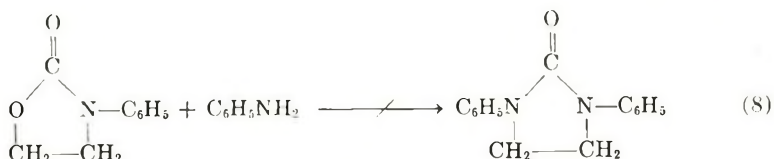
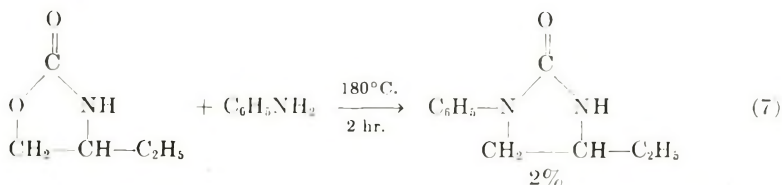
Mechanism of Formation of *N,N'*-Diphenylethylenediamine

The formation of the diamine could be better understood after aniline was allowed to react at 200–205°C. with 3-phenyl-2-oxazolidone under nitrogen. The expected *N,N'*-diphenyl-2-imidazolidone was not formed. Instead, *N,N'*-diphenylethylenediamine (VII) was isolated with a yield of 30–60%, and *N,N'*-diphenylethylenediamine was therefore formed by the reaction of aniline with 3-phenyl-2-oxazolidone [eq. (6)].



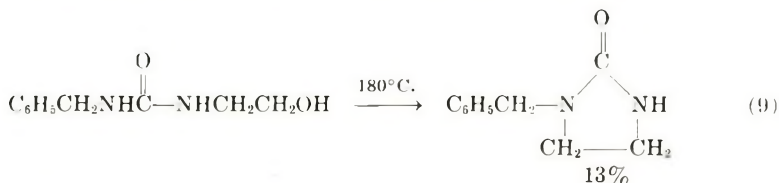
This type of displacement has also been observed by other workers.^{2,13}

The attack of aniline on the methylene group rather than on the carbonyl seemed to be governed by a steric effect. The decrease in reactivity of the carbonyl in a five-membered ring shown by Brown and co-workers¹⁴⁻¹⁶ appeared to be enhanced by the presence of phenyl ring attached to the nitrogen. Aniline reacted with 2-oxazolidone or 4-ethyl-2-oxazolidone to give the corresponding 1-phenyl-2-imidazolidones.^{17,18} No such reaction occurred with 3-phenyl-2-oxazolidone.

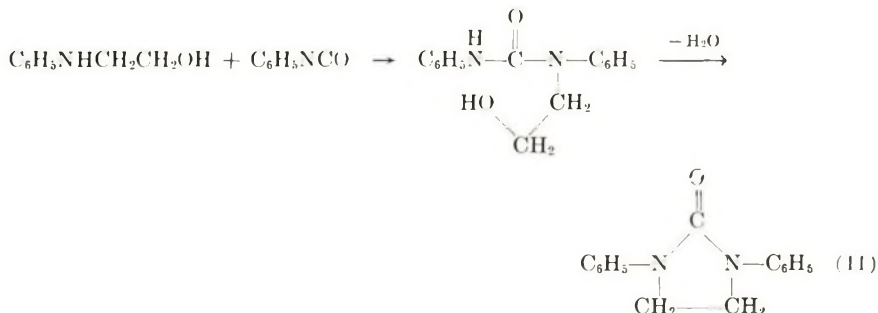
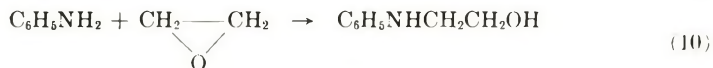


Formation of *N,N'*-Diphenyl-2-imidazolidone

The formation of *N,N'*-diphenyl-2-imidazolidone could not be attributed to the reaction of aniline with 3-phenyl-2-oxazolidone. It had been shown that *N*-benzyl-*N'*-(β -hydroxyethyl)urea cyclized by elimination of 1 mole of water to *N*-benzyl-2-imidazolidone,¹⁹ as indicated in eq. (9).



By analogy, it was presumed that VIII would be formed by the same process from *N*-(β -hydroxyethyl)-*N,N'*-diphenylurea [eqs. (10) and (11)]



However, this reaction did not take place in our experiments. No *N*-(β -hydroxyethyl)-*N,N'*-diphenylurea was isolated in any experiment. Also, the latter compound obtained by the reaction of 2-anilinoethanol with C_6H_5NCO did not give any imidazolidone in the thermal degradation (Table IV).

TABLE IV
Degradation of *N*-(β -hydroxyethyl)-*N,N'*-diphenylurea

	Expt. 1	Expt. 2	Expt. 3
Temperature, °C.	192 \pm 2	212 \pm 2	214 \pm 2
Time, min.	120	85	300
Amount <i>N</i> -(β -hydroxyethyl)- <i>N,N'</i> -diphenylurea, mmoles	20	15	15
Products, mmoles			
Carbon dioxide	8.04	7.4	10
Aniline	^a	^a	^a
Urea	1.61	1	0.5
Imidazolidone	0	0	0

^a Identified but not determined.

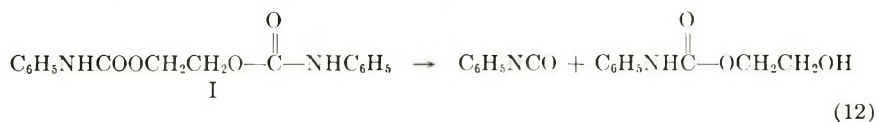
Table I showed also that degradation of EBPC for a short period gave an appreciable amount of SDPU and no imidazolidone. For longer periods the amount of SDPU decreased when VIII was obtained. SDPU seems to be an intermediate in the formation of VIII, as it was found experimentally that *N,N'*-diphenylethylenediamine reacted with SDPU to give a 15% yield of VIII.

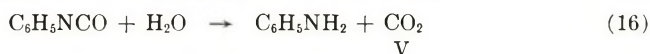
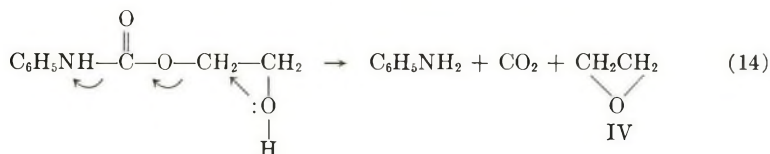
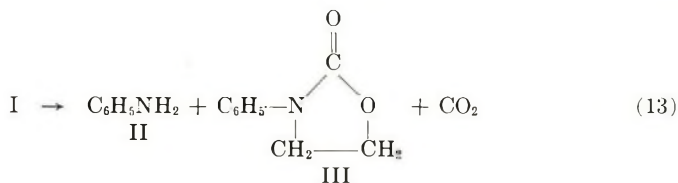
Ratio of CO₂ to Oxazolidone in the Degradation of EBPC

The amount of carbon dioxide found experimentally was the sum of the carbon dioxide liberated during the formation of the oxazolidone, the diamine, aniline, and ethylene oxide. By subtraction of the quantity of CO₂ corresponding to the formation of the diamine, the amount evolved initially, was obtained. The oxazolidone initially formed was equal to the amount found experimentally plus the amount corresponding to the diamine and the imidazolidone found experimentally. This ratio was found to be 1.58, 1.35, and 1.44, respectively in experiments 4, 5, and 6 in Table I.

Mechanism of Degradation of EBPC

From this study the final mechanism of degradation of EBPC was proposed to follow eqs. (12)–(19).





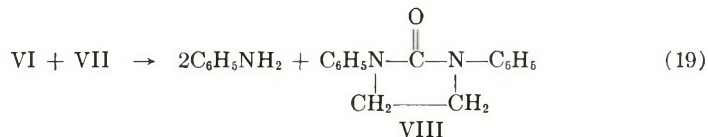
V



VI



VII



EXPERIMENTAL

Preparation of Compounds

Ethylene bis (*N*-phenylcarbamate). Ethylene glycol (Matheson, Coleman and Bell, b.p. 195–197°) was shown to contain no free chloride,²⁰ no propylene glycol.²¹ On distillation under reduced pressure (67°C./6–7 mm.) it gave a single peak on gas chromatography.²²

Phenyl isocyanate (Matheson, Coleman and Bell, b.p. 60–62°C./20 mm.) was purified by distillation in vacuo at 53°C. and 15 mm.; the heart cut was used.

EBPC was obtained by the reaction of ethylene glycol with equimolar quantity of phenyl isocyanate in dry, reagent grade ethyl acetate as solvent. The urethane was dissolved in chloroform and ethanol and recrystallized by addition of ether (yield 90%). It melted at 156–157°C. then resolidified and melted finally at 168–170°C. (lit. mp.: 157°C.²³). The NMR spectrum of the compound dissolved in acetone run on a A60 Varian NMR spectrometer, showed peaks at 4.4, 7.1–7.7, and 8.8 ppm, corresponding respectively to the methylene, aromatic, and carbamate H; the ratios of the peaks were 4, 10, 2. The infrared spectrum was typical of a urethane with a

NH stretching band at 3μ , a C=O stretching band at 5.9μ , and a C=O deformation band at 8.1 – 8.2μ . The use of dry benzene as solvent gave a 90–95% yield of dicarbamate.

ANAL. Calculated for $C_{16}H_{16}N_2O_4$: C, 64.00%; H, 5.33%; N, 9.33%. Found: C, 64.05%; H, 5.56%; N, 9.32%.

β -Hydroxyethyl-*N*-Phenylcarbamate. A solution of phenyl isocyanate (0.12 mole, 15 g.) in 30 cc. of ethyl acetate (or benzene) was added dropwise at reflux to a solution of ethylene glycol (1 mole, 62 g.) dissolved in 60 cc. ethyl acetate (or benzene) and refluxed for 8 hr. Dilution and slow addition were necessary to minimize the formation of the dicarbamate.

After evaporation of solvent and distillation of the excess of ethylene glycol (80°C ., 7–9 mm. Hg) the monocarbamate was obtained as a very viscous liquid which solidified partially on standing. The monocarbamate containing about 3% of EBPC failed to recrystallize in chloroform, *n*-pentane, ether, petroleum ether, alcohol–water. Infrared spectrum of the compound showed carbamate bands at 5.9 and 8.1μ .

The monocarbamate reacted with phenyl isocyanate and *p*-tolyl isocyanate and gave respectively EBPC (yield 87%) and ethylene-(*N*-phenyl-*N'*-*p*-tolyl) dicarbamate (yield 86%, m.p. 134 – 136°C .).

ANAL. Calculated for ethylene-(*N*-phenyl-*N'*-*p*-tolyl) dicarbonate, $C_{17}H_{18}N_2O_4$: C, 64.96%; H, 5.73%; N, 8.91%. Found: C, 65.18%; H, 5.88%; N, 8.68%.

***N*-(β -Hydroxyethyl)-*N,N'*-Diphenylurea.** A slight excess of 2-anilinoethanol (0.11 mole, 15.07 g.) was allowed to react in benzene with phenyl isocyanate (0.1 mole, 11.9 g.) for 4 hr. The carbamate was recrystallized from ether, petroleum ether, m.p. 82 – 83°C ., yield 93%. The infrared spectrum showed a large band at 2.9 – 3μ and an urea band at 6.1μ ; no urethane band was present. The product gave a positive ceric nitrate test and on reaction with 1 equiv. of phenyl isocyanate gave quantitatively *N*-(β -ethylcarbanilate)-*N,N'*-diphenylurea, melting at 136°C . (lit. m.p.: 136 – 137°C .)²⁴ This compound was identical to the product obtained by reacting 2 equiv. of isocyanate with 1 equiv. of 2-anilinoethanol. The infrared spectrum showed a carbamate band at 5.85μ .

3-Phenyl-2-Oxazolidone. This compound was obtained by the reaction of 2-anilinoethanol with diethylcarbonate in the presence of sodium methoxide according to the procedure of Caldwell;²⁵ the yield was 80%; m.p. 120 – 121°C ., (lit. m.p.: 121°C .)²⁵.

1,3-Diphenyl-2-Imidazolidone. The compound was obtained by the reaction of phosgene on *N,N'*-diphenylethylenediamine.^{26–28} When phosgene was bubbled slowly into a cold solution of the diamine in benzene, the dicarbamoyl chloride was obtained with a yield of 80%. It melted at 180°C . (lit. m.p.: 183°C .)²⁷ and gave 1,3-diphenyl-2-imidazolidone upon heating at 228 – 230°C . for 2 hr. Sublimation of the crude product gave the imidazolidone melting at 210°C . (lit. m.p.: 209°C .). The substance was obtained with a 15% yield (based on the dicarbamoyl chloride) and did not show any depression of the mixed melting point.

Thermal Degradation of Urethanes

Apparatus. The degradation of EBPC and related compounds was carried out in a 100-cc. three-necked flask. A slow current of dry and CO₂-free nitrogen was obtained by passing nitrogen through a washing bottle of concentrated sulfuric acid, a tower of calcium chloride, a tower of Ascarite, and a tower of molecular sieves. The nitrogen swept at a rate 20–22 cc./minute the whole apparatus including the reaction flask, a receiver surrounded by Dry Ice in acetone, connected to the reaction flask by an adapter, a trap cooled by Dry Ice in acetone, a U-tube filled with CaCl₂ connected to a three-way stopcock, each of the other two ends of which carried an Ascarite tube. The regular passage of the carrier gas was controlled by a bubble counter. By turning the stopcock in a suitable direction, it was possible to measure without any loss the amount of CO₂ evolved as a function of time.

Detection of Ethylene Oxide. The gas mixture from the reaction flask passed through a CaCl₂ tube, an Ascarite tube, another CaCl₂ tube before bubbling into a tube containing 4–5 cc. of an aqueous solution of 40% KSCN and 2 drops of 0.1% phenolphthalein. As ethylene oxide evolved a red-pink color was observed; a blank remained colorless during the pyrolysis. Ethylene oxide was also identified by its infrared spectrum when the gas was collected in a gas cell.

Isolation of the Products. After pyrolysis, the residue was dissolved in a small amount of cold dry ether and filtered. Dry HCl was bubbled into the ether solution, the amine hydrochlorides precipitated. Dissolution of the amine hydrochlorides in water followed by neutralization with 3*N* NaOH liberated the amines. *N,N'*-Diphenylethylenediamine was filtered, dried, and recrystallized from ether, petroleum ether (m.p. 61–63°C.; mixed m.p. with a sample from Eastman Kodak, 61°C.).

Aniline was obtained by difference after making sure that it was only aniline by extraction of the aqueous solution with ether and reprecipitation of the aniline hydrochloride, m.p. 192–195°C. (mixed m.p.: 194°C.; lit. m.p.: 194–195°C.). The oxazolidone was separated from the solid residue by extraction with a mixture of ether and chloroform (ratio 4:1). After recrystallization in ether-*n*-pentane, it melted at 118–119°C. (mixed m.p. 119–120°C., lit. m.p.: 121°C.). The imidazolidone was recrystallized from alcohol, m.p. 207–214°C. (mixed m.p.: 209–210°C.). If the imidazolidone and SDPU were present, the first one was separated from the latter by partial extraction with a mixture of equal volume of ether and CHCl₃. In some experiments the amines were titrated by perchloric acid in glacial acetic acid²⁹ in presence of crystal violet as indicator. The change of color was checked first by potentiometric titration.

ANAL. (a) 3-phenyl-2-oxazolidone from degradation: Calculated for C₉H₉NO₂: C, 66.24%; H, 5.52%; N, 8.58%. Found: C, 66.71%; H, 5.73%; N, 8.57%.

(b) 1,3-diphenyl-2-imidazolidone from degradation: Calculated for C₁₅H₁₄N₂O: C, 75.63%; H, 5.88%; N, 6.73%. Found: C, 75.56%; H, 5.64%; N, 7.03%.

Degradation of EBPC in the Presence of DABCO. DABCO was mixed with the urethane before being added rapidly to the reaction flask, heated previously at 181–182°C. When the temperature reached 170°C., bubbles were seen in the flask, and CO₂ started to evolve. The origin of time was taken when the temperature was 175°C., at which temperature the reaction was quite vigorous. It took 2 min. to reach 181–182°C. The amount of CO₂ evolved was measured every 5 or 10 min.

The isolation of products was carried out as previously described. Aniline was isolated by its hydrochloride or by its titration with perchloric acid in glacial acetic acid.

Reaction of 3-Phenyl-2-oxazolidone with Aniline

Oxazolidone (18.4 mmole, 3 g.) and 3 cc. aniline were heated at 210°C. for 8 hr. with an oil bath. The amine mixture was extracted from the unreacted oxazolidone with cold ether. The diamine was separated from aniline as previously described. The impure diamine melting at 57–59°C. was obtained with a 58% yield.

Reaction of SDPU with *N,N'*-Diphenylethylenediamine

N,N'-Diphenylethylenediamine (2 g.) was allowed to react with 1 g. of SDPU at 205–210°C. in a 100-cc. three-necked flask completely immersed in an oil bath for 6 hr. The reaction would not occur if all the urea sublimed at the top of the flask. The reaction flask was cooled, then ether was added, the imidazolidone crystallized in lightly rose plates. The amount of imidazolidone isolated was 190–120 mg. (10–18% yield); it melted at 208–212°C.

The authors are indebted to the National Lead Company for the grant provided during this research.

References

1. Dyer, E., and G. E. Newborn, Jr., *J. Am. Chem. Soc.*, **80**, 5495 (1958).
2. Dyer, E., and G. C. Wright, *J. Am. Chem. Soc.*, **81**, 2138 (1959).
3. Dyer, E., and D. W. Osborne, *J. Polymer Sci.*, **47**, 349 (1960).
4. Read, R. E., Ph.D. Dissertation, University of Delaware, June 1960.
5. Metayer, M., *Bull. Soc. Chim. France*, **1951**, 802.
6. Schweitzer, C. E. (E. I. du Pont de Nemours & Company), U. S. Pat. 2,409,712, October 22, 1946.
7. McKay, A. F., and G. R. Vasavour, *Can. J. Chem.*, **31**, 688 (1953).
8. Siefken, W., *Ann.*, **562**, 75 (1949).
9. Illari, G., I. Marengi, and T. Tarantelli, *Ann. Chim. (Rome)*, **43**, 55 (1953).
10. Laakso, T. M., and D. D. Reynolds, *J. Am. Chem. Soc.*, **79**, 5717 (1957).
11. Deckert, W., *Angew. Chem.*, **45**, 758 (1932).
12. Gulbins, K., and K. Hamann, *Ber.*, **94**, 3287 (1961).
13. Scott, H., Ph.D. Dissertation, University of Delaware, June 1955.
14. Brown, H. C., and M. Borkowski, *J. Am. Chem. Soc.*, **74**, 1894 (1952).
15. Brown, H. C., R. S. Fletcher, and R. B. Johannesen, *J. Am. Chem. Soc.*, **73**, 212 (1951).
16. Brown, H. C., J. M. Brewster, and H. Schechter, *J. Am. Chem. Soc.*, **76**, 467 (1954).

17. Gabriel, S., and G. Eschenbach, *Ber.*, **30**, 2494 (1897).
18. Najer, H., P. Chabrier, R. Guidicelli, J. Menin, and J. Duchemin, *Bull. Soc. Chim. France*, **1959**, 1841.
19. Najer, H., P. Chabrier, and R. Giudicelli, *Bull. Soc. Chim. France*, **1957**, 1069.
20. Hanna, J. G., and J. Jura, *Anal. Chem.*, **31**, 1820 (1959).
21. Jones, L. R., and J. A. Riddick, *Anal. Chem.*, **29**, 1214 (1957).
22. Ginsburg, L., *Anal. Chem.*, **31**, 1822 (1959).
23. Snape, H. L., *Ber.*, **18**, 2428 (1885).
24. Dains, F. B., R. Q. Brewster, and J. J. Blair, *J. Am. Chem. Soc.*, **44**, 2640 (1922).
25. Caldwell, J. R., U. S. Pat. 2,656,328, October 20, 1953.
26. Michler, W., and E. Keller, *Ber.*, **14**, 2183 (1881).
27. Hanssen, A., *Ber.*, **20**, 784 (1887).
28. Lob, G., *Rec. Trav. Chim.*, **55**, 866 (1936).
29. Seaman, W., and E. Allen, *Anal. Chem.*, **23**, 592 (1951).

Résumé

On a étudié la pyrolyse du bis(*N*-phénylcarbamate) d'éthylène comme modèle le plus simple de polyuréthane. La dégradation se fait par un double processus de décomposition qui résulte en la formation simultanée du 3-phényl-2-oxazolidone, d'anhydride carbonique, d'aniline et d'une dissociation partielle en monocarbamate et en isocyanate de phényle. La réaction ultérieure produit de l'oxyde d'éthylène, de la *N,N'*-diphényl-éthylènediamine, de la *N,N'*-diphényle-2-imidazolidone et de la *N,N'*-diphénylurée.

Zusammenfassung

Die Pyrolyse von Äthylenbis-(*N*-phenylcarbamate) als des einfachsten Modells eines Polyurethans wurde untersucht. Der Abbau erfolgt über einen doppelten Zersetzungsprozess unter gleichzeitiger Bildung von 3-Phenyl-2-oxazolidon, Kohlendioxyd, Anilin und einer partiellen Dissoziation in Monocarbamat und Phenylisocyanat. Die weitere Reaktion führt Äthylenoxyd, *N,N'*-Diphenyläthylendiamin, *N,N'*-Diphenyl-2-imidazolidon und *N,N'*-Diphenylharnstoff.

Received May 1, 1963

Revised February 10, 1964

Degradation of Polycarbonates.

IV. Effect of Molecular Weight on Flexural Properties

J. H. GOLDEN, B. L. HAMMANT, and E. A. HAZELL, *Explosives Research and Development Establishment, Ministry of Aviation, Waltham Abbey, Essex, England*

Synopsis

The effect of radiation dose and molecular weight on the tensile and flexural properties of polycarbonate, poly-[2,2-propane bis(4-phenyl carbonate)], have been examined in detail. Tensile strength, flexural strength, and flexural modulus can be expressed as linear functions of radiation dose and are almost completely independent of molecular weight when the material is ductile. The strength of the brittle material (molecular weights less than 13,000) is however shown to be a linear function of reciprocal molecular weight. The effect of molecular weight on flexural modulus is also discussed. The presence of the equilibrium water content in the plastic has been shown to cause a four-fold increase in the rate of chain scission and an explanation of this effect is advanced.

INTRODUCTION

Our previous work¹ has shown that irradiation provides a convenient method for the production of a range of polycarbonate specimens of different molecular weight initially prepared under identical conditions. As little information is available on the effect of molecular weight on the flexural properties of plastics we have examined a range of irradiated specimens of polycarbonate in flexure to determine the behavior of this polymer with changing molecular weight in both the ductile and brittle regions.

EXPERIMENTAL

Preparation of Specimens

Makrolon Grade S (Farbenfabriken Bayer), poly-[2,2-propane bis(4-phenyl carbonate)] was employed throughout. Bars ($4 \times 0.5 \times 0.125$ in.) were machined from extruded sheet and allowed to attain equilibrium moisture content (0.23% at $20 \pm 1^\circ\text{C}$. /70% R.H.) before irradiation.

Irradiation

The bars were irradiated in vacuum (10^{-3} mm.) with external water cooling, using the equipment previously described.¹ A linear accelerator electron beam (4 m.e.v.) was employed at a dose rate of 1 Mrad/min.

Test Methods

Specimens were tested after a period of not less than two weeks ($20 \pm 1^\circ\text{C.}/70\%$ R.H.) after irradiation.

Viscosity Measurements. The intrinsic viscosity of the polycarbonate bars was determined in methylene chloride solution in a modified dilution viscometer.² Molecular weights (\bar{M}_v) were calculated from the relationship $[\eta] = 1.23 \times 10^{-5} M^{0.83}$ derived by Schnell.³

Tensile Measurements. Tensile strength σ_T was measured on a Hounsfield Tensometer at a crosshead speed of 0.1 in./min.

Flexural Measurements. Flexural properties were measured in general accordance with A.S.T.M. Designation D790-58T, Procedure B, except that the samples were conditioned and tested at $20 \pm 1^\circ\text{C.}/70 \pm 2\%$ R.H. at a crosshead speed of 0.5 in./min.

Flexural modulus μ_F was calculated from the autographic load-deflection curve. The maximum yield strength, or brittle strength in the absence of yield, and the outer fiber strain at which this stress obtained were also calculated.

RESULTS

All the experimental results are shown graphically in Figures 1-5. All points indicated in Figures 2-5 represent the mean of four determinations and scatter limits have been added. Assuming a linear relationship of the form $y = mR + c$ between various properties (y) and radiation dose (R),

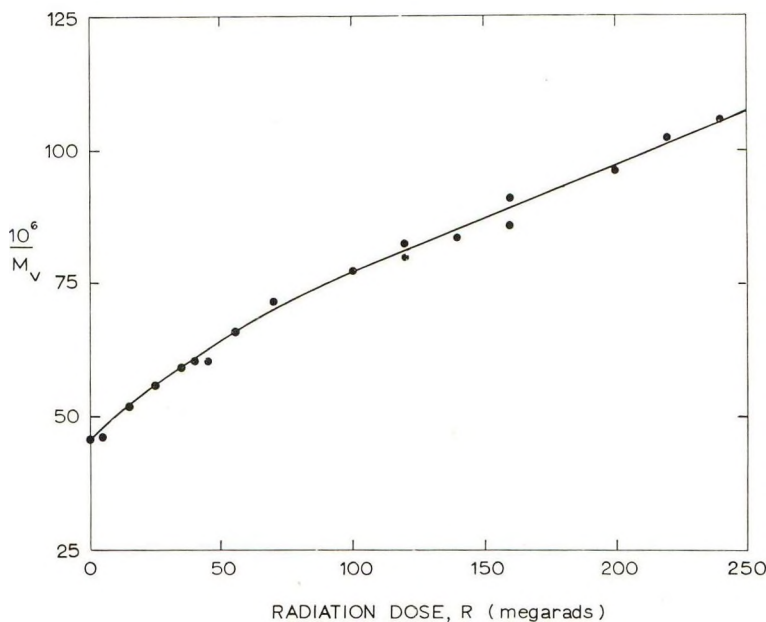


Fig. 1. Effect of radiation dose R on reciprocal viscometric-average molecular weight of polycarbonate bars.

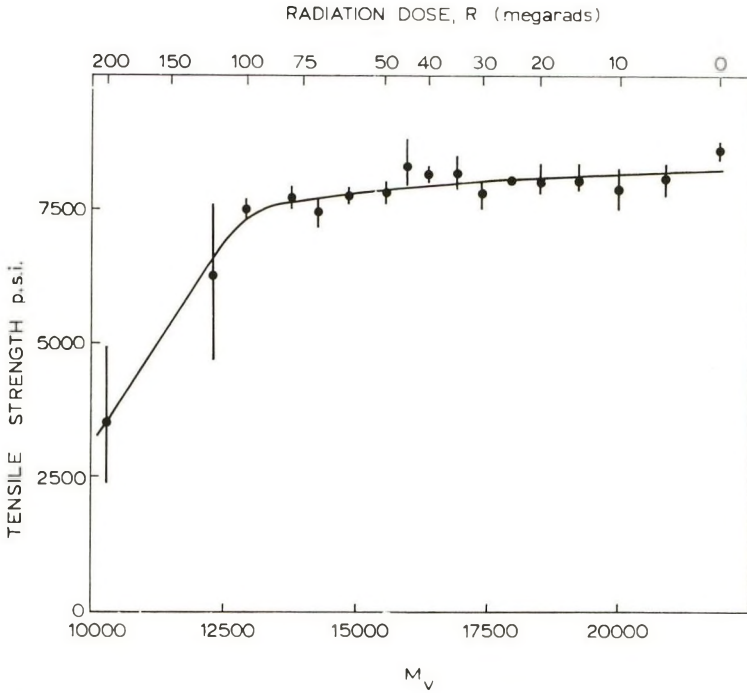


Fig. 2. Tensile strength vs. viscometric-average molecular weight for polycarbonate bars.

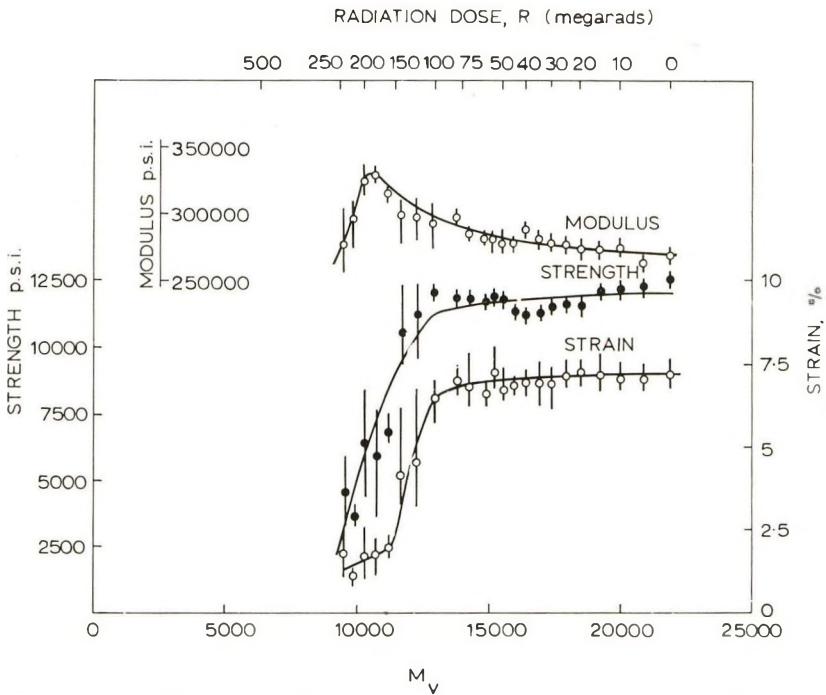


Fig. 3. Flexural properties vs. viscometric-average molecular weight for polycarbonate bars.

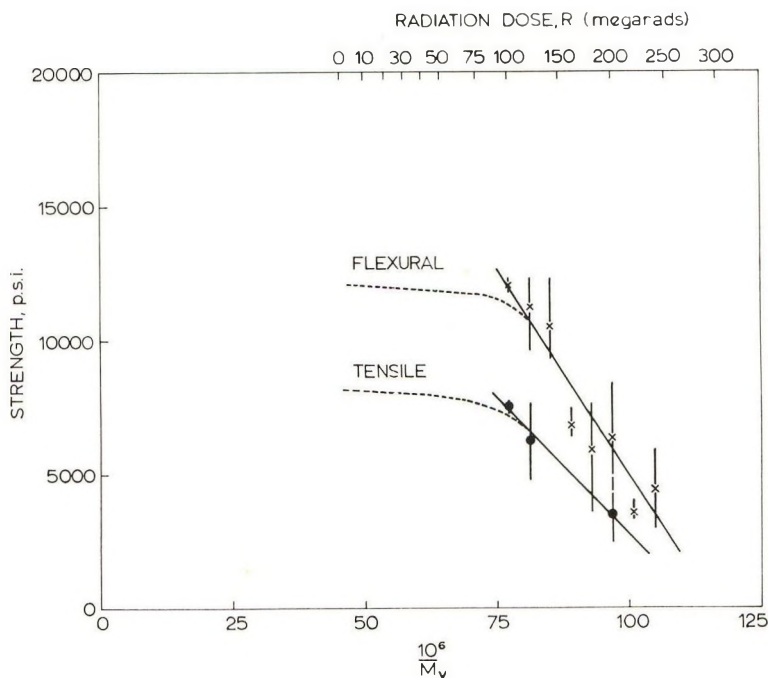


Fig. 4. Tensile and flexural strength vs. reciprocal viscometric-average molecular weight: (---) region of ductile failures; (—) region of brittle failures.

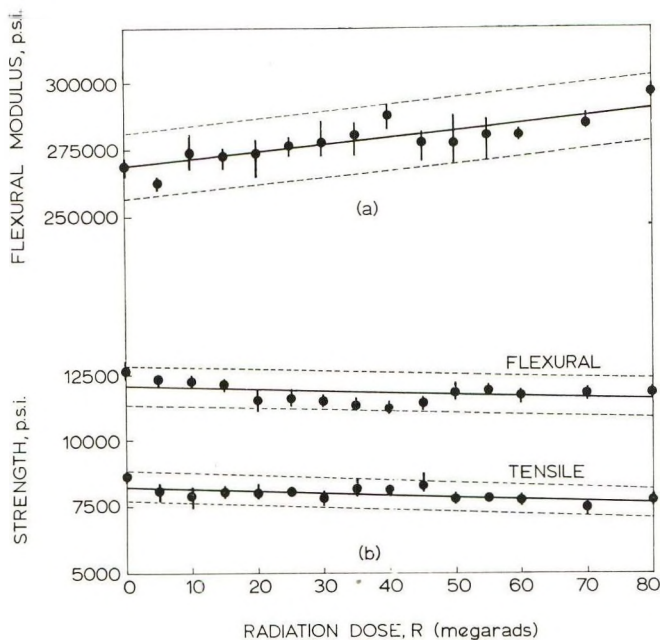


Fig. 5. Relationship between radiation dose R and (a) modulus and (b) strength (flexural and tensile).

TABLE I
Statistical Data for Measured Properties and Radiation Dose
for a Linear Relationship $y = mR + c$

Property (y)	Range of radiation dose R , Mrad	De- grees of free- dom	Constants		Variance ratio	Signifi- cance level	95% Confi- dence limits, psi
			m	c			
1 Tensile yield (σ_T)	0-80	59	-7.8	8250	25.8	0.001	± 530
2 Flexural yield (σ_F)	0-80	64	-6.8	12050	11.25	$\ll 0.01$	± 740
3 Flexural modulus (μ_F)	0-80	62	270	269000	62.4	0.001	± 12200
4 Flexural yield (σ_F)	100-240	42	-61	18130	18.2	0.001	—
5 $10^6 \times \bar{M}_v^{-1}$	70-240	12	0.197	57.8	526	0.001	—

where m and c are constants, a statistical analysis of some of the results has been made. Regression data (property on to radiation dose), variance ratios, significance levels, and 95% confidence limits are shown in Table I.

By elimination of R (radiation dose) from the regressions in rows 4 and 5 of Table I a relationship between flexural yield strength σ_F and molecular weight \bar{M}_v , eq. (2) (below) was obtained.

DISCUSSION

Effect of Water on Changes in Molecular Weight

When irradiated, polycarbonate undergoes chain scission without crosslinking and therefore the molecular weight changes of specimens can be determined by viscometry. The present results are shown in Figure 1 as reciprocal viscosity-average molecular weight \bar{M}_v^{-1} versus radiation dose R . As found previously¹ the initial molecular weight distribution is not random but rapidly becomes so (at a dose of approximately 75 Mrad); thereafter the present results can be expressed by

$$10^6/\bar{M}_v = 0.197R + 57.8 \quad (1)$$

From this equation it follows that the total energy absorbed per chain scission, E , is 274 e.v., and the corresponding G value (number of scissions per 100 e.v. of energy absorbed) is 0.36. This value is considerably different from that ($G = 0.09$) previously¹ obtained for specimens irradiated in vacuum. However, the additional results given in Table II prove that this discrepancy is due to the presence of the equilibrium water content in the present specimens as these were unconditioned whereas those previously examined were rigorously predried. This conclusion is also borne out by

TABLE II
 Molecular Weight of Polycarbonate Specimens

Form	Molecular weight		
	Unirradiated	Irradiated ^a	
		Predried (10 ⁻⁶ mm.)	Not predried
Bars	21,900	15,150	11,200 ^b
Granules	22,000	15,500	11,300 ^c

^a Irradiated in vacuum, total dose 200 Mrad.

^b 0.24% moisture.

^c 0.23% moisture.

the G value (0.34) calculated from viscosity results previously reported¹ for unconditioned specimens.

The marked effect of water can readily be explained on the basis of the mechanism⁴ previously advanced for the radiation-induced degradation of polycarbonates, since water would react with free radicals produced on scission of a carbonate linkage and thus prevent the cage recombination which appears to exert a great protective influence on the polymer. The deleterious effect of water, present only to the extent of approximately three molecules per polymer chain is noteworthy.

Influence of Molecular Weight on Mechanical Properties

The tensile yield strength results obtained in the present study are shown versus molecular weight \bar{M}_v in Figure 2. Similarly the flexural results (yield strength, strain, and modulus) are presented in Figure 3. Corresponding scales of radiation dose have been included in both figures for reference. The similar form of the tensile and flexural yield strength curves (Figs. 2 and 3) indicates a closely related dependence of the two properties on molecular weight. This observation is of considerable value as the behavior of highly irradiated (brittle) material can be more reliably assessed in flexure than in tension, since problems associated with the gripping and loading of specimens can be overcome more easily and hence the modulus can be determined more precisely. For polymers of molecular weight greater than 15,000 the yield strength is essentially constant although below this value the strength decreases rapidly and, at about 8000, appears to become negligible.

As shown in Figure 4 the flexural strength σ_F in the region of brittle failure (i.e., up to a molecular weight of approximately 13,000 at the rate of strain employed) is dependent on reciprocal molecular weight according to the equation

$$\sigma_F = -(309 \times 10^6 / \bar{M}_v) + 36,000 \quad (2)$$

to a high level of significance.

Although fewer tensile strength results are available, Figure 4 suggests that these obey a similar linear relationship. This finding supports the work of Flory,⁵ who has shown that the tensile strength σ_T of cellulose acetate can be expressed by:

$$\sigma_T = a_0 + (a_1/M) \quad (3)$$

where a_0 and a_1 are constants.

The dependence of tensile strength on reciprocal molecular weight has also been observed for other polymers,⁶ at least in the region of brittle failures. It is clear from Figure 4 that in the present case the linear relationships obtained are valid only in this region since in the ductile region the strength appears to be almost completely independent of molecular weight. The results suggest that the ductile strength of a polymer can be almost entirely attributed to interchain cohesive forces. With reduction in the molecular weight and consequent increase in the number of endgroups the material becomes brittle and the strength is rapidly reduced.

We have examined the ductile region in some detail, as we have noted⁷ that in other materials irradiation causes an initial increase in strength before the onset of brittle behavior and the accompanying rapid loss of strength which occurs at high radiation doses. However, in this region we find that tensile yield strength σ_T , flexural yield strength σ_F , and flexural modulus μ_F results (Figure 5) are all linearly dependent on radiation dose according to eqs. (4)–(6):

$$\sigma_T = -7.8R + 8,250 \quad (4)$$

$$\sigma_F = -6.8R + 12,050 \quad (5)$$

$$\mu_F = 270R + 269,000 \quad (6)$$

where σ_T , σ_F , and μ_F are in psi and R is in Mrad (see Results).

The results in Figure 3 show that the modulus is comparatively independent of molecular weight over the complete range studied; the slight maximum which occurs between molecular weights of 9,000 and 13,000 may be associated with the transition from ductile to brittle behavior. Thus, over a wide range of the molecular weight, modulus appears to be dependent solely on the stiffness of the polymer chain and independent of chain length, a conclusion supported by results for other materials, e.g., polyethylene,⁸ polypropylene,⁹ and polystyrene.¹⁰

If we consider the flexural yield strength and modulus results it is possible to predict that the strain will follow a pattern of behavior similar to that of the strength. This conclusion was substantiated by calculation of the maximum strain in the outer fiber from flexural data, and the results are presented in Figure 3. This use of flexural measurements permits a reliable measure of strain to be obtained over the range of brittle failures where accurate measurement of tensile strain is difficult. Thus we conclude that flexural measurements provide a reliable means for following the changes in mechanical properties (yield strength, strain, and modulus)

accompanying the degradation of a material, particularly where a transition from ductile to brittle behavior occurs.

The authors thank Messrs. J. McCann and F. Hazell (Technological Irradiation Group, Wantage) for assistance in the irradiation of samples.

References

1. Golden, J. H., and E. A. Hazell, *J. Polymer Sci.*, **A1**, 1671 (1963).
2. Harding, G. W., *J. Polymer Sci.*, **55**, S27 (1961).
3. Schnell, H., *Angew. Chem.*, **68**, 633 (1956).
4. Golden, J. H., *Makromol. Chem.*, **66**, 73 (1963).
5. Flory, P. J., *J. Am. Chem. Soc.*, **67**, 2048 (1945).
6. Vincent, P. I., *Plastics (London)*, **27**, 105 (August 1962).
7. Golden, J. H., and E. A. Hazell, *J. Polymer Sci.*, **A2**, 4017 (1964).
8. Tung, L. H., *S.P.E. Journal*, **14**, 25 (July 1958).
9. Shearer, N. H., J. E. Guillet, and H. W. Coover, *S.P.E. Journal*, **17**, 83 (January 1961).
10. Maigeldinov, I. A., A. V. Grigoreva, and K. I. Tsyur, *Soviet Plastics*, **3**, 8 (1961).

Résumé

On a examiné en détails l'effet des radiations sur les propriétés mécaniques en tension et en flexion du polycarbonate, poly[2-2-propane bis-phénol-4-(phényl carbonate)] en faisant varier le poids moléculaire. La force de rupture en tension et en flexion, et le module de flexion peuvent être exprimés comme des fonctions linéaires de la dose de radiation et sont à peu près insensibles au poids moléculaire tant le matériel reste ductile. La force de rupture du matériel cassant (poids moléculaire inférieur à 13.000) se présente cependant comme une fonction de l'inverse du poids moléculaire. On discute également de l'effet du poids moléculaire sur le module de flexion. Par suite de la présence d'une certaine quantité d'eau en équilibre avec le polymère, il se produit une augmentation quadruple de la vitesse de scission de chaîne. On propose une explication de cet effet.

Zusammenfassung

Der Einfluss von Strahlungs-dosis und Molekulargewicht auf die Zug- und Biegeeigenschaften des Polycarbonates Poly[-2,2-propan-bis-(4-phenylkarbonat)] wurde im einzelnen untersucht. Zugfestigkeit, Biegefestigkeit und Biegemodul können als lineare Funktion der Strahlungs-dosis ausgedrückt werden und sind bei duktilem Material vom Molekulargewicht fast völlig unabhängig. Die Festigkeit des spröden Materials (Molekulargewicht kleiner als 13000) erweist sich aber als lineare Funktion des reziproken Molekulargewichts. Weiters wird der Einfluss des Molekulargewichts auf den Biegemodul diskutiert. Der Gleichgewichtswassergehalt in der plastischen Masse verursacht eine Zunahme der Kettenspaltungsgeschwindigkeit auf das vierfache; eine Erklärung für diesen Effekt wird vorgeschlagen.

Received February 3, 1964

Polybenzimidazoles. I. Reaction Mechanism and Kinetics*

WOLFGANG WRASIDLO and HAROLD H. LEVINE, *Narmco Research & Development, Division of Telecomputing Corporation, San Diego, California*

Synopsis

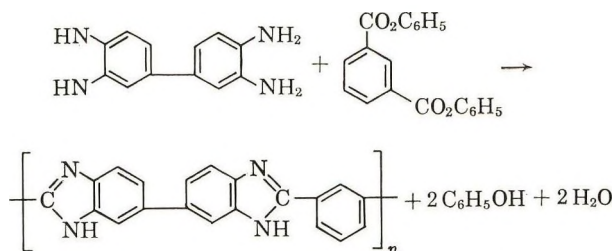
Poly-2,2'-(*m*-phenylene)-5,5'-bibenzimidazole forms, via two or three intermediates, when 3,3'-diaminobenzidine and diphenyl isophthalate are condensed. Kinetic data indicate rapid consumption of 3,3'-diaminobenzidine to form an aldol type intermediate which evolves water to form a Schiff base which in turn evolves phenol to form the final polymer. Phenol evolution is the rate-determining step. The postulated Schiff base can possess stereoisomerism. Intramolecular hydrogen bonding which can occur in the *syn*-isomer offers an explanation why the condensation affords a linear polymer. The combined effects of intramolecular hydrogen bonding and added resonance stabilization in the Schiff base are possible reasons why phenol evolution is the rate-determining step and why the condensation requires high reaction temperatures.

INTRODUCTION

Completely aromatic polybenzimidazoles (PBI) are a new family of thermally stable, high molecular weight polymers. Brinker and Robinson¹ disclosed the synthesis of aliphatic PBI, and two years later, Vogel and Marvel² published their findings on wholly aromatic PBI structures; increased stability resulted from this structural modification.

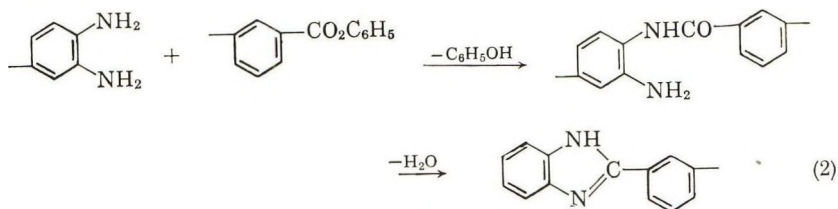
As part of a new program,³ the synthesis of low molecular weight PBI was studied. Modifications in the original synthesis² resulted in some apparently anomalous behavior. This mechanism and kinetic study was undertaken to gain further insight into the condensation.

The overall reaction can be represented by eq. (1):

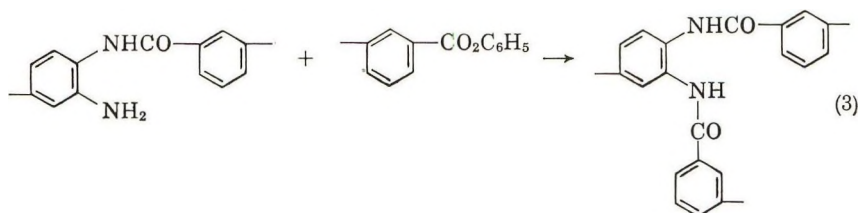


* Paper presented at the 145th Meeting of the American Chemical Society, New York, N. Y., September 1963.

It was originally believed that the first reaction was amidolysis of the phenyl ester to give an aminoamide which then closed the ring by means of dehydration.



Attempts to synthesize ester terminated polymers resulted in evolution of volatiles that exceeded theory. A reasonable explanation seemed to be that the polyaminoamide could condense with unreacted phenyl ester to evolve more phenol instead of cyclizing with liberation of water. Such a reaction would lead to a polymer containing polyamide linkages in place of the more thermally and hydrolytically stable benzimidazole structures. This postulate was based upon the belief that amidolysis was more rapid than dehydration.



This paper describes the reaction mechanism and kinetic study that resulted from the above considerations.

EXPERIMENTAL

A. Synthesis of Model Compounds

1. *N*-Benzoyl-*o*-nitroaniline. A 500-ml., three-necked flask was equipped with a sealed stirrer, dropping funnel, and reflux condenser. A solution of 27.6 g. (0.2 mole) of *o*-nitroaniline was made in the flask by using 300 ml. dry benzene and 100 ml. freshly distilled pyridine. Benzoyl chloride, 28.0 g. (0.2 mole), was added dropwise during 1 hr., with stirring, at room temperature. A slight exotherm was noted as the solution became cloudy. After an additional hour of stirring, an addition of 50 ml. of water caused the turbidity to disappear. The organic layer was separated in separatory funnel and evaporated to dryness by aspiration and heating with a warm water bath. The yellow residue was dissolved in petroleum ether, washed twice with 30 ml. portions of water, and crystallized twice from petroleum ether to give a 41.0 g. (85%) yield of product, m.p. 92.5–93.0°C.; λ_{\max} 248 μ , $\log \epsilon_{\max} = 4.057$ (methanol). An infrared spectrum showed no $-\text{NH}_2$ peak at 2.86–3.03 μ but carbonyl absorption at 5.95 μ .

2. *N*-Benzoyl-*o*-phenylenediamine. A 1-liter, three-necked flask was charged with 20 g. (0.0825 mole) *N*-benzoyl-*o*-nitroaniline and 250 ml. each of ethanol and water. A solution of 60 g. of sodium sulfide in 250 ml. of water was added, during 10 min., with stirring. The resultant reddish solution was refluxed for 1 hr., and on cooling and standing overnight deposited light yellow crystals. After removing the precipitate, the filtrate was concentrated to half its original volume to afford more product. The crude yield was 15.5 g. (88.5%). Recrystallization from ethanol-water gave white crystals, m.p. 153.2–153.6°C., λ_{\max} 296 m μ , $\log \epsilon_{\max} = 3.405$ (methanol). An infrared spectrum showed the —NH₂ doublet at 3.0 μ and carbonyl peak at 6.1 μ .

ANAL. Calculated for C₁₃H₁₂ON₂: C, 74.0%; H, 5.70%; N, 13.21%. Found: C, 73.85%; H, 6.23%; N, 13.54%.

3. *N,N'*-Dibenzoyl-*o*-phenylenediamine. A solution of 10.8 g. (0.1 mole) of *o*-phenylenediamine was prepared in 400 ml. of *N*-methylpyrrolidone and put in a 1-liter flask. A solution of 31.0 g. (0.2 mole) of benzoyl chloride in 100 ml. of *N*-methylpyrrolidone was added dropwise during 1 hr. with stirring. The resulting pink precipitate was collected on a funnel, washed several times with methanol and recrystallized from hot *N*-methylpyrrolidone to give white needles, m.p. 319–320°C.; $\lambda_{\max} = 257$ m μ , $\log \epsilon_{\max} = 4.210$ (methanol). An infrared spectrum failed to show an —NH₂ absorption, indicating that the desired *N,N'*-dibenzoyl derivative was obtained instead of the *N*-benzoyl derivative. This was further substantiated by the fact that the product could not be acetylated with acetic anhydride in pyridine.

4. *N,N'*-Bis(2-nitrophenyl)isophthalamide. A solution of 40.6 g. (0.2 mole) of isophthaloyl chloride in 300 ml. dry benzene was added slowly, with stirring, to 55.2 g. (0.4 mole) of *o*-nitroaniline dissolved in 100 ml. of dry pyridine. The reaction was slightly exothermic, and a fine yellow precipitate formed in a short time. After the addition was completed, the mixture was left overnight, filtered, washed with pyridine, water, pyridine, and ether; yield 76 g. (93.7%), m.p. 214–219°C. Recrystallization from 3:1 acetonitrile:pyridine gave yellow crystals, m.p. 221–223°C. The expected compound was supported by infrared spectral evidence: $\lambda_{\max} = 360$ m μ , $\log \epsilon_{\max} = 4.636$ and $\lambda_{\max} = 256$ m μ , $\log \epsilon_{\max} = 5.108$ (dioxane). In a similar manner, terephthaloyl chloride gave an 86.3% yield of *N,N'*-bis(2-nitrophenyl)-terephthalamide, m.p. 276–279°C.; $\lambda_{\max} = 260$ m μ , $\log \epsilon_{\max} = 4.688$; $\lambda_{\max} = 276$ m μ , $\log \epsilon_{\max} = 5.094$.

5. *N,N'*-Bis(2-aminophenyl)isophthalamide. To a refluxing solution of 3.0 g. (19.7 moles) of the dinitro compound in 100 ml. of dioxane was added to a solution of 14.8 g. (61.5 moles) of sodium sulfide nonahydrate in 50 ml. of water slowly with stirring. The reaction mixture was refluxed for an extra hour and left overnight. The solvents were removed under aspiration and the yellow-brown residue recrystallized three times from 3:1 ethanol:

water to give white crystals, m.p. 239–241°C., both preheated to 230°C. before immersion of m.p. tube. $\lambda_{\text{max}} = 298 \text{ m}\mu$, $\log \epsilon_{\text{max}} = 3.597$ (dioxane).

ANAL. Calculated for $\text{C}_{20}\text{H}_{16}\text{O}_2\text{N}_4$: N, 16.18%. Found: N, 15.95%.

B. Model Compound Condensations

1. Ring Closure of *N*-Benzoyl-*o*-phenylenediamine. A 20-ml. flask was charged with 1.2 g. of *N*-benzoyl-*o*-phenylenediamine and the flask purged with nitrogen after evacuation. The flask was immersed in an oil bath preheated to 260°C. The solid melted and refluxed with formation of small droplets in the Claisen head. Solidification occurred after 24 min. The crude solid had a m.p. of 294–297°C. and λ_{max} at 301 m μ and 242 m μ (methanol); (literature³ $\lambda_{\text{max}} = 300$ and 242 m μ). Recrystallization from ethanol gave a white solid, m.p. and mixed m.p. with 2-phenylbenzimidazole of 298°–300°C.

2. Ring Closure of *N,N'*-Dibenzoyl-*o*-phenylenediamine. About 2 g. of the dibenzoyl derivative was heated in a test tube at 330°C. for 1 hr.; a sublimate formed at the cool upper portion of the test tube. The melting point and infrared spectrum on the residue showed it to be 2-phenylbenzimidazole. A melting point, infrared spectrum, and neutralization equivalent showed that the sublimate was benzoic acid.

Several attempts were made to hydrolyze the bisamide with potassium hydroxide in diethylene glycol for analytical purposes. Heating at 200°C. resulted in ring closure to the 2-phenylbenzimidazole, while at lower temperatures no reactions occurred.

3. Ring Closure of *N,N'*-Bis(2-aminophenyl)isophthalamide. About 0.5 g. of *N,N'*-bis(2-aminophenyl)isophthalamide was placed in a test tube and immersed in a preheated oil bath. Four different conditions were used: (1) 20 min. at 295°C. in the presence of air; (2) 30 min. at 285°C. in nitrogen atmosphere; (3) 5 hr. at 300°C. in the presence of air; (4) 80 min. at 255°C. with small amount of added phenol and in the presence of air. All these conditions yielded a solid which had identical infrared spectra and melted around 180°C., solidified around 240°C., and remelted around 310°C. The expected *m*-phenylene-bibenzimidazole was reported to melt at 330–332°C.⁴ A sample of *m*-phenylene bibenzimidazole was obtained from Prof. C. S. Marvel. The infrared spectra of the two materials were identical and the mixed melting points undepressed at 308°–310°C.

4. Reaction of *o*-phenylenediamine and Phenyl Benzoate. Stoichiometric quantities of the reactants were heated at 260°C. under nitrogen and samples removed periodically for ultraviolet spectral analysis.

C. Kinetic Study

After it was shown that small quantities of tetramine and phenol could be detected in the ultraviolet at 310 and 269 m μ , respectively, an experimental procedure was designed to obtain kinetic data at 200°C. and 260°C.

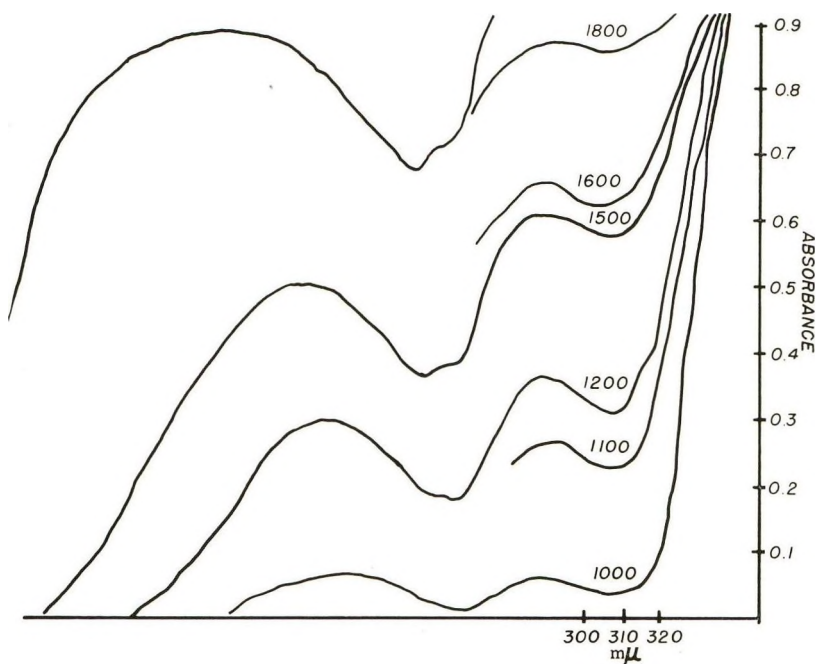


Fig. 1. Tetramine consumption in condensation of 3,3'-diaminobenzidine and diphenyl isophthalate at 200°C.

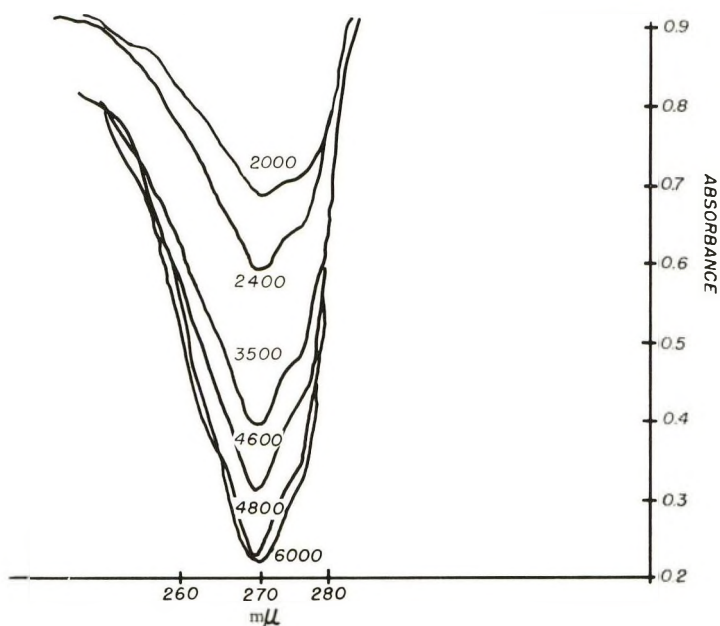


Fig. 2. Phenol formation in condensation of 3,3'-diaminobenzidine and diphenyl isophthalate at 200°C.

Stoichiometric amounts of 3,3'-diaminobenzidine and diphenyl isophthalate were weighed out on an analytical balance and thoroughly mixed on a vibrator with stainless steel balls. Melting point capillary tubes were charged with 10.0 ± 0.1 mg. of the mixture and the ends carefully sealed. All the tubes were completely immersed, simultaneously, into a preheated bath maintained at either $200 \pm 1^\circ\text{C}$. or $260 \pm 1^\circ\text{C}$. and individual tubes removed at certain intervals. After rapid chilling and rinsing with acetone

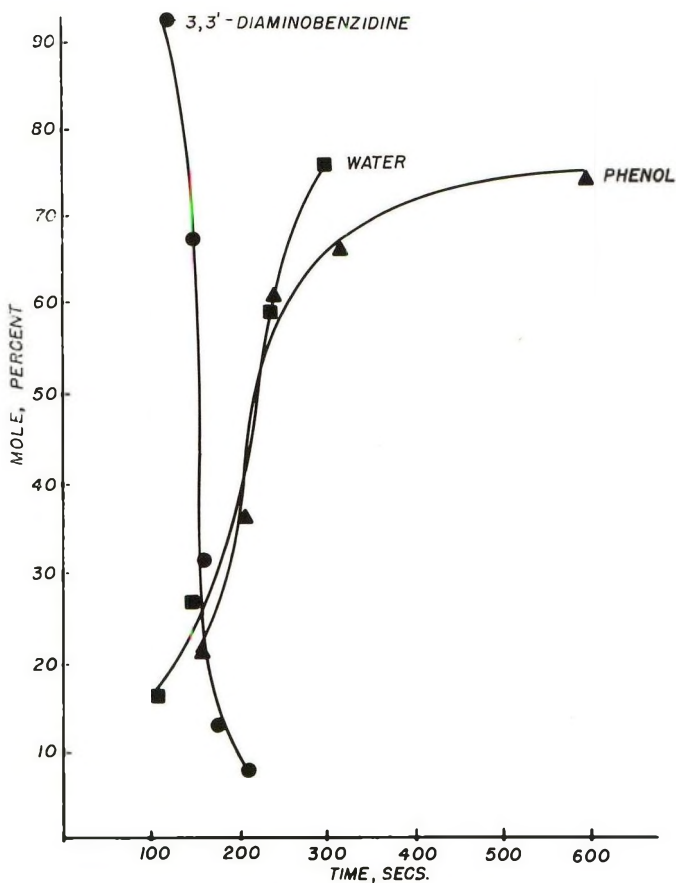


Fig. 3. Condensation of 3,3'-diaminobenzidine and diphenyl isophthalate at 200°C .

and water, the tubes were broken with a rod under 20 ml. of distilled water, heated 5 min., the solution transferred quantitatively to a 50 ml. volumetric flask and diluted with more water to volume. The ultraviolet spectra were recorded for phenol formation as a function of tetramine consumption (Figs. 1-4).

The above technique assumed that the reaction was irreversible under the experimental conditions, that the reaction mixture became homogeneous instantaneously and that ideal heat transfer occurred throughout the reaction mass.

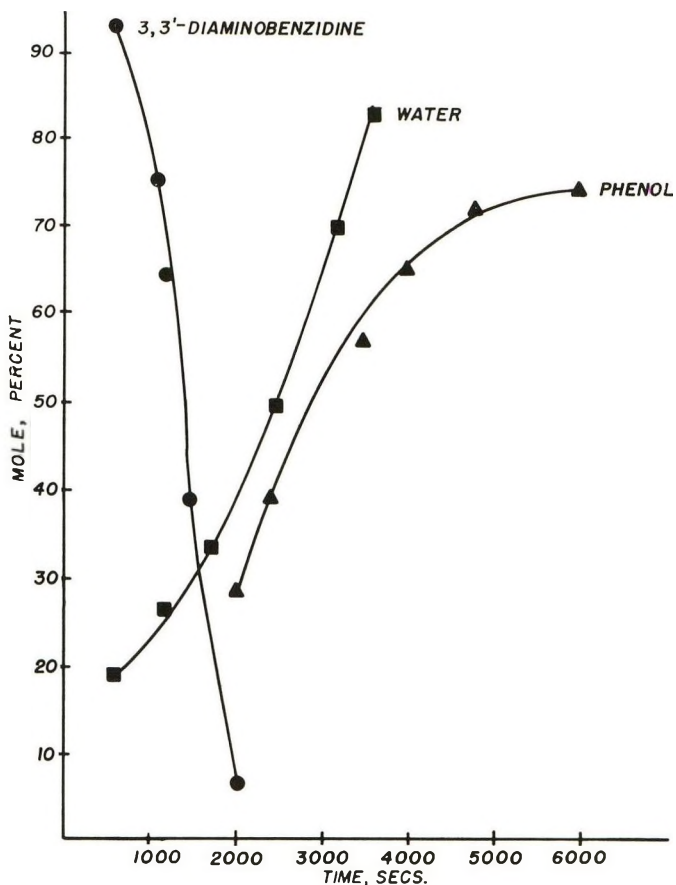


Fig. 4. Condensation of 3,3'-diaminobenzidine and diphenyl isophthalate at 260°C.

Attempts to follow water formation as a function of tetramine consumption by Karl Fisher titration were unsuccessful because of interference

TABLE I

Reaction of 3,3'-Diaminobenzidine and Diphenyl Isophthalate at 200°C. Consumption of 3,3'-Diaminobenzidine (See Figure 1)

Sample	Time, sec.	$\log I_0/I = A^a$	Tetramine remaining, mole-%	$1/M \times 10^{-3b}$
1	600	0.96 ± 0.02	93.0	2.85
2	1100	0.78	75.0	3.55
3	1200	0.69	64.0	4.17
4	1500	0.42	38.9	6.85
5	1600	0.37	37.5	7.10
6	1800	0.15	14.8	16.67
7	2000	0.07	6.4	50.00

^a Absorbance.

^b Molarity.

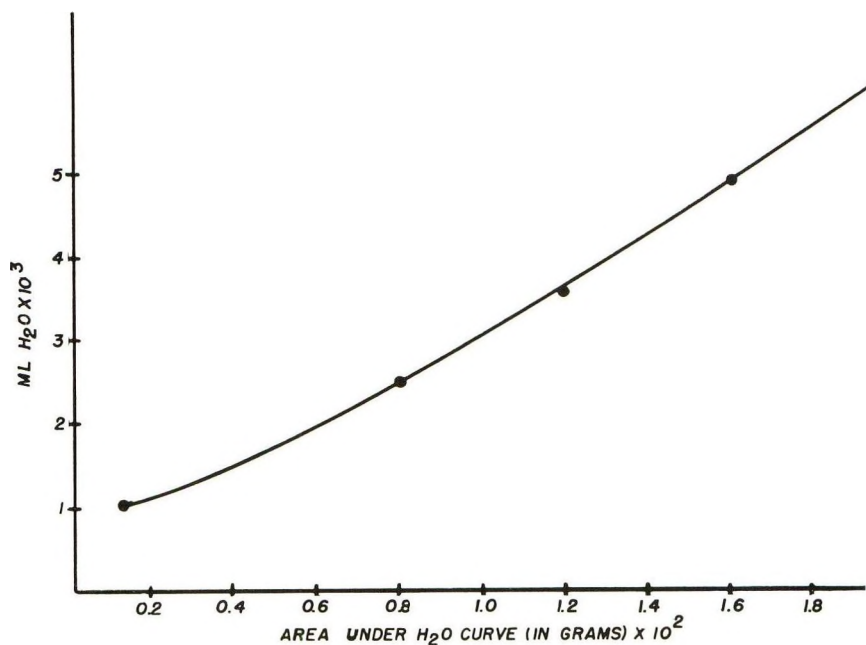


Fig. 5. Water calibration curve for vapor phase chromatography.

TABLE II

Reaction of 3,3'-Diaminobenzidine and Diphenyl Isophthalate at 200°C. Formation of Phenol (See Figure 2)

Sample	Time, sec.	$\log I_0/I = A$	Phenol formed, mole-%	$1/M \times 10^{-3}$
1	2000	0.32 ± 0.02	28.1	4.55
2	2400	0.42	38.5	3.30
3	3500	0.61	56.0	2.38
4	4000	0.69	64.0	2.08
5	4800	0.77	70.5	1.85
6	6000	0.79	72.5	1.83

TABLE III

Reaction of 3,3'-Diaminobenzidine and Diphenyl Isophthalate at 200°C. Formation of Water

Sample	Time, sec.	Wt. H ₂ O, g.	H ₂ O, mole-% formed	$1/M \times 10^{-3}$
1	600	0.030	19.3	6.90
2	1500	0.059	28.6	4.64
3	1700	0.070	33.3	4.00
4	1800	0.096	43.7	3.05
5	2500	0.109	49.2	2.70
6	3200	0.153	69.2	1.92
7	3600	0.170	81.9	1.62

TABLE IV

Reaction of 3,3'-Diaminobenzidine and Diphenyl Isophthalate at 200°C. Summary of Reaction Kinetics

	Rate constant, l. mole ⁻¹ -sec. ⁻¹	$\Delta M/\Delta t$, mole-%-sec. ⁻¹ $\times 10^7$	Ratio of rate constants
3,3'-Diaminobenzidine	77.8	0.070	13.7
Water	15.7	0.018	2.8
Phenol	5.7	0.004	1.0

TABLE V

Reaction of 3,3'-Diaminobenzidine and Diphenyl Isophthalate at 260°C. Consumption of 3,3'-Diaminobenzidine

Sample	Time, sec.	$\log I_0/I = A$	Tetramine concentration, mole l. ⁻¹ $\times 10^4$	Tetramine remaining, mole-%
1	120	0.98	3.42	93.0
2	150	0.73	2.54	87.2
3	155	0.34	1.18	68.9
4	180	0.14	0.48	32.8
5	210	0.08	0.28	6.9

TABLE VI

Reaction of 3,3'-Diaminobenzidine and Diphenyl Isophthalate at 260°C. Formation of Phenol

Sample	Time, sec.	$\log I_0/I = A$	Phenol concentration, mole l. ⁻¹ $\times 10^4$	Phenol formed, mole-%
1	155	0.22	1.53	20.8
2	180	0.38	2.63	34.8
3	210	0.44	2.77	36.6
4	220	0.52	3.60	47.6
5	240	0.64	4.50	59.5
6	320	0.72	5.00	66.1
7	480	0.76	5.26	69.5
8	600	0.80	5.53	73.2
9	1200	0.82	5.67	73.4

TABLE VII

Reaction of 3,3'-Diaminobenzidine and Diphenyl Isophthalate at 260°C. Formation of Water

Sample	Time, sec.	Wt. H ₂ O, g. $\times 10^3$	H ₂ O, formed, mole-%	$1/M \times 10^{-3}$
1	120	1.0	16.3	8.2
2	150	1.8	26.6	5.0
3	200	2.4	35.5	3.7
4	220	3.4	49.5	2.7
5	240	4.0	58.5	2.2
6	300	5.1	75.6	1.8

TABLE VIII
Reaction of 3,3'-Diaminobenzidine and Diphenyl Isophthalate at 260°C. Summary of Reaction Kinetics

	Rate constant, l. mole ⁻¹ -sec. ⁻¹	$\Delta M/\Delta t$, mole-%-sec. ⁻¹	Ratio of rate constants
3,3'-Diaminobenzidine	506	0.97	15
Water	167	0.32	5
Phenol	34.1	0.12	1

TABLE IX
Water Calibration^a

Sample	MeOH, ml.	H ₂ O, ml.	Sample size, μ l.	Attenuation \times absorbance	MeOH time, min.	H ₂ O time, min.
1	1.0	0.01	10	64 \times 4.1	5.4	7.3
2	1.0	0.005	10	64 \times 3.9	5.4	7.6
3	1.0	0.005	50	256 \times 2.4	5.2	6.8
4	1.0	0.005	50	256 \times 2.4	5.2	6.8
5	0.5	0.005	50	256 \times 2.4	5.2	6.8

^a Sample: MeOH + H₂O; column: Perkin-Elmer Type F; column pressure: 30 psi; column temperature: 81°C.; gas carrier: He; flow 6.5 scale div.; attenuation = 1.

apparently caused by the unreacted tetramine. Water was readily determined by vapor phase chromatography. The above experimental technique was modified so that the tubes were broken under anhydrous methanol and the solution made up to volume with more methanol. The amount of water formed was calculated by weighing the paper area under the curve after calibration against known amounts of water (Fig. 5).

The results of these measurements are shown in Tables I-IX.

DISCUSSION

A. Model Compound Study

The formation of 2-phenylbenzimidazole from *N,N'*-dibenzoyl-*o*-phenylenediamine indicated that the condensation could give the desired polymer even if diamide formation occurred. Formation of *m*-phenylenebiphenylbenzimidazole from *N,N'*-bis(2-aminophenyl)isophthalamide indicated that a structure more closely allied to a polyaminoamide than *N*-benzoyl-*o*-phenylenediamine would also give the desired polymer.

B. Kinetic Study

Plotting either $\log c$ versus t or $1/c$ versus t gave a straight line, making the reaction order questionable. However, a plot of dc/dt versus Δc ruled out a first-order reaction and indicated a second-order reaction, overall,

with respect to phenol evolution; the reaction depended on the concentration of both reactants.

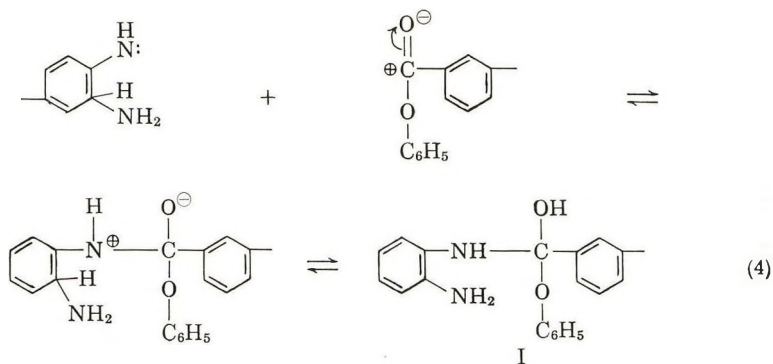
When the evolution of phenol as a function of 3,3'-diaminobenzidine consumption was determined (Figs. 3 and 4) it became clear that amide formation was not an intermediate step in the condensation. For amide formation to occur it would be necessary to have phenol evolution begin with tetramine consumption. The data showed that phenol evolution first started after 70–80 mole % of the tetramine had been consumed. This suggested an intermediate which could split out either phenol, water, or both.

Data on water evolution as a function of 3,3'-diaminobenzidine showed that water formed as soon as the amine started to react (Figs. 3 and 4). Furthermore, the curves showed that water evolution preceded phenol evolution from this intermediate. At the lower reaction temperature, the time interval between water and phenol evolution was the greatest. The data in Tables IV and VIII showed that phenol evolution was the rate-determining step in the condensation, the 3,3'-diaminobenzidine consumption to form the first intermediate being most rapid; the evolution of water to give a new intermediate was the second most rapid reaction in the condensation.

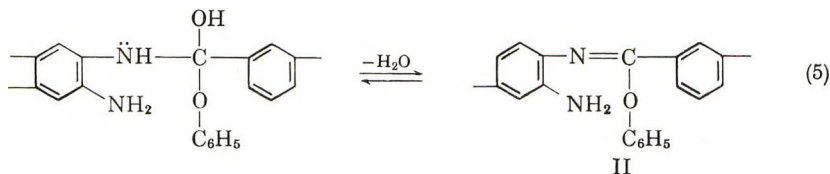
C. Proposed Condensation Mechanism

It was now possible to postulate a mechanism for the preparation of polybenzimidazole from diphenyl isophthalate and 3,3'-diaminobenzidine which fit the kinetic data.

Step 1. The primary amino group added to the ester by donation of the free electron pair on nitrogen to the carbonyl carbon atom, and this was followed by migration of a proton from the now positive charged nitrogen atom to the carbonyl oxygen atom [eq. (4)]



Step 2. Dehydration of the aldol type intermediate (I) then occurred to give the new intermediate (II) which has a Schiff base-type structure. Such a reaction can also be considered to be reversible.



Evidence of the C=N moiety was obtained from the ultraviolet spectra obtained during the condensation of phenyl benzoate and *o*-phenylenediamine (Fig. 6). New, increasing absorptions, which disappeared at the conclusion of the reaction, were found at 275 and 284 m μ . Elderfield and Meyer⁶ studied the condensation of benzophenone and *o*-phenylenediamine and isolated the Schiff base which exhibited absorptions at 275 and 282 m μ (also see Keasling and Schueler⁵ for >C=N-spectra).

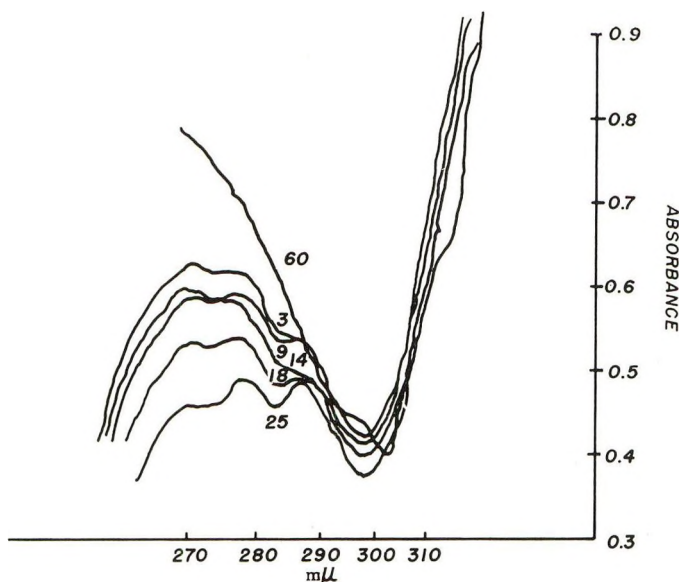
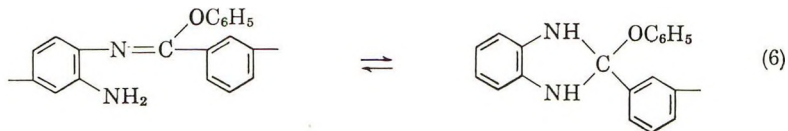


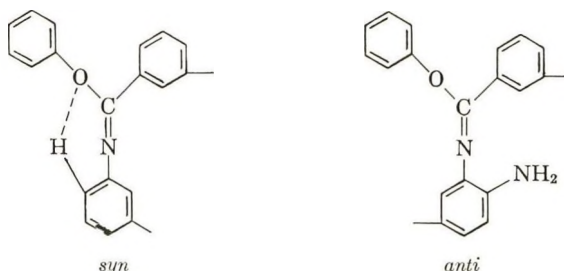
Fig. 6. Reaction of *o*-phenylenediamine and phenyl benzoate at 260°C.

Intermediate II is a most interesting entity for several reasons: (1) It probably can exist in equilibrium with benzimidazoline structure⁶ as shown in eq. (6), although our study did not attempt to investigate this;



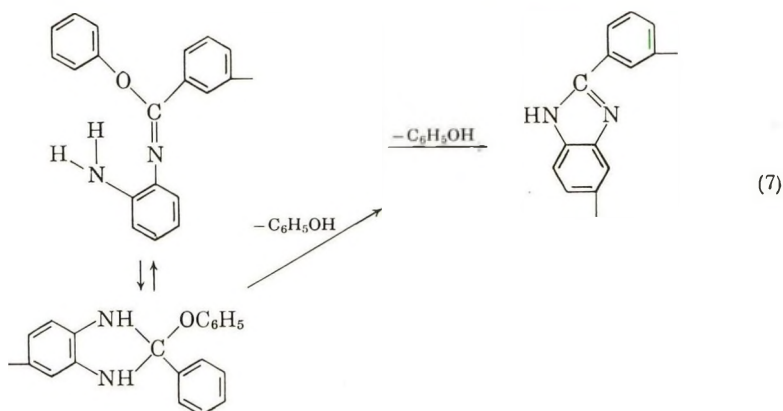
(2) the C=N-moiety is in conjugation with the other double bonds in the

molecule and could cause resonance stabilization of intermediate II; (3) stereoisomerism is possible and the *syn* form could undergo intramolecular hydrogen bonding.



Construction of the isomers with Fisher-Herschfelder models showed that the amino hydrogen in the *syn* form actually contacted the phenoxy oxygen atom, while in the *anti* form intramolecular hydrogen bonding appeared impossible. The implications of this hydrogen bonding are important. This could explain why the condensation affords essentially a purely linear polymer; the internal hydrogen bonding forced the elimination of phenol to be intramolecular; intermolecular phenol evolution would lead to branching and/or crosslinking. Internal hydrogen bonding probably added further stabilization to the molecule, in addition to that from resonance stabilization; these factors are likely reasons for the high reaction temperatures needed and why phenol evolution was the rate-determining step.

Step 3. The final event in the condensation was phenol evolution with the formation of the benzimidazole ring. This could result from either the Schiff base or the benzimidazole structure as shown in eq. (7).



The work presented in this paper was a part of the program sponsored by the United States Air Force under Contract No. AF 33(657)-8047; this program was monitored by the Air Force Materials Laboratory, Plastics and Composites Branch, Research and Technology Division, Wright-Patterson Air Force Base, Ohio.

References

1. Brinker, K. C., and I. M. Robinson (to E. I. du Pont de Nemours), U. S. Pat. 2,895,948 (July 21, 1959).
2. Vogel, H., and C. S. Marvel, *J. Polymer Sci.*, **50**, 511 (1961).
3. Narmco Research & Development, San Diego, California, Contract No. AF 33(657)-8047, Research and Technology Division, Wright-Patterson Air Force Base, Ohio.
4. Vogel, H., and Marvel, C. S., *J. Polymer Sci.*, **A1**, 1531 (1963).
5. Keasling, H. H., and F. W. Schueler, *J. Am. Pharm. Assoc., Sci. Ed.*, **39**, 87 (1950).
6. Elderfield, R. C., and V. B. Meyer, *J. Am. Chem. Soc.*, **76**, 1887 (1954).

Résumé

Il y a formation de poly-2,2'-(*m*-phénylène)-5,5'-bibenzimidazole quand on condense la 3,3'-diaminobenzidine et l'isophthalate de diphenyle via deux ou trois produits intermédiaires. Les données cinétiques indiquent une consommation rapide de la 3,3'-diaminobenzidine qui forme un intermédiaire du type aldol. Celui-ci perd de l'eau pour former une base de Schiff qui à son tour perd un phénol pour former le polymère final. La libération du phénol est l'étape déterminante de la vitesse. La base de Schiff postulée peut présenter le phénomène de stéréoisomérisation. La liaison hydrogène intramoléculaire qui peut exister dans le *syn*-isomère, donne une explication du fait que la condensation donne un polymère linéaire. Les effets combinés de la liaison hydrogène intramoléculaire et la stabilisation due à la résonance dans la base de Schiff peuvent expliquer pourquoi la libération du phénol est l'étape déterminante de la vitesse et pourquoi la condensation requiert une température de réaction aussi élevée.

Zusammenfassung

Poly-2,2'-(*m*-phenylen)-5,5'-bibenzimidazol bildet sich über zwei oder drei Zwischenstufen bei der Kondensation von 3,3'-Diaminobenzidin und Diphenylisophthalat. Die kinetischen Daten lassen einen raschen Verbrauch von 3,3'-Diaminobenzidin unter Bildung von aldol-artigen Zwischenprodukten erkennen, welche unter Bildung einer Schiff'schen Base Wasser entwickeln, die ihrerseits wieder Phenol abspaltet und das Endpolymere bildet. Die Phenolabspaltung ist der geschwindigkeitsbestimmende Schritt. Die postulierte Schiff'sche Base kann in stereoisomeren Formen auftreten. Intramolekulare Wasserstoffbindungen, wie sie in *Syn*isomeren auftreten können, bieten eine Erklärung für die Bildung eines linearen Polymeren bei der Kondensation. Die kombinierten Einflüsse der intramolekularen Wasserstoffbindung und die zusätzliche Resonanzstabilisierung in der Schiff'schen Base sind möglicherweise die Gründe dafür, dass die Phenolabspaltung der geschwindigkeitsbestimmende Schritt ist und die Reaktion hohe Reaktionstemperaturen erfordert.

Received January 29, 1964

Copolymerization of Divinylbenzene with Monovinyl Monomers

WILLIAM E. GIBBS, *Polymer Branch, Nonmetallic Materials Division,
Wright-Patterson Air Force Base, Ohio*

Synopsis

Composition relations for the copolymerization of vinyl monomers with divinyl monomers incapable of undergoing short-range cyclization or alternating inter-intramolecular propagation have been derived both for the general case, including crosslinking reactions, and for the approximate case where the concentration of pendant unsaturation may be assumed unaffected by crosslinking reactions. The general case composition equation has a complexity similar to that for the ternary polymerization of three vinyl monomers. The approximate case closely resembles the usual binary copolymerization relationship:

$$\frac{d[m_1]}{d[m_2]} = \frac{(r_1[M_1] + [M_2])[M_1]}{([M_1] + r_2[M_2])[M_2]}$$

where $r_1 = k_{11}/k_{12}$, $r_2 = k_{44}/k_{41}$, $[M_2]$ is the molar concentration of vinyl comonomer, but where $[M_1]$ is the molar concentration of divinyl monomer double bonds, i.e., twice the molar concentration of divinyl monomer.

INTRODUCTION

The copolymerization of divinylbenzenes with vinyl monomers such as styrene and methyl methacrylate has been of interest, but no composition relationships have been derived for these systems. Wiley and co-workers^{1,2} have presented a composition relationship which they have used successfully but do not indicate a basis for its origin. Composition relationships for these systems may be derived as illustrated in the following.

The composition relationships presented here should be generally applicable to any divinyl type monomer that cannot undergo short-range cyclization, such as the *m*- and *p*-divinylbenzenes, the long-chain dimethacrylates, etc. They are not applicable to monomers which may undergo alternating inter-intramolecular propagation or other short-range cyclization to a significant degree. The composition relations for these type systems are the subject of another paper.³

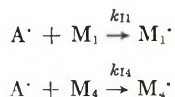
One feature in particular which makes this derivation suited to the divinylbenzene case and to other monomers where the double bonds may interact electronically is the assignment of different rate constants for the reaction of the first and second double bonds. Hence, it need not be assumed that these two types of double bonds have the same reactivity.

However, it is necessary that the two double bonds be equivalent in the unreacted monomer.

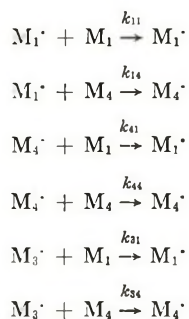
GENERAL CASE

A general scheme is as follows.

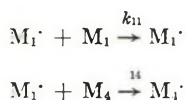
Chain initiation:



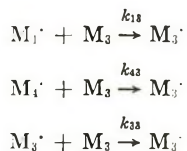
Chain propagation:



Formation of M_3 :



Crosslinking:



In the above, $A \cdot$ is an initiator fragment; M_1 is either double bond of a previously unreacted divinyl monomer having equivalent double bonds; M_4 is the vinyl comonomer, $M_1 \cdot$ is the radical derived from M_1 ; $M_4 \cdot$ is the radical derived from M_4 ; M_3 is the pendant double bond formed; $M_3 \cdot$ is the radical derived from the pendant double bond. In what follows, m_1 and m_4 are the chain elements of type M_1 and M_4 , respectively, incorporated into the polymer.

The concentrations of all species, except M_1 , are in moles/liter. M_1 is given in units of moles double bonds/liter. The M_1 concentration is, then, twice the divinyl monomer concentration.

The rate of formation of M_1 and M_4 type chain elements in the polymer may be expressed according to the above as:

$$d[m_1]/dt = k_{11}[M_1^{\cdot}][M_1] + k_{31}[M_3^{\cdot}][M_1] + k_{41}[M_4^{\cdot}][M_1] \quad (1)$$

$$d[m_4]/dt = k_{14}[M_1^{\cdot}][M_4] + k_{34}[M_3^{\cdot}][M_4] + k_{44}[M_4^{\cdot}][M_4] \quad (2)$$

The rate of formation of M_3 type elements in the polymer may be written as:

$$d[M_3]/dt = k_{11}[M_1^{\cdot}][M_3] + k_{13}[M_1^{\cdot}][M_3] + k_{14}[M_1^{\cdot}][M_4] \\ - k_{13}[M_1^{\cdot}][M_3] - k_{33}[M_3^{\cdot}][M_3] - k_{43}[M_4^{\cdot}][M_3] \quad (3)$$

The rate of change of radical concentrations may be expressed as:

$$d[M_1^{\cdot}]/dt = k_{31}[M_3^{\cdot}][M_1] \\ + k_{41}[M_4^{\cdot}][M_1] - k_{13}[M_1^{\cdot}][M_3] - k_{14}[M_1^{\cdot}][M_4] \quad (4)$$

$$d[M_3^{\cdot}]/dt = k_{13}[M_1^{\cdot}][M_3] \\ + k_{43}[M_4^{\cdot}][M_3] - k_{31}[M_3^{\cdot}][M_1] - k_{34}[M_3^{\cdot}][M_4] \quad (5)$$

$$d[M_4^{\cdot}]/dt = k_{14}[M_1^{\cdot}][M_4] \\ + k_{34}[M_3^{\cdot}][M_4] - k_{41}[M_4^{\cdot}][M_1] - k_{43}[M_4^{\cdot}][M_3] \quad (6)$$

If one makes a stationary-state assumption such that the rate of change of radical concentration is very small compared with either the rate of formation or rate of disappearance of radicals, the above equations may be written as:

$$(k_{13}[M_3] + k_{14}[M_4])[M_1^{\cdot}] = k_{31}[M_3^{\cdot}][M_1] + k_{41}[M_4^{\cdot}][M_1] \quad (4a)$$

$$(k_{31}[M_1] + k_{34}[M_4])[M_3^{\cdot}] = k_{13}[M_1^{\cdot}][M_3] + k_{43}[M_4^{\cdot}][M_3] \quad (5a)$$

$$(k_{41}[M_1] + k_{43}[M_3])[M_4^{\cdot}] = k_{14}[M_1^{\cdot}][M_4] + k_{34}[M_3^{\cdot}][M_4] \quad (6a)$$

This series of equations may be solved to give each radical concentration in terms of one of the other radical concentrations by means of determinants.⁴

$$[M_1^{\cdot}] = \frac{\begin{vmatrix} (k_{41}[M_1][M_4^{\cdot}]) & (-k_{31}[M_1]) \\ (k_{43}[M_3][M_4^{\cdot}]) & (k_{31}[M_1] + k_{34}[M_4]) \end{vmatrix}}{\begin{vmatrix} (k_{13}[M_3] + k_{14}[M_4]) & (-k_{31}[M_1]) \\ (-k_{13}[M_3]) & (k_{31}[M_1] + k_{34}[M_4]) \end{vmatrix}} \quad (7)$$

$$[M_3^{\cdot}] = \frac{\begin{vmatrix} (k_{13}[M_3] + k_{14}[M_4]) & (k_{41}[M_1][M_4^{\cdot}]) \\ (-k_{13}[M_3]) & (k_{43}[M_3][M_4^{\cdot}]) \end{vmatrix}}{\begin{vmatrix} (k_{13}[M_3] + k_{14}[M_4]) & (-k_{31}[M_1]) \\ (-k_{13}[M_3]) & (k_{31}[M_1] + k_{34}[M_4]) \end{vmatrix}} \quad (8)$$

The relative reactivity ratios may be introduced at this point by division of each of the columns of the determinant by the appropriate rate constant, i.e., k_{11} , k_{33} , or k_{44} . Following this procedure and expanding:

$$[M_1'] = \frac{[M_1][M_4'](k_{44})\{Z_1(Y_1[M_1] + Y_4[M_4]) + Y_1(Z_3[M_3])\}}{(k_{11})\{(W_3[M_3] + W_4[M_4])(Y_1[M_1] + Y_4[M_4]) - (Y_1[M_1])(W_3[M_3])\}} \quad (9)$$

$$[M_3'] = \frac{[M_3][M_4'](k_{44})\{(W_3[M_3] + W_4[M_4])(Z_3) + (Z_1[M_1])(W_3)\}}{k_{33}\{(W_3[M_3] + W_4[M_4])(Y_1[M_1] + Y_4[M_4]) - (Y_1[M_1])(W_3[M_3])\}} \quad (10)$$

where $W_3 = k_{13}/k_{11}$; $W_4 = k_{14}/k_{11}$; $Y_1 = k_{31}/k_{33}$; $Y_4 = k_{34}/k_{33}$; $Z_1 = k_{41}/k_{44}$; $Z_3 = k_{43}/k_{44}$.

The right sides of eqs. (4a), (5a), and (6a), are identical with parts of eqs. (1), (2), and (3). Making the indicated substitutions yields

$$d[m_1]/dt = (k_{11}[M_1] + k_{13}[M_3] + k_{14}[M_4])[M_1'] \quad (1a)$$

$$d[m_4]/dt = (k_{41}[M_1] + k_{43}[M_3] + k_{44}[M_4])[M_4'] \quad (2a)$$

$$d[M_3]/dt = (k_{31}[M_1] + k_{33}[M_3] + k_{34}[M_4])[M_3'] - (k_{13}[M_3] + k_{14}[M_4])[M_1'] \quad (3a)$$

Substituting the value of M_1' obtained in eq. (9) into eq. (1a) and carrying out the division by k_{11} yields:

$$\frac{d[m_1]}{dt} = \frac{[M_1][M_4'](k_{44})\{([M_1] + W_3[M_3]) + W_4[M_4]\}\{Z_1(Y_1[M_1] + Y_4[M_4]) + Y_1(Z_3[M_3])\}}{(W_3[M_3] + W_4[M_4])(Y_1[M_1] + Y_4[M_4]) - (Y_1[M_1])(W_3[M_3])} \quad (11)$$

Dividing eq. (11) by eq. (2a), multiplying out the denominator and collecting terms, we have

$$\frac{d[m_1]}{d[m_4]} = \frac{[M_1]\{([M_1] + W_3[M_3] + W_4[M_4])(Z_1Y_1[M_1] + Y_4Z_1[M_4] + Y_1Z_3[M_3])\}}{[M_4]\{Z_1[M_1] + Z_3[M_3] + [M_4]\}(W_3[M_4] + W_3Y_4[M_3] + W_4Y_4[M_4])} \quad (12)$$

Equation (12) represents the composition relationship in terms of m_1 and m_4 for these types of copolymerizations. The complexity is about that for a ternary copolymerization system.

APPROXIMATION OF THE GENERAL CASE

If it may be assumed that the concentration of pendant unsaturated groups is not significantly changed by crosslinking reactions, and hence, that the reactions of the various radicals with M_3 and the reaction of M_3'

with the monomers may be disregarded, a simplification of the above may be obtained.

The rates of formation of m_1 and m_4 chain elements may then be written as:

$$d[m_1]/dt = k_{11}[M_1^{\cdot}][M_1] + k_{41}[M_4^{\cdot}][M_1] \quad (13)$$

$$d[m_4]/dt = k_{14}[M_1^{\cdot}][M_4] + k_{44}[M_4^{\cdot}][M_4] \quad (14)$$

The rate of change of radical concentrations here is then:

$$d[M_1^{\cdot}]/dt = k_{41}[M_4^{\cdot}][M_1] - k_{14}[M_1^{\cdot}][M_4] \quad (15)$$

$$d[M_4^{\cdot}]/dt = k_{14}[M_1^{\cdot}][M_4] - k_{41}[M_4^{\cdot}][M_1]$$

Using the same stationary-state condition as before we have:

$$k_{41}[M_4^{\cdot}][M_1] = k_{14}[M_1^{\cdot}][M_4] \quad (16)$$

$$[M_4] = k_{14}[M_1][M_4]/k_{41}[M_1] \quad (17)$$

Equations (13) and (14) may then be written as:

$$d[m_1]/dt = (k_{11}[M_1] + k_{14}[M_4])[M_1^{\cdot}] \quad (18)$$

$$d[m_4]/dt = (k_{41}[M_1] + k_{44}[M_4])[M_4^{\cdot}] \quad (19)$$

Substituting for $[M_4^{\cdot}]$ in eq. (19) and dividing eq. (18) by the result yields

$$\frac{d[m_1]}{d[m_4]} = \frac{\{(k_{11}[M_1]/k_{14}) + [M_4]\} [M_1]}{\{[M_1] + (k_{44}[M_4]/k_{41})\} [M_4]} \quad (20)$$

$$\frac{d[m_1]}{d[m_4]} = \frac{(r_1[M_1] + [M_4])[M_1]}{([M_1] + r_2[M_4])[M_4]}$$

where $r_1 = k_{11}/k_{14}$ and $r_2 = k_{44}/k_{41}$.

This equation is almost identical with that derived for the binary copolymerization system. There is one important difference, and this lies in the fact that M_1 is not the molar concentration of divinyl monomer, but rather the molar concentration of divinyl monomer double bonds.

References

1. Wiley, R. H., and E. E. Sale, *J. Polymer Sci.*, **42**, 479 (1960).
2. Wiley, R. H., and E. E. Sale, *J. Polymer Sci.*, **42**, 491 (1960).
3. Gibbs, W. E., to be submitted to *J. Polymer Sci.*
4. Walling, C., and E. R. Briggs, *J. Am. Chem. Soc.*, **67**, 1774 (1945).

Résumé

Des relations de compositions pour la copolymérisation de monomères vinyliques avec des monomères divinylés incapables de subir la cyclisation ou la propagation alternativement inter-intramoléculaire ont été obtenues pour le cas général comprenant des réactions de pontage et pour le cas approximatif où la concentration en groupement latéral insaturé semble ne pas être affectée par des réactions de pontage. L'équation de composition dans le cas général possède une complexité semblable à celle des polymérisa-

tions ternaires de trois monomères vinyliques. Le cas approximatif ressemble très fort à la relation habituelle de la copolymérisation binaire:

$$\frac{d[m_1]}{d[m_4]} = \frac{(r_1[M_1] + [M_4])[M_1]}{([M_1] + r_2[M_4])[M_4]}$$

où $r_1 = k_{11}/k_{14}$, $r_2 = k_{44}/k_{41}$, $[M_4]$ est la concentration molaire du comonomère vinylique, mais où $[M_1]$ est la concentration molaire des double liaisons du monomère divinylique, c.a.d. deux fois la concentration molaire en monomère divinylique.

Zusammenfassung

Beziehungen für die Zusammensetzung der Polymeren bei der Copolymerisation von Vinylmonomeren mit Divinylmonomeren ohne Nahcyclisierung oder alternierendes inter-intramolekulares Wachstum wurden sowohl für den allgemeinen Fall bei Berücksichtigung von Vernetzungsreaktionen als auch für die Näherung, bei der keine Änderung der Konzentration der anhängenden Vinylgruppen durch Vernetzungsreaktionen angenommen wird, abgeleitet. Die Zusammensetzungsgleichung für den allgemeinen Fall ist ähnlich komplex wie diejenige bei der ternären Copolymerisation von drei Vinylmonomeren. Die Näherungslösung weist eine starke Ähnlichkeit zur Beziehung für die binäre Copolymerisation auf:

$$\frac{d[m_1]}{d[m_4]} = \frac{(r_1[M_1] + [M_4])[M_1]}{([M_1] + r_2[M_4])[M_4]}$$

wo $r_1 = k_{11}/k_{14}$, $r_2 = k_{44}/k_{41}$, $[M_4]$ die molare Konzentration des Vinylcomonomeren und $[M_1]$ die molare Konzentration der Doppelbindung des Divinylmonomeren, d.h. das Doppelte der molaren Konzentration des Divinylmonomeren ist.

Received July 1, 1963

Revised October 11, 1963

Mechanism of Alternating Inter-Intramolecular Propagation. II. General Kinetics

WILLIAM E. GIBBS, *Polymer Branch, Nonmetallic Materials Division, Wright-Patterson Air Force Base, Ohio*

Synopsis

The general kinetics of alternating inter-intramolecular propagation are presented and discussed. The major factor which determines the microstructure of the polymer, the relative rates of the intramolecular and intermolecular reactions is examined. From the general kinetics methods are proposed for the determination of the ratio of rate constants for these reactions. A simple method utilizes the equation: $[m_1]/[M_3] = 1 + (k_c/k_{11})(1/[M_1]_0)$, where $[m_1]$ is the concentration of monomer units in the polymer, $[M_3]$ is the concentration of uncyclized units, $[M_1]$ is a parameter related to monomer concentration, k_c is the rate constant for cyclization and k_{11} the rate constant for linear propagation. Other methods which may give information on the nature of the termination reaction are discussed.

INTRODUCTION

Although several investigations have been reported concerning the mechanism of alternating inter-intramolecular propagation (or cyclopolymerization)¹⁻³ as yet no attempt has been made to present the kinetics of this system of reactions on a general basis. There are many advantages to be gained from a general consideration of cyclopolymerization kinetics, not the least important of which is a systematic and quantitative approach to the effect of monomer structure and reaction conditions on the structure and properties of the polymers formed.

It is the primary purpose of the present paper to present general treatments of the polymerization kinetics of symmetrical, nonconjugated diolefins. The relationships developed are applicable to systems where the extent of cyclization is zero and cover the range to where cyclization is quantitative. The polymerization of symmetrical nonconjugated diolefins was selected for this because the very large proportion of interest in cyclopolymerization has been centered on these monomers and because the considerations used in the development of pertinent relationships in these cases are fundamental to the cyclopolymerization of any monomer.

DERIVATION OF RELATIONSHIPS

The following terminology will be used: A_2 denotes a thermally dissociating free radical initiator; A' , an initiator fragment; M_1 , either double

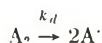
bond of a previously unreacted monomer; M_1' , the initial radical derived from the attack of a radical on M_1 ; M_2' , the radical formed by the intramolecular cyclization of M_1' ; and M_3 , the pendant double bond formed when M_1' does not cyclize and reacts with additional monomer. DB is the concentration of all carbon-carbon double bonds in the system capable of reacting. In certain places reference will also be made to overall monomer concentration $[M]$ and to $[m_1]$, the concentration of M_1 units in the polymer. Concentrations are given in moles per liter; M_1 is given as moles of double bonds per liter.

Polymerizations Involving Biradical Termination

The manner in which growing radicals disappear during polymerization is very important in determining the nature of the rate expressions. For the purposes of this paper it is sufficient to distinguish between two types of termination reactions. This section deals with those polymerizations where termination occurs by the reaction of pairs of radicals—biradical termination. This category includes termination by combination and by disproportionation. The second type of termination, treated in a following section, involves degradative chain transfer,⁴ where a growing radical abstracts a hydrogen atom from monomer thereby forming an unreactive allylic radical.

The general scheme involved in the polymerizations covered in this section is given below.

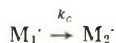
Initiator decomposition:



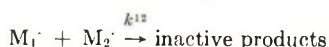
Chain initiation:



Chain propagation:



Chain termination:



The propagation reactions are those reactions important in determining the loss in overall double bond concentration. Providing the kinetic chain length is sufficiently large, the loss of double bonds by the initiation reaction

is negligible. The overall loss of double bonds (DB) may then be written as:

$$-d[\text{DB}]/dt = k_c[M_1\cdot] + k_{11}[M_1\cdot][M_1] + k_{21}[M_2\cdot][M_1] \quad (1)$$

This expression is strictly true only in the absence of crosslinking reactions, since these reactions will also consume double bonds. However, in the general regions of conversion of interest in kinetic studies, the loss in double bonds by the crosslinking reaction should be small compared with that lost during propagation.

In a way analogous to vinyl copolymerization,⁵ the relative concentrations of $M_1\cdot$ and $M_2\cdot$ type radicals are not determined by the overall radical concentration, but rather by the rate at which a chain-end of one type is converted to a chain-end of the other type. In vinyl copolymerization this change is due to reactions of the chain-ends with the different types of monomers. Here, a chain-end of type $M_1\cdot$ is converted to a chain-end of type $M_2\cdot$ by the cyclization reaction. An $M_2\cdot$ chain-end is converted to an $M_1\cdot$ chain-end by reaction with M_1 . The rate of change of $M_1\cdot$ with time is given by:

$$d[M_1\cdot]/dt = k_{21}[M_2\cdot][M_1] - k_c[M_1\cdot] \quad (2)$$

Making use of the "steady-state" approximation where the rate of change of $M_1\cdot$ with time is very much smaller than either its rate of formation or disappearance we have

$$k_{21}[M_2\cdot][M_1] \simeq k_c[M_1\cdot] \quad (3)$$

Hence:

$$[M_2\cdot] = k_c[M_1\cdot]/k_{21}[M_1] \quad (4)$$

Upon substitution of this expression for $[M_2\cdot]$ in eq. (1) there results:

$$-d[\text{DB}]/dt = (2k_c + k_{11}[M_1])[M_1\cdot] \quad (5)$$

The concentration of all chain radicals in the system at any time is determined by their rates of formation and disappearance at that time. The rate of formation of chain radicals is given by the initiation reaction:

$$R_I = k_I[A\cdot][M_1] \quad (6)$$

while the rate of disappearance is given by the sum of the three possible termination reactions:

$$R_t = 2k^{11}[M_1\cdot]^2 + 2k^{22}[M_2\cdot]^2 + 2k^{12}[M_1\cdot][M_2\cdot] \quad (7)$$

If one type of termination is responsible for essentially all the termination in a given system, simple expressions for the overall rate may be found. The three cases are treated below.

1. Termination by $M_1\cdot + M_1\cdot$. Here, the rate of formation and termination of chain radicals may be written as:

$$R_I = R_t$$

$$k_t[A^\cdot][M_1] = 2k^{11}[M_1^\cdot]^2 \quad (8)$$

$$[M_1^\cdot] = (k_t[A^\cdot][M_1]/2k^{11})^{1/2} \quad (9)$$

Following a similar approach, equating the rate of formation of A[·] radicals ($2fk_d[A_2]$) with the rate of disappearance of A[·] radicals ($k_t[A^\cdot][M_1]$) yields:

$$[A^\cdot] = 2fk_d[A_2]/k_t[M_1] \quad (10)$$

where f is the efficiency of initiation of chain radicals by A[·].

Equation (9) may then be written as:

$$[M_1^\cdot] = (fk_d[A_2]/k^{11})^{1/2} \quad (12)$$

Equation (5) then becomes:

$$-d[DB]/dt = (2k_c + k_{11}[M_1])(fk_d[A_2]/k^{11})^{1/2} \quad (13)$$

2. Termination by M₂[·] + M₂[·]. As in the previous case, the rates of formation and disappearance of chain radicals are equated:

$$k_t[A^\cdot][M_1] = 2k^{22}[M_2^\cdot] \quad (14)$$

$$fk_d[A_2] = k^{22}[M_2^\cdot]^2 \quad (15)$$

$$[M_2^\cdot] = (fk_d[A_2]/k^{22})^{1/2} \quad (16)$$

On substituting M₁[·] for M₂[·] by using eq. (4), eq. (16) becomes:

$$[M_1^\cdot] = k_{21}[M_1](fk_d[A_2]/k^{22})^{1/2}/k_c \quad (17)$$

Upon substitution of this in eq. (5) we have:

$$-d[DB]/dt = (2k_c + k_{11}[M_1])(k_{21}[M_1]/k_c)(fk_d[A_2]/k^{22})^{1/2} \quad (18)$$

3. Termination by M₁[·] + M₂[·]. As before:

$$k_t[A^\cdot][M_1] = 2k^{12}[M_1^\cdot][M_2^\cdot] \quad (19)$$

Hence:

$$fk_d[A_2] = k^{12}[M_1^\cdot][M_2^\cdot] \quad (20)$$

On substituting for M₂[·] by using eq. (4) we have:

$$fk_d[A_2] = k^{12}k_c[M_1^\cdot]^2/k_{21}[M_1] \quad (21)$$

$$[M_1^\cdot] = (fk_d k_{21}[M_1][A_2]/k^{12}k_c)^{1/2} \quad (22)$$

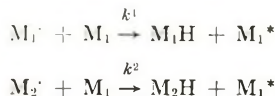
Equation (5) may be written then as:

$$-d[DB]/dt = (2k_c + k_{11}[M_1])(fk_d k_{21}[M_1][A_2]/k^{12}k_c)^{1/2} \quad (23)$$

Polymerizations Involving Degradative Chain Transfer

The classes of symmetrical, nonconjugated diolefins excluded from the previous section were those which have a degradative chain transfer reaction⁴ as the effective means of chain termination. The allyl and diallyl

monomers are important members of these classes. The same initiator decomposition, chain initiation, and chain propagation reactions may be written for these cases as were written for the previous section. The termination reactions here, however, are written as follows:



It may also be possible to have intramolecular termination:



by the transfer of the allylic hydrogen in the same chain element. It would appear, however, that this latter reaction would probably constitute only a small part, if any, of the total termination.

The polymerization of allyl monomers, in general, leads to polymers of relatively low number-average molecular weight. The diallyl monomers usually polymerize to somewhat higher molecular weights than do the corresponding monoallyl compounds. Mikulasova and Hrivik,⁶ in an investigation of the polymerization of allyl- and diallylmethylsilanes initiated by *t*-butyl peroxide, report \overline{DP}_n values of about 3–5 and 10–15 for the allyltrimethylsilane and the diallyldimethylsilanes, respectively. At low \overline{DP}_n values the loss of double bonds by the initiation reaction in these systems may be significant compared with that lost during propagation. In such cases the expression giving the rate of double bond consumption may be written as:

$$\begin{aligned} -d[DB]/dt &= k_f[A\cdot][M_1] + k_{11}[M_1\cdot][M_1] + k_c[M_1\cdot] + k_{21}[M_2\cdot][M_1] \\ -d[DB]/dt &= 2fk_d[A_2] + (2k_c + k_{11}[M_1])[M_1\cdot] \end{aligned} \quad (24)$$

If the contribution of the initiation reaction is not significant, then eq. (5) may be used.

$$-d[DB]/dt = (2k_c + k_{11}[M_1])[M_1\cdot] \quad (5)$$

If the \overline{DP}_n values are in the 10–20 range, the error arising from neglecting initiation will be of the order of 5–10%, and will decrease as \overline{DP}_n increases.

Considering the likely termination reactions, rate expressions may be derived as follows.

1. Termination by $M_1\cdot + M_1$. Equating the rates of formation and disappearance of chain radicals:

$$\begin{aligned} R_f &= R_t \\ k_f[A\cdot][M_1] &= k^1[M_1\cdot][M_1] \\ [M_1\cdot] &= 2fk_d[A_2]/k^1[M_1] \end{aligned}$$

Substitution of this in eq. (24) leads to:

$$-d[DB]/dt = \left\{ 1 + (2k_c + k_{11}[M_1])/k^1[M_1] \right\} 2fk_d[A_2] \quad (24A)$$

If the initiation reaction is not important in determining loss of double bonds:

$$-d[\text{DB}]/dt = (2k_c + k_{11}[\text{M}_1])(2fk_d[\text{A}_2]/k^1[\text{M}_1]) \quad (25)$$

2. Termination by $\text{M}_2' + \text{M}_1$. By following the same procedures used above and in the preceding sections, the rate expressions obtained are:

$$-d[\text{DB}]/dt = \{1 + (2k_c + k_{11}[\text{M}_1])k_{21}/k^2k_c\}2fk_d[\text{A}_2] \quad (24\text{B})$$

for cases where the loss of double bonds by initiation is important, and:

$$-d[\text{DB}]/dt = (2k_c + k_{11}[\text{M}_1])(2fk_d[\text{A}_2])k_{21}/k^2k_c \quad (26)$$

for cases where it is not.

Relative Rates of Formation of M_1 and M_3 Units in the Polymer

In addition to the rate of loss of double bonds in these polymerizations, it is also of use to consider the relative rates of formation of various structures in the polymer in a way analogous also to vinyl copolymerization. If we consider that each time an M_1 monomer reacts there is incorporated in the polymer a structure which may be identified with it (as for example, the number of moles of M_1 units contained in a sample of polymer is the weight of the sample divided by the molecular weight of the diolefin), we may speak of the rate of formation of M_1 units in the chain with respect to the rate of formation of other chain elements, such as uncyclized groups. The rate of formation of M_1 units in the polymer may be written (using the symbol m_1 to denote M_1 units in the polymer):

$$d[m_1]/dt = k_{11}[\text{M}_1'][\text{M}_1] + k_{21}[\text{M}_2'][\text{M}_1] \quad (27)$$

$$= (k_c + k_{11}[\text{M}_1])[\text{M}_1'] \quad (28)$$

following the original kinetic scheme and substituting M_1' for M_2' through eq. (4). The rate of formation of M_3 units in the chain may be expressed as:

$$d[\text{M}_3]/dt = k_{11}[\text{M}_1'][\text{M}_1] \quad (29)$$

since every time an M_1' radical reacts with M_1 monomer a pendant double bond (M_3) is formed.

The relative rates of formation of m_1 and M_3 units are then:

$$d[m_1]/d[\text{M}_3] = 1 + (k_c/k_{11})(1/[\text{M}_2]) \quad (30)$$

If certain conditions are satisfied, primarily that the conversion is low to avoid compositional changes in the polymer due to change in monomer concentration and the loss of M_3 by crosslinking is negligible, this differential form may be approximated by:

$$[m_1]/[\text{M}_3] = 1 + (k_c/k_{11})(1/[\text{M}_1]_0) \quad (31)$$

where $[m_1]$ and $[M_3]$ are the actual concentrations of m_1 and M_3 elements in the chain and $[M_1]_0$ refers to the initial concentration of monomer double bonds.

DISCUSSION

Rate Expressions

By means of the steps outlined in the preceding sections it is possible to derive expressions giving the rate of loss of double bonds or the rate of loss of monomer for cyclopolymerization in terms of the initial monomer and initiator concentrations and the associated rate constants. These expressions are summarized in Table I.

TABLE I
Rate Expressions for Cyclopolymerization

Termination reaction	Rate expression
$M_1 \cdot + M_1 \cdot$	$-d[\text{DB}]/dt = (2k_c + k_{11}[M_1])(fk_d[A_2]/k^{11})^{1/2}$
$M_2 \cdot + M_2 \cdot$	$-d[\text{DB}]/dt = (2k_c + k_{11}[M_1])(k_{21}[M_1]/k_c)(fk_d[A_2]/k^{22})^{1/2}$
$M_1 \cdot + M_2 \cdot$	$-d[\text{DB}]/dt = (2k_c + k_{11}[M_1])(k_d k_{21}[M_1][A_2]/k^{12}k_c)^{1/2}$
$M_1 \cdot + M_1$	$-d[\text{DB}]/dt = (2k_c + k_{11}[M_1])(2fk_d[A_2]/k^1[M_1])$
$M_2 \cdot + M_1$	$-d[\text{DB}]/dt = (2k_c + k_{11}[M_1])(2fk_d[A_2]k_{21}/k^2k_c)$

All three of the expressions pertaining to biradical termination predict a dependence of the rate on the square-root of the initiator concentration. This dependence has been noted in the case of methacrylic anhydride polymerization initiated by azobisisobutyronitrile.⁷ A more complex relationship has been found by Smets and Mercier⁸ for acrylic anhydride. However, they noted that their polymerization was carried out under heterogeneous conditions, and an unusual result might, therefore, be expected.

The relationships derived for the cases involving degradative chain transfer predict a dependence of rate on the first power of the initiator concentration. This is as expected from the polymerization of monoallyl monomers. This dependence has been verified experimentally by Mikulasova and Hrivik,⁶ who investigated the *tert*-butyl peroxide-initiated polymerization of diallyldimethylsilane. Holt and Simpson,⁹ in the investigation of a variety of diallyl esters of dicarboxylic acids, did not find an exact proportionality between the rate of loss of monomer and the first power of the initiator for diallyl *o*-phthalate and concluded that some reinitiation by the allylic radicals was responsible.

The dependence of rate on M_1 concentration is different within the two general cases, depending upon the type of termination reaction. For the biradical termination case, the rate of loss of double bonds divided by the M_1 concentration raised to a power of 0, $1/2$, or 1, should be linear when plotted versus the M_1 concentration. Thus, for $M_1 \cdot + M_1 \cdot$ termination, the exponent of $[M_1]$ is zero, and the rate itself plotted versus M_1 concen-

tration should be a linear relationship with a slope of $k_{11}(fk_d[A_2]/k^{11})^{1/2}$. The intercept of this line on the $M_1 = 0$ axis is $2k_c(fk_d[A_2]/k^{11})^{1/2}$. The ratio of the slope to the intercept is $k_{11}/2k_c$.

For $M_2 \cdot + M_2 \cdot$ termination, the exponent of $[M_1]$ is 1, and the rate divided by $[M_1]$ plotted versus $[M_1]$ should be linear with a slope/intercept ratio also of $k_{11}/2k_c$.

For $M_2 \cdot + M_1 \cdot$ termination, the exponent of $[M_1]$ is $1/2$, and the rate divided by $[M_1]^{1/2}$ plotted versus $[M_1]$ should be linear. The slope/intercept ratio here is also $k_{11}/2k_c$.

The expressions resulting from the polymerizations where degradative chain transfer occurs may also be plotted in this manner. Thus, for $M_1 \cdot + M_1$ termination the rate may be plotted versus the reciprocal M_1 concentration to give a slope/intercept ratio of $k_{11}/2k_c$. For $M_2 \cdot + M_1$ termination the rate plotted versus the M_1 concentration leads to the desired slope/intercept ratio.

The k_c/k_{11} Ratio

In cyclopolymerization the critical factor determining the microstructure of the polymer is the rate of the k_c reaction to relative the k_{11} reaction. If the intramolecular process is slow compared with the intermolecular reaction, the polymer will have a large number of pendant unsaturated groups scattered along the chain. As the reaction proceeds farther this will lead to highly branched and/or crosslinked material. If the intramolecular process is fast relative to the intermolecular reaction, the polymer formed will be saturated and linear.

The k_c/k_{11} ratio, which has the units of moles per liter, may be interpreted¹⁰ as the concentration of M_1 necessary for the rate of the intermolecular reaction to equal the rate of the intramolecular reaction. Thus, if for a given system the k_c/k_{11} ratio is 0.50 moles/l., the concentration of M_1 required for the two processes to proceed at equal rates is 0.50 moles/l. At M_1 concentrations greater than this the intermolecular process is faster, while at lower M_1 levels the intramolecular reaction is favored.

In the sections preceding, two general methods for the determination of the k_c/k_{11} ratio have been outlined. For the first method information is required both on the rate of polymerization as a function of $[M_1]$ and the general mechanism of termination. For the second method information is required on the concentration of uncyclized units in the polymer as a function of the monomer concentration. Of these two the second method offers the more straightforward approach to the determination of k_c/k_{11} because it is not dependent upon the nature of the termination reaction. The only general stipulations are that the intermolecular and intramolecular reactions are as described, and that the conversions be held low to prevent large changes in M_1 concentration and polymer composition.

The first method is perhaps best applied to the determination of the general mechanism of termination in these systems by using the k_c/k_{11} ratio supplied by the second method. The rate data may be plotted according

to the two or three types of terminations and the slope/intercept value compared with the $k_{11}/2k_c$ value from the second method. This may give important information on the nature of the radical species present.

Unfortunately there is available in the literature only very few data on either the rates of polymerization or the composition of the polymer as a function of M_1 concentration. Most of those which are available represent high conversion reactions and are, therefore, unsuitable. However, Holt and Simpson⁹ record the data on variation in unsaturation of the polymer as a function of monomer concentration for the polymerization to low conversions of diallyl *o*-phthalate initiated by benzoyl peroxide at 80°C. Their data, converted to the appropriate parameters, are shown plotted in Figure 1. The fit of the experimental points to a linear relationship, as predicted by eq. (31), is excellent. The intercept of the line on the $M_1 = \infty$ axis is slightly higher than the value predicted, 1.25 as opposed to 1.00. The value of k_c/k_{11} obtained from the slope of this plot is 4.25 moles/l. Thus, the M_1 concentration required for the rates of the intermolecular and intramolecular reactions to be equal is 4.25 moles/l. which corresponds to about a 50% dilution of the pure monomer.

It is interesting to compare the values of cyclized versus non cyclized units found for diallyl *o*-phthalate as the M_1 concentration changes. At an $[M_1]$ value of 8.68 moles/l. about 44% of the groups are cyclized. At an $[M_1]$ value of 6.40 moles/l. the cyclized groups represent about 50%, while at an M_1 concentration of 4.22 moles/l. they represent about 57%. At an $[M_1]$ value of 2.50 moles/l. they have increased to 68%. Thus, even with this relatively high k_c/k_{11} value the residual unsaturation in the polymer at an $[M_1]$ value of 2.50 moles/l. is still 16% of the unsaturation of the monomer.

References

1. Butler, G. B., *J. Polymer Sci.*, **48**, 279 (1960).
2. Marvel, C. S., *J. Polymer Sci.*, **48**, 101 (1960).
3. Kolesnikov, G. S., and S. L. Davydova, *Russian Chem. Rev.*, **29**, 679 (1960).
4. Bartlett, P. D., and R. Altschul, *J. Am. Chem. Soc.*, **67**, 816 (1945).
5. Alfrey, T., J. J. Bohrer, and H. Mark, *Copolymerization*, Interscience, New York-London, 1952.
6. Mikulasova, D., and A. Hrivik, *Chem. Zvesti*, **11**, 708 (1957).
7. Gibbs, W. E., and J. T. Murray, *J. Polymer Sci.*, **58**, 1211 (1962).
8. Smets, G., and Mercier, *J. Polymer Sci.*, **A1**, 1491 (1963).
9. Holt, T., and W. Simpson, *Proc. Roy. Soc. (London)*, **A238**, 154 (1956).
10. Bennett, G. M., *Trans. Faraday Soc.*, **37**, 794 (1941).

Résumé

Les cinétiques générales de la propagation alternée interintra-moléculaire sont présentées et discutées. Le fait majeur qui détermine la microstructure du polymère, les vitesses relatives des réactions intra-moléculaires et inter-moléculaires est examiné. A partir des cinétiques générales, des méthodes sont proposées pour la détermination du rapport des constantes de vitesse pour ces réactions. Une méthode simple utilise l'équation: $[m_1]/[M_3] = 1 + (k_c/k_{11})(1/[M_1]_0)$, où $[m_1]$ = la concentration en unités monomériques dans le polymère, $[M_3]$ = la concentration des unités noncyclisées, $[M_1]_0$ =

un paramètre relié à la concentration en monomère k_c = la constante de vitesse de cyclisation et k_{11} = la constante de vitesse pour la propagation linéaire. D'autres méthodes qui peuvent donner des informations sur la vitesse de la réaction de terminaison sont discutées.

Zusammenfassung

Die allgemeine Kinetik des alternierenden inter-intramolekularen Wachstums wird entwickelt und diskutiert. Der Hauptfaktor für die Mikrostruktur des Polymeren, die relative Geschwindigkeit der intramolekularen und der intermolekularen Reaktion, wird untersucht. Aus dem kinetischen Schema werden Methoden zur Bestimmung des Verhältnisses der Geschwindigkeitskonstanten dieser Reaktionen hergeleitet. Eine einfache Methode geht von der Gleichung: $[m_1]/[M_3] = 1 + (k_c/k_{11})(1/[M_1]_0)$ aus, wo $[m_1]$ die Konzentration der Monomereinheiten im Polymeren, $[M_3]$ die Konzentration der nicht-cyclisierten Einheiten, $[M_1]$ ein Parameter für die Monomerkonzentration, k_c die Geschwindigkeitskonstante für die Cyclisierung und k_{11} die Geschwindigkeitskonstante für das lineare Wachstum ist. Andere Methoden, die eine Information über die Natur der Abbruchsreaktion liefern können, werden diskutiert.

Received July 1, 1963

Revised October 2, 1963

Cyclopolymerization. IV. Structure of Polymethacrylic Anhydride and Kinetics of Polymerization of Methacrylic Anhydride*

G. SMETS, P. HOUS, and N. DEVAL, *Laboratoire de Chimie Macromoléculaire, University of Louvain, Belgium*

Synopsis

The cyclopolymerization of methacrylic anhydride at 36.6°C. produces a polymer whose structure has been examined by infrared spectrometry and bromometric analysis. This polymer contains mainly hexaatomic rings of the A type (absorption bands at 1800 and 1760 cm.^{-1}) and open anhydride units with unsaturated side-groups, the content of which varies only slightly with the monomer concentration. Polymerization at 100°C. produces some syndiotactic hexaatomic rings (1730 cm.^{-1}). Chemical analysis of the polymers obtained at 36.6°C. for different monomer concentrations permitted the ratio of the rate constants of vinyl propagation to that of cyclization to be evaluated. This ratio is 0.022 l./mole, compared to 0.17 l./mole for acrylic anhydride. From a plot of the reciprocal of the degree of cyclization against the monomer concentration the values of the ordinate intercepts are interpreted on the basis of chain transfer reaction with monomer and intramolecular isomerization. From a kinetic point of view, the order of reaction at 36.6°C. with respect to the concentration of initiator varies from 0.66 to 0.58 for monomer concentrations of 0.656 and 3.282 mole/l., respectively. With respect to the monomer concentration, the order of reaction is one up to a concentration of 3 mole/l.; above this concentration, the order increases progressively. This behavior can be easily explained by the progressive insolubilization of the polymer and the increasing viscosity of the solution.

I. INTRODUCTION

The chemical structure of polyacrylic anhydride has been discussed recently² on the basis of infrared spectrometric and analytical data. It was found that two different types of cyclized hexaatomic anhydrides can be formed. Although the isotactic (meso) variety is the more stable, nevertheless the syndiotactic (racemic) one is first formed and isomerizes under the influence of the temperature or of the solvent. The possibility of isomerization is related to the presence of the α -hydrogen atoms and would involve enolization. It was therefore of interest to examine the stereochemical structure of the polymethacrylic homolog where this enolization and consequently the isomerization are impossible. On the other hand, it has been found that polyacrylic anhydride always contains appreciable unsaturation, which is responsible for further gelation and insolubilization

* For the preceding paper in this series see Roovers and Smets.¹

of the polymer. These results differ considerably from those of Jones³ and Butler,⁴ who ascribed a completely cyclized structure to such polymers. From this point of view again a difference between the acrylic and methacrylic series may be expected, α -methyl groups favoring cyclization. The stereochemical configuration of polymethacrylic anhydride has already been discussed by several authors. Tiers and Bovey⁵ on the basis of nuclear magnetic resonance measurements on the derived polymethyl methacrylates,⁶ evaluated the apparent difference in activation enthalpy for the isotactic and syndiotactic propagation steps to be approximately 440 cal. The stereoconfiguration was reexamined more recently by Hwa.⁷

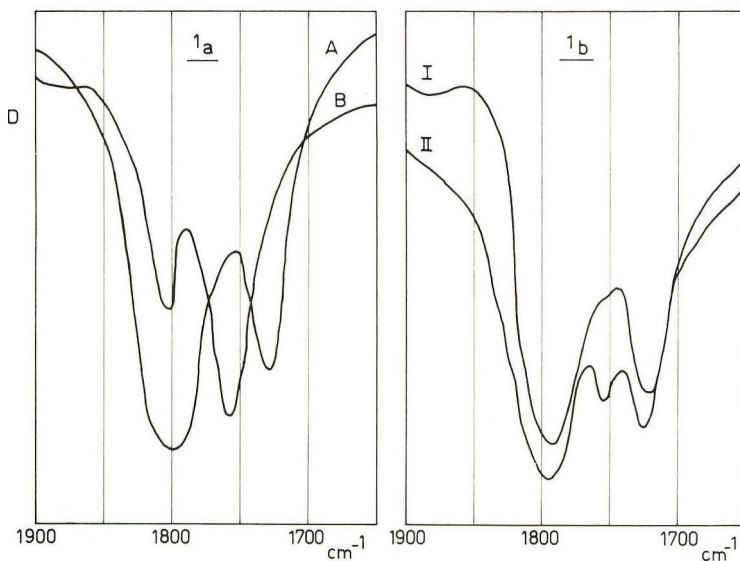


Fig. 1. Infrared spectra of methacrylic anhydride polymers: (a) polymethacrylic anhydride prepared (A) in bulk at 100°C. and (B) in cyclohexanone solution at 36.6°C.; (b) copolymers of methacrylic anhydride (M_1) and styrene prepared in cyclohexanone at 36.6°C.

Using the same NMR technique, Miller, Brey, and Butler⁸ described the polymerization of methacrylic anhydride under various conditions in order to determine whether the cyclopolymerization exerts any influence on the stereoconfiguration and have found that the percentage of isotactic units increases with the polymerization temperature and predominates at higher temperatures (60–80°C.). At lower temperatures (30°C.) more random distribution prevails.

We will consider in the present paper the kinetics of polymerization especially in relation with the unsaturation of the polymer. Some new infrared data will also be reported; their interpretation and band assignments remain however unclear, in view of the previously described NMR data.

II. INFRARED SPECTROSCOPY

Hexaatomic Cyclic Anhydrides

All the polymers prepared by cyclopolymerization of the anhydride at 36.6°C. show a pair of carbonyl absorption bands at 1800 and 1760 cm.^{-1} , the band at 1760 cm.^{-1} showing the highest intensity (isomer A) (Fig. 1a). When the polymerization was carried out in bulk at 100°C., two absorption bands appear at 1800 and 1730 cm.^{-1} of which the 1800 cm.^{-1} one is the most intense (isomer B). The relative intensity dissymmetry of the two bands has been found in most cases, and is usually considered to be characteristic of the system.⁹ It may be worthwhile to point out that in copolymers of methacrylic anhydride with styrene and methacrylonitrile (which are reported in another paper¹⁰) three C=O absorption bands are present and consequently both types of isomers are present simultaneously; the absorption at 1760 cm.^{-1} increases, however, with increasing molar fraction of the anhydride (Fig. 1b).

Vinyl Side Groups

The presence of open anhydride units with vinyl side groups has been demonstrated on the basis of the C=C stretching vibrations absorption at 1625 cm.^{-1} ; its intensity increases with the monomer concentration. This unsaturation was quantitatively confirmed by bromometric measurements and has been related to the kinetics of polymerization.

In copolymers with styrene the unsaturation is higher than in the homopolymer and increases with increasing styrene concentration. Contrarily, the presence of methacrylonitrile has no influence on the degree of unsaturation of the polymers. These effects are likely to be related to differences in polarities of the monomers.

Pentaatomic Cyclic Anhydrides

On the contrary, no five-membered cyclized anhydrides have been detected for methacrylic polymers, any absorption at higher frequency due to the strain of a five-membered ring being absent.¹¹

Infrared analysis has also been applied to polymethacrylic anhydride prepared by dehydration of polymethacrylic acid. Indeed, it is well known that this reaction can be carried out by heating up the acid in the solid state^{12,13} or in the presence of acetic anhydride as it was in our experiments. This last reaction proceeds quantitatively. In addition to formation of cyclic anhydride units, some crosslinking occurs, causing the insolubility of the polymer. No mixed acrylic-acetic acid anhydride units are formed; this has been proved by the absence of any volatile acid on steam distillation, when carried out in the presence of the solid polyanhydride after its isolation. The C=O absorption frequencies are identical with those of the isomer A (1800 and 1760 cm.^{-1}), the lowest frequency band being also the most intense.

III. KINETICS

Cyclization and Vinyl Propagation

If one assumes that the degree of unsaturation is determined only by the relative importance of the bimolecular propagation reaction with respect to the intramolecular cyclization reaction, the reciprocal of the molar fraction of cyclization units f_c should be related to the monomer concentration by the equation

$$1/f_c = 1 + (2k_{11}/k_c)[M] = 1 + 2K[M]$$

where k_{11} and k_c are the respective rate constants.² Experimentally it was found that the unsaturation of the polymers is independent of the amount of initiator (AIBN) and varies with the monomer concentration. By plotting the ratio of vinyl unsaturated/cyclized units ($1/f_c - 1$) against the monomer concentration, a linear diagram is obtained; however, an intercept of 0.3 has been found instead of a plot passing through the origin (Fig. 2).

In all these experiments the degree of conversion was kept below 10%. The polymer was precipitated in dry ether and the degree of unsaturation determined by bromometry. Curve *m* of Figure 2 shows that the unsaturation of the polymers varies only slightly with the monomer concentration; from the slope a value of $K = 0.022$ l./mole has been determined. Curve *a* corresponds to the polymerization of acrylic anhydride, of which the unsaturation was studied as a function of the monomer concentration (intercept equal to 0.13).

Table I shows that the relative cyclization tendency is much more pronounced for methacrylic anhydride than for acrylic anhydride. As expected, the presence of the α -methyl groups is responsible for both effects.

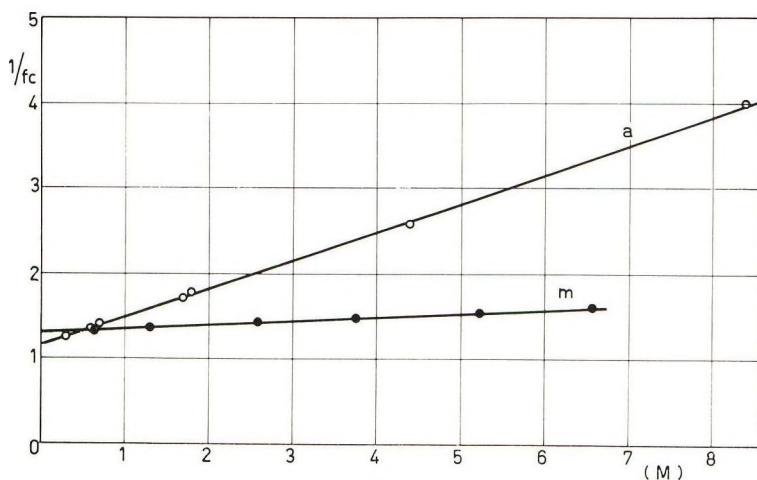


Fig. 2. Dependence of the degree of cyclization f_c on the monomer concentration: (a) acrylic anhydride; (m) methacrylic anhydride.

TABLE I
Influence of the Monomer Concentration on the Degree of Cyclization^a

Methacrylic anhydride (36.6°C.)			Acrylic anhydride (35°C.)		
[M], mole/l.	1/ <i>f_c</i>	<i>K</i> = <i>k₁₁</i> / <i>k_c</i> , l./mole	[M], mole/l.	1/ <i>f_c</i>	<i>K</i> = <i>k₁₁</i> / <i>k_c</i> , l./mole
6.572	1.59	0.022	8.4	4	0.17
5.256	1.54		4.4	2.57	
3.751	1.47		1.8	1.75	
2.624	1.43		1.7	1.72	
1.311	1.35		0.7	1.40	
0.656	1.33		0.6	1.33	
			0.3	1.25	

^a Solvent: cyclohexanone; [AIBN]: 0.0194 mole/l.

The degree of unsaturation is only slightly affected by the monomer concentration. Several factors may account for intercept values higher than unity; they will be considered successively, although they could intervene simultaneously.

(1) The bromometric method used for the determination of the unsaturation usually gives higher values than infrared spectrometry, although reproducible. Therefore a value a little higher than unity could be expected.

(2) Chain transfer reactions between an open unit radical (*k'_{trM}*) and/or a cyclized radical (*k'_{trM}*) with monomer are possible. In our experiments chain transfer with initiator (AIBN) are not considered. On the other hand the chain transfer constant between a methyl acrylate growing chain and cyclohexanone is only equal to 5.5×10^{-4} at 80°C.,⁹ so that by analogy transfer with solvent may be neglected. Consequently the rate of production of unsaturated units becomes

$$R_v = 2/[M](k_{11}[M^0] + k_{trM}[M^0] + k'_{trM}[m^0])$$

while the rate of cyclization *R₂* remains unchanged, i.e. *k₂*[*M₀*]. In this equation [*M⁰*] and [*m⁰*] are the concentrations of open and cyclized radi-

$$[m^0] = k_c[M^0]/2[M](k_{31} + k'_{trM})$$

cals, respectively. Assuming steady-state conditions the concentration of cyclized radicals is equal to *k₃₁* being the rate of addition of a cyclic radical to a double bond of a monomer molecule. The reciprocal of the degree of cyclization is then expressed by

$$1/f_c = 1 + R_t/R_c = 1 + [1/(1 + k_{31}/k'_{trM})] + 2[M][(K + k_{trM})/k_c]$$

A plot of 1/*f_c* against [M] gives an intercept higher than unity, depending on the relative importance of propagation with respect to transfer with monomer; the slope of the plot is a measure of *K* (= *k₁₁*/*k₂*), considering that *k_{trM}* ≪ *k₂* < *k₂*. This interpretation alone is however insufficient, because it affords much too high values for the ratio *k'_{trM}*/*k₃₁*.

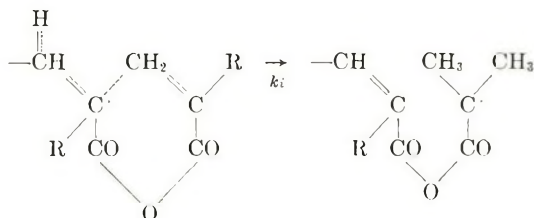
(3) Another possibility resides in an eventual intramolecular isomerization of an open unit with production of more stable radicals; this isomerization should be favored by the pseudo-cyclic structure of the system. In this case the rate of production of unsaturated units is given by the expression

$$R_p = 2[M]k_{11}[M^0] + k_i[M^0]$$

and the reciprocal of the degree of cyclization f_c becomes:

$$1/f_c = 1 + R_p/R_c = 1 + k_i/k_c + (2k_{11}/k_c)[M]$$

for the reaction



Influence of the Initiator and Monomer Concentrations

Two series of experiments were carried out at constant monomer concentration in cyclohexanone solution. The data are given in Table II. From a logarithmic plot of the rate of polymerization versus the initiator concentration, an apparent order of reaction of 0.66 and 0.58 has been found. At the same temperature of 36.6°C. the pure thermal rate of polymerization of methacrylic anhydride in bulk is only 3×10^{-6} mole/l./min., a value negligible compared to that of the rate of chemically initiated polymerization.

With respect to the monomer concentration, the order of reaction is one for a concentration range up to about 3 mole/l.; above that, the rate in-

TABLE II
Influence of the Initiator Concentration on Polymerization of Methacrylic Anhydride^a

[M], mole/l.	[Initiator] $\times 10^2$, mole/l.	$R_p \times 10^4$, mole/l.-min.	$\log R_p$ $\log [I]$
0.656	1.94	2.2	0.66
	3.68	3.5	
	6.39	5.1	
	10.67	6.8	
3.282	0.4	7.0	0.58
	0.63	9.8	
	1.29	13.3	
	1.97	19.6	

^a Temp.: 36.6°C.; solvent: cyclohexanone.

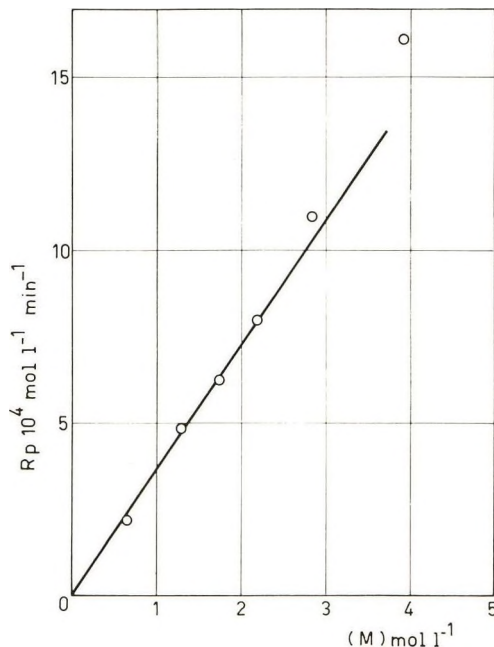


Fig. 3. Dependence of rate on the monomer concentration. Polymerization in cyclohexanone at 36.6°C.; [Init] = 1.94×10^{-2} mole/l.

creases more rapidly. The data are given in Table III and represented in Figure 3.

This order of reaction higher than unity for the monomer dependence has also been found recently by Gibbs and Murray¹⁵ and has been known for a long time for the case of methyl methacrylate,¹⁶ methyl acrylate, and acrylic acid.¹⁷ The increasing viscosity of the solution, the progressive heterogeneity of the reaction medium, as well as some trapping of radicals (which was demonstrated previously for the polymerization of acrylic anhydride²) can easily account for the changing order of reaction with respect to initiator and monomer concentration.

TABLE III
Influence of the Monomer Concentration on Polymerization of
Methacrylic Anhydride at 36.6°C.^a

[M], mole/l.	$R_p \times 10^4$, mole/l.-min.
0.655	2.2
1.312	4.8
1.749	6.2
2.187	8.0
2.844	11.0
3.939	16.1
6.572	81.2

^a Solvent: cyclohexanone; [AIBN]: 0.0194 mole/l.

IV. EXPERIMENTAL

Methacrylic anhydride was prepared by reaction of 40 ml. methacryloyl chloride with 50 g. dry sodium methacrylate. The monomer was purified by repeated fraction distillation; boiling point 44°C./0.6 mm. Hg. Its purity was determined by infrared and chemical analyses.

Cyclohexanone was freshly distilled under nitrogen before use.

The rate of polymerization was measured dilatometrically. The high vacuum filling technique described by Matheson et al. was used.¹⁷ As previously, it was assumed that the volume contraction remains the same, whatever new unit may be included or not in a cycle. Table IV gives a typical series of measurements obtained for the rate determination.

TABLE IV
Polymerization of Methacrylic Anhydride in Cyclohexanone at 36.6°C.^a

Time, min.	$-\Delta[M] \times 10^4$, mole/l. ⁻¹
5	21
10	42
15	55
20	66
25	83
30	94
35	113
40	130
45	154
50	182
55	193
60	205
65	220
70	232
75	248
80	269
85	297
90	314
95	324
100	347

^a [M]: 0.657 mole/l.; [AIBN]: 0.0376 mole/l.

The isolation of the polymer was carried out by adding dry diethyl ether to the polymer solution. The powdery precipitate was washed repeatedly with dry ether and dried under high vacuum.

The infrared spectra were recorded in Nujol suspension with a Perkin-Elmer 21 double-beam spectrometer equipped with rock salt prism. The degree of unsaturation was determined by bromometry by using the method of Polgar and Jungnickel;^{2,18} it was determined that polyacrylic and polymethacrylic acids are inert toward bromine in these experimental conditions.

The transformation of *polymethacrylic acid into polymethacrylic anhydride* was carried out by dissolving the polyacid in dimethyl sulfoxide adding an

excess of acetic anhydride and heating up at 80°C. After reaction, the solution was diluted with dimethylformamide and poured into diethyl ether. After washing the precipitate with diethyl ether it was dried under high vacuum.

V. CONCLUSIONS

The radical cyclopolymerization of methacrylic acid produces a polymer containing large amounts of cyclized hexaatomic units and some side unsaturated acrylic groups; the content of these vinyl units varies only slightly with the monomer concentration. The relative cyclization tendency of methacrylic anhydride versus propagation is much higher than that of acrylic anhydride. On account of the progressive insolubilization of the polymer and the increasing viscosity of solution, the order of polymerization reaction versus monomer and initiator concentrations deviates progressively from the normal behavior.

The authors are indebted to the Institut pour l'encouragement de la Recherche Scientifique dans l'Industrie et l'Agriculture (I.R.S.I.A.) for a fellowship to two of them (P. H. and N. D.), and to the Centre des Hauts Polymères and Gevaert Photoproducten N.V. Antwerp for supporting this research.

References

1. Roovers, J., and G. Smets, *Makromol. Chem.*, **60**, 89 (1963).
2. Mercier, J., and G. Smets, *J. Polymer Sci.*, **A1**, 1491 (1963); *J. Polymer Sci.*, **57**, 763 (1962).
3. Jones, J. F., *J. Polymer Sci.*, **33**, 7, 15 (1958).
4. Butler, G. B., and A. Crawshaw, *J. Am. Chem. Soc.*, **80**, 5464 (1958).
5. Bovey, F. A., and G. V. D. Tiers, *J. Polymer Sci.*, **44**, 173 (1960).
6. Tiers, G. V. D., and F. A. Bovey, *J. Polymer Sci.*, **47**, 479 (1960).
7. Hwa, J. C. H., *J. Polymer Sci.*, **60**, S12 (1962).
8. Miller, W. L., W. S. Brey, Jr., and G. B. Butler, *J. Polymer Sci.*, **54**, 329 (1961).
9. Jones, R. N., and C. Sandorfy, *Techniques of Organic Chemistry*, Vol. IX, A. Weissberger, Ed., Interscience, New York (1956) p. 496.
10. Smets, G., N. Deval, and P. Hous, *J. Polymer Sci.*, **A2**, 4835 (1964).
11. Zbinden, R., and M. K. Hall, *J. Am. Chem. Soc.*, **80**, 6428 (1958); *ibid.*, **82**, 1215 (1960).
12. Grant, D. H., and N. Grassie, *Polymer*, **1**, 125 (1960).
13. Bresler, S. E., N. M. Koton, A. T. Os'minskaia, A. G. Popov, and M. N. Savitskai, *Polymer Sci. U.S.S.R.*, **1**, 393 (1960).
14. Thomas, W. M., *J. Polymer Sci.*, **11**, 399 (1953); *ibid.*, **14**, 489 (1954); *ibid.*, **17**, 275 (1955); *Makromol. Chem.*, **17**, 29 (1955).
15. Gibbs, W. E., and J. T. Murray, *J. Polymer Sci.*, **58**, 1211 (1962).
16. Norrish, R. G. W., and R. R. Smith, *Nature*, **150**, 336 (1942); G. V. Schulz and G. Harborth, *Makromol. Chem.*, **1**, 106 (1947).
17. Matheson, M. S., E. E. Auer, E. B. Bevilacqua, and E. J. Hart, *J. Am. Chem. Soc.*, **71**, 497 (1949); *ibid.*, **73**, 5395 (1951).
18. Polgar, A., and J. L. Jungnickel, *Organic Analysis*, Vol. III, J. Mitchell, Jr., I. M. Kolthoff, E. S. Proskauer, and A. Weissberger, Eds. Interscience, New York, 1956, p. 240.

Résumé

La cyclopolymérisation de l'anhydride méthacrylique à 36,6°C produit un polymère dont la structure a été étudiée par spectrométrie infrarouge et par bromométrie; ce polymère contient principalement des cycles hexaatomiques de type-A (bandes à 1800 et 1760 cm^{-1}) et des unités anhydrides ouverts à groupe insaturé latéral, dont la teneur ne varie que faiblement avec la concentration en monomère. La polymérisation à 100°C fournit quelques cycles hexaatomiques syndiotactiques (1730 cm^{-1}). Par analyse chimique des polymères obtenus à 36,6°C à différentes concentrations en monomère, on a pu évaluer le rapport des constantes de vitesse de propagation vinylique à celle de cyclisation; il est égal à 0.022 l/mole au lieu de 0.17 pour l'anhydride acrylique. Au départ d'un diagramme portant l'inverse du degré de cyclisation en fonction de la concentration en monomère, on obtient des valeurs extrapolées à l'axe des ordonnées, dont l'interprétation est basée sur des réactions de transfert sur monomère, et d'isomérisation intramoléculaire. Du point de vue de la cinétique globale, l'ordre de réaction à 36,6°C par rapport à la concentration en initiateur varie de 0.66 à 0.58 pour des concentrations en monomère de 0.656 et 3.282 mole/l respectivement. Par rapport à la concentration en monomère, l'ordre est unitaire jusqu'à 3 mole/l; au-delà l'ordre croît à des valeurs plus élevées. Ce comportement peut aisément être expliqué par l'insolubilisation progressive du polymère et l'augmentation de la viscosité de la solution.

Zusammenfassung

Die Cyclopolymerisation von Methacrylsäureanhydrid bei 36,6°C führt zu einem Polymeren, dessen Struktur durch Infrarotspektrometrie und bromometrische Analyse untersucht wurde. Das Polymere enthält hauptsächlich sechsatomige Ringe vom A-Typ (Absorptionsbanden bei 1800 und 1760 cm^{-1}) und offene Anhydridbausteine mit ungesättigten Seitengruppen, deren Gehalt nur wenig von der Monomerkonzentration abhängt. Die Polymerisation bei 100°C liefert einige syndiotaktische sechsatomige Ringe (1730 cm^{-1}). Durch chemische Analyse der bei 36,6°C und verschiedenen Monomerkonzentrationen erhaltenen Polymeren konnte das Verhältnis der Geschwindigkeitskonstanten für Vinylwachstum und Zyklisierung bestimmt werden; es beträgt 0,022 l. Mol⁻¹ im Vergleich zu 0,17 bei Acrylsäureanhydrid. In Diagramm reziproker Zyklisierungsgrad gegen Monomerkonzentration werden die Werte des Ordinatenabschnittes auf Grundlage der Kettenübertragung mit dem Monomeren und der intramolekularen Isomerisierung interpretiert. Die kinetische Reaktionsordnung in bezug auf den Starter variiert bei 36,6°C von 0,66 bei einer Monomerkonzentration von 0,656 zu 0,58 bei einer solchen von 3,282 Mol.l⁻¹. In bezug auf das Monomere besteht die Reaktionsordnung eins bis zu einer Konzentration von 3 Mol. l⁻¹; oberhalb dieser Konzentration nimmt die Ordnung stetig zu. Dieses Verhalten kann durch das fortschreitende Unlöslichwerden des Polymeren und die zunehmende Viskosität der Lösung leicht erklärt werden.

Received February 4, 1964

Cyclopolymerization. V. Copolymerization of Acrylic and Methacrylic Anhydrides with Vinyl Monomers

G. SMETS, N. DEVAL, and P. HOUS, *Laboratoire de Chimie Macromoléculaire, University of Louvain, Belgium*

Synopsis

The copolymerizations of acrylic (AA) and methacrylic (MAA) anhydrides (M_1) with styrene (St) and methacrylonitrile (MAN) have been examined; similarly that of acrylic anhydride with allyl chloride. In these systems the reactivity ratio of an open unit radical (r_1) is equal to that of a cyclized radical (r_3), and the usual Alfrey-Price equation is valid. By using a graphical method the ratios of the cross propagation rate constant to the cyclization rate constant (k_{12}/k_c) have been also evaluated. The following values for r_1 , r_2 , and k_{12}/k_c respectively have been found, M_1 being the anhydride: for the system AA (M_1)-St, 0.1, 0.17, and 4; for the system AA-MAN, 0.9, 0.04, and 0.14; for the system AA-allyl chloride, 11.5, 0.01, and 0. For the same systems with MAA, the values of r_1 , r_2 , and k_{12}/k_c were 0.26, 0.12, and 0.2 with St, and 1.6, 0.27, and about zero with MAN. These data indicate also that the cyclization reaction is always more pronounced for methacrylic anhydride than for the acrylic anhydride.

I. INTRODUCTION

The copolymerization of divinyl monomers undergoing cyclization with another monomer has been considered by several authors from the point of view of the solubility of the copolymers; in this sense the copolymerizations of diallyl ether with maleic anhydride¹ and of diallyldimethylammonium chloride with acrylonitrile and acrylamide² have been described.

Marvel and Vest studied the copolymerization of α, α' -dimethylene-pimelic dinitrile and dimethyl ester with acrylonitrile and methyl acrylate and showed also the influence of the monomer ratio on the solubility, and consequently on the degree of branching and crosslinking of the copolymers.³ Similarly, Milford pointed out the influence of the monomer concentration on the solubility of various copolymers of substituted heptadienes.⁴

More recently Matsuyan and co-workers have especially studied the copolymerization of several divinyl acetals with each other or with foreign vinyl monomers; they obtained soluble and fusible divinylbutyral-styrene copolymers.⁵

A quantitative study has been published by one of us⁶ on the case of the copolymerization of vinyl cinnamate, and a more elaborate kinetic analysis of the phenomena has been proposed, assuming an addition of vinyl cinnamate

mate essentially through the vinyl group, and consequently one type of growing radical M_1^* .

In the present paper the same kinetic scheme has been applied to the study of the copolymerization of acrylic and methacrylic anhydrides on the basis of their symmetrical structures.

Hwa and Miller⁷ have already examined the copolymerization of methacrylic anhydride with vinyl monomers and considered the kinetic requirements for producing a soluble copolymer. They assumed that the rate of cyclization is very much greater than the rate of bimolecular propagation with a new anhydride or comonomer molecule. On this basis they obtained a copolymer composition equation similar to the common Alfrey-Price equation, in which the reactivity ratios measure the competition between a methacrylic group and the comonomer for the cyclized radical and for the chain radical ending in the comonomer. Moreover they showed that soluble copolymers were more likely to form: (1) the less reactive the comonomer (e.g., with benzyl vinyl sulfone, 2-chloroethyl vinyl ether, and allyl urea, allyl chloroacetate soluble products are obtained, while with styrene and methyl and hexyl methacrylate the copolymers are always insoluble); (2) the greater the dilution (the cyclization rate being unimolecular is independent of the concentration); (3) the lower the conversion; (4) the greater the difference in moles of the two components in the charge.

It must be pointed out that no determination of unsaturation was reported by these authors. Moreover with highly reactive monomers, such as methacrylates, styrene, and ethyl acrylate, the conversions were too high to permit an evaluation of copolymerization parameters. One major difference between their results⁷ and ours⁸ consists in their claim that pure methacrylic anhydride cyclopolymerizes without gelation; the validity of their solubility criterion, however, may be contested, because on heating at 130–150°C. intramolecular cyclic anhydride formation may proceed easily between neighboring side chains.

Nevertheless, as far as possible, a comparison between the results will be established and discussed in the present paper.

II. COPOLYMER COMPOSITION EQUATIONS

As shown previously by Roovers and Smets,⁶ the copolymerization of a diene monomer undergoing cyclization involves at least six bimolecular propagation steps besides the monomolecular cyclization reaction. Assuming steady-state conditions, the copolymer composition equation becomes:

$$\frac{d[M_1]}{d[M_2]} = \frac{[M_1]}{[M_2]} \left\{ \frac{r_1[M_1] + [M_2] + K'_c}{r_2[M_2] + [M_1] + K'_c \left(\frac{r_2[M_2] + [M_1]}{r_3[M_1] + [M_2]} \right)} \right\} \quad (1)$$

where $[M_1]$, $[M_2]$, r_1 , and r_2 have the usual significance, while $r_3 = k_{31}/k_{32}$ is the reactivity ratio of the cyclized radical towards the monomers M_1 and

M_2 , and $K_c = k_c/k_{11}$, and $K'_c = k_c/k_{12}$ are the ratios of the monomolecular cyclization rate constant k_c to that of monomer and comonomer addition to an open unit.

Equation (1) relates the copolymer composition to the absolute monomer concentration; it becomes equal to the usual Alfrey-Price equation, when the cyclization constants K_c and K'_c are very high, or when r_1 is equal to r_3 .

Similarly the ratio of polymerized diene monomer (M_1) to the amount of cyclized units in the copolymer (m) can be expressed by

$$\frac{d[M_1]}{d[m]} = 1 + \frac{[M_1]}{K_c} + \frac{[M_2]}{K'_c} \quad (2)$$

this equation relates the copolymer composition and the degree of cyclization to the cyclization parameters K_c and K'_c .

When the degree of cyclization of the diene is independent of the presence of the second monomer ($k_{12} \rightarrow 0$) these equations give on simplification:

$$\frac{d[M_1]}{d[M_2]} = \left\{ \frac{[M_1]}{[M_2]} \left(\frac{r_3[M_1] + [M_2]}{r_2[M_2] + [M_1]} \right) \right\} \left(1 + \frac{[M_1]}{K_c} \right) \quad (3)$$

$$\frac{d[M_1]}{d[m]} = 1 + \frac{[M_1]}{K_c} \quad (4)$$

III. RESULTS

Copolymerization with Styrene and Methacrylonitrile

The cyclopolymers of acrylic and methacrylic anhydrides with styrene and methacrylonitrile have been examined and compared to each other. Both comonomers are unreactive toward the anhydride function; moreover the copolymers are soluble in cyclohexanone and their composition can be easily determined by chemical analysis.

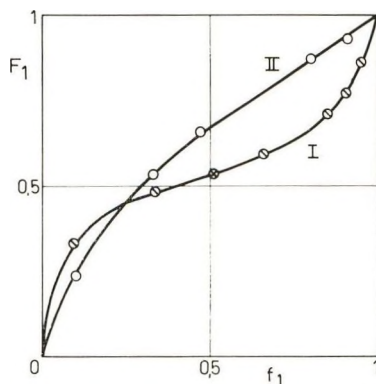


Fig. 1. Copolymerization of methacrylic anhydride with (I) styrene and (II) with methacrylonitrile.

As can be seen from Tables I and II, at the same monomer ratio, the copolymer composition is independent of the overall monomer concentration in both cases, i.e. $r_3 = r_1$; consequently the usual Alfrey-Price equation can be used instead of the more elaborate one. The reactivity ratios r_1 and r_2 were evaluated by the method of Fineman and Ross⁸ (Figs. 1 and 2).

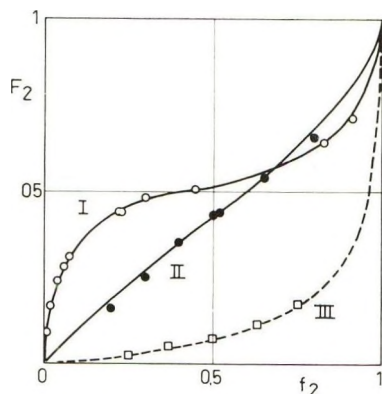


Fig. 2. Copolymerization of acrylic anhydride with (I) styrene, (II) with methacrylonitrile, and (III) with allyl chloride.

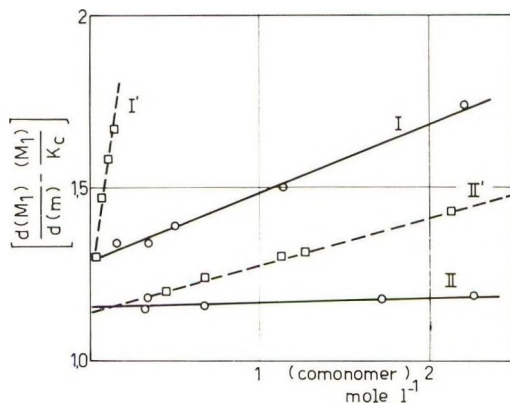


Fig. 3. Copolymerization of methacrylic anhydride (—) and acrylic anhydride (---) with (I) styrene and (II) with methacrylonitrile. Determination of $K'_c = k_c/k_{12}$.

The different K'_c values were determined graphically by plotting $\{[d[M_1]/d[m]] - ([M_1]/K_c)\}$ versus the comonomer concentration (M_2) in agreement with the eq. (2). The values of K_c for acrylic and methacrylic anhydrides used in this equation have been determined and are equal respectively to 6 and 45 per C=C bond.⁹ Some of the data summarized in Tables I and II are represented in Figure 3. F_2 and f_2 represent the mole fractions of monomer M_2 in the copolymer and the unreacted monomer mixture, respectively.

TABLE I
 Copolymerization of Methacrylic Anhydride (M_1)^a

Comonomer (M_2)	$[M_1]$, mole/l.	$[M_2]$, mole/l.	$[M_1]$ + $[M_2]$, mole/l.	f_2	F_2	F_1		$d[M_1]$
						Unsat. units	Cy- clized units	$\frac{d[m]}{[M_1]}$ K_c
Styrene	1.271	1.271	2.542	0.5	0.484			
	1.656	1.656	3.312	0.5	0.473			
	2.21	2.21	4.421	0.5	0.47	0.25	0.28	1.74
	3.167	0.163	3.33	0.049	0.14	0.28	0.58	1.34
	3.052	0.345	3.397	0.101	0.22	0.25	0.52	1.34
	2.979	0.502	3.481	0.145	0.29	0.25	0.47	1.39
	2.253	1.144	3.397	0.335	0.41	0.22	0.37	1.50
	1.156	2.244	3.40	0.66	0.52			
	0.34	3.06	3.40	0.9	0.67			
Methacrylo- nitrile	3.618	0.905	4.523	0.2	0.13			
	2.703	0.676	3.379	0.2	0.13	0.22	0.65	1.16
	1.348	0.337	1.685	0.2	0.13			
	3.071	0.318	3.389	0.094	0.07	0.22	0.71	1.15
	1.356	0.329	1.685	0.195	0.13	0.22	0.65	1.18
	1.497	1.725	3.222	0.53	0.34	0.16	0.50	1.18
	1.127	2.276	3.403	0.67	0.47	0.12	0.41	1.19
	0.34	3.06	3.40	0.9	0.76			

^a Temperature 36.6°C.; $[AIBN] = 0.02$ mole/l.

The plot corresponding to eq. (4) is represented by Figure 4; the slope indicates a K_c value of six, while the intercept at the ordinates is equal to 1.1 instead of one. These results agree remarkably with the data from homopolymerization experiments previously described.⁹

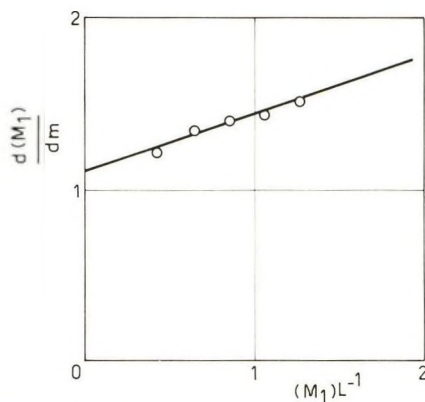


Fig. 4. Copolymerization of acrylic anhydride with allyl chloride. Determination of K_c .

Copolymerization with Allyl Chloride

The low reactivity value of allyl chloride with respect to acrylic derivatives¹⁰⁻¹⁴ makes the system allyl chloride-acrylic anhydride more simple

TABLE II
 Copolymerization of Acrylic Anhydride (M_1)^a

Comonomer (M_2)	$[M_1]$, mole/l.	$[M_2]$, mole/l.	$[M_1]$ + $[M_2]$, mole/l.	f_2	F_2	F_1		$d[M_1]$
						Unsat. units	Cy- clized units	$\frac{d[m]}{[M_1]}$ K_c
Styrene	5.152	1.515	6.66	0.227	0.44			
	3.24	0.95	4.19	0.227	0.44			
	1.94	0.57	2.51	0.227	0.44			
	1.275	1.042	2.137	0.449	0.505			
	1.275	0.554	1.829	0.302	0.48			
	1.275	0.361	1.639	0.219	0.44			
	1.717	0.145	1.862	0.077	0.31	0.38	0.31	1.67
	1.717	0.11	1.827	0.06	0.28	0.39	0.33	1.58
	1.717	0.076	1.793	0.042	0.24	0.39	0.37	1.47
	1.717	0.041	1.758	0.023	0.17	0.39	0.44	1.3
	1.717	0.019	1.737	0.011	0.094			
	0.385	1.77	2.055	0.83	0.64			
	0.112	1.170	1.282	0.913	0.71			
	Methacrylo- nitrile	1.449	0.944	2.393	0.4	0.35		
2.863		1.861	4.724	0.4	0.36			
2.931		1.90	4.831	0.4	0.35			
1.81		0.45	2.26	0.2	0.16	0.38	0.46	1.20
1.58		0.68	2.26	0.3	0.25	0.33	0.42	1.24
1.13		1.13	2.26	0.5	0.43	0.23	0.34	1.3
0.45		1.81	2.26	0.8	0.656			
1.175		1.269	2.444	0.52	0.44	0.23	0.33	1.31
1.178		2.13	3.318	0.65	0.54	0.21	0.25	1.43

^a Temperature 35°C.; $[AIBN] = 0.02$ mole/l.

than those with styrene and methacrylonitrile, and it may be expected that equations (3) and (4) will be valid in this particular case. Indeed as can be seen from Table III, allyl chloride is only poorly incorporated in the copolymers, and exerts practically no influence upon the degree of cyclization of acrylic anhydride polymers (about 65%); the addition of allyl chloride proceeds only with the cyclized radical. The copolymer composition diagram is given in Figure 2, curve III.

 TABLE III
 Copolymerization of Acrylic Anhydride with Allyl Chloride (M_2)^a

$[M_1]$, mole/l.	$[M_2]$, mole/l.	f_2	F_2	F_1		$d[M_1]$
				Unsat. units	Cyclized units	$\frac{d[m]}{[M_1]}$
1.277	0.425	0.25	0.027	0.329	0.644	1.51
1.064	0.638	0.37	0.053	0.292	0.655	1.44
0.851	0.851	0.50	0.076	0.279	0.645	1.40
0.638	1.064	0.63	0.117	0.230	0.653	1.35
0.425	1.277	0.75	0.175	0.151	0.674	1.22

^a Temperature = 35°C.; $[AIBN] = 0.02$ mole/l.; $[M_1] + [M_2] = 1.702$ mole/l.

TABLE IV
 Copolymerization Data of Acrylic and Methacrylic Derivatives

M ₁	Styrene			Methacrylonitrile			Allyl chloride		
	r ₁ = r ₃	r ₂	k ₁₂ /k _c	r ₁ = r ₃	r ₂	k ₁₂ /k _c	r ₃	r ₂	k ₁₂ /k _c
Acrylic anhydride	0.1	0.17	4	0.9	0.4	0.14	11.5	0.01	0
Acrylic acid	0.25	0.15 ^a					—		
Acrylonitrile	0.07	0.37 ^b		0.32	2.68 ^c				
2-Hydroxyethyl acrylate							8.85	0.016 ^d	
Methacrylic anhydride	0.26	0.12	0.2	1.6	0.27	Very low			0.22
Methacrylic acid	0.7	0.15 ^a		1.63	0.59 ^e				
Methacrylonitrile	0.16	0.3 ^f							

^a Data of Chapin et al.¹⁵

^b Data of Thompson and Raines.¹⁶

^c Data of Okamura and Yamashita.¹⁷

^d Data of Ioshi and Kapur.¹⁸

^e Data of Cameron et al.¹⁹

^f Data of Lewis et al.²⁰

IV. DISCUSSION

The copolymerization ratios and cyclization constants for both anhydrides are summarized in the Table IV, together with some values for other acrylic and methacrylic derivatives given in the literature.

For both anhydrides the copolymer composition was independent of the overall monomer concentration, i.e., r_1 is equal to r_3 . The same result was recently found for divinyl acetals²¹ and seems to be a general rule for symmetric dienes.

TABLE V

Monomer polarities	e
Methyl methacrylate	+0.4
Methyl acrylate	+0.6
Methacrylonitrile	+1
Methacrylic anhydride	+1.1
Acrylonitrile	+1.2
Acrylic anhydride	+1.2
Acrylic acid	+1.3

From their r_1r_2 values toward styrene the polarities e of acrylic and methacrylic derivatives can be ranged in order in the series, shown in Table V, e for styrene being equal to -0.8 .

Acrylic derivatives are thus always more positive than their methacrylic homologs, and the same statement can be made from the r_1r_2 values towards methacrylonitrile, differences of polarity Δe of 0.9 and 1.0 being found for methacrylic and acrylic anhydride, respectively. The polarity values, however, in this system are shifted to much higher values, when compared to styrene.

Cross propagation reactions are enhanced by a great difference of polarity between the monomers; for methacrylic anhydride $1/r_1r_2$ is equal to 32 with respect to styrene while only 2.3 with methacrylonitrile. Moreover, the intramolecular cyclization reaction is strongly dominant in the presence of methacrylonitrile. On the other hand, as could be expected from the homopolymerization data, the cyclization tendency is most pronounced for methacrylic anhydride due to the presence of the α -methyl groups.

V. EXPERIMENTAL

The monomers were commercially available products. Before use they were freshly distilled under reduced nitrogen atmosphere.

The copolymerizations were carried out in high vacuum sealed tubes in cyclohexanone solution at 35°C. in the case of acrylic anhydride and at 36.6°C. for methacrylic anhydride. The degree of conversion never exceeds 10%. The copolymers of acrylic anhydride with methacrylonitrile and allyl chloride were precipitated by pouring the solution in dry hexane; acrylic anhydride-styrene copolymers and methacrylic anhydride copoly-

mers were precipitated in dry diethyl ether. The copolymers were filtered off, washed and dried in vacuum at room temperature to constant weight.

The methacrylonitrile content was determined by the Kjeldahl method, that of allyl chloride with the method of Schöniger and Vollhardt, that of styrene by elemental C/H/O determinations (A. Bernhardt, Mikroanalytisches Laboratorium, Mülheim, Germany).

The unsaturation of the copolymers was determined by the bromometric method of Polgar and Jungnickel as for the homopolymers.²² The copolymers were dissolved in 0.1*N* sodium hydroxide; thereafter the solution was neutralized at pH 6 and treated with bromine. The excess of bromine was determined iodometrically. The applicability of this method to copolymers as well as its reliability have been determined. Acrylic acid-styrene and acrylic acid-methacrylonitrile copolymers are inert toward bromine in the same experimental conditions.

VI. CONCLUSIONS

The intramolecular cyclization reaction of acrylic and methacrylic anhydrides is dependent on the presence of foreign monomers, especially when the polarities of the double bonds differ considerably. The tendency for cyclization is always most pronounced for methacrylic anhydride. The reactivity ratios of open and cyclized unit radicals are identical ($r_1 = r_3$); consequently the normal Alfrey-Price copolymerization equation is valid for these symmetrical dienes.

The authors are indebted to the Institut pour l'encouragement de la Recherche Scientifique dans l'Industrie et l'Agriculture (I.R.S.I.A.) for a fellowship to two of them (N. D. and P. H.) and to the Centre des Hauts Polymères and Gevaert Photoproducten N. V. Antwerp for supporting this research.

References

1. Butler, G. B., paper presented at 133rd Meeting, American Chemical Society, San Francisco, April 1958, Division of Polymer Chemistry, Paper 15.
2. Price, J. A., G. Moore, and W. M. Thomas, *J. Chem. Eng. Data*, **4**, 273 (1959).
3. Marvel, C. S., and R. D. Vest, *J. Am. Chem. Soc.*, **81**, 984 (1959).
4. Milford, G. N., *J. Polymer Sci.*, **41**, 302 (1959).
5. Matsoyan, S. G., *J. Polymer Sci.*, **52**, 189 (1961); S. G. Matsoyan, M. G. Avet-yan, and M. G. Voskanyan, *Vysokomol. Soedin.*, **3**, 562 (1961); S. G. Matsoyan, L. M. Akopyan, and M. G. Voskanyan, *ibid.*, **3**, 1010 (1961); *ibid.*, **3**, 1311 (1961).
6. Roovers, J., and G. Smets, *Makromol. Chem.*, **60**, 89 (1963).
7. Hwa, J. C. H., and L. Miller, *J. Polymer Sci.*, **55**, 197 (1961).
8. Smets, G., P. Hous, and N. Deval, *J. Polymer Sci.*, **A2**, 4825 (1964).
9. Fineman, M., and S. D. Ross, *J. Polymer Sci.*, **5**, 259 (1950).
10. Alfrey, T., and J. G. Harrison, *J. Am. Chem. Soc.*, **68**, 299 (1946).
11. Kozaki, K., *J. Polymer Sci.*, **1**, 455 (1946).
12. Chapin, E. C., and G. E. Ham, *J. Polymer Sci.*, **4**, 597 (1949).
13. Mills, C. L., *J. Polymer Sci.*, **22**, 175 (1956).
14. Aelterman, M., and G. Smets, *Bull. Soc. Chim. Belg.*, **60**, 459 (1951).
15. Chapin, E. C., G. E. Ham, and C. L. Mills, *J. Polymer Sci.*, **4**, 597 (1949).
16. Thompson, B. R., and R. H. Raines, *J. Polymer Sci.*, **41**, 265 (1959).

17. Okamura, S., and T. Yamashita, *J. Soc. Textile Cellulose Ind. (Japan)*, **9**, 446 (1953).
18. Joshi, R. M., and S. L. Kapur, *J. Sci. Ind. Res. (India)*, **16B**, 441 (1957).
19. Cameron, G. G., D. H. Grant, N. Grassie, J. E. Lamb, and I. C. McNeill, *J. Polymer Sci.*, **36**, 173 (1959).
20. Lewis, F. M., C. Walling, W. Cummings, E. R. Briggs, and F. R. Mayo, *J. Am. Chem. Soc.*, **70**, 1519 (1948).
21. Eeckman, F., Ph.D. thesis, Louvain, 1963.
22. Polgar, A., and J. L. Jungnickel in *Organic Analysis*, Vol. III, J. Mitchell, I. M. Kolthoff, E. S. Proskauer, and A. Weissberger, Eds., Interscience, New York, 1956, p. 240.

Résumé

On a étudié la copolymérisation des anhydrides (M_1) acrylique (AA) et méthacrylique (MAA) avec le styrène (St) et le méthacrylonitrile (MAN), de même qu'avec le chlorure d'allyle dans le cas de l'anhydride méthacrylique. Le rapport de réactivité d'un radical correspondant à un diène (r_1) ouvert est égal à celui d'un radical cyclisé (r_3), de sorte que l'équation habituelle d'Alfrey-Price reste valide. Sur la base d'une méthode graphique, on a pu évaluer également les rapports de la constante de vitesse de propagation croisée à celle de cyclisation intramoléculaire (k_{12}/k_c). Les valeurs suivantes de r_1 , r_2 et (k_{12}/k_c) ont été trouvées, M_1 désignant l'anhydride: pour la paire AA-St, 0,1, 0,17, et 4; pour la paire AA-MAN, 0,9, 0,04, et 0,14; pour la paire AA-chlorure d'allyle, 11,5, 0,01, et 0. Pour le système MAA-St on a trouvé 0,26, 0,12, et 0,2; et pour le système MAA-MAN, 1,6, 0,27, et environ zéro. De ces résultats il résulte également que la cyclisation est toujours beaucoup plus prononcée avec l'anhydride méthacrylique qu'avec l'anhydride acrylique.

Zusammenfassung

Die Copolymerisation von Acrylsäure-(AA)- und Methacrylsäure-(MMA)-anhydrid (M_1) mit Styrol (St) und Methacrylnitril (MAN) wurde untersucht, und ebenso diejenige von Acrylsäureanhydrid mit Allylchlorid. Bei diesen Systemen ist das Reaktivitätsverhältnis eines Radikals des offenen Bausteins (r_1) gleich demjenigen eines cyclisierten Radikals (r_3) und die übliche Alfrey-Price-Gleichung erweist sich als gültig. Mit Hilfe einer graphischen Methode wurde auch das Verhältnis der Geschwindigkeitskonstanten für das gekreuzte Wachstum zu der Geschwindigkeitskonstanten der Cyclisierung (k_{12}/k_c) ermittelt. Folgende Werte wurden für r_1 , r_2 bzw. k_{12}/k_c , mit Anhydrid = M_1 gefunden: für das System AA(M_1)-St 0,1, 0,17 und 4; für das System AA-MAN 0,9, 0,4 und 0,14; für AA-Allylchlorid 11,5, 0,01 und 0. Für MAA waren sie gleich 0,26, 0,12 und 0,2 mit Styrol und 1,6, 0,27 und etwa 0 mit MAN. Diese Ergebnisse zeigen auch, dass die Cyclisierungsreaktion bei Methacrylsäureanhydrid immer stärker ausgeprägt ist als bei Acrylsäureanhydrid.

Received February 4, 1964

Study of the Hexamethylenediamine-Cellulose Complex*

LEON SEGAL and F. V. EGGERTON,† *Plant Fibers Pioneering Research Laboratory, Southern Utilization Research and Development Division, Agricultural Research Service, U. S. Department of Agriculture, New Orleans, Louisiana*

Synopsis

Complete conversion of the cellulose crystal lattice to that of the hexamethylene diamine-cellulose complex was attained with diamine solutions of 75% and greater. Solutions of 70% or less produced only partial conversion, although the samples contained high diamine contents. Evaporation temperatures over 90°C. reduced these diamine contents and resulted in partial lattice conversion. Neither this effect nor those following have been observed in the ethylenediamine-cellulose complex. The complex did not change while held in vacuum over sodium hydroxide pellets but gained weight when held in air. After long exposure the yarn was stiff and coated with white powder believed to be hexamethylenediamine carbamate. Attempts to react the complex with cellulose and diamine reactants were not successful. Evidence could not be found for a 2:1 molecular ratio between anhydroglucose units and diamine. Extent of fiber swelling was related to diamine content of the fiber and not to distention of the unit cell. Differences were observed in the intensities of the 101 and 10 $\bar{1}$ x-ray interferences of the cellulose I and cellulose II complexes.

Investigations of the interaction of mono- and diamines with the cellulose molecules of cotton fiber to form hydrogen-bonded complexes have been conducted at this laboratory along with other fundamental studies on the fine structure of cellulosic plant fibers. Segal and Loeb¹ postulated that complexes formed with the longer chain diamines which are either high boiling liquids or solids and already described by Creely, Segal, and Loeb² should have greater stability than that observed with the ethylenediamine-cellulose complex. Hexamethylenediamine (HMDA) was chosen for further investigation in the diamine-cellulose system as it is a solid at room temperature, soluble in water and organic solvents, and has a molecular length three times that of ethylenediamine. Because of the hydrocarbon chain length in HMDA its terminal amine groups are not influenced by any inductive effect. Thus, hydrogen bonding capabilities, base strengths, and the like, are unaffected, which is not true with ethylenediamine where the

* Presented at the 15th Annual Southeastern Regional Meeting of the American Chemical Society, Charlotte, N. C., November 14-16, 1963.

† Present address: U. S. Custom House, New Orleans, Louisiana.

inductive effect operates sufficiently well across the short chain such that the ionization constant of the second amine group is markedly different from that of the first. This difference in the two diamines is a significant indication that there may be differences in behavior between the HMDA-cellulose and the ethylenediamine-cellulose complexes. The present paper reports the results of experiments with cellulose and HMDA designed to determine if differences do exist.

EXPERIMENTAL

For cellulose I a kiered, loose-twist, combed cotton yarn was used. Cellulose II was prepared from the purified cotton by the usual mercerizing process. Essentially complete lattice transformation was verified by x-ray diffractograms. Reagent-grade, crystalline HMDA was used as well as a practical-grade, aqueous solution of 74–80% concentration. The thermal behavior of HMDA necessitated use of distillation apparatus with large passages, a well-stirred oil bath deep enough for complete submergence of the distilling flask, and several infrared heating lamps for auxiliary heat directed at exposed surfaces other than the receiving flask.

The HMDA-cellulose complex was prepared in the same manner described in previous studies on the diamine-cellulose complexes,^{2,3} except that the factors of solution concentration, time of immersion, and time and temperature of the vacuum distillation were varied. These experiments were carried out only with cellulose I. Immersion time of the sample in the solutions and evaporation time in vacuum were measured in the same manner as described by Segal and Creely.⁴ Standard conditions for preparing the complex consisted of immersing a 2–3 g. skein of yarn for 16 hr. in 80% HMDA, followed by evaporation of excess diamine in an 80°C. bath for 2 hr. at a pressure of 2 mm. Hg. HMDA solutions of the desired concentrations were prepared by dissolving weighed amounts of reagent-grade, crystalline HMDA in distilled water, followed by titration. Practical-grade HMDA was found quite suitable for general preparative work and where solution concentration was not a critical factor. The diamine contents of the various samples of complex were determined by titrating weighed portions in distilled water with standard hydrochloric acid, methyl orange being used as the indicator. The stability of the complex in air was followed by attaching portions of the yarn to the hook of a precision Jolley balance placed in an atmosphere controlled at 65% R.H. and 70°F. (21.1°C.). Readings were taken from the balance at timed intervals. Some idea of complex stability in absence of air and moisture was obtained by holding a portion of yarn for 70 hr. in an evacuated desiccator containing sodium hydroxide pellets.

The approximate densities of HMDA solutions at room temperature were obtained with the use of a calibrated 5-ml. volumetric flask as a pycnometer. The deliquescence of crystalline HMDA was followed by observing a layer of crystals placed in a crystallizing dish in a desiccator over saturated sodium nitrite solution (65% R.H.) and taking samples for titration at

timed intervals. Atmospheric carbon dioxide was excluded by flushing and filling the desiccator with nitrogen. Reactivity to atmospheric carbon dioxide was determined by following the weight changes of a layer of crystals in an aluminum pan attached to the Jolley balance held in the controlled atmosphere.

The technique used for obtaining x-ray diffractograms (Norelco wide-angle, precision, x-ray diffractometer equipped with a proportional counter detector and pulse height analyzer), was that given by Segal and Creely.⁴ Infrared spectra were obtained with a Perkin-Elmer Model 21 double-beam infrared spectrophotometer with sodium chloride optics, using the KBr-disk technique described by O'Connor and co-workers.⁵

Area measurements were made by planimetry of $1000\times$ photomicrographs of 100 cross sections of fibers from untreated cotton and from the HMDA-cellulose complex. A correction was made in the cross-sectional area when significant lumen area was apparent.

RESULTS AND DISCUSSION

Effect of Solution Concentration

Decreasing solution concentration from 99% HMDA had little effect on the high amount of diamine retained by the cellulose treated under the standard conditions until the concentration fell below 20% HMDA. This behavior, which can be seen in Figure 1, is decidedly different from that reported by Segal and Creely⁴ for the ethylenediamine-cellulose complex.

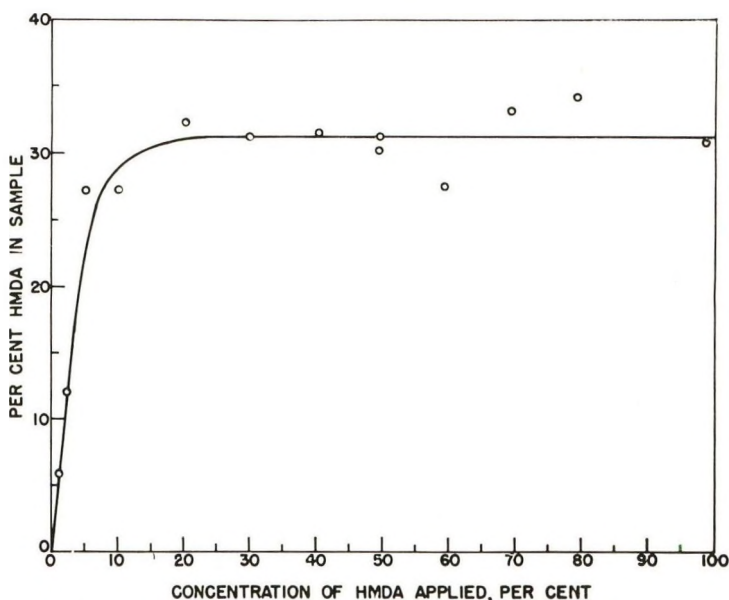


Fig. 1. Relationship between concentration of HMDA applied and HMDA content in the treated cellulose.

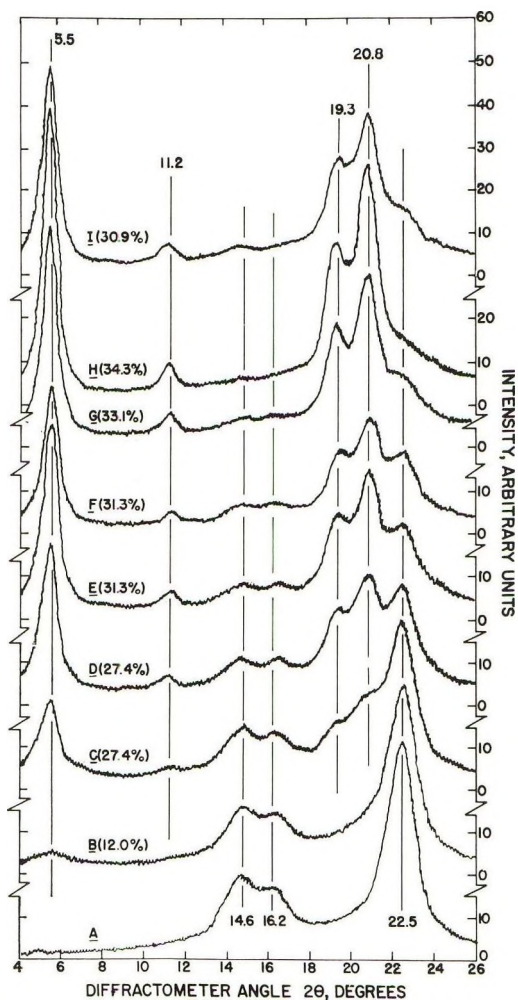


Fig. 2. X-ray diffractograms showing the effect of the concentration of the HMDA applied in preparing the complex: (A) untreated cellulose I; (B) 2.5% diamine; (C) 5% diamine; (D) 10% diamine; (E) 30% diamine; (F) 50% diamine; (G) 70% diamine; (H) 80% diamine; (I) 98.7% diamine. Figures in parentheses are the diamine contents found in the samples.

An anomaly is also found in the x-ray diffractograms of the samples. The diffractogram of the complex (34.3% HMDA) resulting from application of 80% HMDA solution shows no detectable cellulose I interferences (Fig. 2H). With an HMDA content of 26.4% calculated for one diamine molecule crosslinking two cellulose chains in the complex, one would not expect to find much cellulose I in fibers containing 27.4–33.1% HMDA. Yet the diffractograms of such samples clearly show such interferences (Figs. 2C–G). Solutions of 5–70% HMDA were used in preparing these samples.

The quantity of diamine presented to the cellulose had no effect in changing either the x-ray pattern or the amount of retained HMDA. Thus,

treating cellulose I with an 80% HMDA solution resulted in 34.3% diamine in the sample (Fig. 2H), with a 50% solution 31.3% (Fig. 2F). But when to the same weight of cellulose was added a volume of 50% solution such that the same weight of HMDA was present as was contained in the 80% solution used, the x-ray pattern of the product was no different from that of Figure 2F, and the diamine content was 30.3%.

According to the x-ray data, much of the diamine in the samples treated with solutions of less than 80% HMDA must not be truly bound to the cellulose hydroxyl groups. The limiting effective concentration for completely penetrating and converting the cellulose crystalline lattice is apparently between 70 and 80% HMDA, this being the region where the cellu-

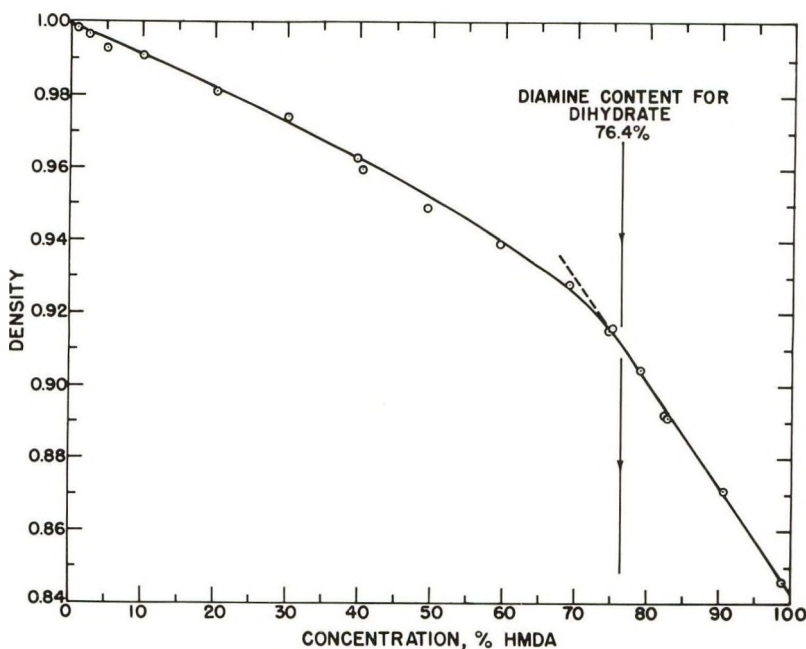


Fig. 3. Variation of the density of HMDA solutions with concentration.

lose I interferences disappear. This conclusion is supported by consideration of the bisquo complex formed when HMDA coordinates with two molecules of water. In that complex the hydrogen-bonding potential of the nitrogen atoms with respect to OH—N bond formation is greatly reduced, and HMDA thus complexed would not be expected to enter into further hydrogen-bond formation with cellulosic hydroxyl groups. In the bisquo-HMDA complex, the diamine content is 76.4%. The above conclusion is further supported by density data. In Figure 3 where densities and concentrations of HMDA solutions are plotted, there is a decided change both in the slope of the curve and its shape in the region of 75% HMDA. Lutsky⁶ has shown that intramolecular hydrogen bonding of a solute and intermolecular hydrogen bonding between solute and solvent

affects the densities of solutions such that the effect can be utilized in studies of association of the dissolved substance.

Effect of Evaporation Temperature and Time

Diamine contents lower than usual, along with the puzzling appearance of cellulose I interferences when none were expected, suggested that the bath temperature of 110°C. used initially in the vacuum distillation was too high. The suspicion that the higher temperature caused the trouble was confirmed by the x-ray diffractograms of samples vacuum-distilled at bath temperatures in the range of 80–120°C. (Fig. 4). The progressive loss of complex as the temperature was raised, indicated by the cellulose

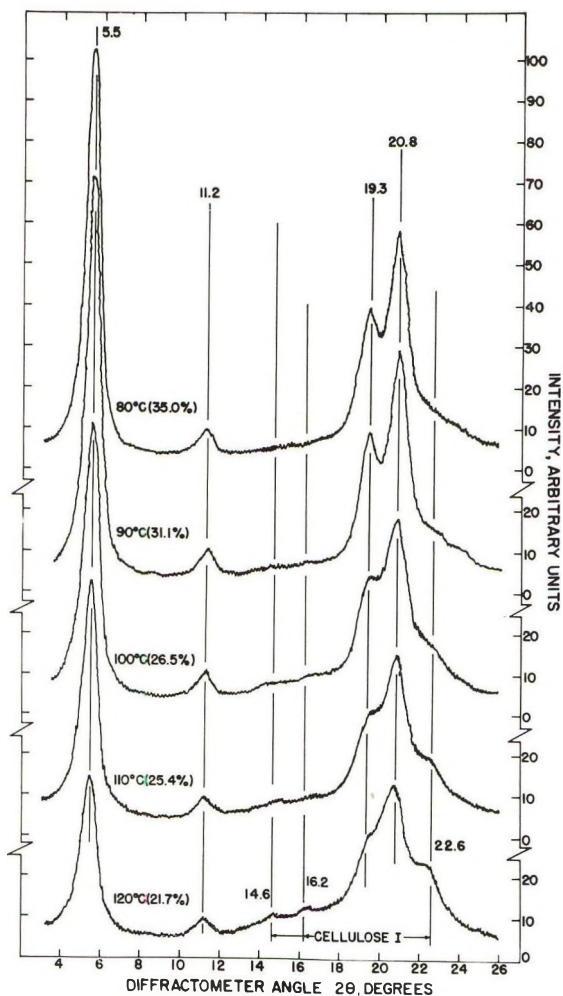


Fig. 4. X-ray diffractograms showing effect of evaporation temperatures on the cellulose I-HMDA complex. Yarns immersed overnight in 85% HMDA, 2 hr. distillation at <2 mm. Hg pressure. Figures in parentheses are diamine contents found in the samples.

I interferences and the decreasing intensity of the interferences of the complex, was paralleled by a linear decrease in diamine content (Fig. 5). Since the diffractograms indicated that the best product was obtained at 80°C.,

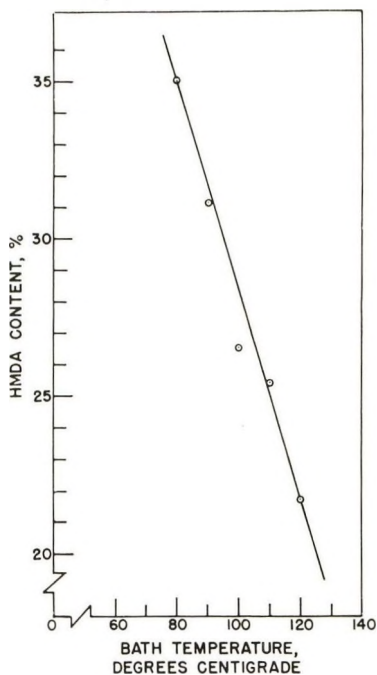


Fig. 5. Change in HMDA content of samples as bath temperature was varied in complex preparation. Yarns immersed overnight in 85% HMDA, 2 hr. distillation at <2 mm. Hg pressure.

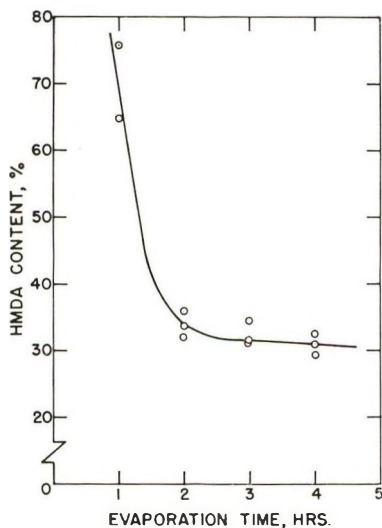


Fig. 6. Relation of HMDA content of the complex to evaporation time after 16 hr. immersion in 85% diamine, evaporated under <2 mm. Hg pressure and in 80°C. bath.

that temperature was selected for use in a standard procedure for complex preparation.

The usual 4 hr. period of evaporation described by Creely and co-workers² for preparing the complex leaves some 29% diamine in the sample. When shorter periods of evaporation were used (Fig. 6), the diamine content of the samples decreased rapidly during the first two hours, after which the rate of change was slight. No cellulose I interferences were detected in the diffractograms of any sample in this series. Evaporation for only 0.5 hr. left the yarn too wet to handle, and samples with HMDA contents above 43% fumed when exposed to the air. These aspects of behavior are similar to those reported for the ethylenediamine-cellulose complex.

The observed behavior of the HMDA-cellulose complex cast considerable doubt on the idea that because HMDA is a solid at room temperature its complex with cellulose should be more stable than the ethylenediamine-cellulose complex. More will be said later concerning the stability of the HMDA complex.

Effect of Time of Immersion in the Solution

Immersion time was found to have a definite influence on both extent of lattice conversion and amount of diamine retained in the cellulose fiber. The effect on lattice conversion was best demonstrated when excess diamine was evaporated with the use of a 110°C. bath, because in the x-ray diffractograms of the products the loss of cellulose I and the increase in complex interferences could be seen very easily (Fig. 7). Applying the same time series but using the 80°C. bath gave parallel results, except that the diffractograms showed little cellulose I to begin with and the diamine contents ranged from 32 to 36%.

Plotting diamine content of the samples against time of immersion showed that longer immersion resulted in significantly higher diamine content in the cellulose. The logarithmic plot of Figure 8 permits easy comparison between the results obtained at the two temperatures and the earlier results of Segal and Creely.⁴ The plotted data for the HMDA samples fall on parallel lines *A* and *B*, which indicates that irrespective of how the diamine is bonded or held by the cellulose, the rate of sorption is independent of the temperature. The steeper slope of lines *A* and *B* relative to the plot for the ethylenediamine-cellulose complex, line *C*, indicates that formation of the HMDA-cellulose complex is more sensitive to time of immersion than is the ethylenediamine-cellulose complex. The cause for this is not clear.

In these series the solution concentration was 85% HMDA. At 40% HMDA, well below the 75% solution concentration for achieving lattice transformation, time of immersion, while not influencing lattice shifts, did affect diamine content. At the end of 16 hr. immersion, 28.6% HMDA was found in the sample; this increased to 31.5% after 64 hr. immersion. However, the x-ray diffractograms, which were very similar to that of the cellulose treated with 30% HMDA (Fig. 2*E*), showed no detectable differences in peak locations or intensities. It is again noteworthy that in this

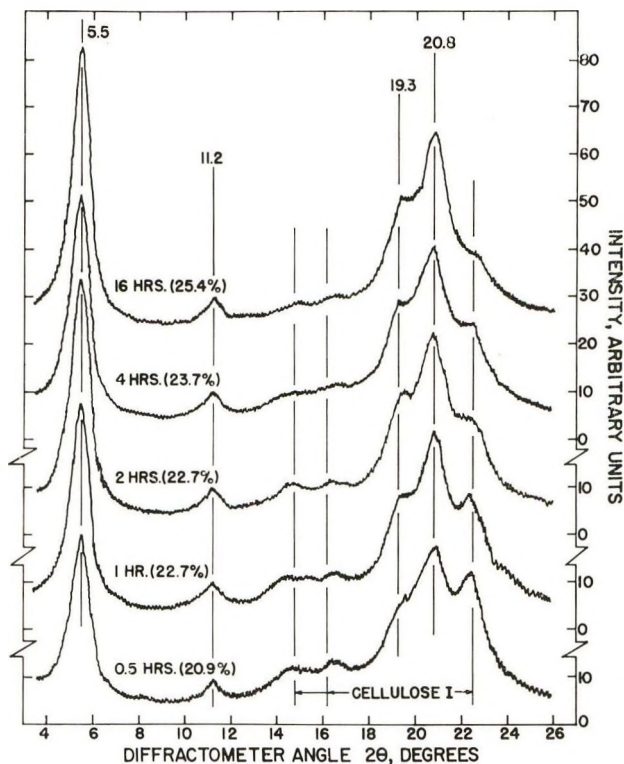


Fig. 7. X-ray diffractograms showing the influence of immersion time in 85% HMDA on complex formation. Evaporation for 2 hr. in 110°C. bath at <2 mm. Hg pressure. Figures in parentheses are diamine contents found in the samples.

64-hr. sample, the diamine content of 31.5% is of the same order as that found in samples with only the lattice of the diamine-cellulose complex, yet the diffractogram of this sample showed much cellulose I. This again shows that while large amounts of diamine may remain in the fiber structure after evaporation, complete lattice shift cannot be attained with solution concentrations of less than 75%.

There seems to be a relation between the intensity of the 101 interference of the complex and the diamine content of the sample, but it is not clear-cut as it seems to be influenced by the conditions under which the diamine is evaporated. Data plotted in Figure 9 show two trend lines. The points of line *A* represent samples prepared under the standardized conditions of temperature, pressure, and time, while the samples giving line *B* were prepared under various conditions. Although the reason for more than one line is not known, there are two interesting aspects to the plots. First, there are no breaks or changes of slope which might be caused by shifts in lattice structure as one molecule of diamine coordinates with two cellulose molecules. Segal and Loeb¹ did observe such shifts with the ethylenediamine-cellulose complex. However, in that study the decomposition of the complex, not its formation, was being followed.

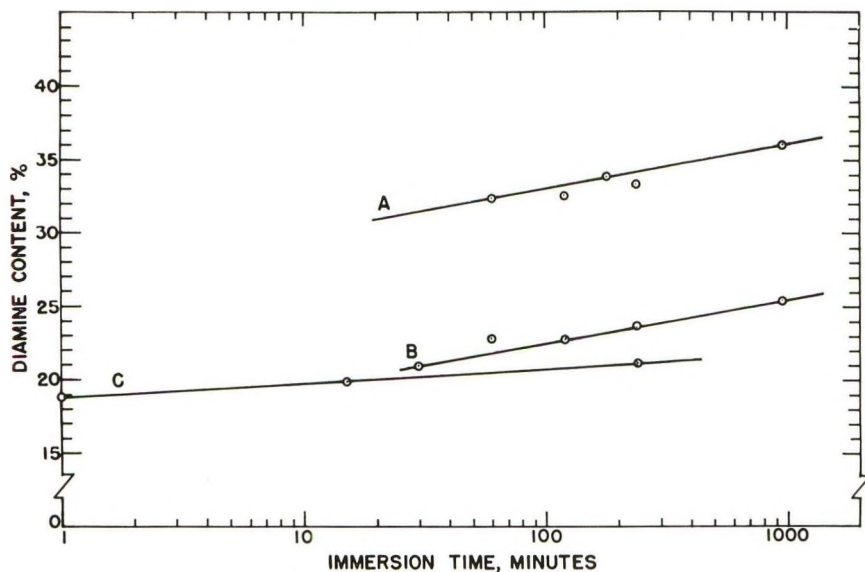


Fig. 8. Relation between diamine content of samples and immersion time in solution: (A) evaporated in 80°C. bath; (B) evaporated in 110°C. bath; (C) ethylenediamine-cellulose complex (from Segal and Creely⁶).

The second aspect to be noted is that when the two trend lines are extrapolated to zero 101 intensity they converge on the abscissa at almost 12% HMDA. This suggests that the first detectable evidence of complex formation should become evident when the increasing diamine content of a sample approaches this value. Among the samples whose diffractograms are given in Figure 2, the sample treated with 2.5% HMDA solution was found to contain 12.0% HMDA, and indeed the 101 interference of the complex at $2\theta = 5.5^\circ$ is readily apparent (Fig. 2B). A sample treated with 1% HMDA, containing 5.9% HMDA, showed no intensity rise at all in that region.

Extent of Fiber Swelling Caused by Complex Formation

An increase in cross-sectional area of a cellulose fiber is to be expected when a swelling compound is formed, but this may or may not be a function of the distention of the crystal lattice. The data given in Table I on cross-sectional area of two samples of HMDA-cellulose complex indicate that fiber swelling in the case of this complex is not related to crystal lattice distention at all, but rather to the diamine content. Diffractograms of the samples were identical with no cellulose I interferences. Creely, Segal, and Loeb² have given the areas of the unit cell projected on the 010 plane for cellulose-diamine complexes of hydrazine through octamethylenediamine, but unfortunately they failed to report any cross-sectional area measurements of the fibers. The distention of the unit cell in going from cellulose I to the HMDA complex, calculated on the basis of the data of Creely and

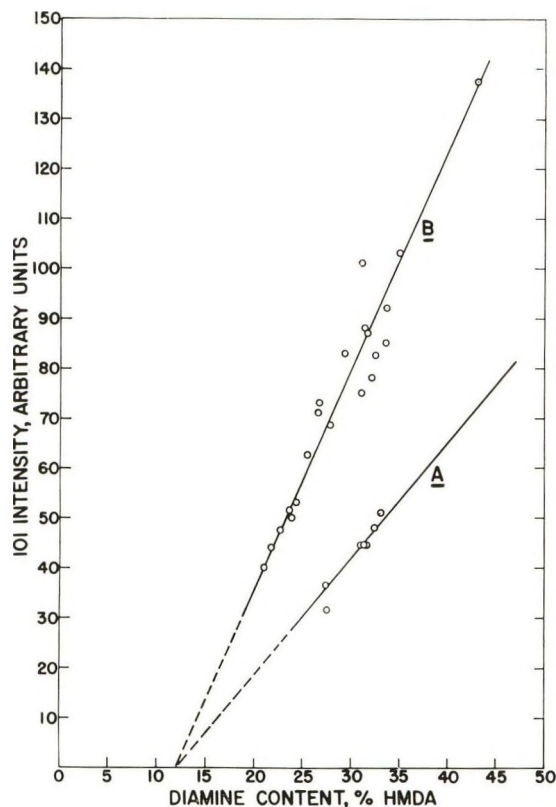


Fig. 9. Relation between diamine content of the sample and intensity of the 101 interference of the complex: (A) samples prepared by the standardized procedure; (B) samples prepared under various conditions.

co-workers, amounts to 121%, but the greatest increase of fiber cross-sectional area actually measured amounts to only 54%. After removal of the diamine from the swollen fibers by water and air-drying, the cross-sectional area was found to be almost the same as that of the untreated fibers, there

TABLE I
Fiber Cross-Sectional Areas of Untreated Cotton and HMDA-Cellulose Complexes

Sample	HMDA, %	Fiber cross-sectional area, μ^2	Increase in area, %	Area of projection of unit cell on 010 plane, \AA^2
Untreated cotton control	—	118	—	66.1 ^a
HMDA-cellulose complex	26.5	156	32	146 ^a
	43.0	182 (122) ^b	54 (3.0) ^b	146 ^a

^a Taken from Creely, Segal, and Loeb.²

^b Figures in parentheses are measurements after drying from exposure to water.

being an increase of only 3%. Segal and Loeb¹ reported for an ethylenediamine-cellulose complex of 19.7% diamine a 40% increase in fiber cross-sectional area, with a 57% increase in the area of the unit cell and a 14% retained swelling after removal of diamine (1.5% diamine content).

Sisson⁷ has contended that in cellulose fibers treated with ethylenediamine most of the fiber swelling may be accounted for by intracellular swelling or compound formation, and this seems to be supported by the findings of Segal and Loeb.¹ A swollen fiber with a cross-sectional area of some 261 μ^2 would be required, however, in order for the present swelling data to agree with the earlier conclusions based on the ethylenediamine work. Although the present data on the HMDA-cellulose complex relative to fiber swelling lead to conclusions different from those arrived at in the earlier ethylenediamine studies, actually the conclusions from both studies are not at variance if the structure of the cotton fiber is taken into account.

As long as the primary wall and the winding layer of the cotton fiber remain intact, as they are in the present cases, an upper limit is placed on the extent of fiber swelling that can possibly be realized with an undamaged fiber. The observed 54% increase in fiber cross-sectional area with the HMDA complex may well be this upper limit, as it falls short of that expected on the basis of the data from the ethylenediamine complex. The 121% distention in the crystalline area which must be accommodated within the confines of the intact cell wall can be accomplished plausibly through compression of the noncrystalline cellulose as the crystalline lattice expands. It is conceivable that the resulting internal forces contained in the structure could contribute much to the observed small swelling retained after removal of the diamine. Further studies on the tensile properties of single fibers of the HMDA-cellulose complex may well lead to highly interesting results.

Stability of the Complex

A sample of complex containing 43.8% HMDA showed no change in x-ray pattern or in diamine content after 70 hr. in vacuum over sodium hydroxide pellets. When the skein was attached to the Jolley balance in the controlled atmosphere, it began increasing in weight immediately. The increase was smooth and regular, leveling off after 6 hr., with little further change after 75 hr. (Fig. 10A). A sample of lower diamine content (33.2%) behaved in exactly the same manner. Per cent weight gains for the two samples were very similar, and no loss of diamine seemed indicated as titrations of the samples, expressed as per cent HMDA, gave percentages of diamine very close to the originals.

Attainment of constant weight which was not found with the ethylenediamine-cellulose complex¹ suggested that the HMDA-cellulose complex is quite stable in air. The observed weight increase could be ascribed to sorption of moisture, except that the duration and the amount of increase was too great for this and there was a crust of HMDA carbamate⁸ on the

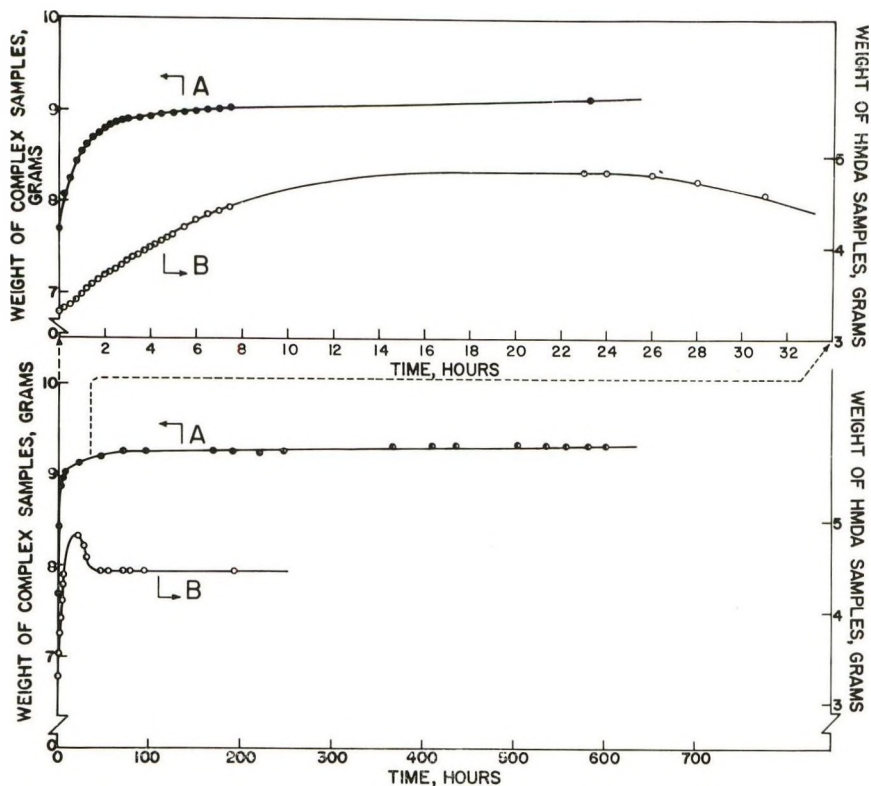


Fig. 10. Weight changes on long exposure of (A) the complex (43.8% HMDA) and (B) solid HMDA: (top) up to 24 hr.; (bottom) up to 600 hr.

yarn. Control tests made with a blank skein of similar weight showed that moisture regain ceased after 15 min. and amounted to some 4%.

Experiments with HMDA gave results which account for the larger part of the weight increase and explains the presence of HMDA carbamate. Figure 10B shows the weight change of a sample of pure, solid HMDA exposed to the controlled atmosphere. The crystals became moist immediately after being placed in the balance pan, and in about 2 $\frac{1}{4}$ hr. the whole pan was completely covered with a layer of liquid. Simultaneous with the deliquescence a white deposit of HMDA carbamate⁸ rimmed the moistened areas, and sample weight increased with the build-up of the deposit. After 23 hr. there was only dry carbamate present. The deliquescence of crystalline HMDA as observed above was more clearly demonstrated when crystals were held in the desiccator at 65% R.H. in a nitrogen atmosphere. Within 9 days all of the crystals had dissolved. Of course with exclusion of atmospheric carbon dioxide no carbamate formed. A marked weight gain should then result with a sample of pure HMDA exposed to the air. Figure 10B, however, shows a decrease in sample weight after about 20 hr., before the sample weight becomes constant. This behavior could be connected with Segal's report⁹ that HMDA carbamate appeared on the outside

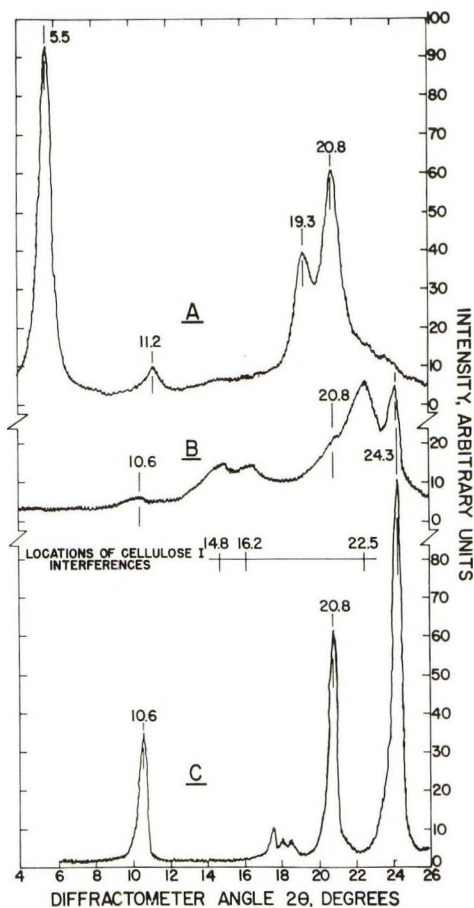


Fig. 11. X-ray diffractograms of (A) cellulose I-HMDA complex, 33.2% HMDA; (B) the complex after 429 hr. in the textile conditioning room at 65% R.H. and 70°F. (21.1°C.); (C) HMDA carbamate (from Segal⁹).

of a thin polyethylene film sealed over a recess containing an aqueous solution of HMDA separated from the film by an air space. He considered this a demonstration of an appreciable vapor pressure for the diamine as well as a strong ability to diffuse. The weight loss of Figure 10B then can be explained by loss of diamine by such vapor diffusion until carbamate formation fixed the bulk of the free diamine whereafter sample weight became constant.

The observed weight behavior of the cellulose-HMDA complex can be explained in light of the above considerations. Deliquescence begins as soon as the anhydrous sample is exposed to the atmosphere, accelerated by the strong sorption of moisture by cellulose itself. With moisture present, the diamine can easily diffuse from the fine structure of the cellulose fibers to react with atmospheric carbon dioxide at the fiber surface, forming there a layer of carbamate.

The indication that HMDA-cellulose complex is not stable in the presence of moisture and carbon dioxide was verified by x-ray diffraction. In Figure 11, which shows a diffractogram (Fig. 11*B*) taken after the second complex referred to above (33.2% HMDA) had stood 429 hr. in the textile conditioning room, the loss of the crystal lattice of the complex is readily apparent. The interferences of cellulose I are easily seen in Figure 11*B*, while the presence of HMDA carbamate is indicated by the interferences at $2\theta = 10.6, 20.8, \text{ and } 24.3^\circ$.

The poor stability of the complex is perplexing, particularly in view of Freedman's¹⁰ studies of the hydrogen bond between hydroxyl and nitrogen. Freedman concludes from his data and that given in the literature by others that the OH—N bond is stronger than the OH—O. In formation of the diamine-cellulose complex, the OH—N bond is formed at the expense of the cellulose-cellulose OH—O bond, but in the decomposition of the complex by moisture, the OH—O bonds are reformed at the expense of the OH—N bonds. A study of the energies of the bonds involved in the system cellulose—H₂O—HMDA required to explain this behavior is, however, beyond the scope of this paper.

Unfortunately the HMDA-cellulose complex does not lend itself very well to direct measurements by the usual techniques used in hydrogen bonding studies. Its KBr infrared absorption spectrum, which is almost identical to that of the ethylenediamine-cellulose complex published by Segal and Creely,⁴ suggests only the presence of a —NH₂ group in the cellulose. Campbell, Cathcart, and Giles¹¹ were faced with problems of a similar nature when they studied the role of hydrogen bonds in the dyeing of cellulose. These workers resorted to model compounds of cellulose, that is, glucose and sucrose, which could be examined by different techniques. They concluded from their data that in the presence of water neither of these sugars forms hydrogen bonds through their OH groups with proton-acceptor dye molecules and that this accounts for many of the effects observed in the dyeing of cellulose fibers. The principal cause for attraction between cellulose and dyes is ascribed to physical or van der Waals forces, and for these forces to exert significant effects, the dye molecules must necessarily have long and planar structures. The question of manner of retention or bonding of diamine in the HMDA-cellulose system, where a high diamine content but an incompletely converted lattice is found, may possibly be resolved through similar considerations. Arshid, Giles, and Jain¹² studied the interaction of glucose and cellobiose with pyridine and other amines. They concluded that when the carbohydrates are in an aqueous environment the hydroxyl groups are inactive because of solvation by water, and the observed interaction with the amines takes place with the carbohydrate molecules in their open-chain (aldehydo) forms. Hydrogen bonding with the amine is by a CH—N bond through the hydrogen of the aldehyde group which is activated by the highly electronegative carbonyl oxygen atom. These workers extend their findings to cellulose, postulating that in the presence of excess water, cellulose does not normally adsorb solutes by hydrogen

bonding. The above experiments, although also contradictory to Freedman's conclusions regarding the OII—N hydrogen bond, suggest other approaches for investigating the interactions of HMDA and cellulose.

Chemical Reactivity of the Complex

The placement of a potentially reactive molecule within the cellulose crystalline region but without chemically modifying cellulose in the usual sense seems to offer a new path for preparing derivatives of fibrous cellulose. The close proximity of —NH₂ and —OH groups along with large distention of the unit cell suggests the possibility of many types of reactions.

Experiments were carried out with a number of reagents, but none were successful. Divinyl sulfone and the chlorides of dibasic organic acids were among the more promising of the reagents as these react with amines and/or cellulose. The cause for failure of the experiments seems to be the requirement for a solvent for the reactant, and as the suitable solvents are generally polar in nature (and usually water), decomposition of the diamine–cellulose complex occurs. The liberated diamine reacts and the cellulose remains unaffected. No better results were obtained in systems where the solvent

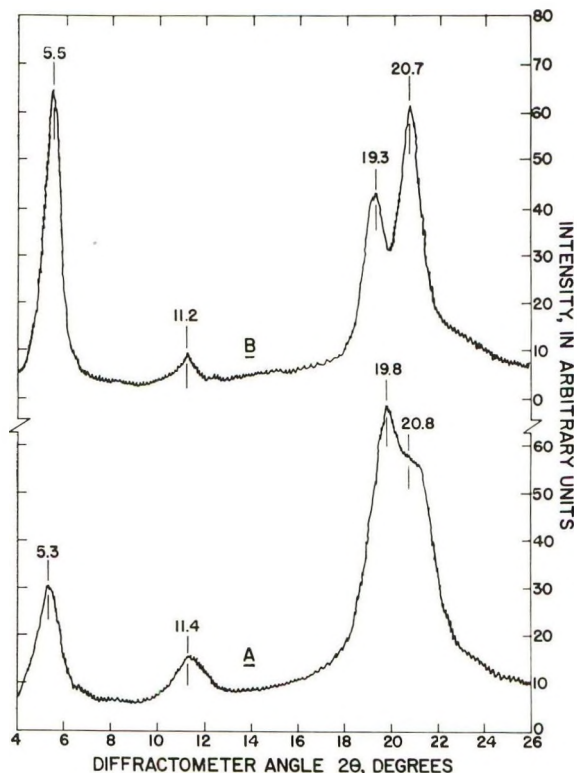


Fig. 12. X-ray diffractograms of the HMDA complexes of (A) cellulose II and (B) cellulose I.

would not affect the complex. The reactant did not or could not diffuse into the cellulose structure to react.

Thoughts have been given to possible effects of activation of the HMDA-cellulose complex by exposure to high energy radiation, but no experiments have been carried out. Speculation here centers about the close proximity of the amine and hydroxyl groups, as well as the distribution of diamine throughout the cellulose structure, both of which would set up favorable conditions for radiation-induced reactions. Another possibility involved inclusion of another substance to the system prior to irradiation, the new compound being one that could also enter into reaction with the products released by the irradiated system.

Aspects of the Cellulose II-HMDA Complex

X-ray diffractograms of the HMDA complex prepared with cellulose II display certain features which suggest that this complex is worthy of detailed x-ray studies that are beyond the scope of the present investigation. The slight differences in peak locations seen in the diffractograms of the cellulose II (Fig. 12A) and the cellulose I (Fig. 12B) complexes are those usually resulting when different initial cellulose polymorphic forms are used. The item to be noted, however, is the greater intensity of the $10\bar{1}$ interference of the cellulose II complex relative to that of its 002 peak. In the diffractogram of the cellulose I complex (Fig. 12B), the intensity of the $10\bar{1}$ interference is seen to be lower than that of the 002. Further, there is a marked difference to be seen in the intensities of the 101 interferences of the two complexes. The same intensity relations were found in diffractograms taken from diamine-wet samples. These factors possibly afford an approach to answering questions regarding the direction in which the diamine molecule is held in the crystalline lattice and to which hydroxyl groups it is bonded.

SUMMARY

Complete conversion of the cellulose crystal lattice to that of the HMDA-cellulose complex can be attained with HMDA solutions of 75% and greater. The extent of lattice conversion, however, is influenced by several factors. Evaporation of excess diamine at reduced pressure carried out at temperatures above 90°C. results in partial conversion, an effect not observed with the ethylenediamine complex. This also results with HMDA solutions of 70% or less, even through diamine contents in the yarns are greater than 26.4%, the value calculated for one HMDA molecule crosslinking two anhydroglucose units of the cellulose chains. In general, immersion of the cellulose yarn in the treating solution for 16 hr. is required to obtain complete conversion of the lattice.

The expected 2:1 molecular ratio between anhydroglucose units and diamine which was found with the ethylenediamine complex could not be verified. Distention of the cellulose unit cell in the 010 basal plane is cal-

culated to be 121%, while the maximum increase in fiber cross-sectional area is only 54%. Fiber swelling is related to HMDA content in the fiber, while first indication of complex formation (appearance of the 101 interference of the complex) occurs at about 12% HMDA content.

The complex was unchanged after 70 hr. in vacuum over sodium hydroxide pellets, but in a controlled atmosphere of 65% R.H. it gained weight rapidly, coming to constant weight after 75 hr. which was not so with the ethylenediamine complex. The yarns were stiff and coated with a white powder. This behavior is explained by sorption of moisture by the sample, followed by diffusion of diamine from the fiber fine structure, and reaction of the diamine with atmospheric carbon dioxide to form HMDA carbamate. Attempts to carry out reactions with the HMDA within the crystalline lattice by using reagents such as divinyl sulfone and chlorides of dibasic organic acids were unsuccessful. The failures are traced back to the solvents required in the reacting system, as these cause decomposition of the complex.

In the diffractogram of the cellulose II-HMDA complex the 101 interference is seen to be of greater intensity than is the 002 interference, while the reverse is true in the diffractogram of the cellulose I complex. The same relations are observed in diffractograms of diamine-wet samples. The intensity of the 101 interference of the cellulose II-HMDA complex is of much lower intensity than that of the cellulose I complex.

The authors wish to acknowledge the contributions of Miss Ines V. deGruy and Mrs. Jarrell H. Carra for the fiber cross sections and photomicrographs, and Mrs. Sylvia Miles for the infrared spectra.

Use of a company name and/or product named by the Department does not imply approval or recommendation of the product to the exclusion of others which may also be suitable.

References

1. Segal, L., and L. Loeb, *J. Polymer Sci.*, **42**, 341 (1960).
2. Creely, J. J., L. Segal, and L. Loeb, *J. Polymer Sci.*, **36**, 205 (1959).
3. Loeb, L., and L. Segal, *J. Polymer Sci.*, **15**, 343 (1955).
4. Segal, L., and J. J. Creely, *J. Polymer Sci.*, **50**, 451 (1961).
5. O'Connor, R. T., E. F. DuPré, and E. R. McCall, *Anal. Chem.*, **29**, 998 (1957).
6. Lutsky, A. E., *J. Gen. Chem. USSR* (Engl. transl.), **24**, 73 (1954).
7. Sisson, W. A., in *Cellulose and Cellulose Derivatives*, 1st Ed., High Polymers Series, Vol. V, E. Ott, Ed., Interscience, New York, 1946, pp. 259, 262.
8. Segal, L., *Appl. Spectry.*, **17**, 21 (1963).
9. Segal, L., *Textile Res. J.*, **32**, 702 (1962).
10. Freedman, H. H., *J. Am. Chem. Soc.*, **83**, 2900 (1961).
11. Campbell, D. S. E., D. Cathcart, and C. H. Giles, *J. Soc. Dyers Colourists*, **73**, 546 (1957).
12. Arshid, F. M., C. H. Giles, and S. K. Jain, *J. Chem. Soc.*, **1956**, 559.

Résumé

La conversion complète du réseau cristallin de la cellulose en celui du complexe hexaméthylènediamine-cellulose a été réalisée avec des solutions de diamine de 75% et plus. Des solutions de 70% ou moins concentrées donnaient seulement une conversion partielle

malgré la grande teneur en diamine des échantillons. Les températures d'évaporation supérieures à 90°C réduisaient cette teneur en diamine et provoquaient une conversion partielle du réseau. On a observé ni cet effet, ni ceux qui suivent pour le complexe éthylènediamine cellulose. Le complexe ne changeait pas quand il était conservé sous vide sur de pastilles de soude caustique, mais gagnait en poids à l'air. Après une longue exposition, le fil devenait rigide et se revêtissait d'une poudre blanche, considérée comme étant le carbamate d'hexaméthylènediamine. Des essais pour faire réagir le complexe avec des réactifs propres à la cellulose et à la diamine furent sans succès. On n'a pas pu mettre en évidence le rapport moléculaire 2:1 entre les unités d'anhydroglucose et celles de diamine. L'importance du gonflement des fibres a été mis en relation avec la teneur en diamine de la fibre, et non avec une dilatation de la cellule unitaire. Des différences dans les intensités des interférences 101 et 10 $\bar{1}$ aux rayons-X des complexes de cellulose I et de cellulose II ont été observées.

Zusammenfassung

Vollständige Umwandlung des Zellulosekristallgitters zu demjenigen eines Hexamethylendiaminzellulosekomplexes wurde mit Diaminlösungen von 75% und höher erzielt. Bei Lösungen von 70% oder geringer war die Umwandlung nicht vollständig, obwohl die Proben einen hohen Diamingehalt aufwiesen. Verdampfungstemperaturen über 90°C vermindern den Diamingehalt und verursachen teilweise Gitterumwandlung. Weder dieser Effekt noch die folgenden konnten an Äthylendiaminzellulosekomplexen beobachtet werden. Der Komplex änderte sich im Vakuum oder über Natriumhydroxydplätzchen nicht, nahm an Luft jedoch an Gewicht zu. Nach langer Expositionsdauer wurde das Garn steif und überzog sich mit einem weissen Pulver, wahrscheinlich Hexamethylendiamincarbat. Versuche zur Reaktion des Komplexes mit Zellulose und Diaminreagenzien waren nicht erfolgreich. Es wurde keinerlei Beweis für ein 2:1-Molverhältnis zwischen den Anhydroglukoseeinheiten und Diamin gefunden. Das Ausmass der Faserquellung wurde mit dem Diamingehalt der Faser und nicht mit dem Abstrand der Einheitszelle in Beziehung gebracht. Es wurden Unterschiede zwischen den Intensitäten der 101 und 10 $\bar{1}$ -Röntgeninterferenz von Zellulose-I- und -II-Komplexen festgestellt.

Received February 11, 1964

An Infrared Study of Polyhydroxymethylene and Deuterated Polyhydroxymethylene

J. R. SCHAEFGEN and R. ZBINDEN,* *Pioneering Research Division,
Textile Fibers Department, E. I. du Pont de Nemours & Company, Inc.,
Wilmington, Delaware*

Synopsis

The polarized infrared spectra of oriented polyhydroxymethylene films were determined in the range 5000-500 cm^{-1} . The films then were deuterated and the spectra again recorded. A tentative assignment of the major absorption bands is proposed on the basis of a simple zigzag chain model with a 2.5 Å repeat distance. The rate of hydrogen-deuterium exchange of a $(\text{-CHOD-})_n$ film with atmospheric water vapor was measured and found to be diffusion-controlled.

An earlier publication¹ described the preparation of clear films of polyhydroxymethylene by hydrolysis of films of high molecular weight poly(vinylene carbonate) in alkaline methanol. Films of polyhydroxymethylene were oriented by stretching and were converted to a high degree to the deuterio form, $(\text{-CHOD-})_n$, by soaking in heavy water. In this paper a tentative assignment is made of most of the major bands in the infrared spectrum of polyhydroxymethylene by use of deuteration and polarized infrared radiation. The results are compared with similar assignments for poly(vinyl alcohol).

Structure

The exact geometrical structure of polyhydroxymethylene in the crystalline state is not known, but from x-ray diffraction patterns of drawn films it is concluded that the longitudinal repeat distance is about 2.5 Å. This indicates that the carbon skeleton is a planar zigzag chain as in polyethylene. It was at first thought that the ring structure of the vinylene carbonate monomer might lead to a polymer in which successive pairs of carbon atoms along the chain had opposite conformations, i.e., *dd*, *ll*, *dd*, *ll*, etc. However, the absence of an x-ray diffraction spot corresponding to a repeat distance of 5.0 Å. in the derived polyhydroxymethylene appears to rule out this possibility. This polymer has, therefore, either an atactic or a stereoregular *d*, *l,d*, *l*, etc. structure. The fact that polyhydroxymethylene can be partially crystallized makes the latter structure more likely. The

* Present address: J. R. Geigy, A.-G., Basel, Switzerland.

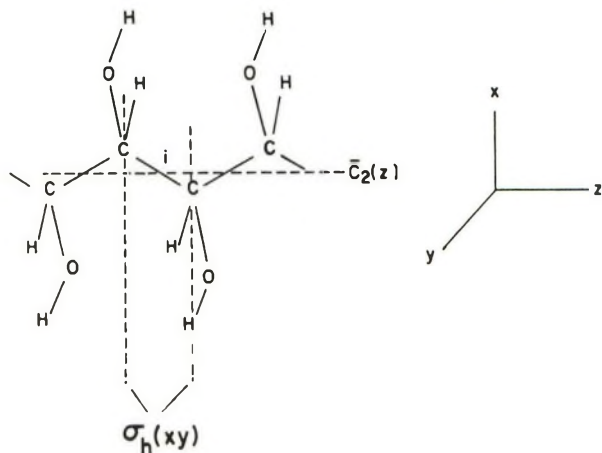


Fig. 1. Structure and symmetry of polyhydroxymethylene assuming a planar zigzag chain.

structure of such a segment is shown in Figure 1. The z axis of the coordinate system is parallel to the chain axis and the carbon atoms lie in the xz plane. The CH and CO bonds are in the xy plane (similar to the CH_2 group of polyethylene). We further assume that the OH bond also lies in this plane with the distance between the hydroxyl and aliphatic hydrogen being the same for all CHOH groups. This assumption may not be correct, and the symmetry of the chain may be lower. This would change somewhat the selection rules discussed below.

We do not want to convey the idea that any further support to this proposed structure of the crystalline regions of the polymer can be provided by the following infrared analysis. It is merely an attempt to assign some of the observed absorption bands to the normal vibrations of the structure most likely at present.

Symmetry Properties

The symmetry of the molecular structure shown in Figure 1 can be described by a one-dimensional space group which is called a line group.² This line group is characterized by the translational repeat unit consisting of two CHOH groups and by the following symmetry operations: a reflection at a plane of symmetry $\sigma_h(xy)$ (through the CHOH group), a screw rotation around the twofold screw-rotation axis $\bar{C}_2(z)$ (parallel to the z -axis) and an inversion at the center i of every C—C bond. These three symmetry operations together with the identity operation E form the factor group of the line group C_{2h} . The character table of this factor group³ is given in Table I. A rigorous vibrational analysis could be based only on a three-dimensional space group. Since the crystal structure of the polymer is not known, however, the line group treatment is probably the best approximation available.

TABLE I
Character Table for Line Group C_{2h} for Polyhydroxymethylene

Species	Symmetry elements				Number of normal vibrations			
	E	$\bar{C}_2(z)$	$\sigma_h(xy)$	i	Skeleton	Whole molecule	Non-genuine vibrations	Infrared activity
	A_g	+1	+1	+1	+1	4	8	R_z
A_u	+1	+1	-1	-1	2	4	T_z	M_z
B_g	+1	-1	-1	+1	2	4		
B_u	+1	-1	+1	-1	4	8	$T_x T_y$	$M_x M_y$

Normal Vibrations and Selection Rules

The number of factor group normal vibrations for an infinitely long single chain is $3N$, where N is the number of atoms per translational repeat unit. Included are four nongenuine normal vibrations: three translations, one each, in the x , y , and z directions, and one rotation around the z axis. In polyhydroxymethylene, therefore, the repeat unit of eight atoms results in twenty-four factor group normal vibrations.

It is convenient to consider first vibrations that mainly involve stretching and deformation of carbon-carbon and carbon-oxygen bonds. The carbon-oxygen skeleton has four atoms per repeat unit and, therefore, only

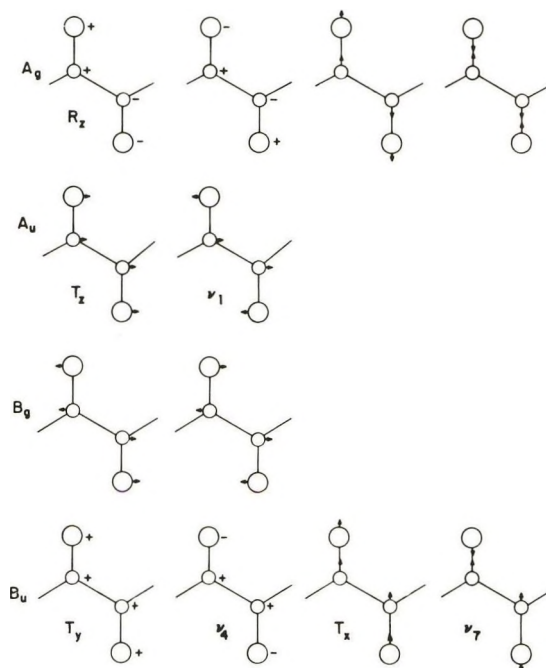


Fig. 2. Normal vibrations of the carbon-oxygen skeleton of polyhydroxymethylene. The large circles represent oxygen atoms; the small circles, carbon atoms.

twelve normal vibrations. These are distributed among the four species as shown in column 6 of Table I. The geometrical form of these vibrations is shown in Figure 2. Four of the vibrations are nongenuine as indicated in column 8, where conventional nomenclature³ is used for translations (T) and rotations (R).

The selection rules for infrared spectra are listed in column 9, where M_x , M_y , and M_z give the direction of the transition moment for the particular species. Only vibrations of species A_u and B_u are infrared-active. In a stretched sample where the z axis of the chain is predominantly parallel to the stretching direction, the A_u vibrations lead to parallel bands, while the B_u vibrations result in perpendicular bands if polarized infrared radiation is used.

If we include the hydrogen atoms in the vibrational analysis we find that there are a total of eight vibrations each of species A_g and of species B_u ,

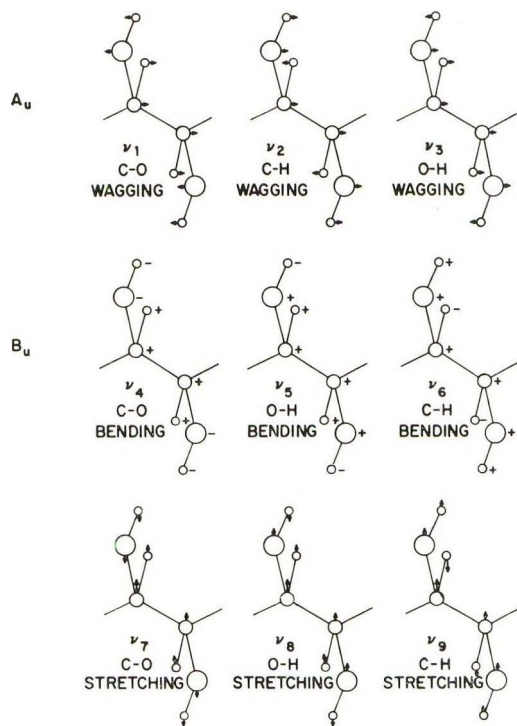


Fig. 3. Infrared-active normal vibrations of polyhydroxymethylene. The large circles represent oxygen atoms; the middle size circles, carbon atoms; the small circles, hydrogen atoms. The vibrations of species B_u shown in this figure correspond only approximately to the designation given, e.g., ν_6 and ν_9 are not pure CH bending and stretching vibrations, respectively. A pure CH stretching vibration would correspond to a combination of ν_6 and ν_9 . Since both these vibrations belong to the same species, two such combinations corresponding to the pure CH bending and CH stretching vibrations could also represent two basic normal vibrations instead of the ones shown in this figure. In analogy, combinations of ν_4 and ν_7 as well as ν_5 and ν_8 would be pure CO and OH bending and stretching vibrations, respectively.

and four vibrations each of species A_u and B_g (see column 7, Table I). The twelve vibrations of species A_u and B_u are expected to be infrared-active; three are pure translations, the remaining nine are shown in Figure 3. They are numbered arbitrarily ν_1 to ν_9 . The assignment of these vibrations to observed absorption bands is discussed in the following section.

Observed Spectra and Band Assignments

Figures 4a and 5a show the polarized infrared spectra of oriented films of polyhydroxymethylene (drawn 400%). The spectra of other less oriented films that had been soaked in D_2O are shown in Figures 4b and 5b. From the relative intensities of the absorption bands due to OH and OD stretching vibrations, the degree of deuteration of the hydroxyl group is estimated to be about 70%. The spectra shown in Figures 4b and 5b were recorded with the sample in a nitrogen atmosphere to prevent the rapid hydrogen-deuterium exchange produced by atmospheric water vapor.

Based on the molecular model described in the previous sections an attempt was made to assign the nine infrared-active fundamental vibrations to observed absorption bands. The results appear in Table II. Both deuteration and polarization spectra helped considerably in the assignment of bands. There is little doubt about the assignment of the vibrations ν_8 and ν_9 , the OH stretching and CH stretching vibrations, respectively. The

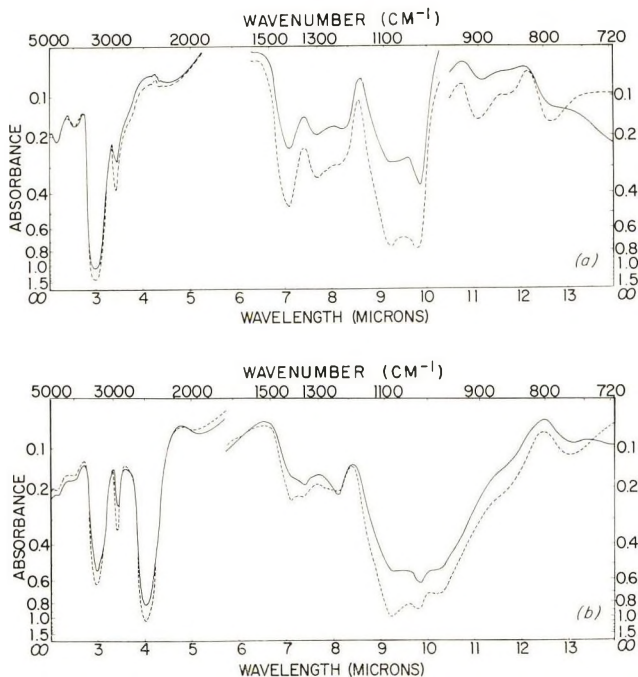


Fig. 4. Polarized infrared spectra of (a) oriented $-(CHOH)-_n$ films and (b) oriented $-(CHOD)-_n$ films, 2 to 14 μ . Electric vector perpendicular to direction of stretch (---) and electric vector parallel to direction of stretch (—).

TABLE II. Infrared Spectra and Tentative Assignment of Fundamental Vibrations for (CHOH)_n and (CHOD)_n

Frequency, cm. ⁻¹ , intensity, and dichroism		Vibration (see Fig. 3)	Group vibration	Some frequencies of corresponding group variations, cm. ⁻¹ ^a	
(CHOH) _n	(CHOD) _n /(CHOH) _n			$\left. \begin{array}{c} -(\text{CH}_2\text{CH})_n \\ \\ \text{OH} \end{array} \right\}$	$\left. \begin{array}{c} -(\text{CH}_2\text{CH})_n \\ \\ \text{OD} \end{array} \right\}$
4800 w ?	4800 vw ?				
3950 w ?	3950 vw ?				
3370 vs ⊥	3370 vs ⊥	<i>ν</i> ₈	OH stretching	3340	
2930 m ⊥	2930 m ⊥	<i>ν</i> ₉	CH stretching	2905 2840	
	2475 s ⊥	<i>ν</i> ₈	OD stretching		2480
2220 vw ?	1905 vw ?				
1410 s ⊥	1410 m ⊥	<i>ν</i> ₅	OH bending	1376 ^b 1326 ^b 1320 ^b	
	1350 m ?	<i>ν</i> ₂	CH bending		1360
1300 m ⊥	1240 m	<i>ν</i> ₆	CH wagging	1235	1230
1215 m ?					
1082 s ⊥	1082 vs	<i>ν</i> ₅	OD bending		
1015 s ⊥	1018 vs 983 vs	<i>ν</i> ₇	CO stretching	1096	
900 w ⊥	860 sh ?				
851 vw ⊥					
790 w ⊥	760 w ?	<i>ν</i> ₃	OH wagging	610 630	
620 m	640 w ⊥ 610 vw ⊥				
		<i>ν</i> ₄	CO bending	480	
		<i>ν</i> ₁	CO wagging	410	

^a After Krimm.⁴ ^b Combination of CH and OH bending vibrations.⁴

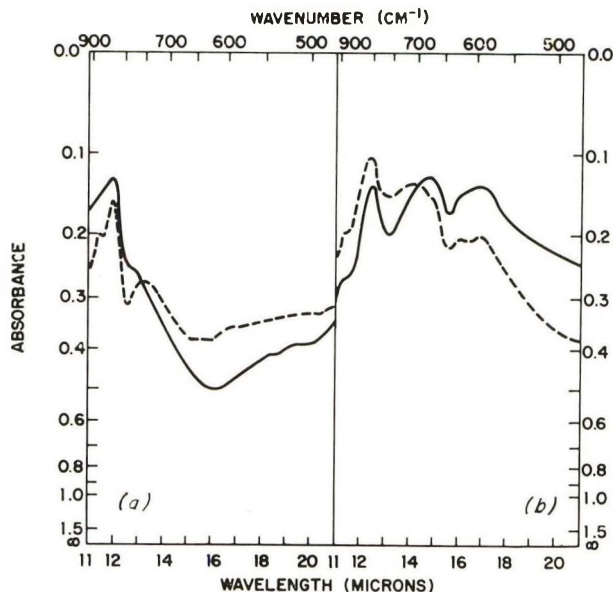


Fig. 5. Polarized infrared spectra of (a) oriented $-(\text{CHOH})_n$ and (b) oriented $-(\text{CHOD})_n$, 11 to 21 μ . Electric vector perpendicular to direction of stretch (---) and electric vector parallel to direction of stretch (—).

strong perpendicular band at 1410 cm.^{-1} disappears on deuteration; it is shifted at least to about 1150 cm.^{-1} or lower. It, therefore, can be identified with ν_5 . In $(\text{CHOD})_n$ two bands are observed between 1200 and 1400 cm.^{-1} . Since this is the region for CH bending and wagging vibrations in other compounds such as polyethylene or poly(vinyl alcohol)⁴ assignment is made of the 1350 cm.^{-1} (perpendicular?) vibration to ν_6 and the 1240 cm.^{-1} (parallel) band to ν_2 , based on the observed dichroism. Note that these two bands cannot be observed clearly in $(\text{CHOH})_n$ due partially to interference of the strong OH bending vibration band. The CO stretching vibration ν_7 is expected to absorb at about 1100 cm.^{-1} in analogy to similar absorption in poly(vinyl alcohol).⁴ Two bands are actually observed at 1082 and 1015 cm.^{-1} for $(\text{CHOH})_n$ and a third band appears at about 983 cm.^{-1} for $(\text{CHOD})_n$. The parallel band at 620 cm.^{-1} for $(\text{CHOH})_n$ is assigned to ν_3 ; the corresponding band for $(\text{CHOD})_n$ is shifted below 500 cm.^{-1} and the frequency of maximum absorption cannot be observed exactly because of absorption by the AgCl polarizers. The vibration ν_1 probably absorbs below 500 cm.^{-1} because apart from the absorptions at 1235 cm.^{-1} (ν_2) and 620 cm.^{-1} (ν_3) no other parallel band above 500 cm.^{-1} is apparent in the observed spectra. The CO bending vibration ν_4 also is expected to absorb below 500 cm.^{-1} .

The assignment of absorption bands given in Table II is only a first attempt at a complete analysis. It seems that the simple molecular model described above cannot account for a number of bands such as the three bands at 790 , 851 , and 900 cm.^{-1} for $(\text{CHOH})_n$ and the two bands at 760

and 860 cm.^{-1} for $(\text{CHOD})_n$. The spectrum of $(\text{CHOH})_n$ also shows additional bands at about 1215 and 1300 cm.^{-1} . Some of these bands might be due to amorphous polymer. Others, as indicated above, may result from lowered symmetry because the OH bonds are not exactly perpendicular to the chain axis. This is indicated by the fact that the dichroism for the OH stretching band seems to be slightly lower than for the same mode of the CH group. Another feature that cannot be accounted for by the simple model is the fact that two strong bands are observed in the region of 1000 – 1100 cm.^{-1} where ν_7 is expected to absorb.

To analyze the spectrum more completely, additional information is required. It will be important to know the crystal structure of this polymer to carry out a vibrational analysis for the space group unit cell. This may lead to somewhat different selection rules. If there is more than one polymer chain passing through the unit cell one would expect to observe band splittings due to intermolecular interaction. It will also be important to study polymer samples with different degrees of crystallinity to distinguish between absorption bands of the crystalline and the amorphous phases. Since the amorphous polymer chains have no symmetry, all vibrations are expected to be infrared-active. It will, furthermore, be useful to observe polarized spectra at frequencies below 500 cm.^{-1} using selenium polarizers to find the absorption bands for the vibrations ν_1 and ν_4 .

Hydrogen-Deuterium Exchange

An oriented film of polyhydroxymethylene, 0.01 mm. thick, was deuterated to the extent of 89% . The hydrogen-deuterium exchange of this deuterated film was then followed at 28% R.H. and 80°F. in a Perkin-Elmer Model 21 spectrometer by use of the 3370 cm.^{-1} OH and 2475 cm.^{-1} OD stretching vibrations. Peak absorption values rather than areas were determined, and these are recorded in Table III. Since hydrogen exchange between protons attached to oxygen is considered to be too fast to measure,⁵ the hydrogen-deuterium exchange was treated as a diffusion-controlled process. The graph of OH absorption versus the square root of time

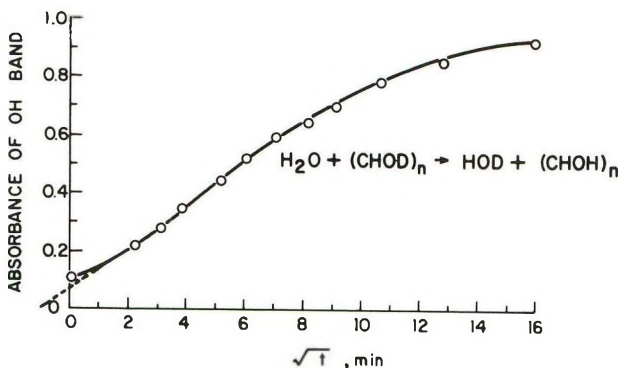


Fig. 6. Rate of hydrogen-deuterium exchange of a 0.4 mil thick $(\text{CHOD})_n$ film with atmospheric water vapor at 28% R.H., 80°C. This corresponds to a partial pressure of water equal to 7.4 mm. Hg.

TABLE III
Hydrogen-Deuterium Exchange in $-(\text{CHOD}_n)_-$ at 28% R.H., 80°F.^a

Time, min.	A_H^b	Time, min.	A_D^c	$(1.00 - A_H)/A_D$
0	0.11	1.1	0.73	1.22
4.7	0.22	5.8	0.70	1.11
9.4	0.28	10.6	0.65	1.11
14.8	0.35	21.3	0.60	1.08
26.0	0.44	32.4	0.52	1.08
36.3	0.52	43.3	0.48	1.00
48.4	0.59	55.0	0.40	1.03
65.1	0.64	84.1	0.32	1.12
82.7	0.70	109	0.24	1.25
107	0.78	165	0.18	1.22
164	0.85	200	0.13	1.15
253	0.92	254	0.08	1.00
368	0.96	370	0.05	0.8
∞^d	1.00	∞^d	0.00	

^a Film is ca. 0.01 mm. thick.

^b Absorbance (peak intensity) of OH stretching band at 3370 cm^{-1} .

^c Absorbance (peak intensity) of OD stretching band at 2475 cm^{-1} .

^d 1080 min.

is shown in Figure 6. [Note: The deuterated film was dried *in vacuo* and timing was started when the film was first exposed to the air. Deuteration may have been nearly complete, since extrapolation to zero OH absorbance (dotted line in Figure 6) shows that an error equivalent to about 1 min. prior exposure would correspond to 100% deuteration.] This is the same type of anomalous curve that is obtained in diffusion of water into poly(vinyl alcohol).⁶ The apparent diffusion constant calculated from the point of half-reaction [see eqs. (3) and (4) of ref. 6] is $13 \times 10^{-10} \text{ cm}^2/\text{min.}$, which is the same order of magnitude as the apparent diffusion constant for water into poly(vinyl alcohol). The strong hydrogen bonding and the fact that this experiment undoubtedly was conducted below the glass transition temperature of polyhydroxymethylene can be cited as reasons for the anomalous diffusion behavior. Since the ratio $(1.00 - A_H)/A_D$ is nearly constant throughout and after completion of the reaction, it is apparent that at 28% R.H. (=7.4 mm. Hg H_2O), the polymer contains very little dissolved water. There is no evidence of a (large) difference in diffusion rate between crystalline and amorphous areas in the film as there is in cellulose, where crystalline regions exchange hydrogen for deuterium only extremely slowly.⁷

Experimental

Poly(vinylene carbonate) was prepared in bulk from monomer treated with NaBH_4 immediately before polymerization by the method previously described.¹ Polymer of inherent viscosity >2.0 was dissolved in *N,N*-dimethylformamide to give a 5% solution. This solution was cast as a 0.25 mm. film on glass and, after drying, the film was hydrolyzed in 1% methanolic sodium methylate solutions (contains traces of water) at 50°C. Some

shrinkage took place on hydrolysis, but the film form was maintained. Films were drawn by hand over a rod heated to 200°C. Water was dripped onto the film during drawing to facilitate this operation. The oriented films which were used were from 0.005 to 0.012 mm. thick.

Oriented films, 1–1.5 cm. in width, were mounted taut on an annular brass holder. Spectra were determined by use of Perkin-Elmer Model 21 (5000–700 cm^{-1}) and Model 221 (700–500 cm^{-1}) infrared spectrometers. Silver chloride polarizers were used in obtaining polarized spectra. These polarizers absorbed so strongly below 500 cm^{-1} that no meaningful spectra could be obtained below this frequency.

Deuteration was accomplished by suspending the film clamped taut on a brass holder in 99.5% deuterium oxide for 24 hr. The reactants were placed in a polyethylene bag. The holder and the film were removed from the bag, evacuated to <1 mm. pressure to remove excess D_2O , and kept in a nitrogen atmosphere to minimize hydrogen–deuterium exchange. The degree of deuteration was 85–90%, assuming nearly equal extinction coefficients of absorption by OH and OD at 3370 and 2475 cm^{-1} , respectively.

The authors acknowledge the helpful technical assistance and advice of Mr. Karl Brandt.

References

1. Field, N. D., and J. R. Schaeffgen, *J. Polymer Sci.*, **58**, 533 (1962).
2. Tobin, M. C., *J. Chem. Phys.*, **23**, 891 (1955).
3. Herzberg, G., *Infrared and Raman Spectra of Polyatomic Molecules*, Van Nostrand, New York, 1945.
4. Krimm, S., C. Y. Liang, and G. B. B. M. Sutherland, *J. Polymer Sci.*, **22**, 227 (1956); H. Tadokoro, *Bull. Chem. Soc. Japan*, **32**, 1252 (1959); H. Tadokoro, H. Nagai, S. Seki, and I. Niha, *ibid.*, **34**, 1504 (1961).
5. Bell, R. P., *The Proton in Chemistry*, Cornell Univ. Press, Ithaca, N. Y., 1959, p. 122.
6. Long, F. A., and L. J. Thompson, *J. Polymer Sci.*, **15**, 413 (1955).
7. Marrinan, H. J. and J. Mann, *Trans. Faraday Soc.*, **52**, 481, 487, 492 (1956); *J. Polymer Sci.*, **21**, 301 (1956).

Résumé

On a pris les spectres infra-rouges en lumière polarisée de films de polyhydroxyméthylène orientés dans le domaine allant de 5000 à 500 cm^{-1} . Après avoir deutéré les films, on a repris les spectres. On a essayé d'expliquer les bandes d'absorption plus grandes, sur la base d'un modèle de chaîne en simple zig-zag avec une distance de 2.5 Å. On a mesuré la vitesse d'échange hydrogène-deutérium d'un film $(-\text{CHOD}-)_n$ avec la vapeur d'eau atmosphérique et on a trouvé qu'elle était contrôlée par la diffusion.

Zusammenfassung

Infrarotspektren orientierter Polyhydroxymethylenfilme in polarisiertem Licht wurden im Bereich von 5000 bis 500 cm^{-1} aufgenommen. Die Filme wurden dann deuteriert und die Spektren neuerlich aufgenommen. Eine versuchsweise Zuordnung der Hauptabsorptionsbanden wird auf Grundlage eines einfachen Zickzack-Kettenmodells mit einer Periodenlänge von 2,5 Å vorgenommen. Die Geschwindigkeit des Wasserstoff-Deuteriumaustausches eines $(-\text{CHOD}-)_n$ -Films mit atmosphärischem Wasserdampf wurde gemessen und als diffusionskontrolliert erwiesen.

Received October 14, 1963

Revised February 5, 1964

Comparison of Polyethylene Molecular Weights Determined by Light-Scattering Measurements in 1-Chloronaphthalene and 1,2,3,4-Tetrahydronaphthalene

L. H. TUNG, *Petrochemicals Research Laboratory, The Dow Chemical Company, Midland, Michigan*

Synopsis

Polyethylene molecular weights were determined by light-scattering measurements in 1-chloronaphthalene and 1,2,3,4-tetrahydronaphthalene at 125°C. Both high density and low density polyethylene fractions were used. The results show that at 125°C. polyethylene molecules do not associate in 1-chloronaphthalene. The disagreement of molecular weights of polyethylene determined in the two solvents is traced to the uncertainty of refractive index increment of polyethylene in 1,2,3,4-tetrahydronaphthalene and to possible oxidation of the polymer in 1-chloronaphthalene.

INTRODUCTION

The solvent 1-chloronaphthalene was first used by Billmeyer¹ in the light-scattering molecular weight determination of polyethylene. It has many desirable properties; a refractive index sufficiently different from that of polyethylene, low volatility, and good stability at elevated temperatures. Many workers have since used it as the solvent for light-scattering measurements of crystalline polyolefins. Later Trementozzi,² however, raised the question whether 1-chloronaphthalene was, after all, a suitable solvent. He compared the molecular weights of polyethylene determined by light scattering in 1-chloronaphthalene with those determined in 1,2,3,4-tetrahydronaphthalene and found agreement for low molecular weight samples only. The disagreement became larger with the increase of molecular weight. At molecular weights of over a million the values determined in 1-chloronaphthalene were two to three times higher than those determined in 1,2,3,4-tetrahydronaphthalene. He attributed this discrepancy to the association of high molecular weight molecules in 1-chloronaphthalene. While Schreiber,³ Schreiber and Waldman,⁴ Wippler,⁵ and also earlier work of Kobayashi et al.,⁶ have given support to Trementozzi's view, Kokle, Billmeyer, Muus and Newitt,⁷ on the other hand failed to confirm his results experimentally. Kokle et al. concluded that the association must have occurred in only a few samples in 1-chloronaphthalene but not in all. De La Cuesta and Billmeyer⁸ analyzed the light-scattering

data of high density polyethylene fractions in 1-chloronaphthalene from three independent sources⁹⁻¹¹ and found that statistically these data belong to a single population and therefore the samples used by them were not likely associated.

Since the molecular weight of polyethylene has far-reaching influences on the interpretation of many physical and rheological studies, dependable light-scattering measurements on the polymer are of great importance. The conclusion that some samples are associated in 1-chloronaphthalene and others not can hardly be taken as a satisfactory explanation for the conflicting sets of data. The purpose of the present work is to provide more experimental evidence aimed at resolving this controversy.

EXPERIMENTAL

Light-Scattering Instrument

A Sofica (Société Française d'Instruments de Contrôle et d'Analyse) photo-gonio-diffusometer was used as the light-scattering photometer in the present study. This instrument is a commercial version of a light-scattering apparatus designed by Wippler and Scheibling.¹² It has a liquid constant temperature bath which provides a faster approach to the measuring temperature for the solutions than the air bath used in an instrument reported earlier.¹¹ Dow Corning 702 fluid was used as the bath liquid as recommended by the manufacturer of the instrument. All measurements were made at 125°C. and with 546 $m\mu$ wavelength light.

Instrument Calibration

A cylindrical glass standard was furnished with the Sofica instrument. This glass standard was calibrated by comparing its scattered light intensity with that of pure benzene at 25°C. and that of a polyethylene solution at 125°C. The value, 16.3×10^{-6} , of Carr and Zimm¹³ was used as the Rayleigh ratio for benzene. The scattering intensity of the polyethylene solution was previously determined by a modified Brice-Phoenix light-scattering photometer of known calibration.¹¹ The results from the two calibrations agreed within 2%. The value obtained from the polyethylene solution was, however, used so that the data would be consistent with those determined previously using the modified Brice-Phoenix instrument.

Refractive Indices and Refractive Index Increments (dn/dc)

TABLE I
Refractive Indices and Refractive Index
Increments at 125°C., 546 $m\mu$ Light

Solvent	Refractive index	dn/dc , cc./g.
1-Chloronaphthalene	1.594	-0.195
1,2,3,4-Tetrahydronaphthalene	1.490	-0.064

In Table I, the refractive index of 1-chloronaphthalene is the measured value reported by Weston and Billmeyer.¹⁴ The dn/dc for polyethylene in 1-chloronaphthalene was the experimental value reported previously.¹¹ It is identical to the value reported recently by Drott and Mendelson¹⁵ and in close agreement with other reported values.¹⁴

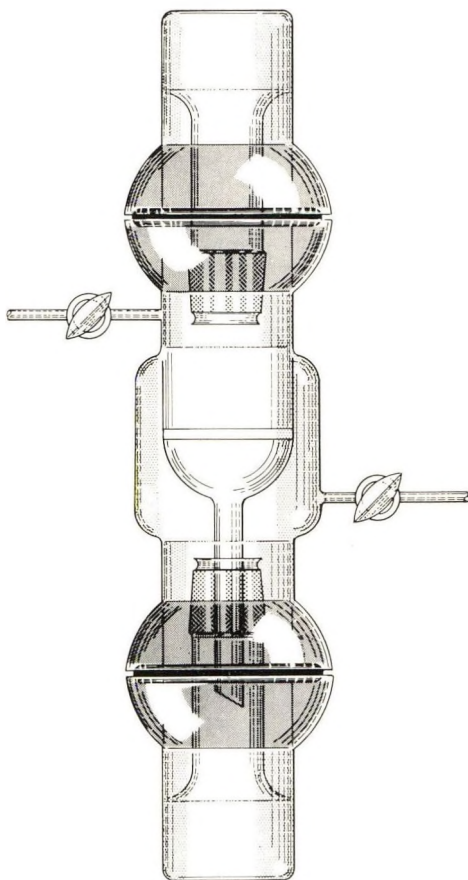


Fig. 1. Filtration apparatus.

The numbers listed in Table I for 1,2,3,4-tetrahydronaphthalene are calculated values; refractive index from room temperature measurement by the Lorentz-Lorenz equation, dn/dc from the value of 1-chloronaphthalene by the Gladstone and Dale rule. The dn/dc value is lower than those used by Trementozzi² and Nicolas,¹⁶ but is in good agreement with that reported by Drott and Mendelson.¹⁵ Drott and Mendelson obtained values of -0.0795 at 81.5°C . and -0.0691 at 105°C ., extrapolation from which gives a value of -0.0602 at 125°C . By using the same temperature coefficient, Trementozzi's value corresponds to -0.0911 at 125°C . Nicolas reported a value of -0.0943 at 125°C .

Materials

Both solvents, 1-chloronaphthalene and 1,2,3,4-tetrahydronaphthalene, were purchased from Eastman Kodak Company. Both were vacuum distilled before use.

Both high density and low density polyethylene fractions were used. These fractions were prepared by the partial precipitation technique from 1% xylene solutions. No refractionation steps were used. They are therefore not particularly narrow in molecular weight distribution but are free from the extra large molecules or particulate matter which may interfere with the light-scattering results.

Solution Preparation

The apparatus shown in Figure 1 was used for dissolution of the polymer and clarification of the solution. The lower reservoir was used for dissolution. After the polymer was completely dissolved, the apparatus was inverted and the solution was filtered through the ultrafine fritted glass filter into the upper reservoir. The entire apparatus was filled with prepurified nitrogen by repeated evacuation from the lower stopcock before heating was started. The filtered solution was then carefully transferred into the light-scattering cells where proper dilution with filtered solvent was made. The scattering intensity of the first solution measured was always checked again at the end to see if any degradation had taken place during the measurement.

RESULTS

TABLE II
Light-Scattering Results of Polyethylene Fractions in 1-Chloronaphthalene and 1,2,3,4-Tetrahydronaphthalene

Sample	In 1-chloronaphthalene			In tetrahydronaphthalene		
	$\langle M \rangle_w \times 10^{-3}$	A_2	$\langle S^2 \rangle^{1/2}$, A.	$\langle M \rangle_w \times 10^{-3}$	A_2	$\langle S^2 \rangle^{1/2}$, A.
A1 HDPE	373	7.9	710	610	13.4	780
B1 HDPE	255	10.9	416	420	13.9	519
B2 HDPE	132	12.1	274	204	16.2	407
C1 HDPE	371	5.3	580	601	6.8	875
D1 HDPE	286	10.4	474	439	14.4	580
D2 HDPE	115	12.0	316	167	16.9	300
E1 LDPE	2160	0.78	709	3480	1.06	845
E2 LDPE	733	2.5	609	1110	3.6	841
E3 LDPE	110	9.2	284	146	11.7	251

All the results listed in Table II are the average of two or more repeated runs. Zimm plots were used to evaluate the weight-average molecular weight $\langle M \rangle_w$, the second virial coefficient A_2 , and the root-mean-square radius $\langle S^2 \rangle^{1/2}$. The reproducibility of the results in 1-chloronaphthalene

was good. Figure 2 shows a Zimm plot of polymer B1 in 1-chloronaphthalene with the experimental points from two duplicated runs plotted together. The reproducibility of the results in 1,2,3,4-tetrahydronaphthalene was less satisfactory, especially for the two low molecular weight fractions D2 and E3. In these cases the excess light scattering of the polymer in a 0.5 g./100 cc. concentration at 90° was only 35% of the solvent light scattering. The numbers listed in Table II for D2 and E3 were the results of

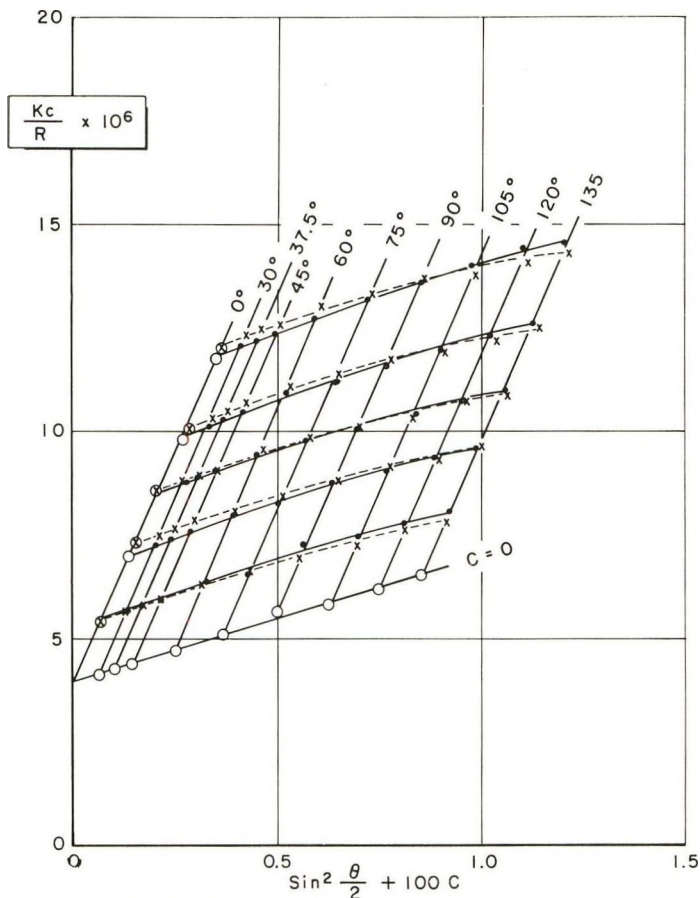


Fig. 2. Zimm plot of two duplicated runs of high density polyethylene fraction B1 in 1-chloronaphthalene.

four repeating runs plotted together. If these runs were plotted separately a difference of close to 30% in molecular weight would have resulted. Figure 3 shows the Zimm plot of D2 in 1,2,3,4-tetrahydronaphthalene with the experimental points of all four repeating runs shown.

Not all the Zimm plots obtained for the fractions give linear extrapolation to zero angle as shown in Figure 2. Figure 4 shows the Zimm plot for fraction E1 in 1-chloronaphthalene. The same amount of curvature exists in

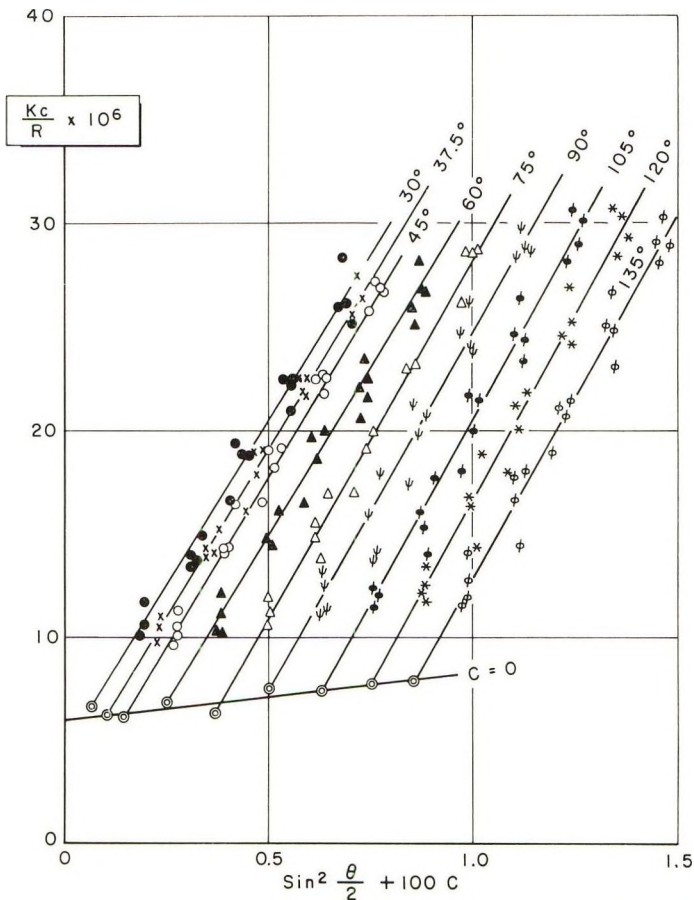


Fig. 3. Zimm plot of four repeated runs of high density polyethylene fraction D2 in 1,2,3,4-tetrahydronaphthalene.

the Zimm plot for the same fraction in 1,2,3,4-tetrahydronaphthalene as shown in Figure 5.

DISCUSSION

There is a large discrepancy of molecular weights determined in 1-chloronaphthalene and those determined in 1,2,3,4-tetrahydronaphthalene as shown in Table II, but this discrepancy remains at a near constant factor with the exception of the two lowest molecular weight fractions. Table III shows the ratio of weight-average molecular weights determined in the two solvents.

The uncertainty in the molecular weight determination for the low molecular samples in 1,2,3,4-tetrahydronaphthalene probably caused the drop-off of the ratios for samples D2 and E3. The results, nevertheless, show that molecular weights determined in 1-chloronaphthalene when compared

TABLE III
Ratio of $\langle M \rangle_w$ Determined in 1,2,3,4-Tetrahydronaphthalene to $\langle M \rangle_w$ in 1-Chloronaphthalene

Sample	$\langle M \rangle_w$ 1,2,3,4-Tetrahydronaphthalene
	$\langle M \rangle_w$ 1-Chloronaphthalene
A1	1.63
B1	1.65
B2	1.55
C1	1.62
D1	1.53
D2	1.45
E1	1.61
E2	1.52
E3	1.33

with those determined in 1,2,3,4-tetrahydronaphthalene did not go up with the increase of molecular weight as found by Trementozzi. The data covered as wide a molecular range as that reported by him. The association of high molecular weight polyethylene molecules in 1-chloronaphthalene observed by him is thus not substantiated by the present data.

One of the causes responsible for the differences in the absolute values of molecular weights measured in the two solvents is perhaps the uncertainty of the refractive index increment of polyethylene in 1,2,3,4-tetrahydro-

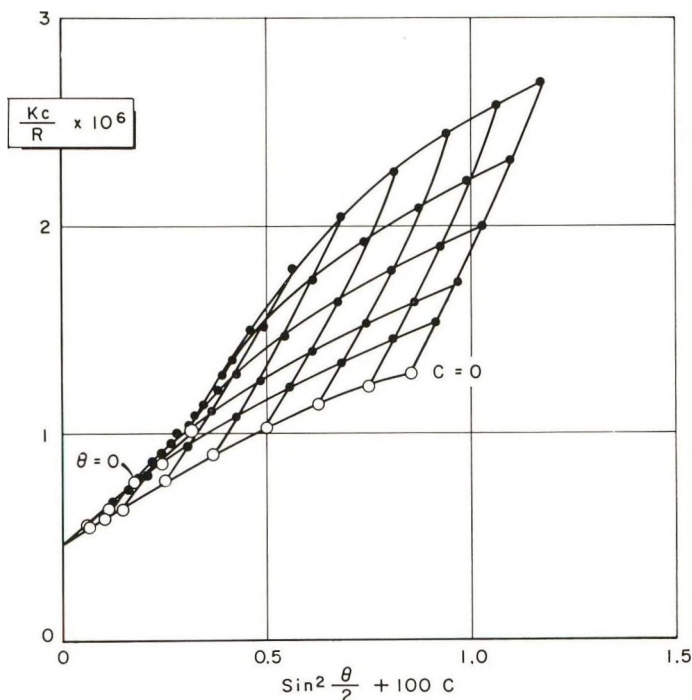


Fig. 4. Zimm plot of low density polyethylene fraction E1 in 1-chloronaphthalene.

naphthalene. The diversity of the values reported has already been shown. Attempts in this laboratory to measure the increment at 125°C. with the use of a Brice-Spenser differential refractometer have not been fruitful. The refractometer has been modified for high temperature work as reported earlier.¹¹ Unlike solutions of 1-chloronaphthalene, the solutions of 1,2,3,4-tetrahydronaphthalene tend to creep up on the cell wall and cause fast evaporation and poor reproducibility. In view of the fact that 1,2,3,4-tetrahydronaphthalene gives also poorer reproducibility in light-scattering measurements, further effort was not made to measure the refractive index

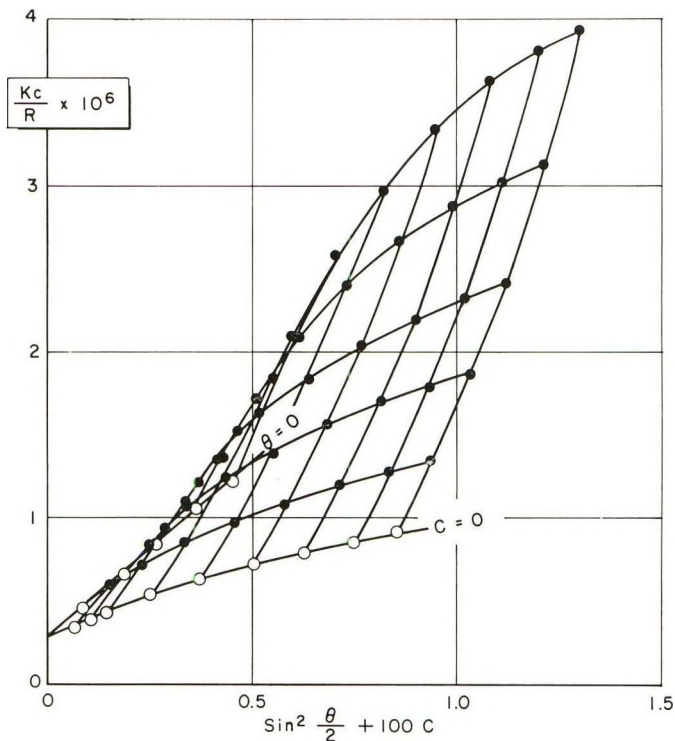


Fig. 5. Zimm plot of low density polyethylene fraction E1 in 1,2,3,4-tetrahydronaphthalene.

increment directly. The ratios of $\langle M \rangle_w$ listed in Table III for the two solvents have an average value of 1.59 (excluding ratios for samples D2 and E3). Assuming that the error is in the refractive index increment of polyethylene in 1,2,3,4-tetrahydronaphthalene, such a discrepancy corresponds to a new refractive index increment value of -0.081 . Table IV shows the recalculated results in 1,2,3,4-tetrahydronaphthalene on the basis of a value of -0.081 as the refractive index increment in comparison with the results determined in 1-chloronaphthalene.

From Table IV it can be seen that the agreement now between the molecular weights measured in 1,2,3,4-tetrahydronaphthalene and 1-chloronaphtha-

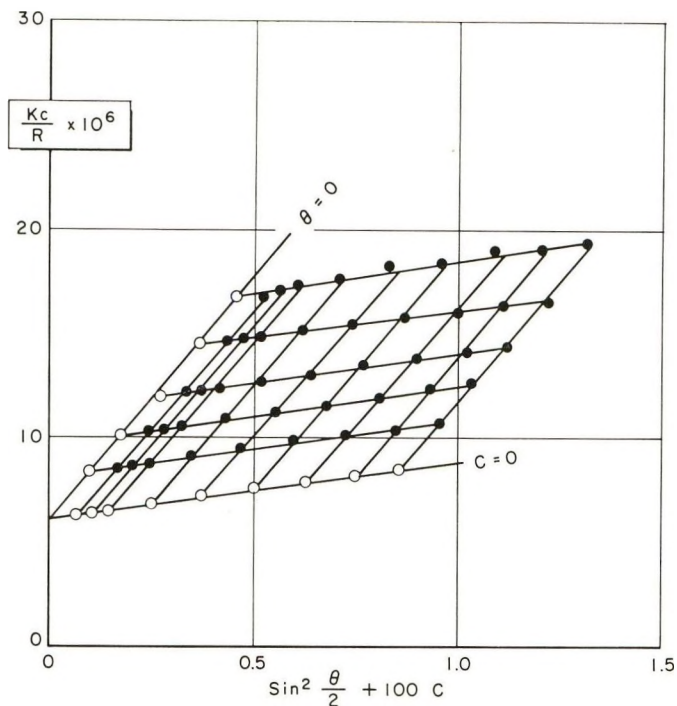


Fig. 6. Zimm plot of high density polyethylene fraction F1 in 1-chloronaphthalene. Clarification of solution was done under nitrogen atmosphere.

lene is quite good. The value of -0.081 is not unreasonable, since it is within the range of published values.

Among the high density polyethylene fractions measured, sample C1 contains some long chain branches. The inherent viscosity (measured in 1,2,3,4-tetrahydronaphthalene at $130^{\circ}\text{C}.$) of the sample is 3.1 dl./g. as compared

TABLE IV
Light-Scattering Results of Polyethylene Fractions in 1-Chloronaphthalene and Recalculated Results in 1,2,3,4-Tetrahydronaphthalene

Sample	In 1-chloronaphthalene			In 1,2,3,4-tetrahydronaphthalene		
	$\langle M \rangle_w \times 10^{-3}$	A_2	$\langle S^2 \rangle^{1/2}$, A.	$\langle M \rangle_w \times 10^{-3}$	A_2	$\langle S^2 \rangle^{1/2}$, A.
A1	373	7.9	710	384	21.3	780
B1	255	10.9	416	264	22.1	519
B2	132	12.1	274	128	25.8	407
C1	371	5.3	580	378	10.8	875
D1	286	10.4	474	276	22.9	580
D2	115	12.0	316	105	26.8	300
E1	2160	0.78	709	2190	1.68	845
E2	733	2.5	609	699	5.7	841
E3	110	9.2	284	92	18.6	251

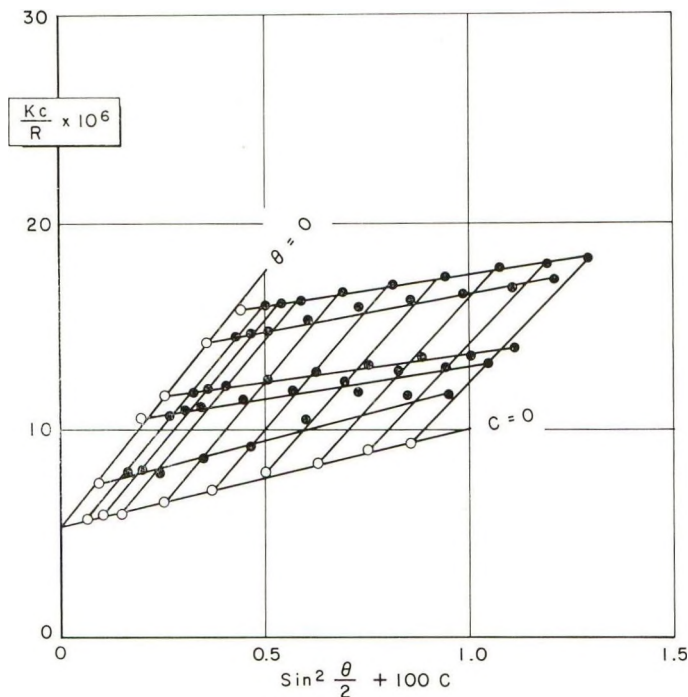


Fig. 7. Zimm plot of high density polyethylene fraction F1 in 1-chloronaphthalene. Solution was filtered twice in the presence of air.

to 4.0 dl./g. for sample A1 of almost identical weight-average molecular weight measured in both 1-chloronaphthalene and 1,2,3,4-tetrahydronaphthalene. In our previous work,¹¹ a few samples of high density polyethylene fractions were believed to contain long-chain branches based on light-scattering measurements in 1-chloronaphthalene. The present result on sample C1 indicates that the interpretation used then was correct. Those results could not have been caused by association as suspected by Schreiber and Waldman.⁴

In the present work the clarification of solutions by filtration was done under nitrogen atmosphere. The nitrogen atmosphere is not always necessary in producing satisfactory light-scattering results as there is some variation in the stability of polyethylene from sample to sample. Usually a sample which has been handled carefully will give identical light-scattering results whether the clarification step is done in air or in nitrogen. However, if the sample has been exposed excessively to high temperatures in the presence of air, filtration under nitrogen is essential for 1-chloronaphthalene solutions of polyethylene. Figure 6 shows the Zimm plot of a high density polyethylene fraction F1 determined in 1-chloronaphthalene when nitrogen protected filtration was used. Figure 7 shows the Zimm plot of the same sample, the solution of which had been filtered twice in the presence of air. Figure 7 gives a higher weight-average molecular weight in

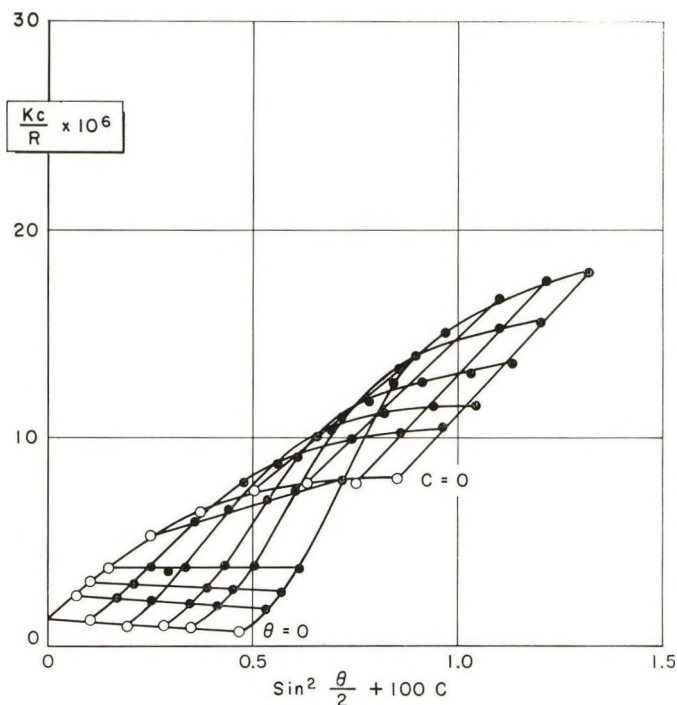


Fig. 8. Zimm plot of high density polyethylene fraction F1 in 1-chloronaphthalene. Solvent was vacuum-distilled through a nickel-packed column.

excess of the experimental error. Chemical crosslinking must have taken place during the double filtration. Filtration in the presence of air has less effect on 1,2,3,4-tetrahydronaphthalene solution of polyethylene. In Trementozzi's work the solutions were filtered four times. It is possible that such treatment on 1-chloronaphthalene solutions of polyethylene caused some crosslinking which he identified as association.

The quality of solvent is also important. For example, a batch of 1-chloronaphthalene distilled through a nickel packed column under vacuum was found to be entirely unsatisfactory for light-scattering work. Figure 8 shows the Zimm plot of fraction F1 determined in such a batch of solvent. Mass spectrometry analysis of the solvent showed only a small amount of impurity at m/e 166 or 168. Such impurities were also found in batches of 1-chloronaphthalene which produced normal light-scattering results. A slight amount of hydroperoxides was, however, found in the 1-chloronaphthalene distilled through the nickel-packed column by the iodometric method of Kokatnur and Jelling.¹⁷ Table V shows the hydroperoxide contents determined. Although 1,2,3,4-tetrahydronaphthalene contained a larger amount of hydroperoxide it did not cause crosslinking of polyethylene as in the case of 1-chloronaphthalene. It is not sure whether the 1-chloronaphthalene or the small amount of halogenated impurities actually formed the hydroperoxide.

TABLE V
Hydroperoxide Contents in 1-Chloronaphthalene and 1,2,3,4-Tetrahydronaphthalene

	Hydroperoxides, ppm	
	In 1-chloronaphthalene	In 1,2,3,4-tetrahydronaphthalene
Vacuum-distilled in all-glass Oldershaw column	undetectable	4
Vacuum-distilled in nickel- packed column	10	35

The temperature of measurement can also influence the results of light-scattering measurements in 1-chloronaphthalene. Schreiber and Waldman⁴ have shown that at 100°C. the molecular weights measured in 1-chloronaphthalene were some 20–30% higher than those measured at 140°C. Presumably, residue crystalline forces at 100°C. caused the clustering of polyethylene molecules in the solvent. The majority of runs reported by Trementozzi were made at 105°C., which could be too low a temperature. 1,2,3,4-Tetrahydronaphthalene, being a better solvent for polyethylene, does not cause the clustering of the polymer molecules. The temperature effect alone is, however, too small to account for the two- to three-fold differences between the molecular weights measured in 1,2,3,4-tetrahydronaphthalene and 1-chloronaphthalene reported by Trementozzi.

In conclusion, the present data indicate that light-scattering molecular weights of polyethylene determined in 1-chloronaphthalene at 125°C. are reliable provided that certain care is exercised. Although 1,2,3,4-tetrahydronaphthalene seems to be a more stable solvent for polyethylene under adverse conditions, it is not a recommended solvent because of the low excess light-scattering intensity of polyethylene in this solvent and the uncertainty of the refractive index increment.

References

1. Billmeyer, F. W., Jr., *J. Am. Chem. Soc.*, **75**, 6118 (1953).
2. Trementozzi, Q. A., *J. Polymer Sci.*, **36**, 113 (1959).
3. Schreiber, H. P., *Can. J. Chem.*, **39**, 1557 (1961).
4. Schreiber, H. P., and M. H. Waldman, *J. Polymer Sci.*, **A2**, 1655 (1964).
5. Wippler, C., through Kokle et al., ref. 6.
6. Kobayashi, T., A. Chitale, and H. P. Frank, *J. Polymer Sci.*, **24**, 156 (1957).
7. Kokle, V., F. W. Billmeyer, Jr., L. T. Muus, and E. J. Newitt, *J. Polymer Sci.*, **62**, 251 (1962).
8. De La Cuesta, M. O., and F. W. Billmeyer, Jr., *J. Polymer Sci.*, **A1**, 1721 (1963).
9. Henry, P. M., *J. Polymer Sci.*, **36** (1959).
10. Chiang, R., *J. Polymer Sci.*, **36**, 91 (1959).
11. Tung, L. H., *J. Polymer Sci.*, **36**, 287 (1959).
12. Wippler, C., and G. Scheibling, *J. Phys. Chim.*, **51**, 201 (1954).
13. Carr, C. O., and B. H. Zimm, *J. Chem. Phys.*, **18**, 1616 (1950).
14. Weston, N. E., and F. W. Billmeyer, Jr., *J. Phys. Chem.*, **65**, 576 (1961).
15. Drott, E. E., and R. A. Mendelson, *Polymer Letters*, **B2**, 187 (1964).

16. Nicolas, L., *J. Polymer Sci.*, **29**, 191 (1958).
17. Kokatnur, V. R., and M. Jelling, *J. Am. Chem. Soc.*, **63**, 1432 (1941).

Résumé

Les poids moléculaires du polyéthylène ont été déterminés par des mesures de diffusion lumineuse dans le 1-chloronaphtalène et le 1,2,3,4-tétrahydronaphtalène à 125°C. On a utilisé des fractions de polyéthylène de haute densité et de faible densité. Les résultats montrent qu'à 125°C, les molécules de polyéthylène ne sont pas associées dans le 1-chloronaphtalène. La différence des poids moléculaires du polyéthylène déterminés dans les deux solvants est due à l'incertitude de l'incrément de l'indice de réfraction du polyéthylène dans le 1,2,3,4-tétrahydronaphtalène et à l'oxydation possible du polymère dans le 1-chloronaphtalène.

Zusammenfassung

Molekulargewichte von Polyäthylenen wurden durch Lichtstreuungsmessungen in 1-Chlornaphthalin und 1,2,3,4-Tetrahydronaphthalin bei 125°C bestimmt. Es wurden Polyäthylenfraktionen hoher und niedriger Dichte verwendet. Die Ergebnisse zeigen, dass Polyäthylenmoleküle bei 125°C in 1-Chlornaphthalin nicht assoziieren. Der Widerspruch zwischen den in den beiden Lösungsmitteln bestimmten Molekulargewichten von Polyäthylen wird auf die Ungenauigkeit des Brechungsindexinkrements von Polyäthylen in 1,2,3,4-Tetrahydronaphthalin und auf eine mögliche Oxydation des Polymeren in 1-Chlornaphthalin zurückgeführt.

Received December 26, 1963

Revised January 28, 1964

Some Elastic Moduli of Bisphenol A Polycarbonate

RICHARD E. ROBERTSON and ROBERT J. BUENKER,* *General Electric Research Laboratory, Schenectady, New York*

Synopsis

The Young's modulus of oriented bisphenol A polycarbonate films were measured along, 45° to, and normal to the direction of orientation by the vibrating reed technique. The change in modulus with the degree of orientation was fitted to a theoretical curve, using an IBM 704 electronic computer. The basis for fitting the data to the theoretical curve was the assumption that the process of orienting the polymer molecules could be described by an affine transformation. The elastic moduli calculated are as follows: The Young's modulus for stretching the chain is 5.4×10^{11} dyne/cm.²; the Young's modulus for separating a bundle of parallel chains laterally is 1.76×10^{10} dyne/cm.²; and the shear modulus for the relative displacement of a bundle of parallel chains along their length is 2.00×10^{10} dyne/cm.².

1. Introduction

In 1936 Meyer and Lotmar¹ calculated the elastic modulus of cellulose along the molecular chain axis from the force constants of the chemical bonds. The values they calculated, 7.7×10^{11} – 12.1×10^{11} dyne/cm.², compared favorably at least with the measured modulus of flax: 8×10^{11} – 11×10^{11} dyne/cm.². More recently, Lyons² calculated the elastic moduli of poly(ethylene terephthalate) and nylon 66 along their chain axes and noted that they were more than an order of magnitude larger than the measured moduli of these materials. But the calculated value of Lyons compares favorably with the modulus of poly(ethylene terephthalate) measured by Dulmage and Contois.³ The latter measured the modulus of the crystalline phase of polyethylene terephthalate by noting the change in the fiber identification period (FIP) deduced from x-ray patterns as the applied stress on a highly drawn specimen was changed. Their result was 1.37×10^{12} dyne/cm.², which compares very well with the best theoretical estimate, that of Treloar,⁴ of 1.22×10^{12} dyne/cm.². Still, however, an exact comparison between theory and experiment has not been made. The theoretical modulus has been calculated for an isolated polymer chain and not for an orderly collection of chains in a crystal. Treloar, for example, postulates that the neglect of the lateral interaction between the chains in the crystal causes the disparity between what we can take for the experimental modulus⁶ of cellulose, 13.4×10^{11} dyne/cm.², and the theoretical

* Present address: Department of Chemistry, Princeton University, Princeton, New Jersey.

modulus,⁴ 5.65×10^{11} dyne/cm². In the present paper, an investigation is described that yields the Young's modulus along a bundle of parallel linear polymers chains that are to a large extent randomly oriented about the chain axis—an experimental condition that may correspond more closely with the theoretical condition of an isolated chain. The moduli of completely oriented, amorphous bisphenol A polycarbonate were calculated from the change in moduli with molecular orientation at low orientation levels.

If an unoriented polymeric material is plastically strained along a single direction, more of the chain axes will be directed along the strain direction than previously and, also, fewer will be directed in a plane normal to the strain direction. This will lead to an anisotropy in a number of properties, including the Young's modulus, simply because of the intrinsic anisotropy of the polymer molecules themselves. If both the intrinsic anisotropic properties of the polymer molecules and the way in which the polymer chains change their orientation with plastic strain, were known, the macroscopic anisotropy resulting from a given plastic strain could be calculated. Or, if instead of the macroscopic anisotropy resulting from a given plastic strain and how the polymer strains changed their orientation with plastic strain were known, the intrinsic anisotropic properties of the polymer molecules could be calculated. Since the macroscopic properties are easily measured, the molecular properties can be obtained if some relationship between plastic strain and molecular orientation can be assumed. We will assume that upon straining the material plastically, the directions of the chain axes undergo an affine transformation. This is the assumption used extensively in the theory of rubber elasticity. Although we will consider the nature of the assumption in detail later, it seems as though the assumption should hold for principally amorphous polymers that are not oriented to the extent that either the material crystallizes or residual crystallites in the unoriented material begin to dominate the behavior. We believe these conditions are satisfied for the bisphenol A polycarbonate investigated in the present work.

The modulus has been measured as a function of plastic strain by a number of investigators on various materials. For example, Hillier and Kolsky⁶ studied polyethylene, neoprene, and nylon; Shinohara and Tanzawa⁷ and Wilson⁸ studied regenerated cellulose; Raumann and Saunders⁹ studied polyethylene; and Wakelin et al.¹⁰ studied nylon 66 and poly(ethylene terephthalate). For the most part these studies cannot be used to find the molecular properties because either a careful accounting of the degree of orientation was not made or crystalline effects intruded.

One must be very careful about interpreting plastic strain, because above the glass transition temperature, molecular relaxation always accompanies plastic strain. Therefore, plastic strain is not often simply related to molecular orientation.

Ward¹¹ has analyzed the data of Raumann and Saunders⁹ on polyethylene according to the procedure we will use with polycarbonate, by assuming

plastic strain to result in an affine transformation of the molecular axes. The result obtained by Ward for the modulus along the chain axis is rather low: Ward calculated 0.2×10^{11} dyne/cm.², which can be compared with an experimental value⁵ of 23.6×10^{11} dyne/cm.². From this we can conclude that the assumption of an affine transformation breaks down if crystalline effects become important, as they are in polyethylene.

As found previously by Raumann and Saunders⁹ on polyethylene, it is extremely difficult to eliminate plastic or anelastic strains from a conventional stress-strain diagram of a polymer because such strains occur at elastic strains even smaller than 1%. We have, therefore, gone to a vibrating reed technique in an attempt to lessen the effect of the plastic or anelastic strains. To obtain the elastic moduli of the polymer chains, we have fitted a theoretical curve by the methods of multiple regression, using an IBM 704 computer.

2. Experimental

The resonant frequency of vibration of a rectangular cantilever beam, vibrating in the mode of lowest frequency is given by¹²

$$f_1 = (a_1/2\pi)(Eh^2/12\rho l^4)^{1/2} \quad (1)$$

In this equation, E is the Young's modulus along the beam, h is the thickness, ρ is the density, and l is the length of the beam. a_1 is a constant describing the first vibrational mode, which we have used in these experiments, and has the value 3.52. Now, the actual size of the beam is not important here so that these equations are perfectly applicable to a thin strip of film clamped at one end. Then, knowing the resonant frequency, the Young's modulus is given by

$$E = (48\pi^2 f_1^2 \rho l^4)/(a_1^2 h^2) \quad (2)$$

It has been found that the preparation of samples requires care. Initial experiments with samples long enough that we could easily observe both the first and the second mode of vibration showed the importance of having the edges of the samples parallel. The theoretical value for the ratio of the frequency of the second mode to that of the first, f_2/f_1 , is 6.25. Let us consider how this ratio changes for trapezoidal samples. If w_f is the width at the free end and w_c the width at the clamped end, the gradient w' is defined by

$$w' = (w_f - w_c)/l \quad (3)$$

We have found empirically that for trapezoidal reeds,

$$f_2/f_1 \approx 6.25 + 130w' \quad (4)$$

This is a rather large effect. But its full importance may not be described by eq. (4) because this equation gives only the ratio of the two frequencies. Although we expect the change from a rectangular to a trapezoidal specimen to affect f_2 to a greater extent than f_1 , it is still likely to be important

for f_1 . What we have said here about width would seem also to hold for thickness.

But even keeping the width the same along the specimen did not solve the problem of reproducibility. We found, however, that for specimens 0.1 mm. and less in thickness we could get reproducibility within $\pm 5\%$ if we kept the length and width within certain ranges:

$$0.75 \text{ cm.} < l < 1.50 \text{ cm.}$$

$$0.20 \text{ cm.} < w < 0.40 \text{ cm., for } h \approx 0.1 \text{ mm.} \quad (5)$$

The samples were first stretched to the proper degree of orientation under various stresses in an oven held at 155°C . Then a paper cutter with a sharp blade was used to obtain the desired dimensions for each specimen. In the actual experiment about six degrees of orientation were achieved and samples of each were cut parallel, perpendicular, and 45° to the direction of orientation. Lengths were measured to 0.0003 cm. with a traveling microscope and thicknesses to $3 \times 10^{-5} \text{ cm.}$ with a Sheffield gauge.

The samples were clamped in place with a jig made from two pieces of clear plastic ($\frac{1}{2} \text{ in.} \times \frac{3}{8} \text{ in.} \times \frac{1}{8} \text{ in.}$) joined with two pins and two screws. This in turn was placed on an earphone connected to an audio oscillator. Frequency measurements were made at 24°C .; the criterion of resonance was maximum amplitude. The latter was kept as low as possible during the measurement as the resonant frequency is slightly amplitude-dependent. The resonant frequency in our experiments ranged between 100 and 400 cycles/sec.; the modulus did not show any frequency dependence between the limits of this range. And the frequency of the oscillator was measured to 0.1 cycle/sec. by an electronic counter.

Finally, it should be mentioned that the procedure of calculating the elastic constants of the molecular chains by measuring the change in modulus with molecular orientation requires only that the modulus in one direction be measured, say, along the direction of orientation. However, since it is generally difficult to obtain high orientations without drastically changing the nature of the material, it is better to measure also both the modulus at an angle of 45° to and normal to the direction of orientation. Because the present experiments were especially limited in the degree of orientation that could be attained, this latter procedure was extremely important.

3. Assumption of an Affine Transformation

An affine transformation is a mathematical term for the linear transformations of a set of points and for which the inverse linear transformations exist. For our purposes, we can think of an affine transformation in terms of the deformation of a perfectly homogeneous, solid body. We consider such a body and imagine a set of points to be imbedded within it. Then, if the body is deformed, the points are displaced such that the fractional displacement of the points along any particular direction is the same

throughout the body. Moreover, if we consider the body to have the shape of a sphere and to be isotropic, deforming the sphere by stretching it uniformly in some direction will yield a prolate spheroid, a body described by the revolution of an ellipse about its major axis. Let us now consider the set of points imbedded in the body to be connected by line elements. We ask with what probability does some element point in a given direction. In the undeformed, isotropic body, there is no preferred direction, so any direction is as likely as any other. We can describe this uniform probability distribution function by a sphere. If we now deform the body by stretching it uniformly in some direction, the probability distribution function for the directions of the line elements changes from the sphere to the same prolate spheroid as the deformation causes the body to take. This correspondence between the probability distribution function and the macroscopic shape of the body is very convenient and is not limited to deformation through uniaxial stretching.

The utility of these concepts in the theory of rubber elasticity is quite direct; the crosslink junctions are taken as the system of points which are connected by the molecular chains. We draw the same type of analogy with linear polymers; but we take the imbedded points as entanglements, which are again connected by polymer chains. To describe the change in the directions of the polymer chains' axes with plastic strain as an affine transformation, therefore, requires the following two conditions. (a) The polymer must be homogeneous so that a macroscopic deformation produces the same strain throughout the body. By the anisotropic nature of a polymer chain this condition cannot be completely satisfied. But we can assume that it is approximately satisfied down to the level of a single polymer chain in an amorphous polymer. (b) There can be no slippage of the polymer chains at the entanglements if we are to keep the simplicity of the macroscopic deformation and the probability function correspondence. This condition is probably satisfied if stretching occurs below the glass transition temperature and if the degree of stretching is not too large. Because polycarbonate necks on cold-drawing, the range of molecular orientation is quite limited. But above the glass transition temperature any degree of orientation can be obtained. But here, molecular relaxation, or slippage at the entanglement point, occurs, accompanying molecular orientation. To overcome the molecular relaxation, we used optical birefringence.

The use of birefringence to compensate for the history of a polymer specimen has been studied in detail by Rudd and Andrews.¹³ In general, they find the relationship between the birefringence and the mechanical properties to be fairly independent of the exact history. The birefringence represents, of course, an average over the distribution of axial directions of the polymer chains. Let us consider a bundle of parallel molecules. If on orienting these molecules there is no particular orientation of each molecule about its axis, we can define refractive indices parallel, n_{\parallel} , and perpendicular to, n_{\perp} , the chain axes. In a partially oriented specimen, the macroscopic

refractive indices, n_{\parallel}' and n_{\perp}' , will each be averages over n_{\parallel} and n_{\perp} . Since the refractive index transforms as a dyadic, if we denote by θ the angle between the molecular axis and the direction of orientation, we have

$$\begin{aligned} n_{\parallel}' &= n_{\parallel}\langle\cos^2\theta\rangle + n_{\perp}\langle\sin^2\theta\rangle \\ n_{\perp}' &= n_{\perp}\langle\cos^2\theta\rangle + \frac{1}{2}(n_{\parallel} + n_{\perp})\langle\sin^2\theta\rangle \end{aligned} \quad (6)$$

where the angular brackets indicate the average over the distribution of chain directions assumed. The birefringence $\Delta n'$ is, then, given by

$$\begin{aligned} \Delta n' &= n_{\parallel}' - n_{\perp}' \\ &= (n_{\parallel} - n_{\perp})(1 - \frac{3}{2}\langle\sin^2\theta\rangle) \end{aligned} \quad (7)$$

(For a more detailed derivation of the above, the reader is referred to Ward's paper.¹¹)

As we have previously noted, because of molecular relaxation accompanying plastic strain in the vicinity of the glass-transition temperature, the actual orientation may not correspond at all to the geometric changes in the body being strained. We will assume, though, that the distribution function for the directions of the polymer chain axes that results is still described by a prolate spheroid. To describe this new function, we will define the affine molecular orientation Ω . Ω is analogous to the plastic strain, but in general

$$1 + \Omega \leq \lambda \quad (8)$$

where λ is the extension ratio. The two sides of this equation are equal only when molecular relaxation does not accompany extension.

The average in eq. (7) can be easily carried out using either the more physical approach of Hsiao¹⁴ or the more mathematical approach of Ward¹¹ to describe the distribution function. The birefringence is given by^{11,15}

$$\Delta n' = \frac{n_{\parallel} - n_{\perp}}{2} \left\{ \frac{2(1 + \Omega)^3 + 1}{(1 + \Omega)^3 - 1} - \frac{3(1 + \Omega)^3}{[(1 + \Omega)^3 - 1]^{2/3}} \tan^{-1}[(1 + \Omega)^3 - 1]^{1/2} \right\} \quad (9)$$

In actual practice, of course, the difference $(n_{\parallel} - n_{\perp})$ is rarely known, and eq. (9) is fairly well approximated, for a moderate degree of molecular orientation, by

$$\Delta n' = \text{const.} \times \Omega \quad (10)$$

In the case of bisphenol A polycarbonate, an extension at room temperature, occurring under the conditions of cold-drawing, is probably not accompanied by molecular relaxation. Therefore, the equality sign in eq. (8) can be used. A typical extension ratio of 1.62 results in a birefringence of 0.01087 at the mercury 5461 Å line. From eq. (9) this gives the molecular birefringence

$$n_{\parallel} - n_{\perp} = 0.0358 \quad (11)$$

Also, for our investigation, eq. (10) becomes

$$\Delta n' = 0.0175\Omega \quad (12)$$

On comparing eq. (12) with the exact eq. (9) we find that Ω as given by eq. (12) does not differ by more than 0.035 from its true value as long as $\Omega \leq 0.75$, which it is for our experiments.

The advantage of using birefringence as a measure of molecular orientation is that it depends on the same probability distribution function for the directions of the polymer chain axes as the elastic modulus. But our assumption that the probability function is described by a prolate spheroid, even if the material is stretched above its glass transition temperature, may not be perfectly correct. In this case, the birefringence loses some of its usefulness. To test our assumption we must look at the calculated moduli that result from the assumption.

4. Results and Discussion

If we orient a piece of film uniaxially, for instance, the elastic modulus will not be the same in the different directions. If we let χ be the angle between the direction of orientation and the direction in which the modulus is measured, then the modulus E_χ will vary as χ varies according to⁹

$$1/E_\chi = s_{11}' \sin^4 \chi + (2s_{13}' + s_{44}') \sin^2 \chi \cos^2 \chi + s_{33}' \cos^4 \chi \quad (13)$$

where s_{11}' , $(2s_{13}' + s_{44}')$, and s_{33}' are elastic constants of the material. In our experiments we measured the modulus along, at an angle of 45° to, and normal to the direction of stretch, giving us

$$1/E_{90} = s_{11}' \quad (14)$$

$$1/E_{45} = (s_{11}' + 2s_{13}' + s_{44}' + s_{33}')/4 \quad (15)$$

$$1/E_0 = s_{33}' \quad (16)$$

The elastic compliances in eqs. (13) and (14), s_{11}' , s_{33}' , s_{13}' , and s_{44}' , are just the macroscopic compliances at the particular degree of orientation (i.e., these compliances are functions of Ω). But they are related to the molecular compliances, s_{11} , s_{33} , s_{13} , and s_{44} ; in particular, the two sets are equal for the case of perfect orientation ($\Omega = \infty$). Therefore, s_{33} is the compliance along the polymer chains, s_{11} is the compliance in a plane perpendicular to the chain axes, s_{13} relates the strain in the plane perpendicular to the chain axes when a stress is applied along the chains and vice versa, and s_{44} is the shear compliance for movement of the polymer chains along their axes. Since we have assumed uniaxial orientation, the material should be isotropic in the plane perpendicular to the direction of stretching. Thus the significant parameter is the angle θ between the direction of stretching and the direction of a polymer segment, or more precisely the average of θ over all the segmental directions in the material. To relate the microscopic and macroscopic compliances, we will assume a series-type model. We assume that the

strain varies from point to point in the polymer sample, as the direction of the molecular axes change. But we assume that the stress is constant everywhere. For these assumptions, Ward¹¹ has given the following relationships.

$$s_{11}' = (1/8) \{ [3\langle \cos^4 \theta \rangle + 2\langle \cos^2 \theta \rangle + 3]s_{11} + 3\langle \sin^4 \theta \rangle s_{33} + [3\langle \cos^2 \theta \sin^2 \theta \rangle + \langle \sin^2 \theta \rangle](2s_{13} + s_{44}) \} \quad (17)$$

$$(2s_{12}' + s_{44}') = [3\langle \cos^2 \theta \sin^2 \theta \rangle + \langle \sin^2 \theta \rangle]s_{11} + 3\langle \sin^2 \theta \cos^3 \theta \rangle s_{33} + 1/2[\langle \sin^4 \theta \rangle + \langle \cos^4 \theta \rangle - 4\langle \sin^2 \theta \cos^2 \theta \rangle + \langle \cos^2 \theta \rangle](2s_{13} + s_{44}) \quad (18)$$

$$s_{33}' = \langle \sin^4 \theta \rangle s_{11} + \langle \cos^4 \theta \rangle s_{33} + \langle \sin^2 \theta \cos^2 \theta \rangle (2s_{13} + s_{44}) \quad (19)$$

The angular bracket indicates the average over all the polymer segments in the material. Again assuming an affine transformation of the chain directions on stretching the material, one can find^{11,16}

$$\langle \sin^4 \theta \rangle = \frac{K^4}{(1 - K^2)^2} \left[1 + \frac{1}{2K^2} + \frac{(1/2 - 2K^2) \cos^{-1} K}{K^3(1 - K^2)^{1/2}} \right] \quad (20)$$

$$\langle \cos^4 \theta \rangle = \frac{1}{(1 - K^2)^2} \left[1 + \frac{K^2}{2} - \frac{3K \cos^{-1} K}{2(1 - K^2)^{1/2}} \right] \quad (21)$$

$$\langle \cos^2 \theta \sin^2 \theta \rangle = \frac{K^2}{(1 - K^2)^2} \left[-\frac{3}{2} + \frac{(1 + 2K^2) \cos^{-1} K}{2K(1 - K^2)^{1/2}} \right] \quad (22)$$

$$\langle \sin^2 \theta \rangle = \frac{K^2}{1 - K^2} \left\{ -1 + \frac{\cos^{-1} K}{K(1 - K^2)^{1/2}} \right\} \quad (23)$$

$$\langle \cos^2 \theta \rangle = 1 - \langle \sin^2 \theta \rangle \quad (24)$$

where

$$K = (1 + \Omega)^{-2/3} \quad (25)$$

Equations (20)–(24) are the same as those given by Ward¹¹ except for a correction of the misprint in $\langle \sin^2 \theta \cos^2 \theta \rangle$; the first term should be $-3/2$, as indicated, rather than $-2/3$.

To find the molecular elastic constants through eqs. (14)–(25), the method of least squares was used. Let

$$\begin{aligned} x(\Omega) &= 1/E_{90}(\Omega) \\ &= A_{x1}(\Omega)s_{11} + A_{x2}(\Omega)(2s_{13} + s_{44}) + A_{x3}(\Omega)s_{33} \end{aligned} \quad (26)$$

$$\begin{aligned} y(\Omega) &= 1/E_{45}(\Omega) \\ &= A_{y1}(\Omega)s_{11} + A_{y2}(\Omega)(2s_{13} + s_{44}) + A_{y3}(\Omega)s_{33} \end{aligned} \quad (27)$$

$$\begin{aligned} z(\Omega) &= 1/E_0(\Omega) \\ &= A_{z1}(\Omega)s_{11} + A_{z2}(\Omega)(2s_{13} + s_{44}) + A_{z3}(\Omega)s_{33} \end{aligned} \quad (28)$$

The basis of our least-squares calculation is the assumption that for a given affine molecular orientation the measured values of the modulus will be

normally distributed about the true value of the modulus with a standard deviation σ that is independent of Ω . For a measurement of E_{90} , say, at an orientation Ω_i , we will denote the reciprocal of this measurement by $x^i(\Omega_i)$ and we denote its true value by $x(\Omega_i)$. The difference $[x^i(\Omega_i) - x(\Omega_i)]$ therefore represents the deviation in the reciprocal of the measured modulus. Because of our assumption of a normal distribution we let L be the likelihood of obtaining in a series of measurements the compliances $x^i(\Omega_i)$, $y^j(\Omega_j)$, $z^k(\Omega_k)$, all i, j, k :¹¹

$$\ln L = -1/2(N_x + N_y + N_z) \ln (2\pi\sigma^2) - \frac{1}{2\sigma^2} \left\{ \sum_{i=1}^{N_x} [x^i(\Omega_i) - \sum_p A_{xp}(\Omega_i)s_p]^2 + \sum_{j=1}^{N_y} [y^j(\Omega_j) - \sum_p A_{yp}(\Omega_j)s_p]^2 + \sum_{k=1}^{N_z} [z^k(\Omega_k) - \sum_p A_{zp}(\Omega_k)s_p]^2 \right\} \quad (29)$$

For convenience here we have let $s_1 = s_{11}$, $s_2 = (2s_{13} + s_{34})$, and $s_3 = s_{33}$. Also, N_x , N_y , and N_z are the number of experimental measurements of E_{90} , E_{45} , and E_0 , respectively. To obtain the molecular parameters s_p , we adjust them so as to make the likelihood L a maximum; i.e., we take the derivative $\partial \ln L / \partial s_p$ and set it equal to zero. This gives the equations, $p = 1, 2, 3$:

$$\sum_{i=1}^{N_x} -A_{xp}(\Omega_i) [x^i(\Omega_i) - \sum_q A_{xq}(\Omega_i)s_q] + \sum_{j=1}^{N_y} -A_{yp}(\Omega_j) [y^j(\Omega_j) - \sum_q A_{yq}(\Omega_j)s_q] + \sum_{k=1}^{N_z} -A_{zp}(\Omega_k) [z^k(\Omega_k) - \sum_q A_{zq}(\Omega_k)s_q] = 0 \quad (30)$$

In a similar fashion the standard deviation σ is found. If we let

$$B_{pq} = \sum_{i=1}^{N_x} A_{xp}(\Omega_i)A_{xq}(\Omega_i) + \sum_{j=1}^{N_y} A_{yp}(\Omega_j)A_{yq}(\Omega_j) + \sum_{k=1}^{N_z} A_{zp}(\Omega_k)A_{zq}(\Omega_k) \quad (31)$$

and

$$\xi_p = \sum_{i=1}^{N_x} A_{xp}(\Omega_i)x^i(\Omega_i) + \sum_{j=1}^{N_y} A_{yp}(\Omega_j)y^j(\Omega_j) + \sum_{k=1}^{N_z} A_{zp}(\Omega_k)z^k(\Omega_k) \quad (32)$$

then we can write eq. (30) as

$$\sum_q B_{pq}s_q = \xi_p \quad (33)$$

B_{pq} is obviously a symmetrical matrix. We can, therefore, find its inverse B_{qp}^{-1} such that $B_{qp}^{-1}B_{pq} = 1$. Then, the molecular moduli are given by

$$s_q = \sum_p B_{qp}^{-1}\xi_p \quad (34)$$

The above procedure for finding the elastic moduli of the polymer chains is not very convenient to carry out manually. We have, therefore, programmed it for an IBM 704 computer. The experimental points and the

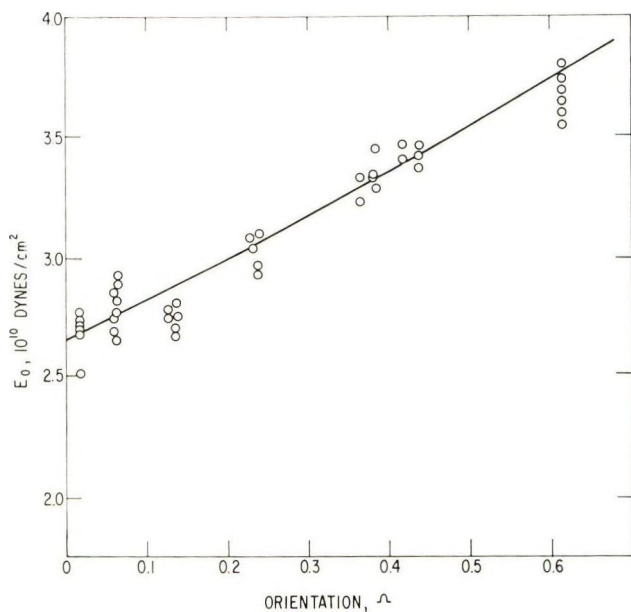


Fig. 1. Young's modulus along the direction of orientation of uniaxially stretched films vs. the affine molecular orientation Ω .

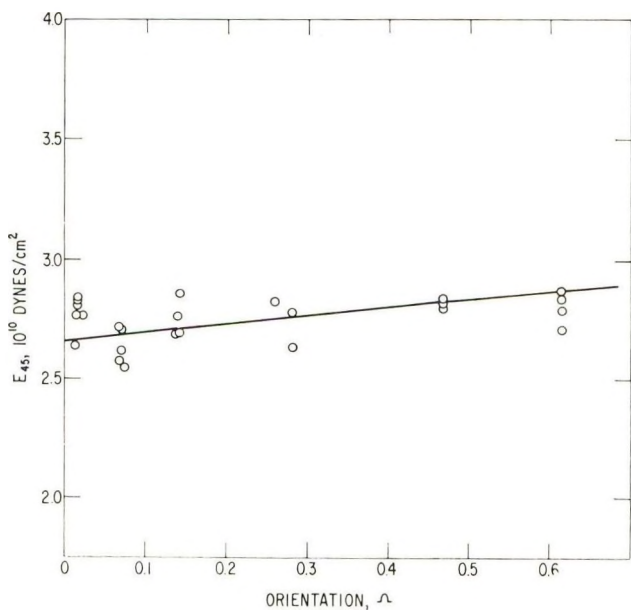


Fig. 2. Young's modulus at 45° to the direction of orientation of uniaxially stretched films vs. the affine molecular orientation Ω .

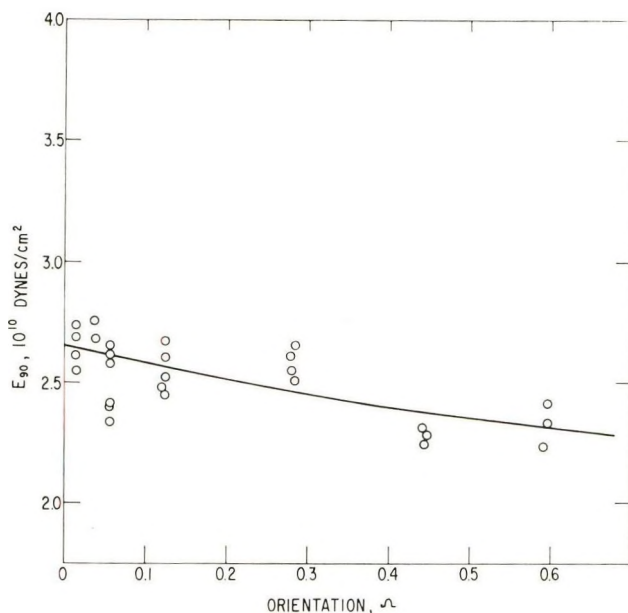


Fig. 3. Young's modulus perpendicular to the direction of uniaxially stretched films vs. the affine molecular orientation Ω .

theoretical curves for E_0 , E_{45} , and E_{90} are shown in Figures 1-3. They are similar to those found by Wilson,⁸ for instance, for regenerated cellulose. The molecular compliances and the standard deviation computed from the data are given in Table I; the results of the computation by means of both eqs. (9) and (12) for relating the birefringence and the affine molecular orientation are given, although that obtained by use of eq. (9) has the more theoretical significance. When the first set of compliances in Table I is

TABLE I

	Molecular compliances $\times 10^{-11}$, cm. ² /dyne			
	s_{11}	s_{33}	$(2s_{13} + s_{44})$	σ
From eq. (9)	5.69	0.187	5.17	0.134
From eq. (12)	5.47	0.0596	6.25	0.132

used, the modulus E_0 ($\Omega = \infty$) is found to be between $1/(s_{33} + \sigma)$ and $1/(s_{33} - \sigma)$ or 3.11×10^{11} to 19×10^{11} dyne/cm.², with the mean at 5.35×10^{11} dyne/cm.². The modulus E_{90} ($\Omega = \infty$) has the value 1.76×10^{10} dyne/cm.². The ratio E_0 ($\Omega = \infty$)/ E_{90} ($\Omega = \infty$) is, therefore, roughly 30. Since we cannot obtain the values of both s_{13} and s_{44} , we will assume values for s_{13} so that we can at least have an indication of s_{44} . If the material is assumed to be incompressible, we have the following relationship for the principal elastic strains, ϵ_1 , ϵ_2 , and ϵ_3 ,

$$\epsilon_1 + \epsilon_2 + \epsilon_3 = 0 \quad (35)$$

and

$$(s_{11} + s_{12} + s_{13})(\sigma_1 + \sigma_2) + (s_{33} + 2s_{13})\sigma_3 = 0 \quad (36)$$

Since the principal stresses σ_1 , σ_2 , and σ_3 are not, in general, equal to zero, we have

$$s_{13} = -1/2s_{33} \quad (37)$$

and

$$s_{12} = (s_{11} - 1/2s_{33})$$

The other extreme from an incompressible body is one in which a stress along the molecular axes produces no strain in the plane perpendicular to it: $s_{13} = 0$. Assuming, then, that s_{13} is between $-s_{33}/2$ and zero gives for s_{44}

$$4.98 \leq s_{44} \leq 5.17(10^{-11} \text{ cm.}^2/\text{dyne}) \quad (38)$$

The shear modulus for the strain tending to cause the chains to slip relative to one another along the axes is, therefore, about 2.00×10^{10} dyne/cm.².

As far as we are aware, the molecular elastic moduli of bisphenol A polycarbonate have neither been measured nor calculated. As a test of the assumptions made, we can compare the modulus along the chain axis with those obtained with other polymers. These are shown in Table II. It

TABLE II
Polymer Moduli Along the Chain Axis

Polymer	Moduli $\times 10^{11}$, dyne/cm. ²	
	Calculated	Experimental
Polyethylene	18.2 ^a	23.6 ^b
Polypropylene		4.1 ^b
Poly(vinyl alcohol)		25.0 ^b
Polyoxymethylene		5.3 ^b
Poly(vinylidene chloride)		4.06 ^b
Cellulose	5.65 ^a	13.4 ^b
Nylon 66	19.6 ^a	
Poly(ethylene terephthalate)	12.2 ^a	13.7 ^c
Bisphenol A polycarbonate		5.35 ^d (3.11-19.0)

^a Data of Treloar.⁴

^b Data of Sakurada, Nukushina, and Ito,⁵ from change in fiber identification period with stress.

^c Dulmage and L. E. Contois,³ from change in fiber identification period with stress.

^d Present work.

should be noted that all of the values in Table II are for the crystalline polymers, except for our data on polycarbonate, which is for the polymer in an amorphous state. In comparison with the other moduli, our results seem to be quite reasonable. The assumptions made in obtaining the molecular moduli here, viz., (1) that an affine transformation of the polymer chains occurs on stretching the material under the conditions stated, and

(2) that the correct relationships between the macroscopic and molecular moduli are those given in eqs. (14)–(19), seem thereby to be justified.

References

1. Meyer, K. H., and W. Lotmar, *Helv. Chim. Acta*, **19**, 68 (1936).
2. Lyons, W. J., *J. Appl. Phys.*, **29**, 1429 (1958).
3. Dulmage, W. J., and L. E. Contois, *J. Polymer Sci.*, **28**, 275 (1958).
4. Treloar, L. R. G., *Polymer*, **1**, 95, 279, 290 (1960).
5. Sakurada, I., Y. Nukushina, and T. Ito, *J. Polymer Sci.*, **57**, 651 (1962).
6. Hillier, K. W., and H. Kolsky, *Proc. Phys. Soc. (London)*, **62B**, 111 (1949).
7. Shinohara, Y., and H. Tanzawa, *Kobunshi Kagaku*, **14**, 488 (1957).
8. Wilson, N., *J. Polymer Sci.*, **43**, 257 (1960).
9. Raumann, G., and D. W. Saunders, *Proc. Phys. Soc. (London)*, **77**, 1028 (1961).
10. Wakelin, J. H., E. T. L. Voong, D. J. Montgomery, and J. H. Dusenbury, *J. Appl. Phys.*, **26**, 786 (1955).
11. Ward, I. M., *Proc. Phys. Soc. (London)*, **80**, 1176 (1962).
12. Den Hartog, J. P., *Mechanical Vibration*, 4th Ed., McGraw-Hill, New York, 1956, pp. 148–155.
13. Rudd, J. F., and R. D. Andrews, *J. Appl. Phys.*, **29**, 1421 (1958).
14. Hsiao, C. C., *J. Appl. Phys.*, **30**, 1492 (1959); *J. Polymer Sci.*, **44**, 71 (1960).
15. Kuhn, W., and F. Grün, *Kolloid-Z.*, **101**, 248 (1942).
16. Robinson, A., J. E. Osborn, and C. C. Hsiao, *J. Appl. Phys.*, **31**, 1602 (1960).
17. Mood, A. M., *Introduction to the Theory of Statistics*, McGraw-Hill, New York, 1950, pp. 301–302.

Résumé

On a mesuré le module de Young de films de polycarbonate de bisphénol-A orientés par la méthode de la bobine vibrante. Le module a été mesuré dans une direction parallèle, à 45°, et dans une direction normale à la direction d'orientation. On a ordonné le changement des modules avec le degré d'orientation dans une courbe théorique en utilisant un ordinateur électronique IBM 704. La base de cette transformation suppose que le processus d'orientation des molécules polymériques peut se décrire par une transformation affine. On a calculé les modules d'élasticité suivants: le module de Young pour étirer la chaîne est égale à 5.4×10^{11} dynes/cm²; le module de Young pour séparer latéralement une gerbe de chaînes parallèles est égale à 1.76×10^{10} dynes/cm²; et le module de cisaillement pour déplacer une gerbe de chaînes parallèles en direction de leur longueur est égale à 2.00×10^{10} dynes/cm².

Zusammenfassung

Der Young-Modul orientierter Bisphenol-A-Polycarbonatfilme wurde nach der Methode des Schwingenden Stäbchens längs, unter 45° und normal zur Orientierungsrichtung gemessen. Die Abhängigkeit des Moduls vom Orientierungsgrad wurde mittels eines IBM 704 Computers einer theoretischen Kurve angepasst. Die Grundlage für die Angleichung der Daten an die theoretische Kurve war die Annahme, dass der Orientierungsprozess der Polymermoleküle durch eine affine Transformation beschrieben werden kann. Folgende Werte wurden für den Elastizitätsmodul berechnet: Der Young-Modul für die Kettenstreckung beträgt $5,4 \times 10^{11}$ dyn/cm²; der Young-Modul für die seitliche Trennung eines Bündels paralleler Ketten beträgt $1,76 \times 10^{10}$ dyn/cm² und der Schermodul für die relative Verrückung eines Bündels paralleler Ketten in der Längsrichtung beträgt $2,00 \times 10^{10}$ dyn/cm².

Received December 26, 1963

Revised February 24, 1964

Salicylaldehyde-Formaldehyde Polymers and Their Metallic Chelates

EUGENE C. WINSLOW and ALBERT A. MANNING, *University of
Rhode Island, Kingston, Rhode Island*

Synopsis

Salicylaldehyde-formaldehyde polymers were prepared with the use of oxalic acid, formic acid, sulfuric acid, and sodium hydroxide as catalysts. A non-catalyzed polymer was prepared also at an elevated temperature with the use of a pressure bomb. Metallic chelates of the oxalic acid-catalyzed polymer were prepared with various metallic cations. Each of the polymers was examined for solubility characteristics and for thermal stability. The chelates were similarly examined. The molecular weights of the polymers were in the 700-800 range as determined by freezing point depression. Chelated polymers were stable in air at temperatures which were about 50°C. higher than the decomposition temperature of the corresponding nonchelated polymers.

INTRODUCTION

An earlier paper discussed the preparation and properties of polymers prepared by condensation of oxine (8-quinolinol) and formaldehyde. The chelating property of oxine was incorporated into the polymer and produced in the polymer the ability to form metallic chelates. The degree of polymerization of such polymers prepared by various techniques was approximately six. This paper discusses the preparation of salicylaldehyde-formaldehyde polymers and their chelates. There was some expectation that salicylaldehyde, which is somewhat less bulky than oxine, could form condensation polymers with formaldehyde which would have a higher degree of polymerization. The polymerization techniques used, however, were unable to produce a polymer which exceeded a degree of polymerization of six.

EXPERIMENTAL

The reagents, treatments, and yields of the variously catalyzed condensations of salicylaldehyde and formaldehyde are summarized in Table I.

Chelation

Chelation was achieved with the bivalent ions of lead, nickel, cadmium, copper, zinc, cobalt, magnesium, and beryllium by dissolving 0.5 g. of the chloride salts of these ions in 15 ml. dimethylformamide (DMF) and add-

TABLE I
Condensations of Salicylaldehyde and Formaldehyde

	Reagents	Reaction time	Treatment	Product weight, g.
A. NaOH ₃ catalyzed	Salicylaldehyde 70 ml., 37% formalin 70 ml., 4 ml. of 10 <i>M</i> NaOH (dropwise with stirring)	5 hr. (reflux)	Sample washed with water to give a neutral pH, then heated in air at 160°C. until gassing ceased. Sample washed in hot water, then dissolved in dimethylformamide and reprecipitated with water; heated at 160°C. in air until gassing ceased	79
B. Sulfuric acid-catalyzed	As above except 500 ml. of 7 <i>N</i> H ₂ SO ₄ used instead of NaOH	50 hr. (reflux) followed by distillation of volatiles		48
C. Oxalic acid-catalyzed	H ₂ O, 800 ml., oxalic acid dihydrate 80 g., salicylaldehyde 35 ml., of 37% formalin 60 ml.	76 hr. (reflux); 15 ml. formalin added twice daily; volatiles distilled off to solid mass	Treatment as in A	46
D. Formic acid-catalyzed	As in A except 85 ml. of formic acid used instead of NaOH	76 hr. (reflux); 10 ml. formic acid and 5 ml. formalin added twice daily; volatiles distilled off	Liquid products heated to 160°C. to give solid product with no further gassing	6.1
E. Non-catalyzed (Bomb)	Salicylaldehyde 35 ml., 91% paraformaldehyde 13.2 g.	2 hr.; sealed bomb in a rocker-heater at 240°C.		13.2

ing the resulting solution to a solution of 15 ml. of DMF and 1 g. oxalic acid-catalyzed polymer. The resulting mixture was heated on a steam bath for 8 hr. and then allowed to stand overnight. The mixture was added to 500 ml. of hot distilled water, stirred, and again filtered. This process was done three times to insure removal of all ions which were not chelated. The chelates were dried in an oven at 180°C.

DISCUSSION

The condensation of formaldehyde with salicylaldehyde can produce only a linear polymer because one of the *ortho* positions of salicylaldehyde is occupied by the formyl group. The inability of the polymer to grow three-dimensionally as can phenol-formaldehyde polymers is possibly the main reason for the limited degree of polymerization observed.

Condensation polymers were prepared with the use of oxalic acid, formic acid, sulfuric acid, and sodium hydroxide as catalysts. A noncatalyzed polymer was also prepared, the reaction being carried out at an elevated temperature in a pressure bomb. Metallic chelates of the oxalic acid-catalyzed polymer were prepared with cadmium, lead, beryllium, magnesium, ferrous, and cupric ions. Each of the polymers was examined for solubility characteristics and for thermal stability. The chelates were similarly examined.

Thermal Stability

All thermogravimetric curves discussed in this paper were determined at a heating rate of 2°C./min. The thermogravimetric curves of

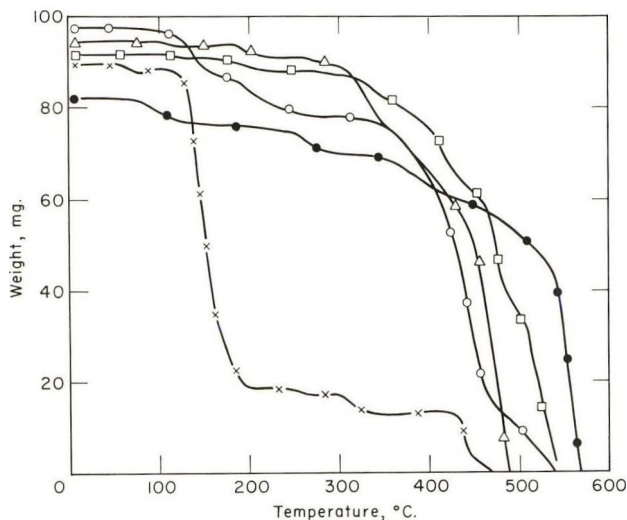


Fig. 1. TGA thermograms for the various catalyzed salicylaldehyde-formaldehyde polymers. Air atmosphere, heating rate 2°C./min.: (Δ) oxalic acid catalyzed; (\square) sulfuric acid catalyzed; (\times) sodium hydroxide catalyzed; (\circ) noncatalyzed; bomb reaction; (\bullet) sodium hydroxide catalyzed, preheated at 210°C. 2 hr.

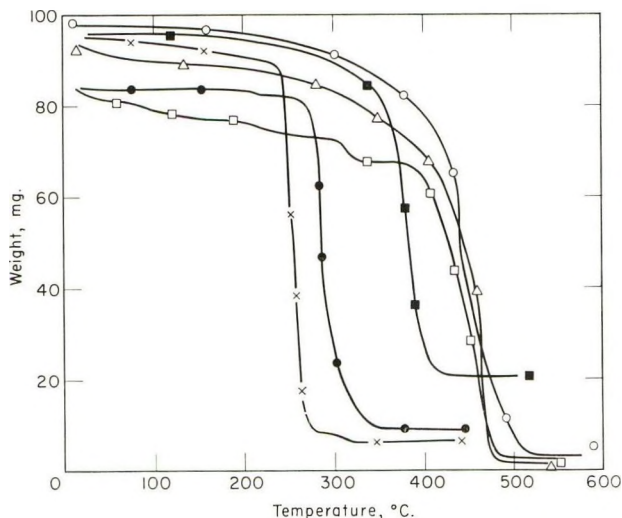


Fig. 2. TGA thermograms for the various bivalent chelates of an oxalic acid catalyzed salicylaldehyde-formaldehyde polymer. Air atmosphere, heating rate 2°C./min. : (Δ) cadmium chelate; (\circ) lead chelate; (\blacksquare) beryllium chelate; (\square) magnesium chelate; (\bullet) iron II chelate; (\times) copper II chelate.

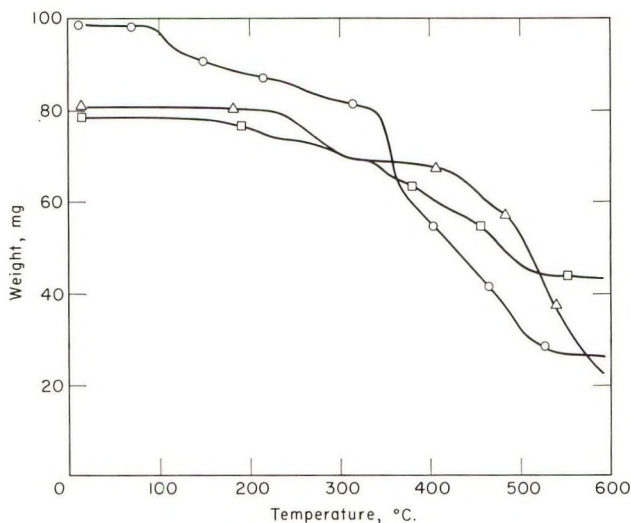


Fig. 3. TGA thermograms for selected salicylaldehyde-formaldehyde bivalent chelates and a polymer. Nitrogen atmosphere, heating rate 2°C./min. : (\circ) copper II chelate; (Δ) magnesium chelate; (\circ) oxalic acid catalyzed polymer.

four polymers are shown in Figure 1. The acid-catalyzed polymers are thermally stable in air to approximately 300°C. at a heating rate of 2°C./min. The noncatalyzed polymer (bomb reaction) has a similar thermogravimetric curve to those of the acid-catalyzed polymers.

The curve for the sodium hydroxide-catalyzed polymer is significantly

different from those of the other polymers. This polymer degrades very rapidly at 120°C., the degradation then levels off, but resumes again at about 420°C. It is reasonable to assume that this polymer has free methylol groups and a considerable amount of attached water. This polymer was preheated for 2 hr. at 210°C. in an air atmosphere and then subjected to thermogravimetric analysis; curve *E* of Figure 1, represents the weight loss of the heat-treated polymer.

Thermal decomposition of several metallic chelates of the oxalic acid-catalyzed polymer is shown in Figure 2. The lower decomposition of the iron and copper chelates is probably caused by the oxidation of the polymer by the catalytic action of iron and copper ions. This was verified by running thermogravimetric curves of the copper chelate and magnesium chelate in a nitrogen atmosphere. Such curves were essentially the same as those for magnesium and copper chelates. The thermogravimetric curves in the nitrogen atmosphere are shown in Figure 3.

The chelated polymers of cadmium, lead, magnesium, and beryllium are significantly more stable than the corresponding polymers before chelation. In general, the thermal decomposition temperature is increased by approximately 50°C. by chelation with bivalent cations which are not good oxidation catalysts. It is possible that metallic chelation inhibits oxidation instead of improving thermal stability; Figure 3 shows that there is very little difference in thermal stability between a chelated polymer and a nonchelated polymer in a nitrogen atmosphere.

Molecular Weight

Viscosity measurements show a reduced viscosity of 0.031 for the oxalic acid-catalyzed polymer in a dimethylformamide. The same polymer in chloroform solution shows a reduced viscosity of 0.037. These values are indicative of a low molecular weight. A viscosity plot is shown in Figure 4. Viscosity data for the oxalic acid-catalyzed polymer are shown in Table II.

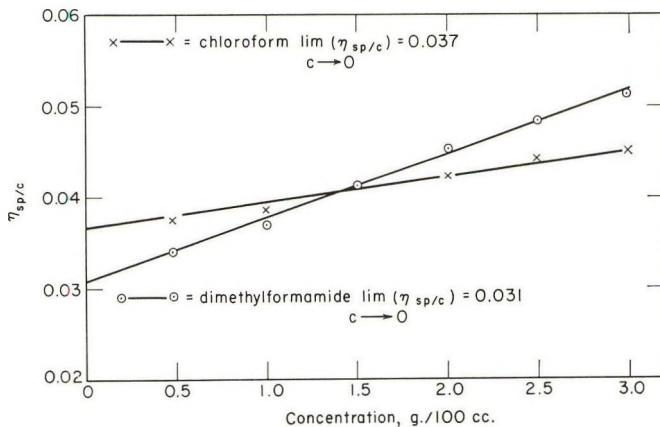


Fig. 4. Plot of viscosity data.

TABLE II
Viscosity Data for Oxalic Acid-Catalyzed Salicylaldehyde-Formaldehyde Polymer

Solvent	Concentration, g./100 cc.	Flow time, sec.	η/η_0	η_{sp}	η_{sp}/c
Dimethyl- formamide	0.0	64.2			
	0.5	65.3	1.017	0.017	0.034
	1.0	66.6	1.037	0.037	0.037
	1.5	68.1	1.061	0.061	0.041
	2.0	70.0	1.090	0.090	0.045
	2.5	71.9	1.119	0.119	0.048
	3.0	74.0	1.153	0.153	0.051
Chloroform	0.0	31.2			
	0.5	31.8	1.019	0.019	0.038
	1.0	32.4	1.039	0.039	0.039
	1.5	33.1	1.062	0.062	0.041
	2.0	33.8	1.083	0.083	0.042
	2.5	34.6	1.110	0.110	0.044
	3.0	35.4	1.134	0.134	0.045

A freezing point depression measurement was made of 0.2 g. of oxalic acid-catalyzed polymer in 20 ml. nitrobenzene. This showed an average molecular weight of 750. The sodium hydroxide-catalyzed polymer showed an average molecular weight of 675. After heating this polymer at 210°C. for 2 hr. the molecular weight by freezing point depression was 880. Additional condensation probably occurred during the heating process.

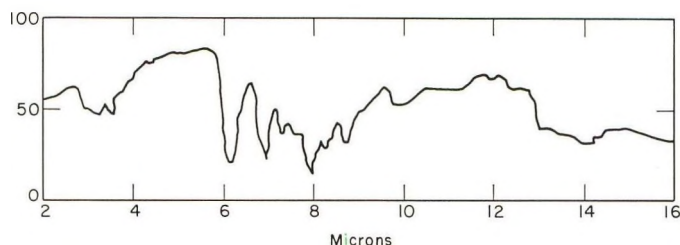


Fig. 5. Infrared spectra of oxalic acid catalyzed polymer.

Figure 5 shows the infrared spectrum of the sodium hydroxide-catalyzed polymer. Infrared spectra of the oxalic acid-catalyzed polymer and the sodium hydroxide-catalyzed polymer were virtually identical.

This research was supported in part by Research Participation funds of the National Science Foundation.

References

1. Winslow, E. C., and R. Horrocks, *J. Polymer Sci.*, **A1**, 3655 (1963).

Résumé

On a préparé des polymères de l'aldéhyde salicylique et du formaldéhyde en employant l'acide oxalique, l'acide formique, l'acide sulfurique et l'hydroxyde de sodium comme catalyseurs. On a préparé également un polymère sans catalyseur à une température élevée et sous pression. On a préparé, en employant divers cations métalliques, des chélates métalliques du polymère catalysé par l'acide oxalique. On a étudié les caractéristiques de solubilité et la stabilité thermique de chacun de ces polymères. Les chélates ont été étudiés de la même façon. Les poids moléculaires de ces polymères situés dans le domaine 700–800 ont été diminués par cryoscopie. Les polymères chélatés sont stables à l'air jusqu'à des températures d'environ 50°C plus élevés que les températures de décomposition des polymères correspondants non-chélatés.

Zusammenfassung

Salicylaldehyd-Formaldehydpolymeren wurden unter Verwendung von Oxalsäure, Ameisensäure, Schwefelsäure und Natriumhydroxyd als Katalysatoren dargestellt. Auch ein nichtkatalysiertes Polymeres wurde bei erhöhter Temperatur in einem Druckrohr hergestellt. Metallchelate der Oxalsäure-katalysierten Polymeren wurden unter Verwendung verschiedener Metallkationen dargestellt. Jedes dieser Polymeren wird auf seine Löslichkeitscharakteristika und thermische Stabilität untersucht. In ähnlicher Weise wurden die Chelate untersucht. Das kryoskopisch bestimmte Molekulargewicht der Polymeren lag im Bereich von 700–800. Chelatpolymere waren in Luft bei Temperaturen beständig, die um etwa 50°C höher als die Zersetzungstemperaturen der entsprechenden nichtchelierten Polymeren waren.

Received January 8, 1964

Revised February 24, 1964

Apparent Transfer Constants of Mercaptans in Emulsion Polymerization. II. Effect of Reactions Other than Polymer Chain Transfer*

E. J. MEEHAN, I. M. KOLTHOFF, and P. R. SINHA, *School of Chemistry, University of Minnesota, Minneapolis, Minnesota*

Synopsis

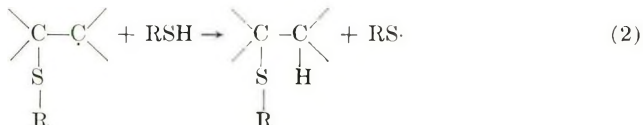
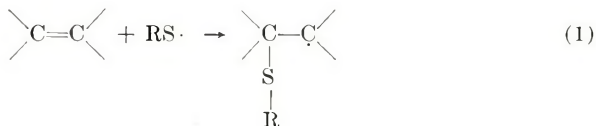
When all the modifier is dissolved in the polymer particles the chain transfer constant, $d \log (\text{RSH})/d \log (\text{M})$ of *n*-octyl mercaptan at 90% conversion in the emulsion polymerization of butadiene (50°C) is 19, the same value as in bulk and in emulsion at 0% conversion. The relative rate of consumption of mercaptan and monomer is unaffected by variation of persulfate and presence of a diluent such as benzene. While mercaptan is consumed by addition to the polymer double bonds (nonmodifying reaction) in monomer-free polybutadiene latex containing persulfate, this addition reaction is virtually suppressed completely in the presence of butadiene monomer. On the basis of the accuracy of the determinations of mercaptan and monomer a slight activation of polymer molecules at high conversion with subsequent cross linking cannot be excluded.

In a previous paper¹ it was shown that the small apparent chain transfer constants of the higher mercaptans (more than eight carbon atoms) in emulsion polymerization of butadiene, butadiene-styrene, and styrene, are due to the slow transport of these mercaptans through the water layer to the polymer particles. The rate of transfer to the particles decreases with increasing molecular weight and is extremely slow for the higher mercaptans. When the experimental conditions are so arranged that all the mercaptan is dissolved in the particles during polymerization, the primary mercaptans with 8-14 carbon atoms have the same transfer constant C ($C = 19$ with both polystyrene and polybutadiene radicals at 50°C.) as in bulk polymerization. Similarly, the tertiary mercaptans with 4-16 carbon atoms have the same value of the constant as in bulk polymerization (4.5 and 3.7, with polybutadiene and polystyrene radicals, respectively, at 50°C.).

The above conclusions are based upon measurement of disappearance of mercaptan during polymerization, the transfer constant C being assumed to be equal to $d \log [\text{RSH}]/d \log [\text{M}]$, where $[\text{RSH}]$ and $[\text{M}]$ are concentrations of unreacted mercaptan and unreacted monomer, respectively. The conclusions would not be valid if an appreciable amount of RSH were consumed in any reaction other than polymer chain transfer. Actually, it has

* This work was begun under the sponsorship of the Office of Synthetic Rubber and completed under a grant from the National Science Foundation.

been shown in previous work² that rapid disappearance of mercaptan occurred at 50°C. when mercaptan was added to monomer-free polybutadiene latex containing persulfate. This is the result of addition to polymer double bonds in a chain reaction:



The addition reaction in monomer-free latex subsequently has been studied in detail. These experiments (to be described in a separate paper) have shown that the rate of disappearance of mercaptan due to the addition is approximately proportional to the square root of the concentration of persulfate, and under some conditions the rate of consumption in the absence of monomer may exceed the rate during polymerization. This is the case, for example, in a monomer-free polybutadiene latex containing (per 100 g. latex) 20 g. polymer, 0.12 g. potassium persulfate (the same ratio as exists during polymerization at 50% conversion), and 0.22 g. *n*-octyl mercaptan. Of the mercaptan, 85% reacts in 1 hr. at 50%, whereas only 40% disappeared when the latex also contained 20 g. of butadiene. Thus there is competition between the polymer double bonds and the monomer for RS·, and possibly competition for RSH between the polymer radical shown in eq. (2) and the polymerization propagating free radical. The main object of the present work was to investigate this competition. In normal emulsion polymerization at 50°C. with persulfate as activator *n*-octyl mercaptan disappears completely before 20% conversion has taken place. Therefore, it appeared desirable to study its chain transfer behavior at higher conversion. The interesting and unexpected result was found that in polybutadiene latex the polymerization chain transfer reaction is not affected by the presence of the polybutadiene, even under the extreme conditions existing in a latex of over 90% conversion, i.e., when the polymer/monomer ratio is more than 10.

n-Octyl mercaptan was used because its rate of consumption in emulsion polymerization is the same as in bulk polymerization, the rate of transport to the latex polymer particles not being a factor.³ This has been confirmed in the present work, and experiment A (see below) was carried out merely to obtain an accurate value of the chain transfer constant under the same conditions as in the other experiments.

In the earlier work,¹ mercaptans were dissolved in monomer-free latex; monomer was added to make the latex equivalent to 25% conversion and the mercaptan content was measured during the subsequent polymeriza-

tion. In the present work the consumption of *n*-octyl mercaptan in the emulsion polymerization of butadiene was measured from 0% conversion and at other initial conversions equivalent to 25, 53, and 90%. In the experiments at initial conversion up to 53%, the conversion was obtained as usual from the polymer content of the latex. In experiments carried out at conversions over 90%, unusually precise measurements of conversion are needed for the present purpose, since with $C = 19$, 90% of the mercaptan present at 90.00% conversion would be consumed by transfer at 91.14% conversion. The ordinary (polymer content of latex) method is not sufficiently accurate for the measurement of the rate of polymerization of added monomer at such conversions. Manometric measurements of vapor pressure of residual butadiene^{4,5} with an accuracy of 1–2 mm. Hg were used to obtain conversion values accurate enough for a severe test of the possible competitive effect of nonmodifying reactions with polymer. At 91% conversion the vapor pressure of residual butadiene (50°C.) changes by 1.2 mm. Hg per 0.01% change in conversion. Substantiation of the results of these studies was obtained from experiments in which the persulfate content was varied. As mentioned earlier the rate of consumption of mercaptan due to addition to polymer double bonds varies approximately as the square root of the concentration of persulfate, whereas in a pure chain transfer process the relative rate, i.e., $d \log [\text{RSH}]/d \log [\text{M}]$ is independent of the initiator concentration.⁶ Also, the effect of benzene upon mercaptan consumption as a butadiene polymerization was determined. The value of $d \log [\text{RSH}]/d \log [\text{M}]$ is the same in bulk and in solution⁶ but the rate, $d [\text{RSH}]/dt$ as a consequence of addition to polymer double bonds in absence of monomer is decreased by addition of benzene.

Experimental

n-Octyl mercaptan (Humphrey-Wilkinson Co.) was vacuum-distilled twice at 30°C. and ca. 1 mm. pressure. Titration both with silver nitrate² and with iodine⁷ gave a mercaptan content of 21.5% (theory 21.9%), the agreement indicating that no tertiary mercaptan was present. A potassium fatty acid soap containing a little peroxide was used. Benzene was shaken with acidic ferrous sulfate, washed with water, dried over calcium chloride, and distilled under nitrogen. Other chemicals and procedures were as described previously.¹ Monomer-free polybutadiene latex (I) used in experiments B, C, and D, was prepared using the recipe (parts by weight): butadiene 100, water 180, fatty acid soap 5, and *n*-dodecyl mercaptan 0.5. The mixtures were rotated at 35 rpm at 50°C. for 30–60 hr. until at least 60% conversion was attained; rates of polymerization with peroxide-containing soaps are not well reproducible in the absence of persulfate. Practically all the mercaptan had been consumed at 60% conversion. Residual butadiene was removed by venting, and then nitrogen was passed through the latex at room temperature for 2 days. No measurable amount of butadiene remained after this treatment. The polymer content was 21.60%. Monomer-free latex II used in experiments E, F, and G was prepared in a

TABLE I
 Composition of Emulsion or of Latices

	Expt. A	Expt. B	Expt. C	Expt. D	Expt. E	Expt. F	Expt. G	Expt. H ^a	Expt. I ^a
Monomer-free latex, g.	—	25.45	37.00	46.07	23.59	24.75	24.02	47.8	47.8
Polybutadiene, g.	—	5.50	7.99	9.95	5.66	5.94	5.77	13.4	13.4
Butadiene, g.	25	14.22	7.76	8.67	17.91	16.43	16.78	1.5	1.5
Initial conversion, %	0	27.9	50.7	53.4	24.0	26.6	25.6	90.0	90.0
Fatty acid soap, g.	5	—	—	—	—	—	—	—	—
Water, g.	40	15.85	—	—	40.75	39.44	41.59	—	—
<i>n</i> -Octyl mercaptan, g.	0.125	0.057 ^b	0.071 ^b	0.090 ^b	0.098 ^b	0.115 ^b	0.101 ^b	0.07 ^e	0.07 ^e
Potassium persulfate, g.	0.10	0.06	0.06	0.06	0.014	0.075	0.356	0.01	0.18
Persulfate, parts per 100 (monomer + polymer)	0.40	0.30	0.38	0.32	0.060	0.34	1.58	0.067	1.21

^a Weights were measured to 0.001 g. in the separate experiments of H and of I.

^b After being dissolved in polymer particles.

^c Approximate amount added before being dissolved in polymer particles.

similar way, the polymer content being 24.00%. A known amount of *n*-octyl mercaptan was dissolved in latex I or II by shaking (room temperature) for 15 hr. at 390 strokes/min. Some mercaptan disappeared during this time. The amount of mercaptan was determined by alcohol coagulation and titration with silver in ammoniacal medium.² Blank experiments showed that all the mercaptan was recovered. Potassium persulfate and butadiene were added to the latex. The subsequent polymerizations then were carried out at 50°C., 35 rpm. Compositions are given in Table I. Monomer-free latex III was prepared from the same mixture as I plus 0.03 part of potassium persulfate. After 24 hr. at 50°C. the conversion was 87.6%. Butadiene was removed as above and the latex was stored two weeks under nitrogen at room temperature. Polymer content was 28.11%.

The relationship between vapor pressure and conversion in latex III was determined as follows. A 50-ml. portion of latex was added to a bottle of accurately known weight and volume and the weight of latex added was determined. All weighings were made to 1 mg. An excess over the calculated amount of liquid butadiene containing a trace of inhibitor to prevent polymerization during the calibration experiments was added, and some was allowed to evaporate to remove air. The bottle was capped tightly and the weight was adjusted by allowing butadiene to escape through a hypodermic needle until the corresponding conversion, $100 \times \text{polymer}/(\text{monomer} + \text{polymer})$ was in the range 90–93%. Correction was made for the weight of air displaced. The mixture was shaken (390 strokes/min.) for 15 min. to dissolve the butadiene in the polymer particles and then rotated (35 rpm) at 50°C. for at least 45 min. before being placed in a 50.00°C. thermostat in which the pressure measurements were made. This thermostat contained a mercury well with a column of suitable height, and a flexible connection provided with a hypodermic needle. Before the connection

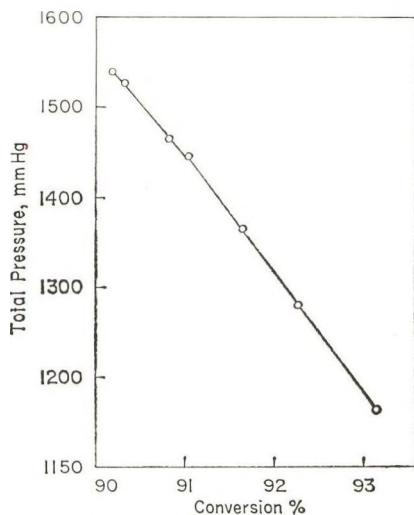


Fig. 1. Pressure-conversion relation in emulsion polymerization of butadiene at 50°C.

to the bottle was made butadiene was added to the manometer so that the pressure in the manometer was equal to the pressure expected to be measured. Then the pressure readings were taken before and after connection through the needle. Since it was impossible to predict the exact pressure to be measured, it was unavoidable that some butadiene should enter or leave the bottle. Therefore after making the pressure reading the bottle was weighed again and the correct value for per cent conversion was obtained. The experiment was repeated if the initial and final pressure differed by more than 20 mm. The data fell on the smooth curve shown in Figure 1. (The reported pressures include the vapor pressure of the aqueous layer, approximately 92 mm.) Mercaptan disappearance above 90% conversion was determined as follows. Latex III (52–54 g.) was added to a bottle of accurately known volume and weight; 0.06–0.07 g. *n*-octyl mercaptan was added and the mixture shaken (390 strokes/min.) for 2 hr. to dissolve the mercaptan in the particles. After the shaking period the mercaptan content was determined amperometrically. Then a suitable amount of latex was removed so that the amount remaining was 47.8 g., i.e., the same weight as was present in the calibration experiment of Figure 1. Butadiene and persulfate were added as described above. Three mixtures each of the compositions H and I (see Table I) were prepared. Each was polymerized for a suitable time, after which the pressure was measured and the mercaptan content determined.

Results

The results are given in Figures 2 and 3. Short induction periods were observed in some of the experiments. Considering first the rates of polymerization (Fig. 2), it is of interest to note that a 25-fold variation of concentration of persulfate had practically no effect on the rate of polymerization at 25% conversion (E, F, G) while an 18-fold increase in persulfate increased the rate by about 50% at 90% conversion (H, I). The rate of conversion of the added monomer at 50% conversion (C, D) of 6.0%/hr. corresponds to about 3.0%/hr. when expressed in the usual way, i.e., on the basis of total monomer, or about the same value as at 0% conversion. The corresponding rates at 25% conversion (B, E, F) however, were about 25% lower than in A. The figures 5.0 and 7.8% of added monomer/hr. at 90% conversion (H, I) correspond to 0.5 and 0.8%/hr. on the basis of total monomer. The rate of 3.3%/hr. in A, which is an ordinary polymerization experiment, is substantially smaller than the value of about 4.5%/hr. found when *n*-dodecyl mercaptan is used in the persulfate-initiated emulsion polymerization of butadiene at 50°C. The reason apparently is that *n*-octyl mercaptan is not as effective a promoter of butadiene or butadiene-styrene polymerization as *n*-dodecyl mercaptan.⁸

The mercaptan-monomer data are shown on a log-log plot in Figure 3. The straight line drawn in Figure 3, which is fitted by least squares to the 38 separate mercaptan conversion experiments, has a slope of 18.7. The six high conversion experiments, H and I, yield a least-squares value of d

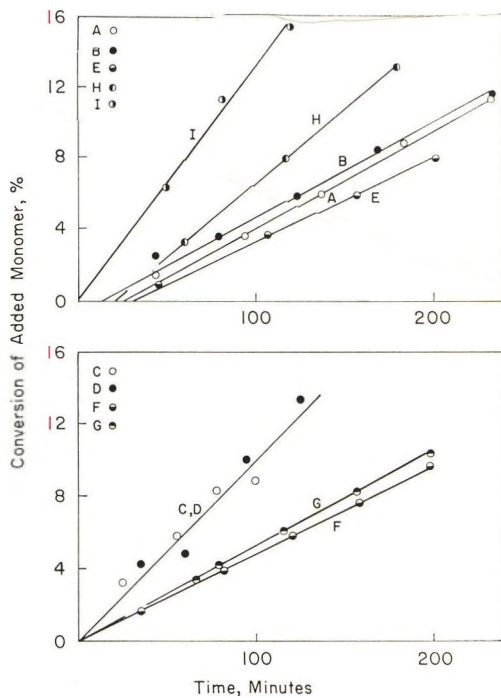


Fig. 2. Conversion of added butadiene.

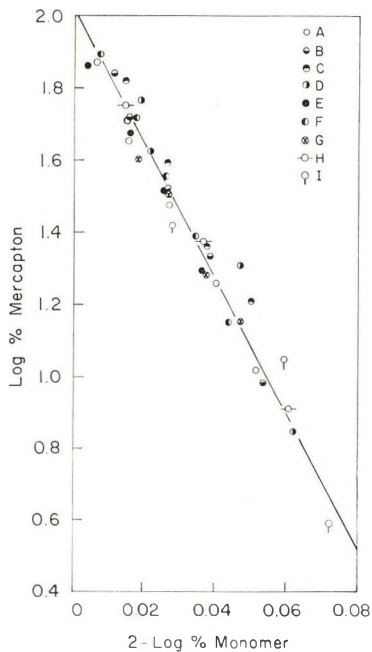


Fig. 3. Relative rate and consumption of mercaptan.

$\log [\text{RSH}]/d \log [M]$ of 19.3. The values are identical within experimental uncertainty. Variation of persulfate over wide limits did not affect the value of $d \log [\text{RSH}]/d \log [M]$, even at 90% conversion. Experiments in the presence of different amounts of benzene in a mixture similar to A (0, 0.5, 1, 5, or 10 g., respectively, of benzene/25 g. butadiene) showed that the addition of benzene reduced the rate ($-d[M]/dt$) of polymerization⁹ but did not affect the value of $d \log [\text{RSH}]/d \log [M]$.

Discussion

The results show conclusively that the relative rate of consumption of mercaptan is exactly the same at 90% conversion as it is at 0%. Therefore the presence of polybutadiene is of no consequence (other than to provide a locus for the reaction), and addition of mercaptan to the unsaturated polymer is suppressed completely in the presence of the relatively small amount of butadiene remaining at 90% conversion and above. This is confirmed by the fact that the variation of persulfate and the addition of benzene, each of which affects the rate of reaction of mercaptan with polymer in the absence of monomer, have no effect on the relative rate of mercaptan disappearance in the presence of monomer. It is also of interest to note that the transfer constant during the initial few per cent of polymerization in a polymer-free charge (mixture A) has the normal value of 19, indicating that the *n*-octyl mercaptan and the butadiene both have ready access to the locus of the initial reaction (soap micelles).

Finally, it should be stated that crosslinking of the polymer in the later stages of conversion cannot be excluded on the basis of our analytical results. Polymer molecules can be activated by SO_4^- radicals produced by thermal dissociation of persulfate, and additions of a few monomer molecules may bring about crosslinking.

Assistance of Mr. Y. T. Okinaka with the high conversion experiments is acknowledged.

References

1. Meehan, E. J., I. M. Kolthoff, and P. R. Sinha, *J. Polymer Sci.*, **16**, 471 (1955).
2. Kolthoff, I. M., and W. E. Harris, *J. Polymer Sci.*, **2**, 49 (1947).
3. Smith, W. V., *J. Am. Chem. Soc.*, **68**, 2059 (1946).
4. Houston, R. J., and R. A. Briggs, communication to Office of Rubber Reserve, Nov. 1, 1945.
5. Meehan, E. J., *J. Am. Chem. Soc.*, **71**, 628 (1949).
6. Mayo, F. R., *J. Am. Chem. Soc.*, **65**, 2324 (1943).
7. Kolthoff, I. M., and W. E. Harris, *Anal. Chem.*, **21**, 963 (1949).
8. Kolthoff, I. M., and W. E. Harris, *J. Polymer Sci.*, **2**, 41 (1947).
9. Bovey, F. A., I. M. Kolthoff, A. I. Medalia, and E. J. Meehan, *Emulsion Polymerization*, Interscience, New York, 1955, p. 357.

Résumé

Quand tout le régulateur de chaîne est dissous dans les particules du polymère, la constante de transfert de chaîne $d \log (\text{RSH})/d \log (M)$ du mercaptan *n*-octylique à 90% de conversion dans la polymérisation en émulsion du butadiène (50°C) est égale à

19, la même valeur que pour la polymérisation en bloc ou en émulsion à un taux de conversion de 0%. La vitesse relative de la consommation du mercaptan et du monomère n'est pas affectée par la variation du persulfate ni par la présence d'un diluant comme le benzène. Tandis que le mercaptan est consommé par addition aux doubles liaisons du polymère (réaction non régulatrice) dans un latex de polybutadiène exempt de monomère et contenant du persulfate, cette réaction d'addition est virtuellement supprimée complètement en présence du monomère butadiène. Sur la base de la précision des déterminations du mercaptan et du monomère, une légère activation des molécules du polymère à des taux de conversion élevés accompagnée d'un pontage subséquent ne peut être exclue.

Zusammenfassung

Wenn der gesamte Regler in den Polymerteilchen gelöst ist, so beträgt die Kettenübertragungskonstante $d \log(RSH)/d \log(M)$ *n*-Octylmercaptan bei 90% Umsatz bei Emulsionspolymerisation von Butadien (50°C) 19, das ist derselbe Wert wie in Substanz und Emulsion bei 0% Umsatz. Die relative Verbrauchsgeschwindigkeit von Mercaptan und Monomeren wird durch Variation des Persulfates und Anwesenheit eines Verdünnungsmittels wie Benzol nicht beeinflusst. In monomerfreiem Polybutadienlatex mit Persulfat wird Mercaptan durch Addition an die Polymerdoppelbindungen verbraucht (Nicht-Regelreaktion), während diese Additionsreaktion bei Anwesenheit von Butadienmonomerem praktisch vollständig unterdrückt ist. Auf Grundlage der Genauigkeit der Mercaptan- und Monomerbestimmung kann eine geringe Aktivierung der Polymerelemente mit folgender Vernetzung bei hohem Umsatz nicht ausgeschlossen werden.

Received February 11, 1964

Electron Radiation of Aqueous Methyl Cellulose Solutions*

W. JACK HILLEND and HAROLD A. SWENSON, *The Institute of Paper Chemistry, Appleton, Wisconsin*

Synopsis

Solutions (4%) of commercial methyl cellulose (85,000 weight-average molecular weight) were radiated with electrons under varied atmospheres of oxygen at dose rates of 0.15, 0.45, and 4.5 Mrad/min. to total doses of 0.45, 4.5 and 10.0 Mrad. Samples irradiated at the highest dose rates formed gels whose strength was estimated in a Brookfield viscometer. After dispersing by stirring, the gels were clarified by centrifugation before viscosity, light-scattering, and sedimentation measurements were made. Molecular weight increases to as high as 270,000 were found, and the sedimentation coefficients increased correspondingly. The intrinsic viscosity of the irradiated polymer solutions, on the other hand, did not increase as the molecular weight doubled or tripled. This is interpreted to be the result of recoupling of hydrolyzed fragments to produce branched molecules of smaller volume and greater weight. High dose rates promoted molecular weight increases while the presence of oxygen, low dose rates, and low polymer concentration favored degradation. The carboxyls evidently produced in the oxidative degradation resulted in a lowered pH of the irradiated solution and in polyelectrolyte viscosity behavior. Boiling an irradiated polymer solution at pH 10.5 reduced molecular weight from 270,000 to 165,000, showing the presence of alkali-labile as well as alkali-stable bonds. The gels on the other hand could be dispersed by stirring or heat as well as by alkali. Although branching may affect gelation to some extent, the molecular weight and sedimentation of the samples in solution appear to be approaching a maximum at the dosage level where the more labile bonding of the gelation phenomenon sets in.

INTRODUCTION

Conflicting effects of branching and crosslinking on the one hand and degradation and chain scission on the other result from the radiation of polymers. A number of workers have reported evidence for degradation of carbohydrates during electron radiation, as shown by increase in chain cleavage, carbonyl and carboxyl production, rate of acid hydrolysis, solubility in water and alkali, and decrease in tensile strength, modulus of elasticity, and intrinsic viscosity.¹⁻⁶ The extent of degradation is slightly less when radiations were made under nitrogen than under oxygen.³⁻¹⁵

Radiation also appears to induce branching in polymeric carbohydrates.

* Abstracted from a thesis submitted in partial fulfillment of the requirements of The Institute of Paper Chemistry for the degree of Doctor of Philosophy from Lawrence College, Appleton, Wis., June 1963.

Samec¹⁴ found that γ -radiation of an aqueous wheat starch solution increased the molecular weight from 164,000 to 264,000, while the relative viscosity decreased from 1.16 to 1.07. Granath and Kinell¹⁵ presented evidence that γ -radiation of solid dextran caused branching even though the molecular weight was continuously decreased.

Miller¹⁶ and Leavitt¹⁷ showed that electron radiation promotes gelation of methyl cellulose in aqueous solution.

The present study concerns branching and molecular weight increases produced by electron radiation of water solutions of methyl cellulose short of the gel point and their relation to gelation which occurs at higher dose rates. The stability of the bonds involved in the crosslinking phenomena was also investigated.

MATERIALS AND METHODS

Preparation of Methyl Cellulose Solutions

Stock solutions in 4% concentration were prepared from Dow "Methocel" (15 cpoise technical grade) in deionized water. The methoxyl content of this methyl cellulose was $29.4 \pm 0.1\%$ as determined by the method of Zeisel.¹⁸ The ash content was $0.60 \pm 0.01\%$ determined as the amount of material remaining after heating the samples for 6 hr. at 900°C. The weight-average molecular weight of this sample was found to be 85,000. The air space above the solutions was evacuated and replaced with nitrogen three times at room temperature and finally stored under a 0.4 psig pressure of nitrogen. To minimize the possibility of degradation by microorganisms, solutions were stored at 1°C. until ready for use.

The solutions were irradiated in glass pans which had bottom dimensions of 9.5×20 cm. A 100-ml. quantity of nitrogen-saturated solution, the volume radiated in each case, gave a solution depth of 0.53 cm. The pans were placed in polyethylene bags which were sealed and then flushed and filled with a positive pressure of nitrogen through a small hole which was then resealed. The procedure resulted in an initial atmosphere above the solutions of about 4% oxygen when carried out in air and 0.3% when done in a nitrogen atmosphere. Irradiations were done the next day. The extent of oxygen diffusion into the bag during this interval was believed to be small.

Radiation of Solutions

All solutions were radiated at $23 \pm 2^\circ\text{C}$. with electrons at a potential of 2×10^6 e.v. The electron source was a 2-M.e.v., 2-ma. resonant transformer* which delivered a beam with a diameter of approximately 1.5 in. The beam was swept 180 times/sec. along the length of the sample and 56 times across the width of the sample. The beam current was pulsed 180 times/sec. and had a square-wave form. The average dose rate in the

* Located in the Application Laboratory, General Electric Co., Milwaukee, Wisconsin.

solutions, based on the density and thickness of the solution, was obtained from calibrations by General Electric Company. The distance from the beam window to the sample was 7.5 in., and average dose rates were varied from 0.15 to 10.0 Mrad/min. Beam currents of 0.0050–0.15 ma. were used. Radiation doses of 0.45 to 2.1 Mrad were obtained by controlling the exposure time.

Light-Scattering Measurements

Methyl cellulose solutions were stored at 1°C. prior to measurement to discourage aggregation which has been found to occur above 30°C.^{19,20} No aggregation was observed upon rewarming the solutions. The samples which gelled as a result of irradiation were dispersed by dilution to 0.8% followed by stirring in a Waring Blendor at 1000 rpm for 15 min. This treatment, which was sufficient to disperse 90% of the two gelled samples, did not degrade a like concentration of unirradiated methyl cellulose.

The ungelled solutions and dispersed gel solutions were clarified by centrifuging at 100,000 gravity for 1/2 hr. followed by pressure filtration through Millipore filters (Millipore Filter Corp., Bedford, Mass.) with a rated pore size of 450 m μ . The refractive index increment in water was found to be 0.145 ± 0.002 ml./g. determined at a wavelength of 546 m μ in a Rayleigh interferometer. Irradiation did not change dn/dc .

Dissymmetry ratios were found to range from 1.3 to 1.8, too high to be accounted for by molecules of the size involved, and corrections for the particle scattering factor²¹ were neglected. From an estimate of the coil dimensions,²² at molecular weights of 85,000 and 200,000, omission of the particle-scattering factor $P(\theta)$ would result in molecular weights approximately 6–13% too low, respectively. Apparent depolarization corrections were less than 3% and were neglected, and no fluorescence was detected in the solutions. Five replicate determinations of the unirradiated methyl cellulose were between 80,900 and 90,600, a precision of $\pm 6.0\%$. The measurements of the irradiated sample were made five weeks after irradiation.

Sedimentation Measurement

A Beckman Model E ultracentrifuge, with Analytical-D rotor, was used for sedimentation velocity experiments. All runs were made at 43,040 rpm at $20.2 \pm 0.1^\circ\text{C}$., at a polymer concentration of 0.82 ± 0.01 g./100 ml. A double-sector cell was used with irradiated methyl cellulose in one sector and an equal volume of nonirradiated methyl cellulose in the other. Schlieren patterns were recorded photographically at known times, t . The distance, x , of the peak of the boundary curve from the center of rotation was measured with a microcomparator. The sedimentation coefficient s was obtained by finding the slope (by least-squares) of the $\ln x$ versus t plot according to the equation

$$s = (1/\omega^2)(d \ln x/dt)$$

where ω is the angular velocity in radians per second. Data were taken eight weeks after radiation.

Intrinsic Viscosity Measurements

A modified Ubbelohde viscometer²³ was used at $25 \pm 0.02^\circ\text{C}$. The determinations which were obtained in water (Table I and Fig. 1) are relative values, since polyelectrolyte effects on the viscosity were very marked due apparently to carboxyl groups produced during irradiation. Sample 8, for

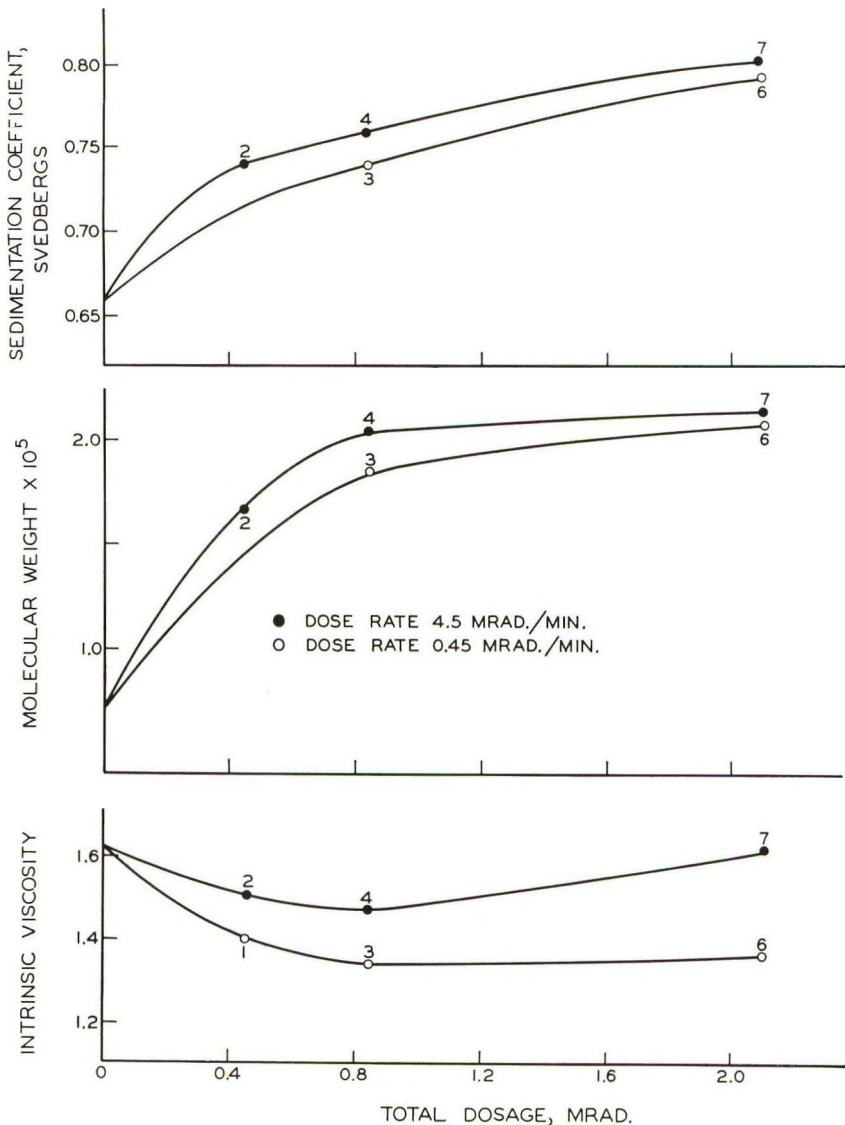


Fig. 1. Intrinsic viscosity, molecular weight, and sedimentation coefficient as a function of total dosage at various dose rates.

TABLE I
Influence of Dose and Dose Rate on Molecular Weight Sedimentation Coefficient, Intrinsic Viscosity, pH, and Brookfield Viscosity of Methyl Cellulose

Sample	Dose, Mrad	Dose rate, Mrad/min.	Molecular wt. ^a	Sedimentation coefficient, Svedbergs	pH	Intrinsic viscosity, dl./g.	Brookfield viscosity, cpoise
0	0	0	85,000	0.666	5.8	1.62	96
1	0.45	0.45	—	—	4.7	1.40	51
2	0.45	4.50	167,000	0.740	4.8	1.50	86
3	0.84	0.45	185,000	0.740	4.5	1.33	47
4	0.84	4.50	204,000	0.758	4.7	1.47	92
5	2.10	0.15	—	—	3.9	0.86	32
6	2.10	0.45	207,000	0.792	4.1	1.36	148
7	2.10	4.50	215,000	0.801	4.2	1.61	6200
8 ^b	2.10	4.50	270,000	0.992	4.4	2.32	>100,000

^a By light scattering.

^b This sample had an initial atmosphere of 0.3% oxygen in nitrogen above the solution. The other samples initially had 4% oxygen above the solution.

example, had intrinsic viscosities of 2.32, 1.41, and 1.31 dl./g. when measured in water, in 0.2*M* NaCl, and in 0.2*M* borate buffer at pH 9.0, respectively. Increased polymolecularity might be expected from the radiation. Its effect on the viscosity and on the molecular weight average obtained by light scattering and on the sedimentation coefficient was not investigated. The Waring Blendor dispersed 90% of the two gelled samples (Samples 7 and 8 in Table I). Material of higher molecular weight could have been left in the remaining undispersed gel.

RESULTS AND DISCUSSION

Influence of Dose Rate and Total Dosage on Molecular Weight

The 100-ml. portions from a 4% stock solution of methyl cellulose after nitrogen flushing and sealing, as previously described, were subjected to total dosages of 0.45, 4.5, and 2.10 Mrad at dose rates of 0.45 and 4.50 Mrad/min. The influence upon the molecular weight, sedimentation coefficient, and intrinsic viscosity of the methyl cellulose solutions is seen in Table I and in Fig. 1.

Figure 1 shows that there was no increase in intrinsic viscosity while both molecular weight and sedimentation coefficient increased with increasing radiation. This can be explained by assuming that degraded fragments reunite to form branched molecules of greater weight with no increase in volume. Actually, an appreciable decrease in hydrodynamic volume apparently occurred, since the viscosities in water as judged by the one sample mentioned above are over 50% higher than they would be had polyelectrolyte effects been suppressed in the viscosity measurements shown.

An increase in molecular weight, viscosity, sedimentation coefficient, and gel strength occurred between samples 7 and 8 when the oxygen initially above the solution was reduced from 4.0 to 0.3% as seen in Table I. The pH of the solution following radiation also increased slightly apparently reflecting decreased oxidation.

Apparent Absence of Molecular Association

Aggregation could be expected, particularly in the solutions which were originally gels or incipient gels.²⁴ No rapidly sedimenting fraction was observed during the sedimentation, however, following the clarification procedure already described. The slopes of the light-scattering plots were also strongly positive, indicating lack of aggregation.²⁵ The Schlieren sedimentation patterns were also single-peaked. Therefore, the observed increases in molecular weight appear to be true increases in true mass of the molecule and not due to aggregation.

Stability of the Radiated Methyl Cellulose

The viscosity and molecular weight determinations reported in Table I and Figure 1 were done within a one-week period, nine weeks after radiation. The molecular weight of samples 7 and 8 (Table I) had also been de-

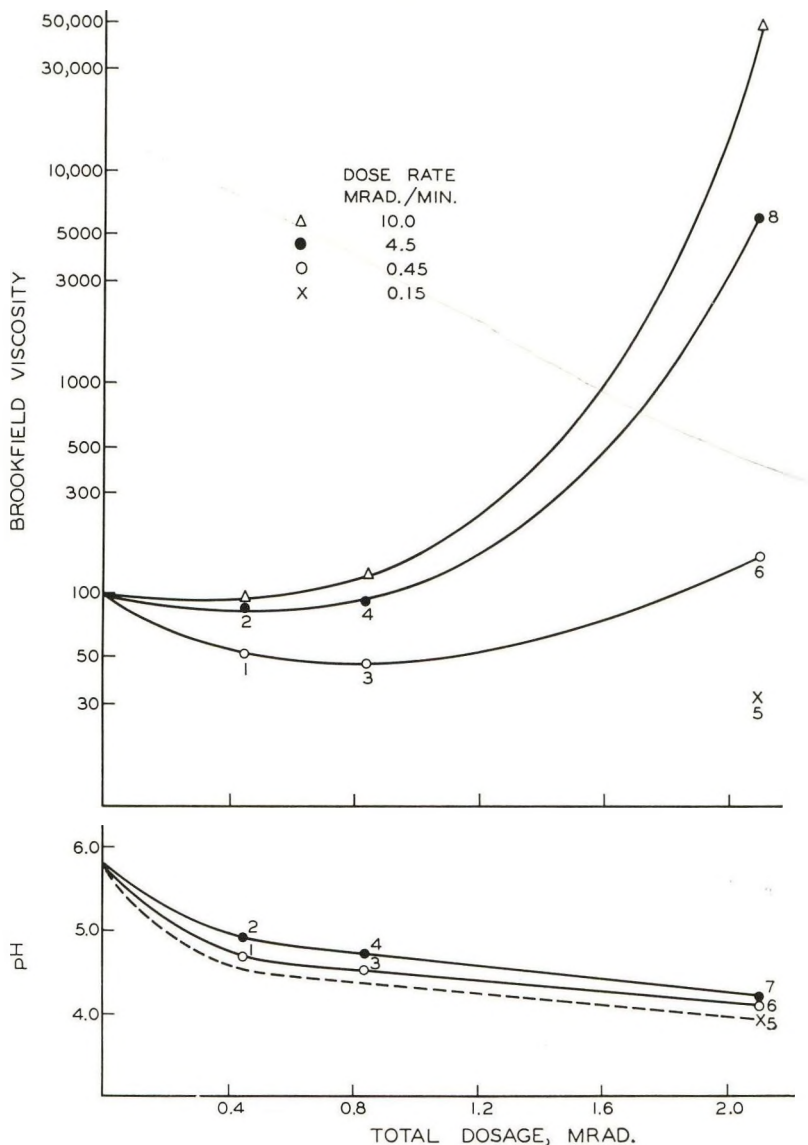


Fig. 2. pH and Brookfield viscosity of irradiated methyl cellulose.

terminated earlier, three weeks after radiation. In the six-week period, sample 7 dropped in molecular weight from 241,000 to 215,000 and sample 8 from 308,000 to 270,000. The unirradiated control remained unchanged.

The dispersed gel of sample 8 was boiled in a solution of 0.05M sodium borohydride at pH 10 for 1 hr. As seen in Table II, the radiated sample shows appreciable breakdown compared to the unirradiated control. Bonds stable to alkali, as well as bonds unstable to alkali, appear to be present in the branched methyl cellulose structure. A portion of these alkali-unstable bonds, however, conceivably could include bonds along the original

TABLE II
Alkali Stability of Methyl Cellulose Crosslinked by Radiation

Sample	Molecular weight		Sedimentation coefficient, Svedbergs		Intrinsic viscosity, dl./g.	
	Before treatment ^a	After treatment	Before treatment	After treatment	Before treatment	After treatment
	Nonirradiated	85,000	81,000	0.666	0.658	1.62
8	270,000	165,000	0.972	0.820	2.32	1.23

^a In boiling 0.05M sodium borohydride at pH 10.0 for 1 hr.

polymer chain that were weakened during radiation. Peroxy ester and hemiacetal linkages might be cleaved by the alkaline treatment,^{26,27} whereas carbon-carbon, ether, acetal, or glycosidic linkages could be expected to be stable.

Influence of Dose Rate on Gelation and Oxidation

The extent of gelation was highly dependent upon the rate of radiation. This is shown in Figure 2 by the Brookfield viscosity of the radiated samples. When a low dose rate of 0.15 Mrad/min. was used to obtain a total dosage of 2.1 Mrad, the Brookfield viscosity decreased from 96, that of the unirradiated 4% solution, to 31 cpoise after radiation. When a 10.0 Mrad/min. dose rate was used to obtain the same total dosage, on the other hand, a firm gel which had a Brookfield viscosity of 58,000 was formed, as shown in Figure 2. That gelation occurs in preference to degradation at higher dose rates has been shown by Leavitt.¹⁷

Although branching prior to gelation may affect the degree of gelation, comparison of Figures 1 and 2 indicate that the molecular weights of the samples in solution are near a maximum at the dosage level where the weaker bonding of gelation sets in.

References

1. Teszler, O., L. H. Kiser, P. W. Campbell, and H. A. Rutherford, *Textile Res. J.*, **28**, 456 (1958).
2. Glegg, R. E., and Z. I. Kertesz, *J. Polymer Sci.*, **26**, 289 (1957).
3. Arthur, J. C., F. A. Blouin, and R. J. Demint, *Am. Dyestuff Repr.*, **49**, 383 (1960).
4. Pan, H., B. E. Proctor, S. A. Goldblith, H. M. Morgan, and R. Z. Naar, *Textile Res. J.*, **29**, 415 (1959).
5. Arthur, J. C., and R. J. Demint, *Textile Res. J.*, **32**, 108 (1962).
6. Harman, D. J., *Textile Res. J.*, **27**, 318 (1957).
7. Skinner, R. E., and Z. I. Kertesz, *J. Polymer Sci.*, **47**, 99 (1960).
8. Price, F. P., W. D. Bellamy, and E. J. Lawton, *J. Phys. Chem.*, **58**, 821 (1954).
9. Samec, M., *Stärke*, **10**, 76 (1958).
10. Moody, G. J., and G. O. Phillips, *Chem. Ind. (London)*, **1959**, 1247.
11. Barker, S. A., P. M. Grant, M. Stacey, and R. B. Ward, *J. Chem. Soc.*, **1959**, 2871.
12. Phillips, G. O., G. J. Moody, and G. L. Mattok, *J. Chem. Soc.*, **1958**, 3522.
13. Barker, S. A., F. R. S. Stacey, P. M. Grant, and R. B. Ward, *J. Chem. Soc.*, **1959**, 2648.

14. Samec, M., *J. Appl. Polymer Sci.*, **3**, 224 (1960).
15. Granath, K. A., and P. Kinell, *Acta Chem. Scand.*, **15**, 141 (1961).
16. Miller, A. A., U. S. Pat. 2,895,891 (July 21, 1959).
17. Leavitt, F. C., *J. Polymer Sci.*, **51**, 349 (1961).
18. Samsel, E. P., and J. H. McHard, *Ind. Eng. Chem. Anal. Ed.*, **14**, 750 (1942).
19. Kuhn, W., and P. Moser, *Makromol. Chem.*, **44**, 71 (1961).
20. Neely, W. B., private communication, 1962.
21. Doty, P., and R. Steiner, *J. Chem. Phys.*, **18**, 1211 (1950).
22. Beattie, W. H., and C. Booth, *J. Polymer Sci.*, **44**, 81 (1960).
23. Craig, A. W., and D. A. Henderson, *J. Polymer Sci.*, **19**, 215 (1956).
24. Doty, P., H. Wagner, and S. Singer, *J. Phys. Colloid Chem.*, **51**, 32 (1947).
25. Doty, P., and G. E. Myers, *Discussions Faraday Soc.*, No. 13, 51 (1953).
26. Tobolsky, A. V., and R. B. Mesrobian, *Organic Perozides*, Interscience, New York, 1954.
27. Head, F. S. H., *J. Textile Inst.*, **49**, T345 (1958).

Résumé

On a irradié des solutions à 4% de méthylcellulose commerciale (poids moléculaire moyen en poids: 85.000) au moyen d'électrons sous diverses pressions d'oxygène à de vitesses d'irradiation de 0.15, 0.45 et 4.5 Mrad/minute jusqu'à des doses totales de 0.45, 4.5 et 10.0 Mrad. Les échantillons les plus fortement irradiés forment des gels dont l'importance a été déterminée dans un viscosimètre de Brookfield. Après dispersion des gels par agitation, ceux-ci ont été clarifiés par centrifugation préalable, ensuite soumis aux mesures de viscosité, de diffusion lumineuse et de sédimentation. Les poids moléculaires atteignent 270.000 et les coefficients de sédimentation augmentent de manière correspondante. D'autre part, la viscosité intrinsèque des solutions de polymère irradié n'augmente pas même lorsque le poids moléculaire double ou triple. On interprète ceci comme étant dû à la recombinaison de fragments hydrolysés de façon à produire des molécules ramifiées de volume plus petit mais de poids supérieur. Des vitesses d'irradiation élevées favorisent l'augmentation du poids moléculaire tandis que la présence d'oxygène de faible vitesse d'irradiation et de faibles concentrations en polymère, favorisent la dégradation. Les carboxyles, produit de toute évidence au cours de la dégradation oxydante, ont pour résultat d'abaisser le pH de la solution irradiée et de lui conférer, du point de vue viscosité, un comportement polyélectrolytique. En faisant bouillir une solution irradiée de polymère à pH 10.5, on provoque une réduction du poids moléculaire de 270.000 à 165.000 montrant la présence de liaisons labiles aux alcalis aussi bien que de liaisons stables aux alcalis. D'autre part les gels peuvent être dispersés autant par agitation ou chauffage que par l'action d'alcalis. Quoique la ramification puisse affecter la gélification dans une certaine mesure, le poids moléculaire et la sédimentation des échantillons en solution paraît tendre vers un maximum au niveau d'irradiation en solution paraît tendre vers un maximum au niveau d'irradiation examiné (dose) où a lieu la formation des liens labiles de la gélification.

Zusammenfassung

Vierprozentige Lösungen von handelsüblicher Methylzellulose (Gewichtsmittel des Molekulargewichts 85.000) wurden mit Elektronen unter variierter Sauerstoffatmosphäre mit Dosisleistungen von 0,15, 0,45 und 4,5 Mrad pro Minute bis zu einer Gesamtdosis von 0,45, 4,5 und 10,0 Mrad bestrahlt. Mit höchster Dosisleistung bestrahlte Proben bildeten Gele, deren Festigkeit in einem Brookfield-Viskosimeter gemessen wurde. Vor den Viskositäts-, Lichtstreuungs- und Sedimentationsmessungen wurden die Gele nach Dispergierung durch Rühren durch Zentrifugierung geklärt. Ein Molekulargewichtszuwachs bis zu 270.000 wurde festgestellt, der Sedimentationskoeffizient nahm in gleicher Weise zu. Die Viskositätszahl der bestrahlten Polymerlösungen nahm andererseits bei Verdoppelung oder Verdreifachung des Molekulargewichts nicht zu.

Dies wird als Ergebnis der neuerlichen Vereinigung von hydrolysierten Bruchstücken zu verzweigten Molekülen mit geringerem Volumen und höherem Gewicht aufgefasst. Hohe Dosisleistung förderte den Molekulargewichtszuwachs, während Sauerstoff, niedrige Dosisleistung und niedrige Polymerkonzentration den Abbau begünstigten. Die beim oxydativen Abbau offensichtlich gebildeten Carboxylgruppen ergaben einen erniedrigten pH-Wert der bestrahlten Lösung und ein Polyelektrolyten entsprechendes Viskositätsverhalten. Das Kochen einer bestrahlten Polymerlösung bei $\text{pH} = 10,5$ setzte das Molekulargewicht von 270.000 auf 165.000 herab und zeigte damit sowohl Alkali-labile als auch Alkali-stabile Bindungen. Andererseits konnten die Gele genauso durch Rühren und Erhitzen wie durch Alkali dispergiert werden. Obwohl die Verzweigung die Gelbildung zu einem gewissen Ausmass beeinflussen kann, scheinen doch Molekulargewicht und Sedimentation der Proben in Lösung ein Maximum bei einem Dosisniveau zu erreichen, bei dem die labilere Bindung im Gelierungsphänomen einsetzt.

Received April 12, 1963.

Revised February 17, 1963

On the Deformation of Networks of Very Stiff Random Chains Existing in Certain Colloidal Gels

JAN HERMANS, JR.,* *FMC Corporation, American Viscose Division,
Research and Development, Marcus Hook, Pennsylvania*

Synopsis

The deformation of the random chains consisting of stiff particles which occur in gels of certain colloids is analyzed. The results of this analysis are used to obtain an expression for the elasticity modulus of infinite networks consisting of such chains. It is found that the shear modulus is proportional to the number of chains between crosslinks per unit of volume and to the average inverse length of the chains.

INTRODUCTION

Much theoretical work has been done on the elasticity of networks formed by randomly coiling chains and the results obtained form an excellent description of the observed behavior of rubberlike materials.¹⁻³ The force resisting the deformation of the network is taken to be that pulling the two ends of a randomly coiled molecule together, averaged over many such molecules, and is an "entropy force." Recently, the energy of deformation of the individual chains has been introduced in this theory,⁴ since it is more realistic to let both the internal energy and entropy of the chains depend on their conformation. However, the energy changes considered were relatively small.

We wish to present here an attempt at calculating the elastic properties of a random network when these are over whelmingly determined by the energy of deformation. It is, of course, recognized that such networks of stiff chains are themselves very stiff, and that material containing them will not possess rubberlike elasticity. Such networks occur, however, in gels formed in suspensions of rigid particles, such as clays and cellulose microcrystals.^{5,6} These gels owe their characteristic properties (yield stress and high viscosity) to a network of particles extending throughout the solution when it is at rest.⁵ One method of studying these networks is by measuring their elastic modulus. The latter is found to be exceedingly large considering the number of particles in the solution, and this indicates that the deformation of the network requires much energy.⁷ To interpret these data quantitatively, it was obviously of interest to

* Present address: Department of Biochemistry, University of North Carolina, Chapel Hill, N. C.

analyze the deformation of the model. The results of this analysis are presented below. It should be pointed out that we shall consider only small deformation since the mathematical difficulties in doing otherwise are rather formidable. Also, the gels which led us to consider this model can be deformed only small amounts before they yield and are found to follow Hooke's law at these small deformations.

DEFORMATION OF CHAINS

Model

We shall consider a three-dimensional network of random chains. The chains will be built up of rigid rodlike particles of length l and will commence and terminate in two succeeding branch points of the network.* Two particles can be joined in any relative direction, but this direction is not allowed to vary over the time by diffusion. When the number n of particles in a chain is large, the end-to-end distances of the chains will follow a Gaussian distribution

$$W(h)dh = (4b^3/\pi^{1/2})h^2 e^{-b^2h^2}dh \quad (1)$$

where $W(h)dh$ is the probability that a given chain has an end-to-end distance between h and $h+dh$ and b is given by

$$b^2 = 3/2nl^2 \quad (2)$$

The choice of this model is justified by a consideration of the system it is sought to represent: a gelled suspension of rigid particles. When such a gel is made to flow, most of the bonds linking the particles are disrupted, and the particles will soon be randomly oriented by the thermal motion, at least if the velocity gradient is small. When the flow stops, the particles link up to form a network. Experimentally it is found that these gels may be deformed and the deformation recovered after a reasonable length of time.⁷

Mechanics

The deformation of an individual chain occurs by bending and twisting the particles and by a deformation of the bond linking the particles. It is impossible to say *a priori* which will produce the greater change in end-to-end distance. The following equations of elementary mechanics describe the deformation.⁸

Let us first consider a chain with freely moving ends. Let opposite forces, f_p , parallel to the end-to-end line be applied at both endpoints (Fig. 1). A short straight segment of length Δs at a distance r from the straight line joining the two ends is then subjected to a moment

$$M = rf_p \quad (3)$$

* The length l will on the average be equal to one third the length of the rods if the rods are tied together by bonds distributed randomly over their length.

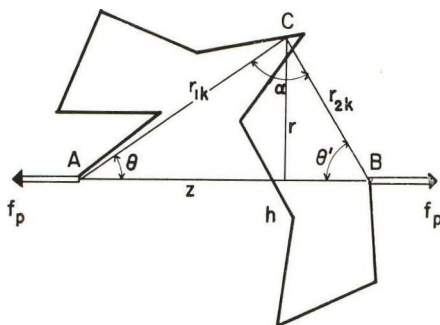


Fig. 1. Diagram illustrating the deformation of a randomly coiled chain.

If the rod lies in one plane with the end-to-end line, it will be bent, and its ends will make an angle

$$\Delta\alpha = M\Delta s/EI \quad (4a)$$

with each other, where

$$I = \pi a^4/4 \quad (4b)$$

for a cylinder of radius a , and E the modulus of the material. The stored energy will be

$$\Delta\epsilon_1 = \Delta s M^2/2EI = EI (\Delta\alpha)^2/2\Delta s \quad (5)$$

When the rod is perpendicular to the plane drawn through its center and the end-to-end line, it is rotated by a moment of the same magnitude. The ends will be turned with respect to each other over an angle

$$\Delta\alpha = 2M \Delta s/\pi G a^4 \quad (6)$$

where G is the shear modulus. Since $2G \leq E \leq 3G$ the values of $\Delta\alpha$ of eqs. (4) and (6) do not differ much. We shall assume that the angular deformation is independent of the direction in space of the part of the chain under consideration and is given by eq. (4) and the stored energy by eq. (5).

The deformation of the bonds we shall let be described by similar equations:

$$\Delta\alpha = M/B \quad (7)$$

for each bond and the stored energy

$$\Delta\epsilon_2 = M^2/2B = B(\Delta\alpha)^2/2 \quad (8)$$

is independent of the direction of the bond. The constant B depends on the chemical nature of the bond and its magnitude will generally be unknown. In the following discussion we shall treat the case in which the rods are distorted and not the bonds. Because of the similarity of eqs. (5) and (8) it is easy to rewrite the resulting equations in such a way that

they describe the behavior of chains in which the bonds are deformed according to eqs. (7) and (8).

Clearly, the distortions characterized by the angle $\Delta\alpha$ will produce a change in the end-to-end distance. It can easily be seen that the distortion of each element produces a lengthening of the chain when both ends are free as is assumed. The component of the lengthening parallel to the original end-to-end distance is

$$\Delta h = r \sin \theta \Delta\alpha = r\Delta\alpha \quad (9)$$

as can be shown by applying the cosine rule to the triangle ABC in Figure 1, differentiating with respect to α while keeping the sides r_1 and r_2 constant, and substituting $h \sin \theta = r_2 \sin \alpha$. The total change in the end-to-end distance is found by summing all Δh , i.e. by writing

$$h' - h = (f_p/EI) \int_s r^2 ds \quad (10)$$

with the energy of deformation given by

$$\epsilon = (h' - h)f_p/2 \quad (11)$$

Here eqs. (3) and (4a) have been used, and the integration is extended over the entire path s of the chain.

Application to Random Chains

When the path s which the chain follows is unique, eq. (11) provides the answer sought. However, the randomness of our chains implies that this path is not known and that only average quantities can be calculated. The probability function describing the distribution in space of the k th element of a Gaussian chain with end-to-end distance h has been obtained by Kuhn, Künzle, and Katchalsky.⁹ It is derived by multiplying two Gaussian distribution functions according to eq. (1), one for a chain with k links beginning in one end point, the other for a chain with $n - k$ links beginning in the other end point, the two chains being constrained to have one end point in common. When this distribution function is expressed in cylindrical polar coordinates, the origin and z axis being chosen to coincide, respectively, with the first end point and the end-to-end line (Fig. 1), this function becomes

$$W_k(r,z)dzdr = \left[\frac{3n}{2l^2k(n-k)\pi} \right]^{3/2} \times \exp \left\{ - \frac{3n}{2l^2k(n-k)} [(z - hk/n)^2 + r^2] \right\} 2\pi r dz dr \quad (12)$$

We may now use this distribution function to obtain the average contribution by the k th element to the elongation of a chain of n units and end-to-end distance h . Using eq. (10) we have:

$$EI\Delta h_k/f_p = l \int_0^\infty \int_{-\infty}^\infty W_k(r,z)r^2 dz dr \quad (13)$$

Both integrations are performed easily to give

$$EI \Delta h_k / f_p = 2l^3 k(n - k) / 3n \tag{14}$$

It will be seen that the result is independent of h and that only summation over k remains:

$$EI(h' - h) / f_p = (2l^3 / 3n) \sum_0^n k(n - k) = (2l^3 / 3n) (n^3 / 6 - n^2 / 6) \tag{15}$$

and when n is large (as is supposed to be the case)

$$EI(h' - h) / f_p = n^2 l^3 / 9 \tag{16}$$

The energy of deformation is, of course,*

$$\epsilon = 9EI(h' - h)^2 / 2n^2 l^3 \tag{17}$$

It is of interest to compare this expression with that for the entropy change on elongation of a random coil with constant internal energy

$$\Delta S = -3k(h'^2 - h^2) / 2nl^2 \tag{18}$$

It will be noted that the dependence on h' , on h , and on n is different for the two types of chain. It is, therefore, to be expected that the deformation of a network of stiff chains follows rather different rules than does the deformation of a rubber.

DEFORMATION OF NETWORKS

We shall follow the analysis given for a rubberlike network of chains by Treloar.² In this analysis it is assumed that the endpoints of each chain—which are branch points in the network and, therefore, end points of (at least) three chains, move “affinely” when the sample is deformed, i.e., as if they were embedded in an elastic continuum. This is not the case, however, for the remaining parts of the chains, which can take up those positions required for a maximum overall entropy. We shall now assume the same to hold for a deformed stiff network, where maximum entropy is to be replaced by minimum energy. To calculate the energy of deformation of the network, the energies of elongation of the individual chains, given by eq. (17), must be summed. The elongation of a given chain is found as follows.

If the deformations of the sample in the three principal directions are λ_1 , λ_2 , and λ_3 , a chain with end-to-end vector of components h_1 , h_2 , and h_3 along these axes, will after deformation have components $\lambda_1 h_1$, $\lambda_2 h_2$, and $\lambda_3 h_3$. The stored energy depends on the length, following eq. (17):

$$\epsilon = (9EI / 2n^2 l^3) \times [(\lambda_1^2 h_1^2 + \lambda_2^2 h_2^2 + \lambda_3^2 h_3^2)^{1/2} - (h_1^2 + h_2^2 + h_3^2)^{1/2}]^2 \tag{19}$$

* It is assumed here that the ratio: average change in length to given applied force is equal to the ratio: given change in length to average applied force.

This expression is to be averaged over all possible combinations (h_1, h_2, h_3), keeping the number of links in the chain constant. This averaging is made much simpler by letting

$$\begin{aligned}\lambda_1 &= 1 + \sigma/2 \\ \lambda_2 &= 1/(1 + \sigma/2) \sim 1 - \sigma/2 + \sigma^2/4 \\ \lambda_3 &= 1\end{aligned}\quad (20)$$

If σ_0 is the (small) amount of simple shear applied,²

$$\sigma_0 = \lambda_1 - \lambda_2 = \sigma + 0(\sigma^2).$$

Equation (19) becomes

$$\epsilon = (9EI/2n^2l^3) \sigma^2 (h_1^2 - h_2^2)^2/4h^2 + 0(\sigma^3) \quad (21)$$

It can easily be shown that for a given h , the average value of $(h_1^2 - h_2^2)^2$ is

$$\langle (h_1^2 - h_2^2)^2 \rangle = 4h^4/15 \quad (22)$$

Hence

$$\epsilon = (6EI/5n^2l^3) \sigma^2 h^2 \quad (23)$$

Averaging over h is simple, since

$$\langle h^2 \rangle = nl^2 \quad (24)$$

Hence

$$\epsilon = 6EI \sigma^2/5nl \quad (25)$$

This result differs significantly from that for the average contribution to the entropy of deformation made by a single flexible chain in a rubber network,

$$\Delta S = k\sigma^2/2 \quad (26)$$

in that it still contains n . The total energy of the network of stiff chains depends not only on the number of chains, but also on the way they are distributed over various contour lengths:

$$\epsilon_{\text{total}} = (6EI \sigma^2/5l) \sum_n N_n/n \quad (27)$$

where N_n is the number of chains containing n links. As a consequence, the shear modulus is given by

$$G = 2\epsilon/\sigma^2 = (12EI/5l) \sum_n N_n/n \quad (28)$$

where N_n is from here on to be taken to represent the number of chains of n links per unit of volume. Formally, we can write this

$$G = (12EI/5l)N_c \langle 1/n \rangle \quad (29)$$

where N_c is the total number of chains per unit of volume and $\langle 1/n \rangle$ the average of the reciprocal of the number of elements per chain. In contrast, for a rubber, the modulus is proportional to N_c , and a term containing n does not appear

$$G = N_c kT \tag{30}$$

An interesting consequence of the inverse dependence on n of the modulus of the network of stiff chains is that for sufficiently large n , the modulus given by eq. (28) will be lower than the value calculated for a rubber. Of course, no matter how stiff the chains are, the entropy of the network will, upon shearing change according to eq. (26). Hence, the modulus should be written as the sum of two terms, given by eqs. (28) and (30), of which in special cases one may predominate, depending on the structure of the network and the value of the constants E and I .

Effect of Distribution of Chain Lengths

The distribution of chain lengths will have to be considered separately, depending on the way the network was formed. Since this point is not under discussion here, we shall limit ourselves to a few general considerations.

If all chains have the same number of elements, n , this number is equal to the ratio of the total number of elements, N_0 , in the network and the number of chains, N_c :

$$n = N_0/N_c$$

(N_0 need not be identified with the total number of particles present since "loose ends" do not contribute to the network). The modulus will be equal to

$$G = (12EI/5l) N_c^2/N_0 \tag{31}$$

For any other type of distribution the modulus will be greater than this, since the average of $1/n$, given N_0/N_c , the number-average of n , is smallest when all n 's are the same.

For example, for a most probable distribution

$$P(n) = (N_c/N_0) (1 - N_c/N_0)^n \tag{32}$$

where $P(n)$ is the probability that a given chain has n links, it follows that

$$G = (12EI/5l) (N_c^2/N_0) \log N_0/N_c \tag{33}$$

Shorter Chains

It may be argued that we have not used the correct energy of deformation for a single chain. When the chains for which we derived relationship (17) are deformed as we assumed, the relative angle which the first and last element of the chain make with one another may change by an amount

equal to the sum of the $\Delta\alpha$ over the entire chain. (In our treatment all $\Delta\alpha$ are positive, i.e. make a positive contribution to $h' - h$.) Now the first and last elements of each chain are part of two other chains and are no more flexible than the other elements. Hence, the angles between the three chain ends may not be changed; at most the branchpoint may be rotated to another position. This means, then, that apart from a force extending the chain, a moment is applied at each end point, and that as a result, the bending of the chain is different. Undoubtedly, more energy will be needed for a given change in end-to-end distance, and a higher value of the modulus would be the result. One will notice, however, that bending which occurs simultaneously in two directly opposed points (i.e., in our cylindrical polar coordinates: with the same z and r , but with values of φ differing by an amount π), produces a lengthening of h , but results in no change of the angles which the first and last elements make with the z axis. If, therefore, the chain length of the random chains under consideration is great enough, the extra condition imposed on the deformation is automatically met.

We find it worth pointing this out, since an extension of the theory to networks containing short chains would have to take this extra energy into account, in addition to the well-known factor of non-Gaussian statistics.

Very Short "Chains"

We would like to conclude this analysis by pointing out some aspects of the treatment of a random network where every "chain" is so short that it is only a segment of rod. This type of problem has been investigated by different authors for the two-dimensional networks occurring in paper.^{10,11} Litt's results (which are in agreement with experimental data on paper) indicate that the modulus, apart from a small proportionality constant, would approximately be given by

$$G = Ed/(l^2/4a^2 + 1) \quad (34)$$

where d is the volume fraction of the network and a the radius of the elements. This result was derived on the assumption that the fibers are deformed and the bonds linking them are not. In such a network every particle-particle link may be considered a crosslink. As N_c/N_0 increases, the average number of crosslinks per particle increases, the average length of the elements decreases to zero, so that the upper limit of G will be in the neighborhood of Ed . More particularly, when N_c/N_0 is large, the average length of the elements of the network will be

$$\langle l \rangle = l_0/(N_c/N_0 + 1) \quad (35)$$

since a line element is divided into $g + 1$ pieces by g points. By substituting eq. (35) into eq. (34) one may obtain an expression relating the modulus to N_c/N_0 when the latter is high.

This expression is very similar to the one obtained by us in the limit of long chains. By letting $N_0 \gg N_c$ in eq. (35), one obtains with eq. (34)

$$G \sim 4Eda^2N_c^2/l_0^2N_0^2 \quad (36)$$

which, since $d = \pi N_0la^2/4$, is nearly identical with the expression for G of eq. (31), in which I is given by eq. (4b). Thus, it would appear possible to apply eqs. (31) or (29) over a much wider range of degrees of crosslinking than was allowed in their derivation.

It is interesting to note an alternative possibility, namely, that the interparticle bonds are responsible for the observed deformation. As is obvious from a comparison of the form of eqs. (5) and (8), the way in which the modulus of a network of long chains depends on N_c/N_0 is in this case still given by eq. (28), except for the proportionality constant. However, when we try to deform a network in which the "chains" are short pieces of rod, it will from a certain value of N_c/N_0 onward be impossible to deform the network by deforming the bond angles, since the six sides suffice to determine each tetrahedron of which the network is composed. In such a case one might expect to find a rather sudden increase in modulus with N_c/N_0 as the point is reached where the deformation must occur by the deformation of the rods rather than by that of the bonds.

Comparison with Experimental Results

The elastic properties of gel of cellulose microcrystals, systems which may be adequately described as random networks of rodlike particles, have been studied by the author as a function of the concentration.⁷ (These results have been submitted for publication.) Unfortunately, the results obtained do not permit one to evaluate the applicability of the theory derived in this article. Such a verification is complicated by the fact that one has to make three basic assumptions when one wishes to analyze these data quantitatively, namely, (1) how the number of particle-particle bonds varies with the concentration, (2) what the structure of the network will be, given the number of links per particle, and (3) what will be its elastic behavior. In first approximation, the simplest possible assumption was made in each case. Thus the importance will be clear of having shown that the elasticity of networks of stiff chains is, in the simplest case, a different function of the structure of the network from that to be assumed for rubberlike networks, even though agreement between theory and experiment was not obtained with the simple assumptions.

It gives the author much pleasure to recognize the help in deriving the results obtained which he received from Dr. Robert Simha during his short stay at our laboratory.

References

1. Kuhn, W., *Kolloid-Z.*, **76**, 258 (1936).
2. Treloar, L. R. G., *The Physics of Rubber Elasticity*, Clarendon Press, Oxford, 1958.
3. Flory, P. J., *The Principles of Polymer Chemistry*, Cornell Univ. Press, Ithaca, N. Y., 1953, p. 432.
4. Flory, P. J., C. A. J. Hoeve, and A. Ciferri, *J. Polymer Sci.*, **34**, 337 (1959).
5. Goodeve, C. F., *Trans. Faraday Soc.*, **35**, 342 (1939).
6. Hermans, J., *J. Polymer Sci.*, **C2**, 129 (1963).
7. Hermans, J., *J. Polymer Sci.*, submitted for publication.
8. Timoshenko, S., and J. N. Goodier, *Theory of Elasticity*, McGraw-Hill, New York, 1951, Chaps. 10-12.
9. Kuhn, W., O. Künzle, and A. Katchalsky, *Helv. Chim. Acta*, **31**, 1994 (1948).
10. Onogi, S., and K. Sasaguri, *Kami-pa Giklshi*, **11**, 233 (1957).
11. Litt, M., *J. Colloid Sci.*, **16**, 297 (1961).

Résumé

On a analysé la déformation de chaînes statistiques constituées de particules rigides, qui se produit dans les gels de certains colloïdes. Les résultats de cette analyse sont utilisés pour obtenir une expression du module d'élasticité des réseaux infinis constitués de chaînes de cette espèce. On a trouvé que le module de cisaillement est proportionnel au nombre de chaînes situées entre les ponts par unité de volume et à l'inverse de la longueur moyenne des chaînes.

Zusammenfassung

Die Deformation der aus steifen Partikeln bestehenden statistischen Ketten, die in Gelen bestimmter Kolloide auftreten, wird untersucht. Die Ergebnisse dieser Analyse werden zur Bildung eines Ausdruckes für den Elastizitätsmodul unendlicher Netzwerke aus solchen Ketten verwendet. Der Scherungsmodul ist der Zahl der Ketten zwischen den Vernetzungsstellen pro Volumeneinheit und der mittleren reziproken Kettenlänge proportional.

Received October 8, 1963

Revised March 6, 1964

Polymer Degradation. II. Mechanism of Thermal Degradation of Polyoxypolypropylene Glycol-Toluene 2,4-Diisocyanate Polymer (POPG-TDI) and a Block Polyether Glycol-TDI Polymer*

J. D. INGHAM and N. S. RAPP, *Jet Propulsion Laboratory, California Institute of Technology, Pasadena, California*

Synopsis

Further studies on the thermal degradation of POPG-TDI polymer have been carried out. It has been shown that at temperatures of $\sim 200^\circ\text{C}$., the predominant degradation process involves random scission of the urethane linkages to give substantial amounts of isocyanate and hydroxyl. Kinetic data suggests that the weakest links in POPG-TDI polymer are spaced at intervals of $\sim 10,000$ in molecular weight and that they may be eliminated by pretreatment of the POPG with ethylene oxide to form a block copolyether which is used to prepare the polyurethane. At temperatures exceeding 250°C . and a greater conversion to volatile fragments ($>10\%$) the kinetics of degradation of POPG-TDI are similar to results for POPG and indicate scission of the polyether bonds by a combination of intramolecular proton abstraction and free radical unzipping reactions, in agreement with previous studies of POPG of much higher molecular weight.

I. INTRODUCTION

Column elution fractionation of an uncrosslinked POPG-TDI polyurethane before and after moderate thermal degradation at 200°C . in a vacuum has shown the molecular weight distribution to be invariant and most probable.¹ This result suggests a random scission process. It does not, of itself, provide unequivocal proof for a random process because other mechanisms, for example free radical unzipping initiated at the chain ends, can also give invariant most probable distributions.² However, such depolymerizations would be accompanied by much larger extents of volatilization for comparable reductions in molecular weight than were observed for these polymers ($<5\%$ volatilization).

For a more detailed consideration of the mechanism, the question arises as to whether scission occurs randomly at the urethane links or randomly along the chains. One method of deciding is to measure the ratio of weight-average to number-average molecular weight, \bar{M}_w/\bar{M}_n in the highly de-

* This paper presents one phase of research performed by the Jet Propulsion Laboratory, California Institute of Technology, sponsored by the National Aeronautics and Space Administration, Contract NAS 7-100.

graded residue. Since urethane scission would effectively regenerate POPG units and the distribution of molecular weights of POPG is very narrow ($\bar{M}_w/\bar{M}_n \sim 1.0$), the degradation residue at high extents of degradation (to about the molecular weight of POPG) should give \bar{M}_w/\bar{M}_n of nearly one if predominant urethane scission occurs. On the other hand, predominant scission at the ether bonds in POPG will not change the ratio.

The origin of these statements is as follows.

For condensation polymers that polymerize to give most probable distributions:^{3a}

$$\bar{M}_w = \bar{M}_u \bar{X}_w = M_u (1 + P)/(1 - P) \quad (1)$$

$$\bar{M}_n = M_u \bar{X}_n = M_u/(1 - P) \quad (2)$$

in which M_u is the unit molecular weight, \bar{X}_n and \bar{X}_w are the number-average and weight-average degrees of polymerization, respectively, and P is the extent of reaction or fraction of functional groups reacted.

Dividing eq. (1) by eq. (2) yields:

$$\bar{M}_w/\bar{M}_n = 1 + P \quad (3)$$

From eq. (2):

$$P = 1 - M_u/\bar{M}_n \quad (4)$$

From eqs. (1), (3), and (4):

$$\bar{M}_w/\bar{M}_n = 2/(1 + M_u/\bar{M}_w) \quad (5)$$

These relationships are also valid for degraded polymers that undergo scission by a random process; M_u can then be considered to be the molecular weight between scissionable bonds. Therefore, by measuring $[\eta]$, calculating \bar{M}_w ,⁴ and using an assumed value for M_u , P and \bar{M}_w/\bar{M}_n can be calculated for degraded polymer. For POPG-TDI degraded to $\bar{M}_w = 3500$, $P = 0.228$ if $M_u = 2200$, assuming only urethane scission, and $P = 0.966$ if $M_u = 60$, assuming ether scission. Therefore, either fractionation of highly degraded POPG-TDI and calculation of \bar{M}_w/\bar{M}_n and P , or independent measurements of \bar{M}_w and \bar{M}_n can be used to determine whether ether or urethane scission predominates.

The required fractionation and subsequent determination of \bar{M}_w/\bar{M}_n is a many-sided problem so, following the Experimental section, the various portions are discussed separately in parts A through C. Part A is concerned with the development of a suitable method for the column fractionation of POPG. Such a procedure could then be used for the fractionation of highly degraded POPG-TDI. It was first applied to a synthetic mixture of POPG 1000 and POPG 2000 to demonstrate that reasonably efficient fractionation could be achieved. Part B consists of a discussion of a similar fractionation of highly degraded POPG-TDI. The results indicated predominant urethane scission rather than ether scission. Further evidence for this conclusion was obtained in part C, in which \bar{M}_n of the

fractions was determined by vapor pressure osmometry. By using estimates of \bar{M}_w of intrinsic viscosities, \bar{M}_w/\bar{M}_n was then calculated and found to be ~ 1.23 . Similarly, a low value of \bar{M}_w/\bar{M}_n was obtained for a series of other degraded POPG-TDI samples to provide additional evidence for predominant urethane scission at 200°C. in an inert atmosphere.

Having established the site of degradation at 200°C., attention is then directed in parts D and E to the mechanism itself. Part D presents a report of an examination of the volatile products and residues from degraded POPG-TDI by infrared spectroscopy. It was found that an important degradative reaction is reversal of the polymerization process to give TDI and free hydroxyl groups. Moreover, it was believed that urethane bonds formed from primary hydroxyls would be less susceptible to scission than those from secondary, so POPG was reacted with ethylene oxide in an effort to convert the terminal groups to primary hydroxyl. A polyurethane prepared from this modified POPG was degraded and the kinetics of scission were compared with an unmodified POPG-TDI as discussed in part E. The results showed that the weakest links had been effectively eliminated in the modified polymer.

All of the preceding studies were carried out at $\sim 200^\circ\text{C}$. Part F is concerned with additional studies at 250–320°C. Volatilization rate measurements were carried out to compare the degradation processes for POPG-TDI with POPG. It was found that after initial volatilization of TDI in the former, the rate curves and activation energies for both polymers were the same, indicating similar mechanisms of degradation. This is further evidence that after initial urethane scission, the POPG-TDI residue is structurally similar to POPG.

II. EXPERIMENTAL

A. Preparation of Polyether-Polyurethanes

For most of the work described in this paper, POPG-TDI was prepared by polymerization in bulk as described previously.^{1,4} The block (polyoxyethylene glycol-polyoxypropylene)-toluene diisocyanate polymer, (POEG-POP)-TDI, and the normal POPG-TDI used for comparison were prepared by adding 2 ml. of TDI containing 2.5 mg./ml. of ferric acetylacetylacetonate (FeAA) from a tube flushed with dry nitrogen to 26.57 g. of dried polyether, with polymerization at 120°C. for 20 min. while the polymer tube was continuously purged with dry helium.

B. Preparation of Block (Polyoxyethylene Glycol-Polyoxypropylene)-Toluene Diisocyanate

The POPG (496.6 g.) was dried by heating to 120°C. in a stream of dry nitrogen followed by the addition of 11 g. of sodium. After heating overnight at 125°C., the sodium had dissolved, and 80 g. of ethylene oxide was added by distillation to the reaction mixture at 130–140°C., with a Dry Ice condenser attached to the flask. The polymer was neutralized with

dilute hydrochloric acid, washed four times with water and dried by heating while being purged with dry nitrogen.

C. Column Fractionation of POPG and Thermally Degraded POPG-TDI

Because of their low molecular weights and high solubilities, POPG and highly degraded POPG-TDI could not be fractionated by elution from a Teflon column as described previously,¹ even at -30°C . Therefore adsorbing substrates were tried. Cellulose powder gave no separation; however, preliminary experiments with thin layer chromatography indicated that good separations could be obtained from silica gel by using an eluent of 75% benzene and 25% acetone. A 2.5×8.5 cm. column of silica gel provided separation of POPG of molecular weights 2000 and 1000 as discussed below. For similar fractionation of highly degraded POPG-TDI it was necessary to increase the eluent polarity after fraction 5 to 30% acetone for fractions 6 to 11; 35% acetone for 12; and 100% acetone followed by methanol for 13, to remove these fractions from the column.

D. Thermal Degradation Experiments

For most degradation experiments, the sample was heated at constant temperature in a test tube fitted with a thermometer and a helium inlet that was below the surface of the polymer. Samples were removed for $[\eta]$ and infrared measurements with 2 mm. glass rods. The highly degraded POPG-TDI of Part B below and Table III was obtained by heating 3.36 g. of polymer at 207°C . in a tube continuously flushed with helium for 429 hr. For the experiments in closed bottles, (Part C and Table V) four 60 to 70 mg. samples were weighed into small aluminum cups and placed in pressure-tight aerosol bottles. The bottles were then evacuated and filled with nitrogen at atmospheric pressure and placed in a thermostatted oven. The results given are the average values for the four samples in each case. For small samples it appeared that more reproducible results were obtained if aluminum containers (rather than Pyrex) were used.

E. Intrinsic Viscosity Measurements

Viscosities were determined in benzene with Ubbelohde suspended-level viscometers at $25 \pm 0.02^{\circ}\text{C}$. at two concentrations. Intrinsic viscosities were calculated from

$$\eta_{sp}/c = [\eta] + k'[\eta]^2c$$

in which $[\eta]$ is the intrinsic viscosity, η_{sp} is the specific viscosity, and c is the polymer concentration in grams per deciliter. A value of k' of 0.39 as determined previously⁴ was assumed; since the two values of $[\eta]$ from the two concentrations were in good agreement, the use of the value of 0.39 for k' was justified. Although not strictly accurate for degraded POPG-TDI or POPG-TDI of $[\eta] > 0.55$, the equation⁴

$$[\eta] = 4.13 \times 10^{-4} M_w^{0.64}$$

was used to estimate weight-average molecular weights.

F. Number-Average Molecular Weights by Vapor Pressure Osmometry

Method A with Benzene as Solvent. The instrument used was the Mechrolab vapor pressure osmometer (Mechrolab, Inc., Mountain View, California); the principle of operation is described in part C below. The instrument was calibrated with a series of biphenyl and squalene solutions. The resistance increments for a series of four or more concentrations (1–10 g./l. in benzene) were determined for each polymer and an apparent molecular weight obtained by extrapolation to infinite dilution. In general, the scatter was rather high and this procedure has no advantage over method B given below. It is mentioned here because the initial data were obtained in this way.

Method B with Toluene as Solvent. Because toluene is a "poorer" solvent for POPG-TDI polymers than benzene, less chain interaction and molecular association was expected when toluene was used. Actually, no concentration dependence outside the limits of error was observed for POPG or highly degraded POPG-TDI polymers below 20 g./l. The 37°C. thermostat temperature varied during the heater on-off cycles. Since this caused variations in the thermistor resistances, the error was reduced by recording the resistances at the same point in the thermostat cycle each time, both for solvent calibration and sample measurements. A number of determinations were made at concentrations of <20 g./l. and the results averaged to give the apparent number-average molecular weight.

G. Weight Loss Measurements in Vacuum

The balance consisted of a fine Pyrex capillary fixed at one end and positioned horizontally within a Pyrex housing that could be evacuated to $<10\mu$ Hg. Sensitivity was 0.9 mm./mg.; it was found to be linear over the range of measurements by adding fractional weights to the pan enclosed by a temporary housing at ambient conditions. The sensitivity varied slightly from run to run, presumably because of temperature changes, but was checked by measuring the total deflection and weighing the sample before and after degradation. Deflection of the capillary was measured with a steel scale and fixed magnifying glass or, more recently and confidently, with a cathetometer. The total load limit was 70 mg., which was found to be more than adequate for these measurements. The 5–15 mg. sample was weighed onto an aluminum foil pan which was attached to the free end of the capillary by means of a thin tungsten wire and suspended in the evacuated Pyrex tube immersed in the furnace. The sample pan was ~ 20 cm. below the top opening of the furnace. An experiment showed that identical weight loss rates were obtained using either aluminum or platinum pans. The furnace consisted of a large test tube wrapped with nichrome wire and controlled to within $\pm 0.5^\circ\text{C}$. with a proportioning controller. The temperature was determined from a thermometer suspended inside the evacuated tube near the sample. Although differences in thermal emis-

sivity of the sample and thermometer could lead to errors in absolute temperature, those were probably not more than 2°C. and were relatively constant for separate runs as indicated by the straight-line activation energy plots obtained.

III. RESULTS AND DISCUSSION

A. Column Elution Fractionation of POPG

Although POPG-TDI polymers of $[\eta] = 0.70\text{--}0.20$ dl./g. were fractionated by elution from a column of Fluoropak 80 (Teflon) with benzene solvent-isooctane nonsolvent at temperatures of 34 and 7°C.,¹ separation of POPG 2000 could not be obtained by similar procedures, presumably because of its lower molecular weight. Even at -30°C . with pure isooctane eluent, all of the polymer was removed from the column with the first solvent increment. Therefore, columns of an adsorbing substrate, silica gel, were used.

Results of the fractionation of a 2 g. sample of POPG 2000 from a column of silica gel at room temperature are shown in Table I. It is not possible

TABLE I
Column Adsorption Fractionation of Polyoxypropylene Glycol (POPG) of Molecular Weight 2000^a

Fraction	Cumulative weight fraction, W^b	Intrinsic viscosity $[\eta]$, dl./g. ^c	Molecular weight M^d
1	0.041	0.049	1750
2	0.163	0.050	1800
3	0.300	0.051	1860
4	0.410	0.053	1970
5	0.531	0.054	2040
6	0.664	0.055	2100
7	0.867	0.056	2150
Initial ^e	...	0.055	2100
Combined ^e	...	0.053	1970

^a Recovery: 100.4%; \bar{M}_w/\bar{M}_n : 0.997.

^b W was calculated from $(1/W_i)[(W_i/2) + \sum_1^{i-1} W_{i-1}]$.

^c $[\eta]$ was determined in duplicate and calculated from $\eta_{sp}/c = [\eta] + k'[\eta]^2c$, for an assumed value of k' of 0.39.⁴

^d M was calculated from $[\eta] = kM^a$ for $K = 4.13 \times 10^{-4}$ and $a = 0.64$.⁴

^e Initial refers to unfractionated polymer; combined are corresponding data calculated from $[\eta] = (1/W_i) \sum_1^i W_i [\eta]_i$ and $M = (1/W_i) \sum_1^i W_i M_i$.

to determine whether POPG has the narrow distribution obtained ($\bar{M}_w/\bar{M}_n = 1.0$), because inefficient fractionation could produce the same experimental results. To further examine the efficiency of fractionation and

TABLE II
Column Adsorption Fractionation of a Bimodal Mixture of Polyoxypropylene Glycol of
Molecular Weights 1000 and 2000^a

Fraction	Cumulative weight fraction W^b	Intrinsic viscosity $[\eta]$, dl./g. ^c	Molecular weight M^d
1	0.0405	0.032	910
2	0.1135	0.034	1000
3	0.1880	0.035	1050
4	0.2625	0.037	1150
5	0.3320	0.040	1300
6	0.4120	0.043	1450
7	0.4975	0.048	1700
8	0.5700	0.051	1850
9	0.6905	0.054	2050
10	0.805	0.055	2100
11	0.924	0.057	2200
Initial ^e	...	0.046	1600
Combined ^e	...	0.046	1600

^a Recovery: 99.7%; \bar{M}_w/\bar{M}_n : 1.09.

^b W was calculated from $(1/W_t) [(W_i/2) + \sum_1^{i-1} W_{i-1}]$.

^c $[\eta]$ was determined in duplicate and calculated from $\eta_{sp}/c = [\eta] + k'[\eta]^2 c$, for an assumed value of k' of 0.39.⁴

^d M was calculated from $[\eta] = KM^a$ for $K = 4.13 \times 10^{-4}$ and $a = 0.64$.⁴

^e Initial refers to unfractionated polymer; combined are corresponding data calculated from $[\eta] = (1/W_t) \sum_1^i W_i[\eta]_i$ and $M = (1/W_t) \sum_1^i W_i M_i$.

determine the utility of the method, a synthetic mixture of 1.40 g. of POPG 1000 and 1.75 g. of POPG 2000 was fractionated. The results of this experiment are given in Table II. The integral data for POPG 2000 and for the POPG 2000-POPG 1000 mixture are given in Figure 1. Curves *A* and *B*, and *C* and *D* are theoretical Poisson distributions for POPG 1000 and POPG 2000. Poisson distributions were calculated for comparison because Flory has shown that polymerization of cyclic monomers, such as ethylene oxide, can give polymers having a Poisson distribution of molecular weights.⁵ Curve *E* is the experimental integral distribution for POPG 2000, which is considerably narrower than the Poisson distribution (*D*). Curve *F* was obtained by adding the Poisson distributions for POPG 1000 and 2000 together. Except at the ends, agreement of the points with the theoretical curves is remarkably close. The value of \bar{M}_w/\bar{M}_n for this fractionation was 1.09. Calculation of \bar{M}_w/\bar{M}_n to be expected from the mixture, assuming both components to have $\bar{M}_w/\bar{M}_n = 1$ gives a result of 1.12, which compares favorably with the experimental value.

Therefore, although Poisson distributions are not obtained for POPG, the fractionation procedure can still be used to detect deviations in polydispersity, in particular, changes in \bar{M}_w/\bar{M}_n from 1.0 to 1.1, or higher, and

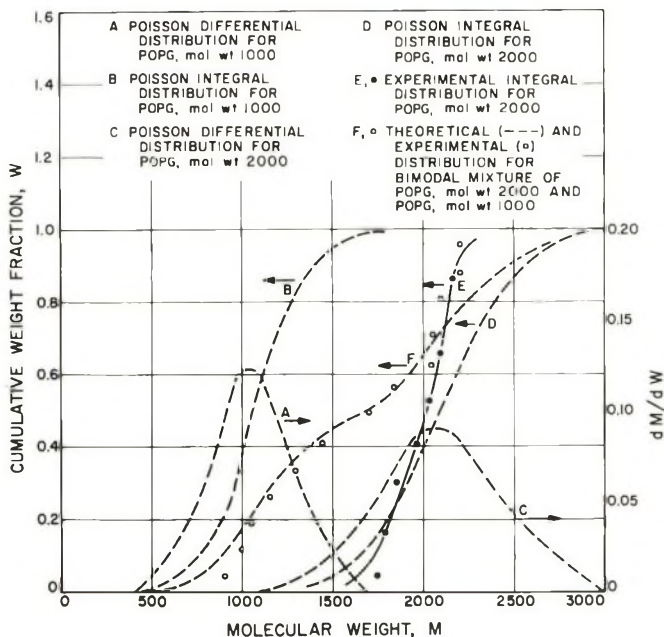


Fig. 1. Molecular weight distributions for polyoxypropylene glycols (POPG, mol. wt. 1000 and 2000) and a bimodal mixture of POPG 1000 and 2000.

has been applied to POPG-TDI residue as discussed below. Although this and other work on the fractionation of POPG⁶ indicates that POPG has a distribution narrower than the Poisson, Flory proposes that fractionation of polymers having such narrow distributions would be difficult if not impossible by any physical method.^{3b} However, it is recognized that the necessary condition of having growing chain ends of equal reactivity, for polymerization to a Poisson distribution, can not be assumed for the polymerization of propylene oxide. The primary hydroxyls add monomer at a faster rate than the secondary; furthermore, because of diffusion effects, the polymerization rate may decrease at higher molecular weights. Therefore, POPG may actually have a distribution more narrow than the Poisson.

B. Fractionation of Low Molecular Weight POPG-TDI Residue

A POPG-TDI sample was degraded from an initial intrinsic viscosity of 0.725 to 0.077 dl./g., corresponding to an M_w decrease from 122,000 to 3,500. The initial \bar{M}_w/\bar{M}_n was ~ 2.0 , as shown previously for polymers prepared by the same procedure.¹

The degraded polymer was then fractionated as described above for POPG, except that more polar eluents were required to remove fractions 6 to 13 from the column. In contrast to the results obtained for POPG, there was no correlation between the order of elution from the column and intrinsic viscosity. Possibly the polymer fragments have a variety of

TABLE III
Column Adsorption Fractionation of Degraded Polyoxypropylene Glycol-Toluene Diisocyanate Polymer (POPG-TDI)^a

Fraction	Cumulative weight fraction W^b	Intrinsic viscosity $[\eta]$, dl./g. ^c	Molecular weight M^d
10	0.042	0.064	2600
9	0.119	0.065	2700
3	0.184	0.066	2800
4	0.250	0.068	2900
5, 8, 11	0.407	0.070	3000
7	0.587	0.075	3400
12	0.681	0.084	4000
2, 6	0.804	0.806	4200
13	0.912	0.088	4300
1	0.965	0.122	7200
Initial ^a	—	0.077	3500
Combined ^a	—	0.077	3500

^a Recovery = 97.6%; $\bar{M}_w/\bar{M}_n = 1.03$.

^b W was calculated from $(1/W_i)[(W_i/2) + \sum_1^{i-1} W_{(i-1)}]$.

^c $[\eta]$ was determined in duplicate and calculated from $\eta_{sp}/c = [\eta] + k'[\eta]^2c$, for an assumed value of k' of 0.39.⁴

^d M was calculated from $[\eta] = KM^a$ using $K = 4.13 \times 10^{-4}$, and $a = 0.64$.⁴

^e Initial refers to unfractionated polymer; combined are corresponding data calculated from $[\eta] = (1/W_i) \sum_1^i W_i [\eta]_i$ and $M = (1/W_i) \sum_1^i W_i M_i$.

types of endgroups and, therefore, variable column adsorption characteristics that are not related to molecular weight. The fractionation data were arranged in order of increasing intrinsic viscosity and the integral distribution was obtained as shown in Table III and Figure 2. Since the separation was not based solely on differences in molecular weight, the results may not be very reliable because large variations in polydispersity of the fractions could exist. As an independent check of fraction polydispersity, the number-average molecular weights of the fractions were measured as discussed in part C below so that a more reliable estimate of \bar{M}_w/\bar{M}_n could be made.

The only quantity required to calculate the theoretical most probable distribution of a polymer is P . For POPG-TDI degraded to $\bar{M}_w = 3500$, $P = 0.228$ if $M_u = 2200$ (assuming urethane scission) and $P = 0.966$ if $M_u = 60$ (assuming ether scission). Therefore, theoretical distributions were calculated for these two cases for comparison with the experimental integral distribution of POPG-TDI of $\bar{M}_w = 3500$ in Figure 2. The experimental value of \bar{M}_w/\bar{M}_n was 1.03, compared with calculated value of ~ 1.23 for exclusive urethane scission and ~ 1.97 for ether scission. If the polydispersity of the fractions is considered, \bar{M}_w/\bar{M}_n is slightly greater than 1.03; therefore, the fractionation data indicate predominate scission at the

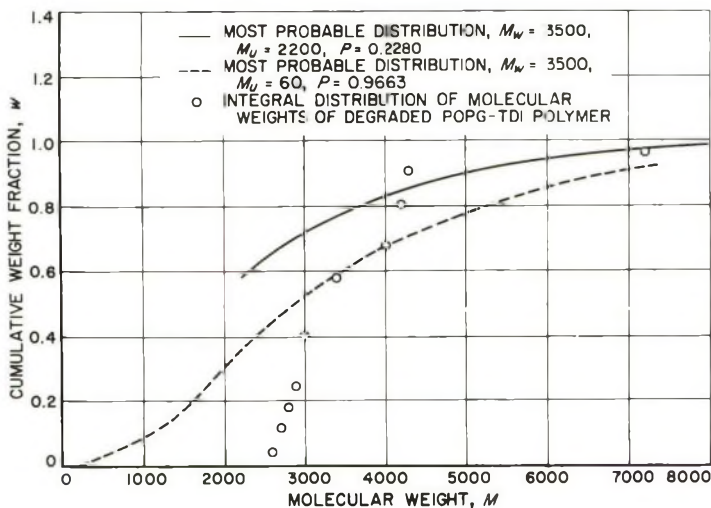


Fig. 2. Integral distribution of degraded polyoxypropylene glycol-toluene diisocyanate polymer (POPG-TDI) and comparison with some most probable distributions.

urethane bonds. The theoretical distributions were calculated by summing Flory's differential equation^{3a}:

$$dW_n/dX = X(1 - P)^2 P^{X-1} \quad (6)$$

to give:¹

$$W_n = 1 + XP^{X+1} - (X + 1) P^X \quad (7)$$

Equation (7) was used to calculate the distributions for the two values of P in Figure 2. The integral form of eq. (7) can be used if P is ~ 1.0 , but for low values of P , such as 0.23, appreciable errors would arise.

C. Measurement of Number-Average Molecular Weights of Fractions from Highly Degraded POPG-TDI

Because of the small amount of sample available from the fractionation of degraded POPG-TDI described above (0.1-0.2 g. per fraction) the Mechrolab vapor pressure osmometer was used for the determination of number-average molecular weights. The principle on which the operation of the instrument is based is that of vapor pressure lowering of the solvent by solute. A drop of solution and a drop of solvent are placed on two thermistor beads next to each other in a closed chamber saturated with solvent vapor. Because of the difference in vapor pressure of the two drops, a differential mass transfer occurs between the drops. The lower rate of evaporation from the solution drop results in a temperature difference between the two that is proportional to the vapor pressure lowering, and, therefore, proportional to the molar concentration of the solute, from which the molecular weight can be calculated. For these measurements, the

samples were dissolved in benzene and run according to method a described in the Experimental section. Some curvature in the M_n versus concentration plot, suggesting extrapolation to molecular weights higher than those given by a straight line, was shown for a few of the samples. However, this was generally ignored because ordinarily at least four points deviated less than 2% from a linearly extrapolated line. In an effort to avoid systematic errors a correction was applied to these apparent molecular weights based on the known number-average molecular weight of POPG. Since this POPG is believed to have a number-average molecular weight of 2000 and an apparent molecular weight of 1850 was obtained by the method described here, the apparent molecular weights were multiplied by a factor of 2000/1850, or 1.08, to give the corrected values shown in Table IV.

TABLE IV

Number-Average Molecular Weights by Vapor Pressure Osmometry and the Corresponding Ratios of Weight-Average to Number-Average Molecular Weights, \bar{M}_w/\bar{M}_n^a

Fraction	Uncorrected apparent number- average molecular weight $M_{n, \text{uncorr}}^b$	Corrected apparent number-average molecular weight, \bar{M}_n^c	Weight-average molecular weight \bar{M}_w^d	\bar{M}_w/\bar{M}_n
1	5300	5720	7200	1.26
2	2900	3130	4200	1.35
3	2200	2376	2800	1.18
4	2080	2247	2900	1.29
5	2480	2678	3000	1.12
6	3120	3370	4200	1.25
7	2820	3045	3400	1.12
8	2680	2890	3000	1.04
9	2310	2490	2700	1.08
10	2180	2350	2600	1.11
11	2190	2370	3000	1.27
12	2580	2790	4000	1.43
13	4100	4430	4300	0.97

$$^a \bar{M}_w/\bar{M}_n = \frac{\sum_i W_i \bar{M}_{wi}}{\sum_i W_i / \bar{M}_{ni}} = 1.228.$$

^b Replicate determinations; the plot of concentration vs. molecular weight showed some curvature; the values shown were obtained by linearly extrapolating to infinite dilution using 3 points at concentrations <2.5 gm./dl.

^c Corrected by multiplying by M_n for POPG 2000/ M_n observed for POPG 2000 = 1.08.

^d From $[\eta]$ by using $[\eta] = 4.13 \times 10^{-4} M^{0.64}$. Ref. 4.

Although replicate runs were made only for fraction 1, these data and a few check points indicate reproducibility of $\pm 7\%$; therefore the \bar{M}_w/\bar{M}_n values obtained for the fractions may not differ significantly. From the results obtained a value of 1.228 was calculated for the whole polymer. This,

TABLE V
Number-Average Molecular Weights by Vapor Pressure Osmometry of POPG and Degraded POPG-TDI

Sample No.	Time in 200°C. oven (helium atmosphere), hr.	$[\eta]$, dl./g. ^a	\bar{M}_w^b	\bar{M}_n^c	M_w/M_n (exp.) ^d	\bar{M}_w/\bar{M}_n (calc.) ^e $M_u = 1100$ $M_u = 2200$	
POPG-TDI							
1	0.25	0.705	117,000	}	2.05-2.2	2.0	2.0
2	0.25	0.743	125,000				
3	0.25	0.731	120,000				
Avg.		0.726	121,000				
POPG-TDI							
4	24	0.081	3,850	2170	1.77	1.56	1.27
5	24	0.076	3,480	2300	1.51	1.52	1.23
6	24	0.076	3,480	2370	1.47	1.52	1.23
Avg.		0.078	3,600	2280	1.58	1.53	1.24
POPG-TDI							
7	48	0.063	2,600	2070	1.26	1.41	1.08
8	48	0.061	2,470	2090	1.18	1.38	1.06
9	48	0.068	2,900	2070	1.40	1.45	1.14
Avg.		0.064	2,650	2080	1.28	1.41	1.09
POPG							
10	0	0.056	2,150	1890	1.14	1.05	
11	0			2015	1.07		
12	0			1990	1.08		
13	0			2010	1.07		
14	0			1795	1.20		
15	0			1910	1.13		
Avg.				1935	1.11		

^a Determined from benzene solutions at 25°C. and calculated from $\eta_{sp}/c = [\eta] + k'[\eta]^2c$ for $k' = 0.39$.⁴

^b Calculated from $[\eta] = 4.13 \times 10^{-4} M^{0.64}$. Ref. 4.

^c Each value is the average of three determinations that agreed within $\pm 4\%$ or better measured on the Mechrolab vapor pressure osmometer.

^d From \bar{M}_w calculated from $[\eta]$ and \bar{M}_n from vapor pressure osmometry, except for undegraded POPG-TDI (1, 2, and 3) for which the range given is that obtained from fractionation data for similar polymers.

^e Calculated from $\bar{M}_w/\bar{M}_n = 2/(1 + M_u/\bar{M}_w)$, where M_u was arbitrarily taken as 1100 and 2200, and \bar{M}_w was the value calculated from $[\eta]$ in b above, except for POPG for which ~ 1.05 is believed to be very near the actual value.

perhaps fortuitously, is the same as that calculated previously assuming $M_u = 2200$ in part B; nevertheless, the conclusion as to urethane scission is sustained. In fact, any value less than 1.3 is consistent with the idea of predominate urethane scission by a random process.

After completion of the work just described, method b (see Experimental)

for determination of number-average molecular weight was developed. Precision and accuracy appear to be well within $\pm 5\%$ for most measurements. Some results obtained for POPG-TDI samples degraded under helium are given in Table V. These results provide further confirmation of urethane scission, since the calculated values of \bar{M}_w/\bar{M}_n assuming a unit chain length $M_u = 1100$ are in good agreement with the experimental values. The polymer samples were degraded in closed bottles so that $<2\%$ volatilization occurred; therefore, $M_u = 1100$ is more reasonable than 2200 for these experiments.

D. Examination of the Products of Degradation of POPG-TDI by Infrared Spectroscopy

Thermal degradation in a vacuum ($<150 \mu$ Hg.) of a 14.4 g. sample of POPG-TDI, initial $[\eta] = 0.75$ dl./g., for 22 hr. at 233°C . resulted in 0.7 g. or 5% weight loss. Recovery of the volatiles was 0.63 g. or 90%, collected in the connecting tubes and a liquid nitrogen trap. The material in the trap, which consisted of 50% of the recovered product, had the same infrared spectrum as TDI. The remaining product in the connecting tubes had a melting range of $55^\circ\text{--}60^\circ\text{C}$. Its infrared spectrum was similar to that of TDI but showed some urethane or urea hydrogen and carbonyl absorption. This reacted isocyanate may have come from volatilization of polymer fragments or from reaction of volatilized TDI with adsorbed water on the pyrex surface. The infrared spectrum of the residual polymer is compared with that of POPG in Figure 3. Comparison of these spectra and spectra for undegraded POPG-TDI and a partially degraded POPG-TDI sample (cf. Fig. 4) shows that urethane hydrogen absorption (3.02μ , 3310 cm.^{-1}), carbonyl (5.75μ , 1740 cm.^{-1}) and absorption at 8.15μ (possibly C—O) decrease, and hydroxyl (2.85μ , 3500 cm.^{-1}) increases. Although not present in these spectra, during degradation in a flowing helium atmosphere, there may be a small absorption at 4.45μ (2247 cm.^{-1}) from isocyanate that may disappear. Apparently little or no carbodiimide is formed:



since absorption at 4.75μ (2100 cm.^{-1}) is not observed. The extensively degraded polymer had an $[\eta]$ of 0.059 dl./g., corresponding to an \bar{M}_w of 2300, using the relationship⁴:

$$[\eta] = 4.13 \times 10^{-4} \bar{M}_w^{0.64}$$

The measured \bar{M}_n by vapor pressure osmometry was 1930.

Thus, the results indicate that scission occurs predominantly at the urethane bonds to give substantial amounts of hydroxyl and isocyanate. However, the small absorptions at 5.8 and 6.2μ in degraded POPG-TDI (Fig. 3) may indicate the presence of carbonyl, aromatics, or unsaturation. Therefore, although there is substantial regeneration of hydroxyl and isocyanate, various other reactions take place. An expected reaction would

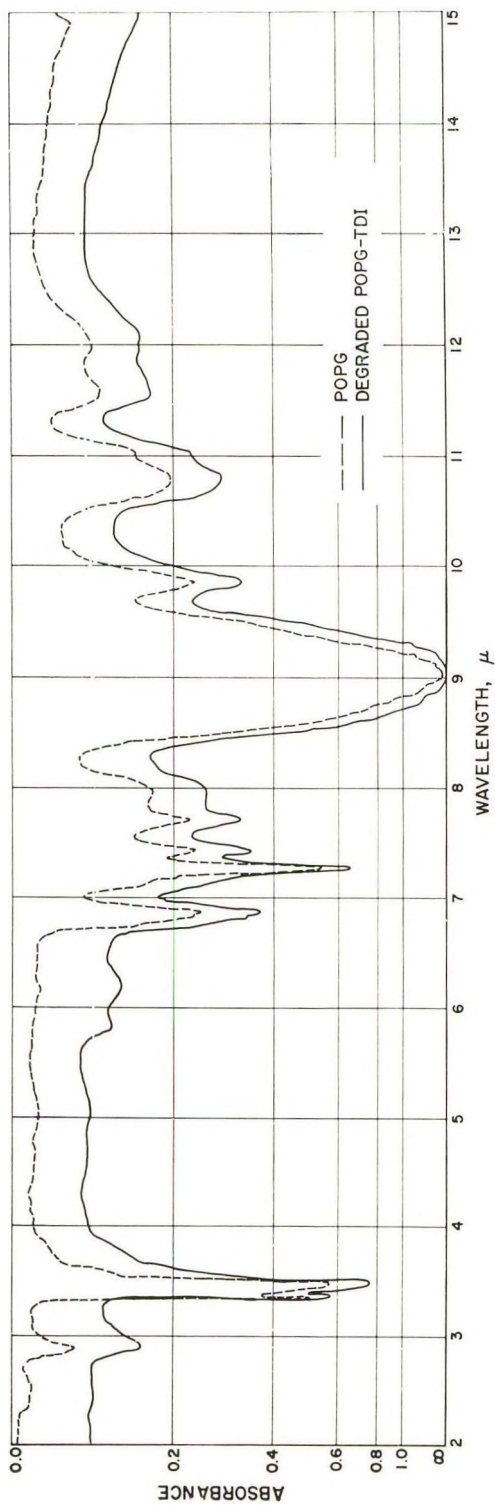


Fig. 3. Comparison of infrared spectra of polyoxypropylene glycol (POPG) and highly degraded polyoxypropylene glycol-toluene diisocyanate (POPG-TDI)

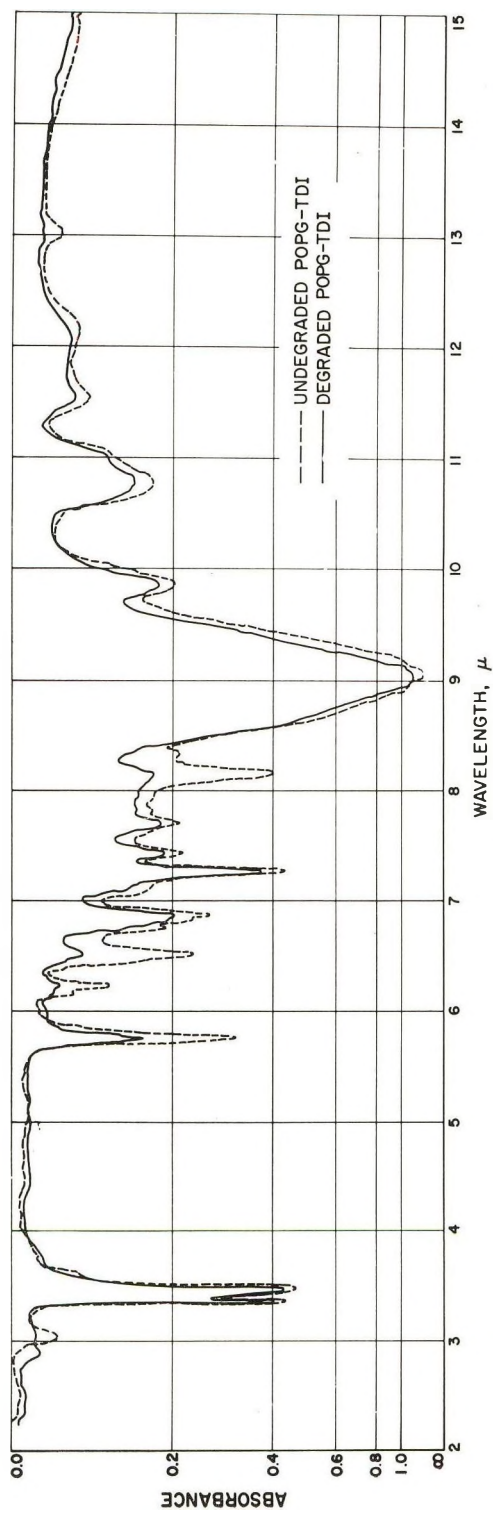


Fig. 4. Infrared spectra of polyoxypropylene glycol-toluene diisocyanate polymer (POPG-TDI) before and after thermal degradation.

be formation of unsaturation, aromatic amine and carbon dioxide, particularly when diffusion of TDI from the polymer is limited. One significant consequence of the importance of the reversal reaction is that it is subject to acidic or basic catalysis and may take place more rapidly at relatively lower temperatures in heterogeneous mixtures. Furthermore, the rate of scission may be decreased by using less active catalysts for urethane formation or by using less hindered reactants, e.g., primary terminal hydroxyl groups on the polyether.

E. Kinetic Studies of Chain Scission of POPG-TDI and a Block (Polyoxyethylene Glycol-Polyoxypropylene)-Toluene Diisocyanate (POEG-POP)-TDI Polymer

Although chain scission of POPG-TDI at 200°C. has been shown to take place predominately at the urethane bonds by a random mechanism it is not expected that all the urethane bonds will break at the same rate. The 2- or 4-isocyanate groups form bonds with primary or secondary hydroxyls of different stability and these four possible urethane types will degrade at different rates. Furthermore, weak links other than urethanes can be postulated, for example, peroxides in the polyether, or dimerized isocyanates. In an attempt to determine whether the initial rate of bond scission would be decreased by a larger concentration of primary hydroxyl groups in the starting polyoxyalkylene glycol, a block (polyoxyethylene glycol-polyoxypropylene)-toluene diisocyanate (POEG-POP)TDI polymer was prepared for degradation. The POPG was reacted with sodium and then treated with ethylene oxide until 3.76 moles of epoxide per equivalent of hydroxyl was reacted. After thorough washing and drying the POEG-POP was reacted with TDI. A similar polyurethane was prepared from unmodified POPG and both samples were degraded at 200°C. under helium. The degradation was followed by withdrawing samples for intrinsic viscosity $[\eta]$ and infrared measurements. Although the infrared studies indicated decreasing urethane hydrogen and increasing hydroxyl at large extents of degradation, because of band overlap and sample and cell variability, quantitative results were not obtained. From $[\eta]$ the weight-average molecular weight \bar{M}_w was estimated.

It has been shown that the ratio of the weight-average molecular weight \bar{M}_w to number-average molecular weight \bar{M}_n for most probable distributions is given by:

$$\bar{M}_w/\bar{M}_n = 2/(1 + M_u/\bar{M}_w)$$

or

$$\bar{M}_n = (\bar{M}_w + M_u)/2$$

Therefore, \bar{M}_n was calculated from \bar{M}_w and an assumed value of the unit molecular weight, $M_u = 1100$, the average spacing of urethane links. This value of M_u was also used to calculate the number-average degree of

polymerization, \bar{X}_n . In addition, the average number of cuts per molecule S and the fraction of urethane links broken α were calculated from

$$S = \bar{X}_{n(0)} / X_{n(t)} - 1$$

and

$$\alpha = S / (\bar{X}_{n(0)} - 1)$$

in which $X_{n(0)}$ and $X_{n(t)}$ are the number-average degrees of polymerization at time zero and time t , respectively. For a system undergoing strictly random degradation, the integrated rate equation is

$$-\log \frac{\bar{X}_{n(t)} - 1}{\bar{X}_{n(0)}} = -\log \frac{\bar{X}_{n(0)} - 1}{\bar{X}_{n(0)}} + kt$$

For such a process a plot of $-\log [(\bar{X}_{n(t)} - 1) / \bar{X}_{n(t)}]$ versus time t , should give a straight line with a slope k and an intercept of $-\log[(\bar{X}_{n(0)} - 1) / X_{n(0)}]$.⁷

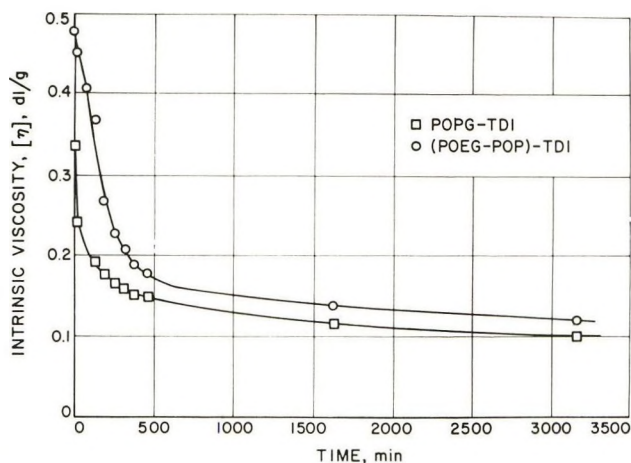


Fig. 5. Decrease of intrinsic viscosity on thermal degradation of POPG-TDI and block (POEG-POP)-TDI polymers at 200°C. under helium.

The results for POPG-TDI and the (POEG-POP)-TDI polymers are given in Table VI and Figure 5 and the $-\log (X_{n(t)} - 1) / X_{n(t)}$ versus t plot in Figure 6. It is apparent from the decrease in $[\eta]$, S , and α that the initial rate of degradation is much less for the block polymer. Figure 6 shows that neither polymer exhibits strictly random degradation since the available cleavable bonds undergo scission at different decreasing rates as degradation proceeds. Extrapolation of the first straight line portion of the curve for POPG-TDI to zero time gives a molecular weight of $\sim 10,000$, which represents the spacing of the very weak links. Since a similar extrapolation for (POEG-POP)-TDI gives the initial molecular weight, such weak links do not appear to be present in this polymer. The results

TABLE VI
 Thermal Degradation of POPC-TDI and a Block (POEG-POP)-TDI Polymer at 200°C. Under Helium

Polymer	Time, min.	Intrinsic viscosity, $[\eta]$, dl./g. ^a	Weight-average molecular weight, $\bar{M}_w \times 10^{-3}$	Number-average molecular weight, $\bar{M}_n \times 10^{-3}$	Number-average chain length, \bar{X}_n^d	$-\log \frac{\bar{X}_n - 1}{\bar{X}_n}$	No. of cuts, S^e	Extent of degradation, a^f
POPC-TDI	0	0.336	35.5	18.29	16.63	0.02664	0.0	0.0
	15	0.243	21.4	11.24	10.22	0.04455	0.6275	0.04015
	75	0.202	16.0	8.55	7.775	0.05973	1.140	0.07295
	135	0.195	15.0	8.055	7.322	0.06374	1.270	0.08125
	195	0.176	12.9	7.000	6.364	0.07417	1.613	0.1032
	255	0.166	11.7	6.400	5.816	0.08176	1.860	0.1190
	315	0.160	11.0	6.050	5.500	0.08725	2.025	0.1296
	375	0.153	10.4	5.750	5.227	0.09232	2.181	0.1395
	460	0.150	10.0	5.550	5.044	0.09583	2.207	0.1469
	1635	0.118	6.95	4.023	3.657	0.13847	3.548	0.2271
	3165	0.102	5.45	3.274	2.977	0.17751	4.585	0.2933
	0	0.478	62.0	31.55	28.69	0.01525	0.0	0.0
	(POEG-POP)-TDI	15	0.450	56.0	28.53	25.95	0.01705	0.1060
75		0.409	49.0	25.04	22.77	0.01932	0.2590	0.009360
135		0.371	41.8	21.45	19.50	0.02273	0.4710	0.01701
255		0.229	19.5	10.30	9.370	0.04905	2.062	0.07450
315		0.206	16.8	8.96	8.145	0.05090	2.522	0.09110
375		0.190	14.6	7.850	7.138	0.06550	3.020	0.1091
460		0.180	13.3	7.200	6.545	0.07186	3.383	0.1222
1635		0.138	8.8	4.950	4.500	0.10902	5.378	0.1943
3195		0.121	7.2	4.147	3.770	0.13401	6.610	0.2388

^a Determined in benzene solutions at 25°C. and calculated

from $\eta_{sp}/c = [\eta] + k'[\eta]^2$, for $k' = 0.39$.

^b From $[\eta] = 0.413 \times 10^{-4} M_w^{0.64}$, Ref. 4.

^c From $M_n = (\bar{M}_w + M_n)/2$, for $M_w = 1100$.

^d From $\bar{X}_n = \bar{M}_w/M_n$ for $M_w = 1100$.

^e From $S = \bar{X}_n(0)/\bar{X}_n(t) - 1$.

^f From $\alpha = S/(\bar{X}_n(0) - 1)$; α is the fraction of urethane bonds broken.

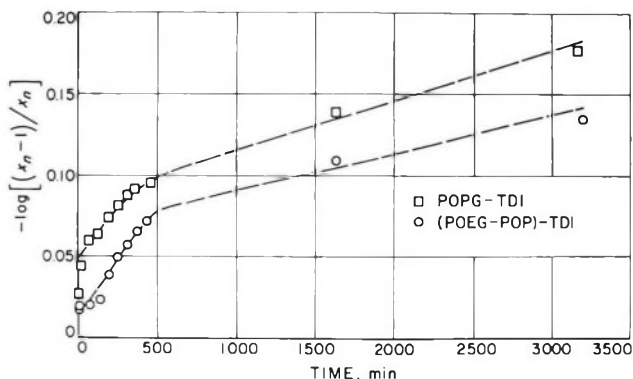


Fig. 6. Kinetic plot of thermal degradation of POPG-TDI and block (POEG-POP)-TDI polymers at 200°C. under helium.

indicate that the weak links involve terminal secondary hydroxyls on the POPG, presumably reacted with *o*-isocyanate groups.

However, it has been shown that commercially prepared POEG-POP containing 40% ethoxy units still retains over 50% secondary hydroxyl;⁸ therefore the POEG-POP prepared in this study probably does not contain 100% primary hydroxyl, although it may contain considerably more than the commercial polyether because of differences in the preparative method. Furthermore, since it has been established that POPG contains over 90% secondary hydroxyl,⁸ it is surprising that this work indicates a weak bond spacing as large as 10,000 in molecular weight. However, of all the possible bond forming reactions, the rate for formation of urethane from *o*-isocyanate and secondary hydroxyl is relatively small, since both reactant groups are sterically hindered. Therefore it may be that fewer urethane bonds of this type are present than would be predicted from a consideration of initial functional group concentrations and the assumption that negligible bond-forming side reactions occur. Also, the rate of degradation of the weak bonds may decrease as the reaction proceeds because of an increase in reaction order or inhibition by the products, giving an erroneous value of weak bond spacing with respect to structure. Therefore, although this study indicates that secondary hydroxyl groups are involved in the formation of weak bonds in POPG-TDI polymers, further work will be required to establish firmly their frequency and chemical structure.

F. Thermal Degradation of POPG and POPG-TDI at High Temperatures

To clarify the degradation mechanism of POPG and POPG-TDI polymers at higher temperatures (250–320°C.) volatilization rate measurements in a vacuum of 10 μ Hg have been carried out. Data for POPG are shown in Figure 7 at 275 and 305°C. Wall et al.⁹ have shown that a maximum in volatilization rate should occur at approximately 25% weight loss, followed at higher conversions by a steadily decreasing rate. Since the results in Figure 7 do not show this behavior, POPG apparently does not degrade

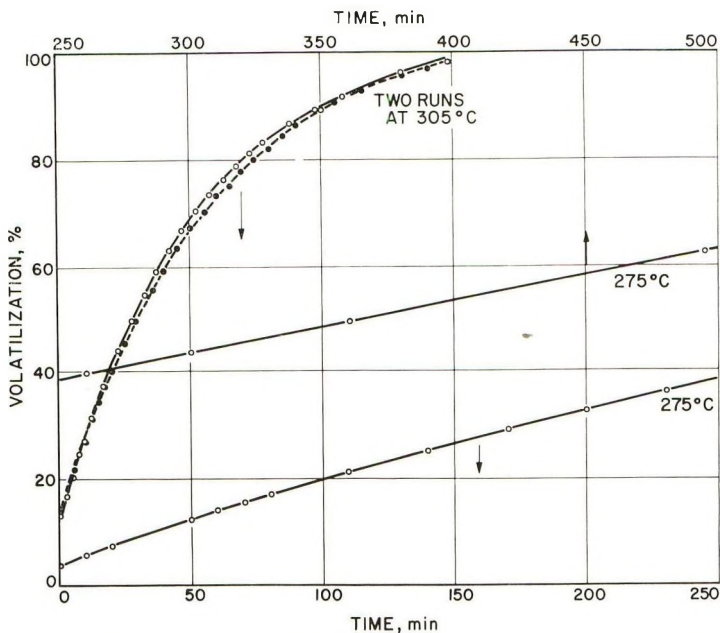


Fig. 7. Volatilization of POPG 2000 vs. time.

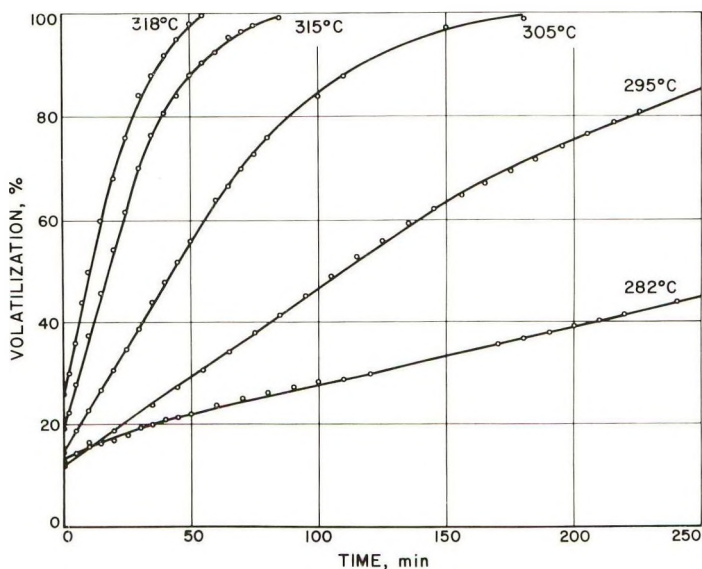


Fig. 8. Volatilization of POPG-TDI vs. time.

randomly. This is in agreement with results obtained previously for POPG of much higher initial molecular weight.¹⁰

In Figure 8 are shown a series of volatilization versus time curves for POPG-TDI polymer having an initial molecular weight M_w of 122,000.

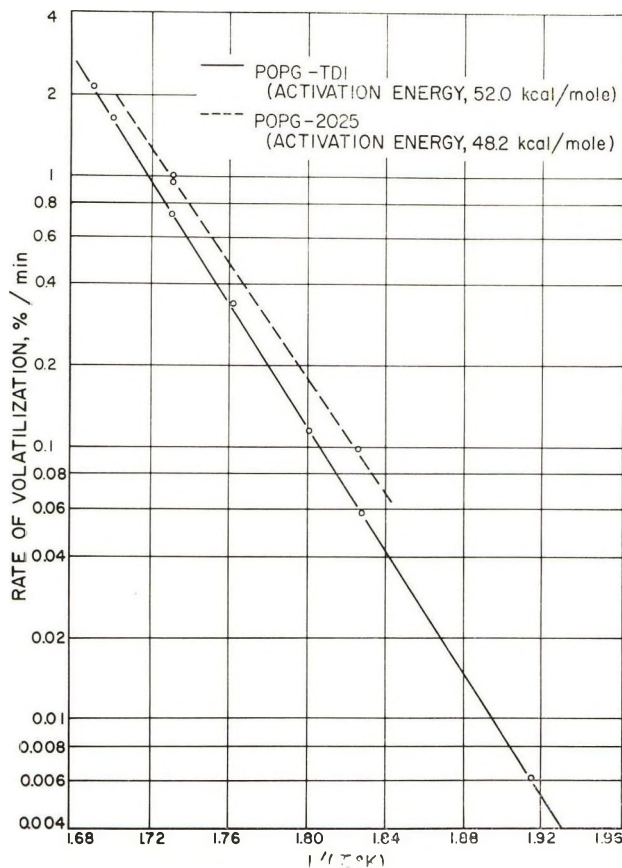


Fig. 9. Rates of volatilization of POPG-TDI polymer and POPG vs. $1/T$, $^{\circ}\text{K}^{-1}$.

The results, strikingly similar to those for POPG, show substantially zero-order dependence for conversions of 20–65% and indicate similar mechanisms of degradation for both polymers, although the rate is slightly less for POPG-TDI. Activation energy plots are given in Figure 9 for rates calculated from the nearly linear portions of the curves (20–65% conversion). The activation energies are the same within experimental error, 52.0 kcal./mole for POPG-TDI and 48.2 kcal./mol for POPG.

A plot of molecular weight of the residue expressed as per cent of initial molecular weight versus per cent volatilization for POPG-TDI is shown in Figure 10. The data points represent separate experiments at different temperatures as shown in the figure. These results are in agreement with the expected scission mechanism. Above 10% conversion, the constancy of the residue molecular weight (which was 2400, with one point at 3800) indicates zip depolymerization with a minimum zip length of about 2400. However, the approximate zero-order dependence of the rate curves of Figure 8 suggests a stepwise depolymerization, presumably occurring at a constant number of chain ends or initiating sites. Since the volatilization

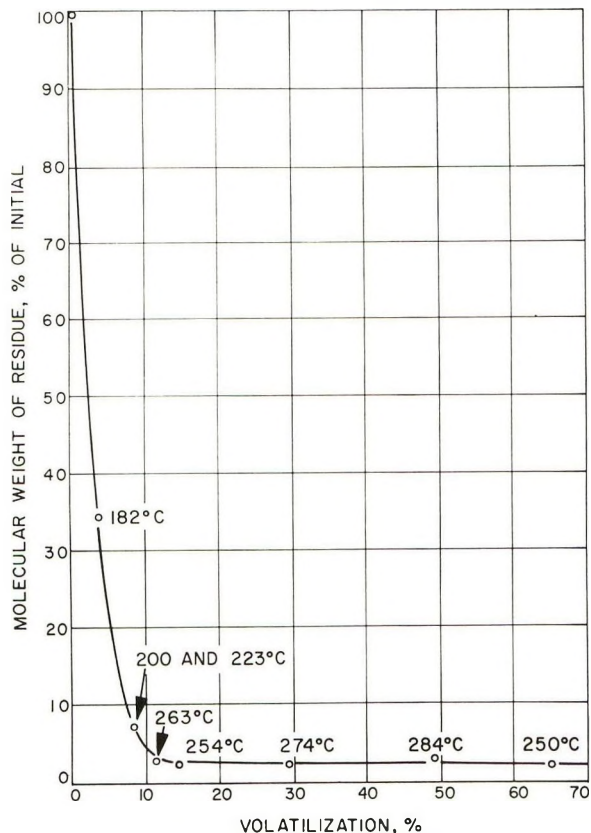


Fig. 10. Decrease in molecular weight vs. volatilization of POPG-TDI.

rates were slightly less for POPG-TDI than for POPG, fewer sites for initiation of depolymerization must be available in the former, suggesting the presence of inactivated chain ends or a slightly higher molecular weight. This work and the study of POPG of molecular weight 16,000 by Madorsky and Straus¹⁰ do not indicate a simple depolymerization of POPG to propylene oxide nor a high kinetic chain length. The wide range of molecular weights observed by Madorsky and Straus and the variety of volatile products observed (acetaldehyde, propene, acetone, and relatively small amount of propylene oxide) in both studies suggests that POPG degrades by a combination of intramolecular proton abstraction and free-radical unzipping reactions.

IV. CONCLUSIONS

For POPG-TDI polymer, the predominant mode of degradation at low conversion to volatiles is essentially random scission of the urethane linkages to regenerate hydroxyl and isocyanate. The evidence for this consists of the results from studies of the molecular weight distributions, intrinsic

viscosities, number-average molecular weights, and infrared spectra of thermally degraded polymer. At very high extents of degradation, the residual polymer has nearly the same infrared spectrum, number-average molecular weight, intrinsic viscosity and observed molecular weight distribution as POPG. Preliminary kinetic data suggests that the weak links in POPG-TDI polymer are spaced at intervals of $\sim 10,000$ in molecular weight and that they may be eliminated by pretreatment of the POPG with ethylene oxide to form a block copolyether which is used to prepare the polyurethane.

At temperatures above 250°C . and a greater conversion to volatile fragments ($>10\%$) the kinetics of degradation of POPG-TDI are similar to results for POPG and indicate scission of the polyether bonds by a combination of intramolecular proton abstraction and free radical unzipping reactions, in agreement with previous studies of POPG of much higher molecular weight.¹⁰

The authors wish to acknowledge the contributions of Professor R. Simha and Dr. R. F. Landel for many helpful discussions during the course of this work.

References

1. Rapp, N. S., and J. D. Ingham, *J. Polymer Sci.*, **A2**, 689 (1964).
2. Gordon, M., in *Thermal Degradation of Polymers*, Macmillan, New York, 1961, p. 163.
3. Flory, P. J., *Principles of Polymer Chemistry*, Cornell Univ. Press, Ithaca, N. Y., 1953, (a) p. 325; (b) pp. 337, 339; (c) p. 320.
4. Moacanin, J., *J. Appl. Polymer Sci.*, **1**, 272 (1959).
5. Flory, P. J., *J. Am. Chem. Soc.*, **62**, 1561 (1940).
6. Morris, R. J., Jr., and H. E. Persinger, *J. Polymer Sci.*, **A1**, 1041 (1963).
7. Grassie, N., *Chemistry of High Polymer Degradation Processes*, Butterworths, London, 1956, p. 126.
8. Hanna, J. G., and S. Siggia, *J. Polymer Sci.*, **56**, 297 (1962).
9. Wall, L. A., S. L. Madorsky, D. W. Brown, S. Straus, and R. Simha, *J. Am. Chem. Soc.*, **76**, 3430 (1954).
10. Madorsky, S. L., and S. Straus, *J. Polymer Sci.*, **36**, 183 (1959).

Résumé

On a poursuivi l'étude de la dégradation thermique du polymère POPG-TDI. On a montré qu'à une température de $\sim 200^{\circ}\text{C}$, le processus de dégradation prédominant comporte une scission de la liaison uréthane en donnant des quantités considérables d'isocyanate et d'hydroxyle. Les données cinétiques suggèrent que les liaisons les plus faibles du polymère POPG-TDI se trouvent à des intervalles de $\sim 10,000$ en poids moléculaire et qu'elles peuvent être éliminées par un traitement préalable du POPG par l'oxyde d'éthylène qui forme un copolyéther à blocs, qui est utilisé dans la préparation du polyuréthane. À des températures supérieures à 250°C et à des degrés de conversion supérieures aux fragments volatils ($>10\%$), ces cinétiques de dégradation du POPG-TDI sont semblables aux résultats obtenus pour le POPG et indiquent une scission des liaisons polyéthers par une combinaison de l'arrachement intramoléculaire d'un proton et des réactions de dépolymérisation par radicaux libres, en accord avec les études antérieures sur le POPG de poids moléculaire plus élevé.

Zusammenfassung

Weitere Untersuchungen des thermischen Abbaus des POPG-TDI-Polymeren wurden durchgeführt. Es zeigte sich, dass bei Temperaturen von $\sim 200^{\circ}\text{C}$ der vorherrschende Abbaumechanismus mit statistischer Spaltung der Urethanbindung unter Bildung grösserer Mengen an Isocyanat und Hydroxyl vor sich geht. Kinetische Daten legen nahe, dass die schwächsten Bindungen im POPG-TDI-Polymeren in Molekulargewichtsintervallen von ~ 10.000 angeordnet sind und dass sie durch Vorbehandlung des POPG mit Äthylenoxyd unter Bildung eines Blockcopolyäthers, der zur Darstellung des Polyurethans verwendet wird, eliminiert werden. Bei Temperaturen oberhalb 250°C und einer grösseren Umwandlung in flüchtige Bruchstücke ($>10\%$) ist die Abbaukinetik von POPG-TDI der von POPG ähnlich und weist auf eine Spaltung der Polyätherbindungen durch eine Kombination von intramolekularem Protonenentzug und radikalischer Zippreaktion in Übereinstimmung mit früheren Untersuchungen an POPG mit viel höherem Molekulargewicht hin.

Received October 29, 1963

Revised March 9, 1964

Diffusion of Oxygen in Gamma-Irradiated Polyethylene

R. C. GIBERSON, *Hanford Laboratories General Electric Company, Richland, Washington*

Synopsis

Theories of gas flow in polymers developed by Michaels and co-workers have been used to calculate the diffusion coefficient for oxygen in γ -irradiated polyethylene. The value obtained is in good agreement with that obtained from an independent method. The possible effect of dose rate on Michaels' theories is presented.

INTRODUCTION

Michaels and co-workers¹⁻³ have presented rather complete theories to account for the sorption and flow behavior of various gases in polyethylene. They have recently⁴ extended these studies to gas transmission in irradiated polyethylene.

The purpose of this paper is to present a correlation between Michaels' work and that reported by Giberson.⁵ An extension of the theories presented to account for the observed dose rate effect on the reaction of oxygen with irradiated polyethylene is presented.

DISCUSSION

Theory of Michaels

If Fick's law of diffusion applies, as has been found in the case of gas-polymer systems,⁶ and if in addition Henry's law is applicable, then the relationship between the permeability constant \bar{P} , diffusion constant D , and solubility constant k , is:

$$\bar{P} = Dk \tag{1}$$

Michaels and Parker¹ and later Michaels and Bixler^{2,3} have shown that D and k in eq. (1) can be written:†

$$k = \alpha k^* \tag{2}$$

$$D = D^*/\tau\beta \tag{3}$$

$$\bar{P} = \alpha k^* D^*/\tau\beta \tag{4}$$

† The nomenclature used by Michaels, et al.¹⁻³ will be adopted here, which will necessitate some changes in nomenclature from the author's previous work.⁵

where α is the volume fraction of amorphous polymer, and k^* and D^* are the solubility and diffusion constants respectively, in a completely amorphous polyethylene. τ is a geometric impedance factor that is effective in reducing the diffusion coefficient because of the necessity of molecules to by-pass crystallites and move through amorphous regions of nonuniform cross-sectional area. β is the chain immobilization factor accounting for the reduction in amorphous chain segment mobility due to the proximity of crystallites.

Before considering what effect irradiation of the polymer should have on the parameters of eq. (4), a brief summary of the previous work⁵ on diffusion in irradiated polyethylene is in order.

Oxygen Diffusion in Irradiated Polyethylene

The final equation derived by Giberson⁵ relating carbonyl formation to sample thickness and total dose was:

$$A = k' (1 - e^{-\eta L}) \quad (5)$$

where A is the optical density of the carbonyl absorption (measured in the infrared at $\sim 1720 \text{ cm}^{-1}$), L is the sample thickness in centimeters k' includes the parameters of η as well as a factor for the total radiation exposure and other physical constants. η is given by:

$$\eta = (\epsilon/D)^{1/2} \quad (6)$$

where ϵ is the reaction probability factor and D is the diffusion coefficient. The assumptions made in arriving at eq. (5) were that: (1) active sites in the polymer were created by the ionizing radiation; (2) the sites are homogeneously distributed and the number available at any given time during the irradiation was constant; (3) the formation of carbonyl depends on the diffusion-limited reaction of oxygen with an active site in the polymer. Furthermore, it was observed that throughout the range of exposures, dose rates and sample thicknesses used in the work, the total carbonyl formation, at a given thickness and dose rate, increased linearly with exposure.

It was further shown that:

$$\epsilon = \rho\delta \quad (7)$$

where δ is the dose rate and ρ is a constant. The constant η was found to increase in a predictable way with dose rate. It was not possible, however, to determine unambiguously the effect of dose rate on the diffusivity. Estimates of that effect are presented in this paper.

Effect of Irradiation on Solubility

X-ray data indicated that α was not significantly changed by irradiation,⁴ and therefore any change in k must be related to a change in k^* . It was observed that k was larger in the irradiated material. Crosslinking caused by irradiation may not affect the solubility appreciably. Indeed,

Sobolev et al.⁷ attributed a decrease in permeability of gases in irradiated polymers solely to a decrease of the diffusion coefficient [see eq. (1)]. Their films were irradiated either in vacuum or under an inert atmosphere, and consequently, no oxidation would occur. In view of these results, it can be assumed that the increase in k^* for the irradiated films is caused by the polyethylene oxide which has been formed. It is interesting that this increase of about 40% is the same for all gases studied by Bixler.⁴ The gases used were He, N₂, CH₄, and C₃H₈. If crosslinking of the polymer were affecting k^* , it would probably have a greater influence on the larger gas molecules. This same conclusion was reached by Bixler et al.,⁴ who attributed increases in k^* to increases in the cohesive energy of the polymer due to the presence of carbonyl and other chemical changes.

Effect of Irradiation on Diffusivity

To determine the effect of irradiation on the diffusivity, the separate and/or combined effects on D^* , τ , and β must be determined.

Bixler et al.⁴ chose not to make any correction for D^* in the irradiated films because the analogy of using natural rubber values for completely amorphous polyethylene is not sufficiently exact. However, it appears that the irradiated D^* would be less than the unirradiated D^* . This conclusion results from the fact that the density of the amorphous phase is greater after irradiation,⁴ and thus the completely amorphous analog of irradiated oxidized polyethylene should resist diffusion more than amorphous polyethylene.

The geometric impedance factor, τ , has been correlated³ with α :

$$\tau = \alpha^{-n} \quad (8)$$

Since α has been shown to not change under irradiation it is tempting as Bixler⁴ has stated to say that τ did not change. However, it was recognized that this is not the case. Crosslinking is very likely to have influenced the ability of even the small helium molecule to diffuse through polyethylene; thus τ could increase on irradiation. Bixler⁴ has chosen only to calculate the product $\tau \beta$ in his work and has successfully demonstrated that τ may be independent of the size of the gas molecule even in the irradiated films.

A second approach is to assume that eq. (8) is still valid in the irradiated films; then irradiation must affect n . Michaels and Bixler³ have shown that n varies with the type of polyethylene. It therefore appears reasonable to assume that n for irradiated, oxidized polyethylene would be different than for normal branched polyethylenes. In the present work a separate value of τ and β for the irradiated material has been calculated, which yields $n = 1.98$ if eq. (8) is valid. This increase of approximately 10% in the irradiated samples is interesting in view of the change in the density of the amorphous phase.

Bixler et al.⁴ have found that β depends more strongly on the size of the gas molecule in the irradiated material. This can reasonably be

attributed to the crosslinking caused by irradiation. β has been correlated with molecular size³

$$\ln \beta = \gamma [d - (\phi^{1/2}/2)]^2 \quad (9)$$

where γ is a constant depending on the material, d is the diameter of the gas molecule, and ϕ is the free volume per unit length of a $-\text{CH}_2-$ group measured along the chain axis. $\phi^{1/2}/2$ is approximately equal to the mean unoccupied distance between two chain segments. Due to the amorphous-phase densification mentioned earlier, this latter quantity changes from 0.9 Å. in unirradiated polymer to 0.8 Å. in the irradiated material. γ is thought to be unfluenced by both α and the size and shape of the crystallites.³ The increase in γ caused by irradiation must evidently be related to other than a change in α , since α was found not to change. A highly crystalline linear polyethylene was found³ to have the highest γ . It may be concluded that the tightening of the polymer structure by crosslinking under irradiation gives a similar increase in γ to that found for increasing crystallinity.

Calculation of k and D for Oxygen in Alathon 3, NC-10

Oxygen was not used in the flow studies of Bixler, et al.;⁴ however, from the previous theories¹⁻³ and results of irradiation on flow parameters of other gases, it is possible to calculate k and D for oxygen in Alathon 3.

The solubility is given by eq. (2)

$$k = \alpha k^* \quad (2)$$

α was determined to be 0.55 in Alathon 3.⁴ k^* can be taken from Michaels and Bixler² as 0.077 cc. (STP)/cc. atm. at 25°C. Hence $k = 0.042$ cc. (STP)/cc. atm. at 25°C. In the irradiated polymer if we assume the same 40% increase found for the other gases, k (irradiated) = 0.059 cc. (STP)/cc. atm. at 25°C.

The diffusion coefficient in the unirradiated material is given by

$$D = D^*/\tau\beta \quad (3)$$

D^* for O_2 from Michaels and Bixler² is 17.3×10^{-7} cm.²/sec. By defining a value of $\beta = 1.00$ for helium in the unirradiated samples,³ τ can be calculated from the helium data:⁴

$$\tau = D^*/1.0D = 2.80$$

This agrees fairly well with a calculation based on eq. (8).³

$$\tau = 0.55^{-1.88} = 3.08 \quad (10)$$

The value $n = 1.88$ for the unirradiated material is used. β for oxygen is given by eq. (9):

$$\ln \beta = 0.045 (2.6)^2 \quad (11)$$

$$\beta = 1.36 \quad (12)$$

γ was found to be 0.045 by Bixler⁴ for Alathon 3, NC-10. Therefore at 25°C. for O₂:

$$D = 17.3/[(2.8)(1.36)] = 4.54 \times 10^{-7} \text{ cm.}^2/\text{sec.} \quad (13)$$

In the irradiated material, if it is assumed that $\beta = 1.10$ for helium[†] and furthermore that D^* changes by 10%, it is again possible to calculate τ from the helium data and β from eq. (9)[‡], viz.:

$$\tau_i = \frac{D_i^*}{1.1 D_i} = 3.27 \quad (14)$$

$$\beta_1 = 1.67 \text{ (for O}_2\text{)} \quad (15)$$

therefore for O₂:

$$D_i = \frac{D_i^*}{\tau_i \beta_i} = 2.87 \times 10^{-7} \text{ cm.}^2/\text{sec.} \quad (16)$$

This result may be compared with the value of 1.75×10^{-7} cm.²/sec. calculated by Giberson⁵ for O₂ diffusion in samples irradiated at the same dose rate. Considering the assumptions involved in both methods, the agreement is good.

Effect of Dose Rate on Reaction

Bixler et al.⁴ have discussed the possible effect on the flow parameters of a nonuniform gradient of chemical composition in the material. It is not necessary to repeat their discussion here other than to point out that as the dose rate increases the gradient for oxidation becomes steeper. *trans*-Vinylene formation is apparently homogeneously distributed in the samples and only slightly affected by oxidation for γ -irradiations at room temperature.⁸

From eqs. (6) and (7)

$$\eta = (\rho \delta / D)^{1/2} \quad (17)$$

Giberson⁵ has shown that the constant η must increase with an increase in dose rate (over the dose rate studied, $1-5 \times 10^6$ r/hr.). As stated previously, it was not possible to predict the effect of dose rate on D . Empirically it was found that D increased with dose rate.

The work of Bixler et al.⁴ was done on polyethylene irradiated at only one dose rate. However, from their theories and Giberson's⁵ results, the following assumptions may be made on the effect of dose rate on the factors of eq. (4).

† It was found by Michaels and Bixler² that it was advantageous to have β increase slightly as α decreased. A similar assumption for the crosslinked polymer seems entirely reasonable.

‡ The subscript i refers to the irradiated value. The value of $\tau_i \beta_i = 5.46$ is lower than that given by Bixler et al.,⁴ as they chose not to apply a correction to D_i^* .

Solubility Constant. As stated earlier k^* is assumed by Bixler⁴ to be a function of the cohesive energy of the polymer, thereby being influenced by both carbonyl and transvinylene. In view of Sobolev's⁷ work it would appear that the carbonyl would be the principal contributor to the increased solubility. A 40% increase in k was observed⁴ for the dose rate of 1.34×10^6 r/hr. Assuming a linear dependence of k^* on carbonyl contact we can determine the solubility trend with dose rates.

Diffusion Coefficient. The effect of dose rate on D must be separated into the effects on D^* , τ , and β [eq. (3)].

The amorphous-phase density which is related to the crosslinking that occurs influences the value of D^* . Since the change (if any) of D^* at the one irradiation dose was small, any additional effect from the different dose rates is likely to be even smaller.

Since τ and β are increased by irradiation as a consequence of the crosslinking of the material (τ still being insensitive to gas-molecule size) any effect of dose rate on these parameters must be explained by the effect of dose rate on crosslinking.

Crosslinking mechanisms have been presented by Pearson,⁹ who showed that *trans*-vinylene decays by crosslinking. Dole et al.¹⁰ have criticized Pearson's mechanism mainly as pertaining to the method of production of the *trans*-vinylene. Dole does, however, conclude that part of the crosslinking which occurs comes by way of *trans*-vinylene decay. In fact 60% of crosslinks formed in one sample of low density polyethylene came about in this manner.¹¹ Vinylidene decay also contributes to crosslinking and possibly endlinking.¹¹ Giberson⁸ has shown that the amount of *trans*-vinylene in the samples after irradiation is a function of dose rate, there being more *trans*-vinylene at higher dose rates. Postulated crosslinking mechanisms involving the *trans*-vinylene structure are time-dependent. For example, Pearson's mechanism involves the reaction of the *trans*-vinylene group with a free radical which must have migrated to an appropriate spot for reaction. This migration of free radicals is well established. Since the total number of radiation induced events is constant at a given total dose for any dose rate, it follows that less of the *trans*-vinylene has an opportunity to decay by crosslink formation at the higher dose rates.

As pointed out above, *trans*-vinylene decay is only one of the ways that

TABLE I
Predicted Effects Due to Increased Dose Rate on Eq. (4)

Parameter	Effect ^a
α	No change
k	Decreases
D^*	Small increase _w
τ	Decreases
β	Decreases

^a Relative to the 1.34×10^6 r/hr base.

crosslinking arises. (The arguments for *trans*-vinylene would appear appropriate for the mechanisms proposed for vinylidene decay.)¹¹ However, the observations are at least consistent with the higher value of D found for the higher dose rates,⁵ since D is influenced most by the crosslinking of the polymer.

A summary of the postulated effect of dose rate on the parameters of eq. (4) is given in Table I. It would be interesting to test these proposals experimentally for they would predict that as the dose rate increases the value of D_i approaches the unirradiated value for irradiation to 1×10^8 r.

References

1. Michaels, A. S., and R. B. Parker, Jr., *J. Polymer Sci.*, **41**, 53 (1959).
2. Michaels, A. S., and H. J. Bixler, *J. Polymer Sci.*, **50**, 393 (1961).
3. Michaels, A. S., and H. J. Bixler, *J. Polymer Sci.*, **50**, 413 (1961).
4. Bixler, H. J., A. S. Michaels, and M. Salame, *J. Polymer Sci.*, **A1**, 895 (1963).
5. Giberson, R. C., *J. Phys. Chem.*, **66**, 463 (1962).
6. Barrer, R. M., *Diffusion in and through Solids*, University Press, Cambridge, England, 1951.
7. Sobolev, I., J. A. Meyer, V. Stannett, and M. Szwarc, *J. Polymer Sci.*, **17**, 417 (1955).
8. Giberson, R. C., *J. Polymer Sci.*, **B2**, 951 (1964).
9. Pearson, R. W., *J. Polymer Sci.*, **25**, 189 (1957).
10. Dole, M., D. C. Milner, and T. F. Williams, *J. Am. Chem. Soc.*, **80**, 1580 (1959).
11. Williams, T. F. and M. Dole, *J. Am. Chem. Soc.*, **81**, 2919 (1959).

Résumé

Les théories des courants gazeux dans les polymères développées par Michael et ses collaborateurs ont été employées pour calculer le coefficient de diffusion de l'oxygène dans le polyéthylène irradié par des rayons-gamma. La valeur obtenue est en bon accord avec celle obtenue par une méthode indépendante. On présente l'effet possible de la vitesse de la dose sur les théories de Michael.

Zusammenfassung

Die von Michaels und Mitarbeitern entwickelten Theorien über die Bewegung von Gasen in Polymeren wurde zur Berechnung des Diffusionskoeffizienten von Sauerstoff in gammabestrahltm Polyäthylm herangezogen. Der erhaltene Wert stimmt mit dem aus einer unabhängigen Methode erhaltenen gut überein. Der mögliche Einfluss der Dosisleistung auf die Theorien von Michaels wird untersucht.

Received November 8, 1963

Revised March 9, 1964

1,5-Hexadiene Polymers. II. Copolymers of Ethylene and 1,5-Hexadiene*

HENRY S. MAKOWSKI, BENJAMIN K. C. SHIM,† and ZIGMOND W. WILCHINSKY, *Chemicals Research Division, Esso Research and Engineering Company, Linden, New Jersey*

Synopsis

A series of crystalline ethylene-1,5-hexadiene copolymers containing 15-93 mole-% ethylene were prepared with an $\text{AlR}_3/\text{TiCl}_3\text{-AlCl}_3$ catalyst system. X-ray diffraction analyses showed two distinct crystalline phases in the copolymers; one phase had the polyethylene structure whereas the other had the poly-1,5-hexadiene structure. However, the unit cell sizes of these two phases were significantly different from those of the respective homopolymers, indicating that both types of monomeric units are present in each of the copolymer phases. Physical property measurements on the copolymers support these conclusions.

INTRODUCTION

In a previous paper¹ the cyclopolymerization of 1,5-hexadiene with aluminum alkyl-titanium halide catalysts to crystalline polymers was described. The major repeating unit in these crystalline polymers was concluded to be the *cis*-1-methylene-3-cyclopentyl group wherein the cyclopentane ring is in an envelope form. The extended polymer chain is very analogous to the simple extended carbon-carbon chain of polyethylene. The similarity of chain conformations suggested that 1,5-hexadiene and ethylene could be copolymerized to crystalline copolymers.

Valvassori et al.² have described the preparation of poly-1,5-hexadiene and copolymers of 1,5-hexadiene and ethylene with combinations of $\text{Al}(\text{C}_2\text{H}_5)_2\text{Cl}$ and vanadium compounds. However, with these catalyst systems approximately 75-80% of the 1,5-hexadiene polymerizes through one double bond only, resulting in polymers which are essentially amorphous in nature.

Although crystalline copolymers have been more common to the polyamide systems,³⁻⁷ more recently crystalline copolymers of α -olefins have been prepared.⁸⁻¹¹ In general, however, the copolymerization of two olefins which produce crystalline homopolymers results in a breakdown of the crystal system at some critical composition. Structural incompati-

* Presented before the Division of Polymer Chemistry, 144th Meeting, American Chemical Society, Los Angeles, California, April 1963.

† Present address: Central Research, Lord Manufacturing Company, Erie, Pennsylvania.

bility of the comonomers in the crystal lattice is the general cause for the crystalline breakdown.^{8,12}

In this paper the preparation and properties of crystalline copolymers of ethylene and 1,5-hexadiene of wide compositional ranges are described.

EXPERIMENTAL

Starting Materials

Ethylene (Matheson C.P.) was purified by passage successively through barium oxide, Drierite, Ascarite, two triethylaluminum in Bayol D scrubbing solutions (25%), and a cotton demisting tower.

The purification of 1,5-hexadiene and *n*-heptane diluent and the preparation of the catalyst have been described in a previous paper.¹

Polymerizations

All fourteen polymerizations effected with the "preformed" $\text{AlEt}_3/\text{TiCl}_3-0.22 \text{ AlCl}_3$ catalyst system were performed under identical conditions. Polymerizations were conducted in glass resin reaction flasks which were thoroughly dried and swept with scrubbed, dry nitrogen. One liter of dry *n*-heptane and 0.90 g. of $\text{TiCl}_3-0.22 \text{ AlCl}_3$ and 0.78 g. of triethyl aluminum were charged to the resin flask. The temperature of the catalyst slurry was raised to 60°C., and the predetermined amount of 1,5-hexadiene was added while immediately introducing the gaseous ethylene feed. Polymerization was allowed to proceed for 40 min. during which time the constant ethylene feed was totally absorbed and the temperature was maintained at around 60°C. The polymerization was then immediately quenched with 100 ml. of isopropanol. The reaction mixture was mixed with a solution of 750 ml. isopropanol and 750 ml. acetone, and the solid, white polymer was suction-filtered, washed twice with acetone, and then vacuum oven-dried at 80°C. for two days.

Ethylene was metered into the polymerization vessel with accurately calibrated rotameters. The volume of ethylene absorbed and the weight of copolymer produced were used to calculate the copolymer macro composition.

Full details of polymerization conditions and polymer yields are given in Table I.

Solvent Extraction of Polymers

n-Heptane-soluble fractions were obtained on all polymers prepared with the "preformed" catalyst system by Soxhlet extraction for 48 hr.

Physical Properties

Softening and melting points were obtained with a Nagel melting point apparatus.

Inherent viscosities were determined from kinematic viscosities in tetralin solution at 125°C.

Densities, tensile properties, and apparent moduli of elasticity were obtained from 20 mil thick 1 in. \times 2 in. micropads which were produced by heating the polymer between sheets of aluminum foil or Mylar film in an aluminum mold at 350–450°C. under pressure. Tensile strengths and elongations were obtained on microdumbbells on a Scott microtester at a jaw speed of 10 in./min. Apparent moduli of elasticity were determined according to ASTM D-1043. Densities were determined by titration of portions of the molded polymer with aqueous calcium nitrate solutions.

The physical properties of the polymers obtained are listed in detail in Table I.

X-Ray Diffraction

Diffraction traces were used for crystal phase identification and precise measurement of interplanar spacings. The latter were carried out with an internal standard of KBrO_3 the (101) line, $d = 4.39 \text{ \AA}$,¹³ being used. A scanning rate of $1/8^\circ$ in 2θ per minute was used with a time constant of 16 sec.; the chart presentation was 4 in. per degree. In addition, diffraction photographs were obtained of stretched fibers with a flat plate camera.

RESULTS AND DISCUSSION

Copolymerization Effects on Monomer Conversion

All copolymerizations were carried out by first adding all the 1,5-hexadiene to the catalyst slurry and then introducing gaseous ethylene at a constant rate over a period of 40 min. The copolymerizations were effected in this manner because of the expected wide differences between the reactivity ratios of ethylene and 1,5-hexadiene. In work reported by Natta et al. on the isomorphism of monomeric units,⁹ monomers were used whose $r_1 r_2$ product of reactivity ratios was practically unity so that the copolymers were essentially randomly distributed in monomers. Unfortunately, this is not the case in ethylene-1,5-hexadiene copolymers. Even though copolymerization conditions were favorable for more random copolymerization, the polymerization rate of ethylene still exerted a powerful effect on copolymer composition.

The copolymerization of ethylene and 1,5-hexadiene with a "preformed" catalyst results in an unusual mutual synergistic effect on polymerization rate. The effect of ethylene on 1,5-hexadiene conversion in this catalyst system is illustrated in Figure 1. In the absence of ethylene the conversion of 1,5-hexadiene is about 40%. The addition of ethylene to the monomer feed results in an increase of 1,5-hexadiene conversion up to about 10 wt.-% ethylene in the feed. Thereafter, the conversion of 1,5-hexadiene remains relatively constant at about 70% with further increases in ethylene concentration.

The inverse effect, i.e., the increased rate of ethylene polymerization by 1,5-hexadiene addition, is shown in Table I. Under the given conditions when ethylene was homopolymerized only 66 liters of the 80-liter feed were

Total polymer properties	1.22	1.13	0.99	1.37	1.48	1.67	1.81	2.28	2.76	3.72	3.76	4.27	4.52	9.16
Inherent viscosity, dl./g.	1580	1930	2990	1880	1220	910	1350	940	1045	1650	1340	2270	2890	6145
Tensile strength, psi	365	290	270	340	360	300	370	260	300	490	300	530	540	420
Elongation, %	114/128	119/130	124/140	100/120	108/122	102/117	108/120	106/120	118/131	112/123	113/124	122/131	124/133	134/146
S.P./M.P., °C.														
% <i>n</i> -Heptane-soluble, %	11.7	10.2	8.6	11.2	15.7	20.3	21.5	24.2	24.8	21.1	23.0	11.8	15.2	0.5
Density, g./cc.	1.0080	1.0063	0.9907	0.9904	0.9848	0.9786	0.9622	0.9604	0.9538	0.9494	0.9455	0.9439	0.9403	0.9314
Apparent modulus of elasticity, psi. $\times 10^{-5}$														
At 25°C.	0.72	0.72	0.46	0.36	0.26	0.32	0.34	0.39	0.46	0.56	0.65	0.62	0.58	1.07
At 0°C.	1.07	1.10	0.99	0.80	0.70	0.78	0.89	1.03	1.03	1.10	1.24	1.17	1.17	1.73
At -25°C.	1.86	1.70	1.61	1.32	1.32	1.22	1.34	1.39	1.62	1.75	1.86	1.93	1.79	2.95

^a Reaction conditions: AlEt₃/TiCl₃-0.22 AlCl₃ catalyst, AlEt₃/Ti ratio 1.26, catalyst concentration 1.68 g./l.; solvent *n*-heptane, total volume 1,000 ml.; length of run 40 min.; temperature 53-64°C.

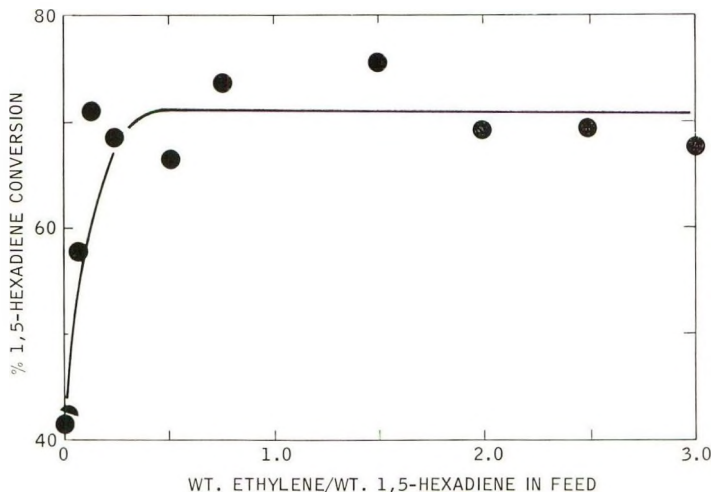


Fig. 1. Effect of ethylene on 1,5-hexadiene conversion.

absorbed and polymerized. On the other hand, in the presence of 1,5-hexadiene as much as 120 liters of ethylene were totally absorbed and polymerized, and, apparently, this was not the upper limit of ethylene absorption.

It would appear from these observations that a chain end 1,5-hexadiene unit prefers to react with ethylene monomer while a chain end ethylene unit prefers to react with 1,5-hexadiene monomer. If this is indeed true, the reasons for these phenomena are not entirely clear. In addition, x-ray analyses of the copolymers show them to consist of two crystalline phases having essentially polyethylene and poly-1,5-hexadiene structures; however, each phase contains some of the other monomer. If the above simple explanation for polymerization rate synergism were true, it might be expected that the copolymers would be quite random in nature. The contrary evidence indicates that the rate controlling mechanism is much more complex.

X-Ray Diffraction Results

From fiber diffraction photographs of poly-1,5-hexadiene, the unit cell was tentatively determined as orthorhombic with constants $a = 13.30 \pm 0.05$ A., $b = 15.52 \pm 0.06$ A., and $c = 4.80 \pm 0.05$ A. In Table II the equatorial spots are indexed, and the observed interplanar spacings are compared with calculated values. On the assumption of eight monomeric units per unit cell, the crystal density is 1.10 g./cm.³; the experimental value obtained on compression-molded pads was 1.01 g./cm.³.

Diffraction traces of the copolymers showed, in general, modified patterns of both polyethylene and poly-1,5-hexadiene; below about 15 wt.-% ethylene only the poly-1,5-hexadiene pattern was detected and above 90% ethylene only the polyethylene pattern was detected. In the

TABLE II
 Comparison of Observed with Calculated Interplanar Spacings
 (Unit Cell Assignment: Orthorhombic, $a = 13.30$ A., $b = 15.52$ A., $c = 4.80$ A.)

Miller Indices	d , A.	
	Obs.	Calc.
030	5.18	5.18
130	4.84	4.82
310	4.26	4.28
040	3.85	3.88
410	3.26	3.26
430	2.79	2.80

intermediate region the positions of the two patterns are shifted from those of the pure homopolymers. This is illustrated in Figure 2. In the co-

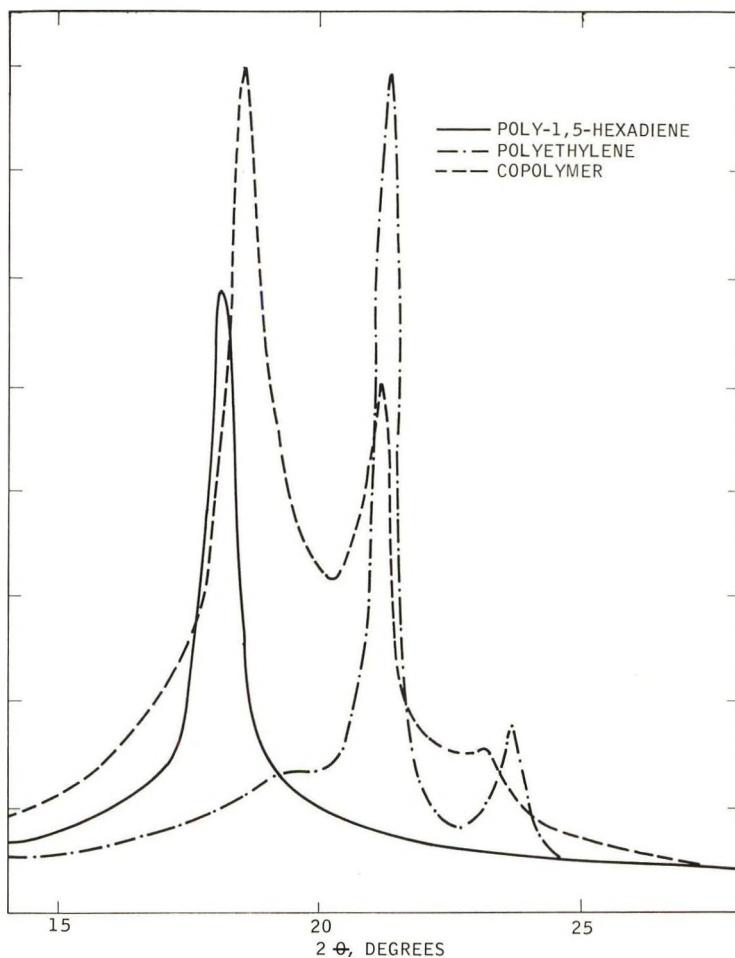


Fig. 2. X-ray diffraction patterns of polyethylene, poly-1,5-hexadiene and ethylene-1,5-hexadiene copolymer.

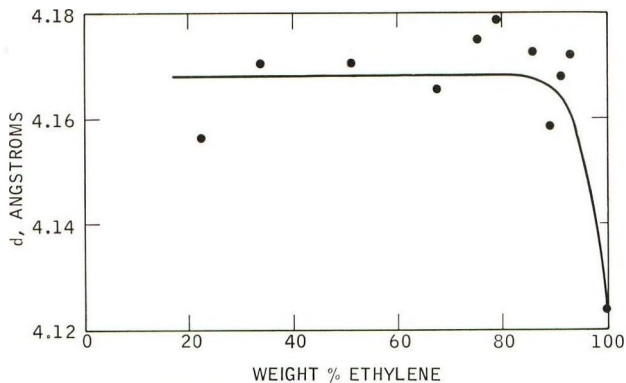


Fig. 3. Effect of copolymer composition on the $\{110\}$ interplanar spacing of the modified polyethylene phase.

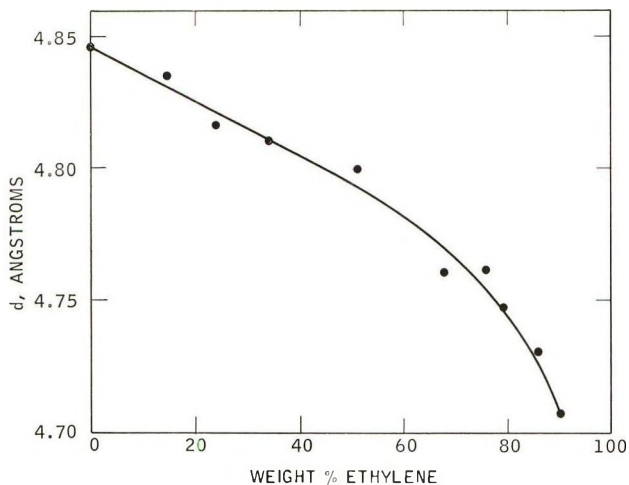


Fig. 4. Effect of copolymer composition on the $\{130\}$ interplanar spacing of the modified poly-1,5-hexadiene phase.

polymers, the interplanar spacings are increased in the modified polyethylene structure and decreased in the modified poly-1,5-hexadiene structure. The variation of the d values for the strongest lines of the two patterns is shown in Figures 3 and 4 as a function of ethylene content. It can be noted that over the entire range of compositions for which the measurements could be made that the d value for the modified polyethylene phase is constant. On the other hand, the d value for the modified poly-1,5-hexadiene decreases continuously with increasing ethylene content.

A direct measurement of the a axis of the polyethylene type phase was obtained from the $\{200\}$ reflection for the copolymers above 75% ethylene content. These results, summarized in Table III, show a constant value of a for the copolymers within the experimental accuracy. For the copolymer, the average expansion along the a axis is 1.96%. From the data for the

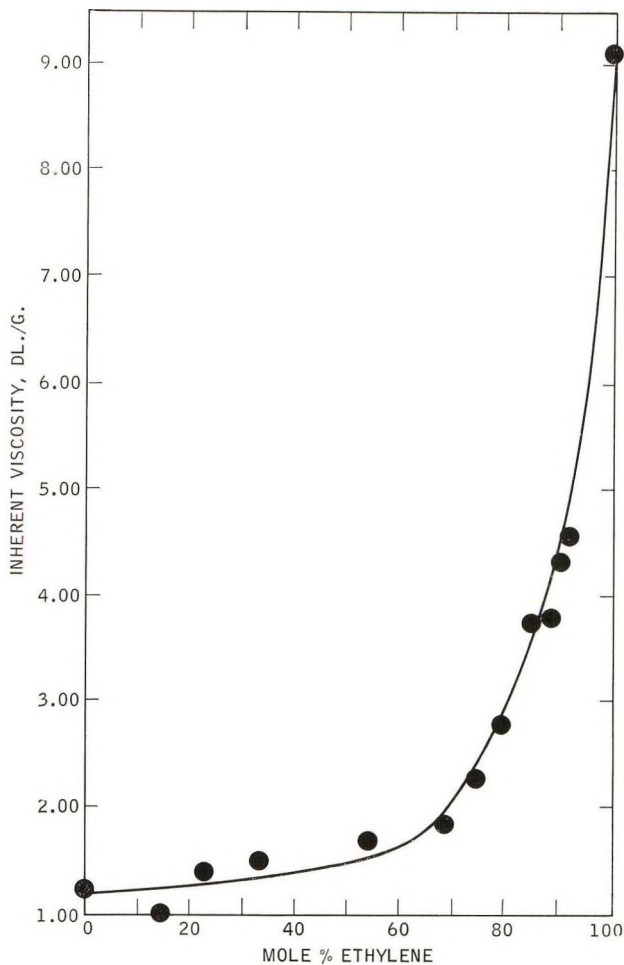


Fig. 5. Effect of copolymer composition on inherent viscosity.

{110} reflection, the average expansion in a direction perpendicular to these {110} planes is 1.025%. On the basis of the measured expansion in these two directions, expansion along the b axis is calculated to be 0.00%. This is in agreement with previous work reported for cell expansions of modified

TABLE III

Expansion of a Axis of Polyethylene Phase as Function of Composition of Ethylene-Hexadiene-1,5 Copolymer

Ethylene, wt.-%	a , A.
75.6	7.582
85.4	7.586
91.0	7.586
93.0	7.582
100	7.438

polyethylenes¹⁴⁻¹⁷ in which the b axis remained nearly constant while the a axis increased.

Effect of Composition on Physical Properties

Inherent Viscosity. The inherent viscosity of the copolymer increases with increasing ethylene content (Fig. 5). The effect is rather small in the region 0-70 mole-% ethylene, but inherent viscosity sharply increases at higher ethylene contents up to a maximum for polyethylene. These

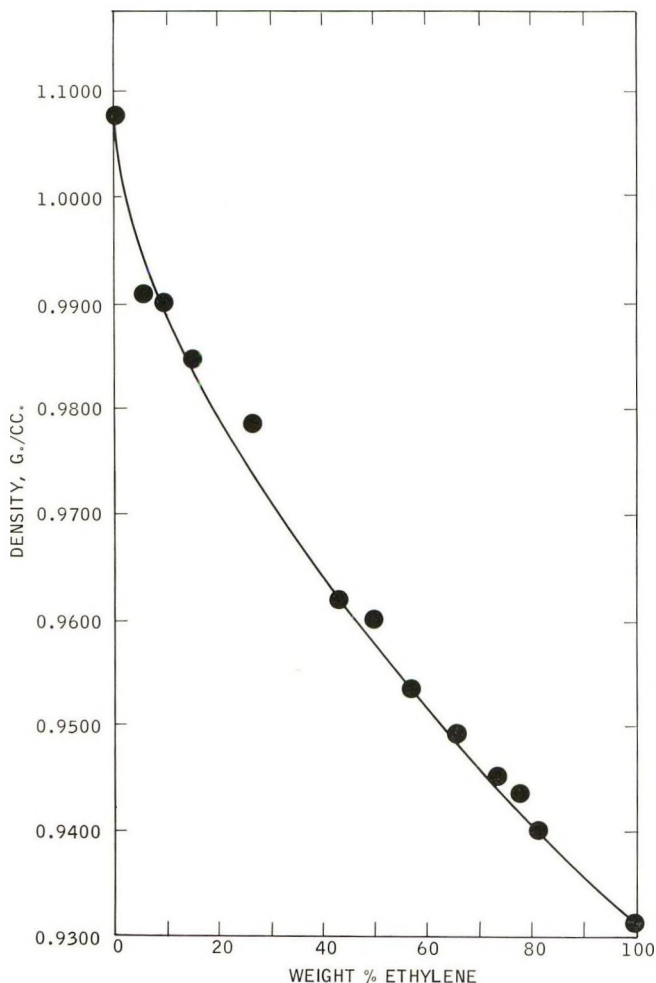


Fig. 6. Effect of copolymer composition on density.

changes in inherent viscosity with composition are assumed to be due primarily to molecular weight differences rather than to compositional effects. Although no molecular weight data are available for splitting out the contributions of each of these effects on inherent viscosity, the assump-

tion is considered reasonable in view of the large differences in inherent viscosity between the homopolymers of ethylene and 1,5-hexadiene.

It appears that 1,5-hexadiene dominates in determining copolymer inherent viscosities. Even in a copolymer containing but 10% 1,5-hexadiene the inherent viscosity is already one-half that of polyethylene, demonstrating the controlling effect of 1,5-hexadiene.

Density. The effect of composition on copolymer density is illustrated in Figure 6. The density of poly-1,5-hexadiene prepared with the preformed catalyst is 1.008 g./cc. As ethylene content is increased the density decreases in an almost linear fashion. It is interesting to note that the

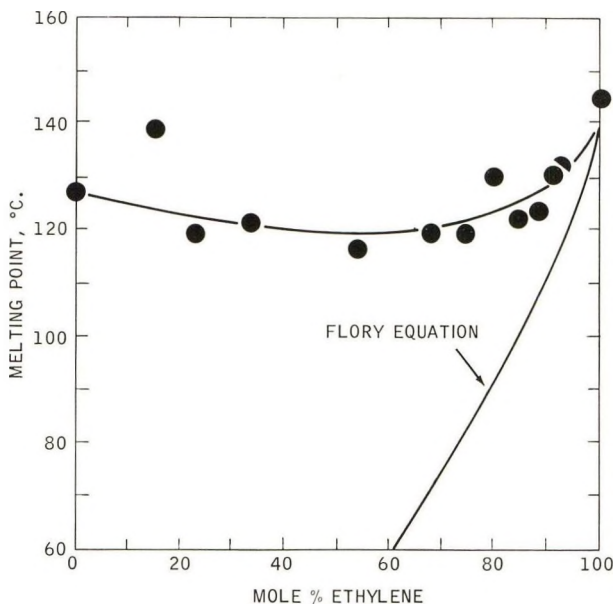


Fig. 7. Effect of copolymer composition on melting point.

minimum density is that for polyethylene. This is rather unusual since most copolymers of ethylene with α -olefins tend to decrease from the polyethylene density.¹⁸ This is interpreted as showing that there is little destruction of crystal systems in these copolymers. If mutual destruction of crystallinity had occurred, the copolymer densities, which are dependent on the extent of crystallinity, would have decreased markedly. For comparison a physical blend of polyethylene and poly-1,5-hexadiene has very nearly the same density as the copolymer containing the same ratio of ethylene to 1,5-hexadiene units.

Melting Point. The melting point curve for the copolymer series resembles that of a eutectic. Figure 7 shows that the copolymer melting point passes through a minimum at about 55 mole-% ethylene content.

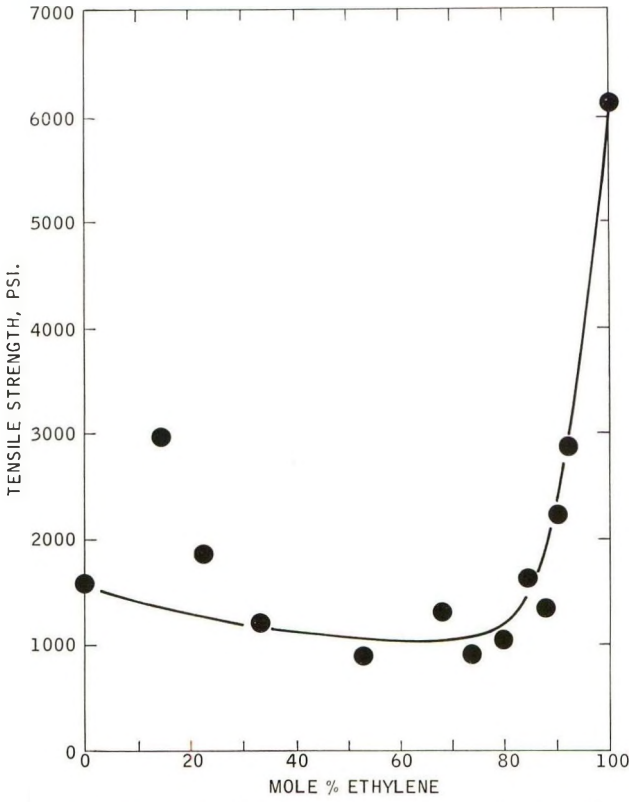


Fig. 8. Effect of copolymer composition on tensile strength.

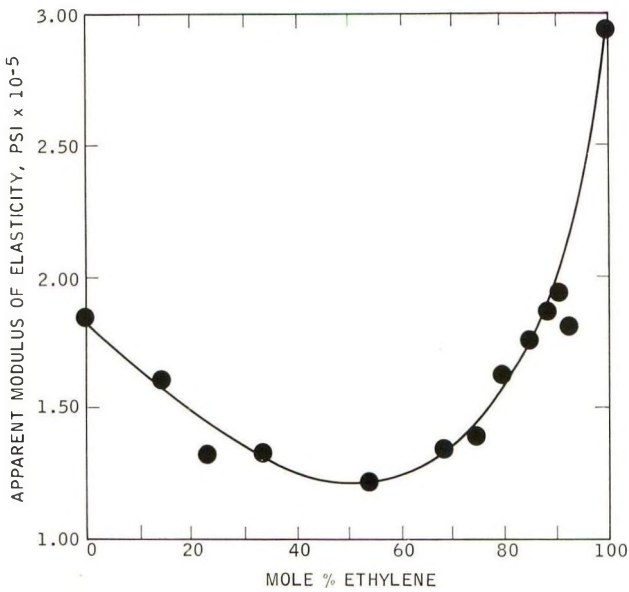


Fig. 9. Effect of copolymer composition on apparent modulus of elasticity.

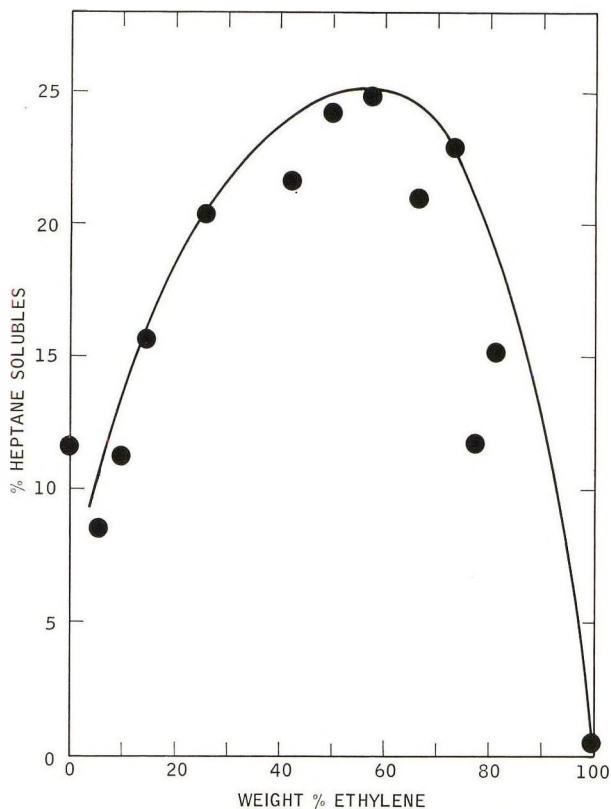


Fig. 10. Effect of copolymer composition on solubility in *n*-heptane.

The melting point curve lies considerably higher than the curve calculated from Flory's equation for copolymer melting point¹⁹ which is given by

$$\frac{1}{T_m} - \frac{1}{T_m^0} = - (R/\Delta H_f) \ln X_A = - (R/\Delta H_f) \ln p$$

where ΔH_f is the heat of fusion for the major component, X_A is the mole fraction of the major component, and p is the probability of A-A linkages. For true random copolymerizations $p = X_A$. Since the ethylene-1,5-hexadiene copolymer melting points are much higher than those calculated by the Flory equation p must, therefore, exceed X_A and, consequently, the monomer units may occur in long sequences or blocks. The existence of a minimum in the melting point curve suggests that the chain units contributed by the monomers, i.e., $-\text{CH}_2-\text{CH}_2-\text{CH}_2-$ and methylene cyclopentane groups, are not truly isomorphous.¹⁰ The accommodation of these comonomer units into the lattices of the homopolymers can, therefore, be accomplished only at the expense of some variation in unit cell dimensions. Indeed the previously discussed x-ray analyses of the copolymers have demonstrated these variations in unit cell dimensions.

Mechanical Properties. The effect of copolymer composition on tensile strength is illustrated in Figure 8. A minimum appears in the region of 55–60 mole-% ethylene content. Figure 9 shows the effect of copolymer composition on the apparent modulus of elasticity (at $-50^{\circ}\text{C}.$). Again the curve passes through a minimum in the region of about 50 mole-% ethylene content. The addition of a comonomer reduces the tensile strength and increases the flexibility of the copolymer from that of the homopolymer. The comonomer appears to be acting largely as a plasticizer in relation to the copolymer physical properties.

Solubility. The effect of composition on the solubility of the copolymer in boiling *n*-heptane is illustrated in Figure 10. This curve passes through a maximum at a composition of about 60 wt.-% (80 mole-%) ethylene content. This maximum coincides with the region of rapidly increasing inherent viscosity (see Fig. 5). The *n*-heptane-soluble copolymer fractions are rich in 1,5-hexadiene. No blocks of ethylene were detected in these fractions. The *n*-heptane-insoluble copolymers have generally higher tensile strengths, melting points, and inherent viscosities than the total polymers. Densities are lower than in the total polymer, as would be expected from the high concentration of 1,5-hexadiene in the *n*-heptane-soluble portions.

CONCLUSIONS

It is concluded from the foregoing that ethylene-1,5-hexadiene copolymers prepared with preformed $\text{AlR}_3/\text{TiCl}_3$ catalysts are probably block copolymers in which the block sequences are rather long. Furthermore, each block is not a homopolymer but is modified by the inclusion of comonomer.

X-ray analysis and physical property measurements do not distinguish between a true block copolymer, on the one hand, and essentially homopolymer sequences on the other. However, the latter would require the presence of two essentially different and reactive types of catalyst sites in the $\text{AlR}_3/\text{TiCl}_3$ catalyst complex, and this is considered unlikely in any large measure.

Good evidence for the block nature of the copolymer is obtained from physical property measurements, especially melting point–composition behavior, and from the observation that the copolymers crystallize into polyethylene and poly-1,5-hexadiene crystals.

Evidence for the block modifications, i.e., each block containing some comonomer, is obtained from the observed expansion or contraction of interplanar spacings.

The authors wish to thank Mr. H. W. Dougherty for his experimental assistance and Dr. E. Tornqvist for the catalyst preparations.

References

1. Makowski, H. S., B. K. C. Shin, and Z. W. Wilchinsky, *J. Polymer Sci.*, **A2**, 1549 (1964).
2. Valvassori, A., G. Sartori, and F. Ciampelli, *Chim. Ind. (Milan)*, **44**, 1095 (1962).
3. Baker, W. O., and C. S. Fuller, *J. Am. Chem. Soc.*, **64**, 2399 (1942).
4. Edgar, O. B., and R. Hill, *J. Polymer Sci.*, **8**, 1 (1952).
5. Cramer, F. B., and R. G. Beaman, *J. Polymer Sci.*, **21**, 237 (1956).
6. Yu, A. J., and R. D. Evans, *J. Polymer Sci.*, **42**, 249 (1960).
7. Ke, B., and A. W. Sisko, *J. Polymer Sci.*, **50**, 87 (1961).
8. Reding, F. P., and E. R. Walter, *J. Polymer Sci.*, **37**, 555 (1959).
9. Natta, G., P. Corradini, D. Sianesi, and D. Morero, *J. Polymer Sci.*, **51**, 527 (1961).
10. Natta, G., G. Dall'Asta, G. Mazzanti, I. Pasquon, A. Valvassori, and A. Zambelli, *J. Am. Chem. Soc.*, **83**, 3343 (1961).
11. Chatani, Y., T. Takizawa, S. Murahashi, Y. Sakata, and Y. Nishimura, *J. Polymer Sci.*, **55**, 811 (1961).
12. Bunn, C. W., *J. Appl. Phys.*, **25**, 820 (1954).
13. National Bureau of Standards, (U.S.), Circular 539, Vol. 7.
14. Walter, E. R., and F. P. Reding, *J. Polymer Sci.*, **21**, 561 (1956).
15. Cole, E. A., and D. R. Holmes, *J. Polymer Sci.*, **46**, 245 (1960).
16. Einhorn, R. M., *J. Polymer Sci.*, **31**, 197 (1958).
17. Swan, P. R., *J. Polymer Sci.*, **56**, 409 (1962).
18. Reding, F. P., and C. M. Lovell, *J. Polymer Sci.*, **21**, 157 (1956).
19. Flory, P. J., *Principles of Polymer Chemistry*, Cornell Univ. Press, Ithaca, N. Y., 1953.

Résumé

On a préparé, avec un catalyseur $\text{AlR}_3/\text{TiCl}_3 \cdot \text{AlCl}_3$, une série de copolymères cristallins d'éthylène-1,5-hexadiène, qui contiennent 15 à 93 mole % d'éthylène. Ces analyses par diffraction aux rayons-X, montrent que dans les copolymères il y a deux phases cristallines distinctes; l'une des deux phases a la structure d'un polyéthylène, tandis que l'autre a une structure poly-1,5-hexadiène. Cependant les dimensions de la cellule unitaire de ces deux phases diffèrent de celles des homopolymères respectifs, ce qui indique que les deux types d'unités monomériques sont présentes dans chacune des phases du copolymère. Des mesures de propriétés physiques sur les copolymères confirment ces conclusions.

Zusammenfassung

Eine Reihe kristalliner Äthylen-1,5-hexadiencopolymerer mit einem Gehalt von 15 bis 93 Mol % Äthylen wurde mit einem $\text{AlR}_3/\text{TiCl}_3 \cdot \text{AlCl}_3$ -Katalysatorsystem hergestellt. Die Röntgenbeugungsanalyse zeigte zwei verschiedene kristalline Phasen im Copolymeren; eine Phase hatte Polyäthylenstruktur, die andere dagegen Poly-1,5-hexadienstruktur. Die Grösse der Elementarzelle dieser beiden Phasen war deutlich von der der Homopolymeren verschieden und zeigte damit, dass beide Arten der Monomereinheit in jeder Copolymerphase vorhanden sind. Messungen der physikalischen Eigenschaften der Copolymeren unterstützen diese Schlüsse.

Received January 22, 1964

Revised March 5, 1964

Synthesis and Characterization of Poly-*s*-Triazinyleneimides*

GERHARD F. L. EHLERS, *Air Force Materials Laboratory, Wright-Patterson Air Force Base, Ohio*, and JAMES D. RAY, *University of Dayton Research Institute, Dayton, Ohio*

Synopsis

Poly-*s*-triazinyleneimides have been prepared from melt reactions between amino- and chloro-substituted *s*-triazine derivatives. The polymers, which have been characterized by melting ranges, inherent viscosity, solubility, elementary analysis, and thermogravimetric analysis, are brittle resins of relatively low molecular weight. Poly-6-phenyl-*N*-methyl-2,4-*s*-triazinyleneimide, with an inherent viscosity of 0.35, had the highest molecular weight of the polymers synthesized. Poly-6-chloro-*N*-phenyl-2,4-*s*-triazinyleneimide, exhibited considerable mechanical strength at room temperature, apparently due to strong secondary bonding forces.

INTRODUCTION

The synthesis of linear *s*-triazinyleneimides has been reported previously by Reimschuessel et al.¹ The polymers which were obtained, preferably by reacting phenoxy with amino derivatives of *s*-triazine, were not fully described at that time, with the exception of the general features of their infrared spectra.

The work of the above authors, which had been initiated in this laboratory, was continued with the purpose of exploring in detail the synthesis of a series of *s*-triazinyleneimides and fully characterizing these polymers.

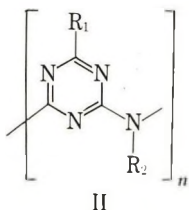
DISCUSSION AND RESULTS

Several approaches to poly-*s*-triazinyleneimides (I) appear feasible and are shown at the top of the following page.

Preference was given to the last two for the following reasons: As exploratory trials indicated, the approaches involving the use of phenoxy derivatives, under elimination of phenol, did not offer any advantages compared to reactions with chlorotriazines. The molecular weights obtained were not higher than those from chlorotriazines; on the other hand, the work-up procedure was more difficult, since phenol had to be removed from the reaction mixture. The progressing reaction could not as easily

* Presented in part at the 145th National Meeting of the American Chemical Society, New York, N. Y., September 9-13, 1963.

A series of poly-*s*-triazinyleneimides of general type (II):



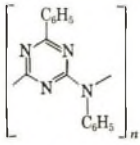
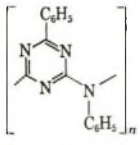
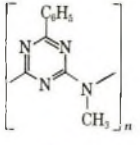
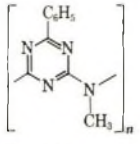
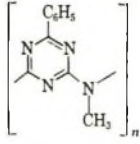
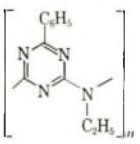
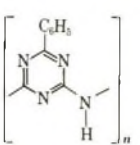
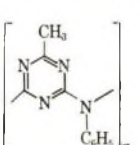
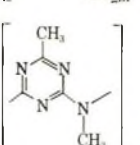
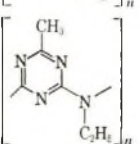
and related, branched and crosslinked structures have subsequently been prepared and identified by elementary analysis, solubility, inherent viscosity, softening under load, and thermogravimetric analysis. Intrinsic viscosities have been obtained for two of the polymers from a solution viscosity versus concentration plot. The intrinsic viscosities are slightly lower than the inherent viscosities, determined at a concentration of 0.5%. Two polymers have also been investigated by differential thermal analysis.

The synthesis of poly-*s*-triazinyleneimides (II) with R_1 phenyl and R_2 phenyl, methyl, ethyl and hydrogen presented no problems. Clear, yellow to brown, brittle resins were obtained from melt reactions which were soluble in benzene, *m*-cresol, or phenol with the exception of the polymer from 2-phenyl-4-chloro-6-amino-*s*-triazine. The analysis results were in good agreement with the calculated values and the inherent viscosities, between 0.07 and 0.35 suggest molecular weights up to the order of 16,000. It seemed that the specific structure played the most important role in determining the degree of polymerization, because identical inherent viscosities were obtained for the same polymer not only in repeated runs, but also from the homocondensation of a chloroaminotriazine as well as from the reaction of a dichlorotriazine with a diaminotriazine. In the latter case it is impossible to sustain a balanced stoichiometry, because both components are different in their tendency to sublime. This, however, did not seem to affect the molecular weight of the so formed polymer. The polymer with the highest molecular weight, poly-2-phenyl-4,6-*N*-methyl-*s*-triazinyleneimide, exhibited a certain degree of toughness.

It was assumed that polymers with higher molecular weights could be obtained by replacing phenyldichlorotriazine by the more reactive phenyldibromotriazine. However, polymers synthesized this way did not give analysis results as good as those of the polymers made previously, were less soluble and the molecular weight was lower in one, about the same in the other case.

The polymers with a methyl group adjacent to the *s*-triazine ring are dark red powders, which retained a considerable amount of chlorine. They soften only partially and at high temperatures (Fig. 1); their infrared spectra are very diffuse and hardly show any bands at all, and the TGA curve (Fig. 4) of one of these polymers is different from those of all the other polytriazinyleneimides, with the exception of the two polymers with pending chlorine groups. Color, softening behavior, chlorine content and infrared

TABLE I. Properties of Poly-

No.	Structure	Starting materials	Reaction time, hr.	Temp., °C.	Conversion, % ^a	Yield, % ^b	Appearance
1		2-Phenyl-4-chloro-6-anilido-s-triazine	67	200	67	98	Clear, brown brittle resin
2		2-Phenyl-4,6-dibromo-s-triazine + 2-phenyl-4,6-dianilido-s-triazine	240	200		87	Gray-brown powder
3		2-Phenyl-4-chloro-6-methyl-amino-s-triazine	29	220	44	93	Clear, light yellow, brittle resin
4		2-Phenyl-4,6-dichloro-s-triazine + 2-phenyl-4,6-dimethyl-amino-s-triazine	46	200	45	90	Clear, light yellow, brittle resin
5		2-Phenyl-4,6-dibromo-s-triazine + 2-phenyl-4,6-dimethyl-amino-s-triazine	430	200		78	Clear, light yellow, brittle resin
6		2-Phenyl-4,6-dichloro-s-triazine + 2-phenyl-4,6-diethyl-amino-s-triazine	43	200	19	92	Clear, light yellow, brittle resin
7		2-Phenyl-4-chloro-6-amino-s-triazine	15	230	85	98	Clear, light yellow, brittle resin
8		2-Methyl-4,6-dichloro-s-triazine + 2-methyl-4,6-dianilido-s-triazine	230	200			Dark red resin
9		2-Methyl-4,6-dichloro-s-triazine + 2-methyl-4,6-dimethyl-amino-s-triazine	49	200	34	75	Dark red powder
10		2-Methyl-4,6-dichloro-s-triazine + 2-methyl-4,6-diethyl-amino-s-triazine	26	200	18	84	Dark red powder

s-triazinyleneimides

Soluble in	Analyses								η_{inh} (% in solvent)	Heat soften- ing temp., °C. ^o
	Calc. for DP = ∞				Found					
	C, %	H, %	N, %	Cl, %	C, %	H, %	N, %	Cl, %		
Benzene	73.2	4.1	22.7	0	73.7	4.5	22.3	0	0.07 (0.4% in benzene)	185
<i>m</i> -Cresol	67.6 ^d	3.9 ^d	21.0 ^d	7.5 ^{d,e}	67.3	4.2	20.9	7.7	0.06 (0.5% in <i>m</i> -cresol)	—
<i>m</i> -Cresol	64.9	4.9	30.2	0	64.0	4.4	30.9	0	0.30 (0.5% in <i>m</i> -cresol)	235, 365
<i>m</i> -Cresol	64.9	4.9	30.2	0	64.1	4.3	30.5	0.8	0.29, 0.35 (0.5% in <i>m</i> -cresol)	—
<i>m</i> -Cresol	64.9	4.9	30.2	0	63.0	3.9	31.4	1.6 ^e	0.11 (0.5% in <i>m</i> -cresol)	250, 315
Phenol	66.7	5.1	28.2	0	66.0	4.7	28.9	0.5	0.07 (0.5% in phenol)	185
Insoluble	63.6	3.5	32.9	0	61.7	3.5	31.9	2.3	—	250, 320
Phenol	62.8	4.7	32.5	0	60.8	4.3	27.9	6.2	0.06 (0.05% in phenol)	250
Phenol (part.)	49.2	4.9	45.9	0	43.1	5.0	40.2	8.7	0.18 (0.25% in phenol)	~490
Phenol	52.9	5.9	41.2	0	46.1	5.0	37.1	8.3	0.07 (0.5% in phenol)	—

(continued)

TABLE I

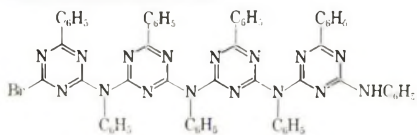
No.	Structure	Starting materials	Reaction time, hr.	Temp. °C.	Conversion, % ^a	Yield, % ^b	Appearance
11		2-Methyl-4,6-dimethyl-amino- <i>s</i> -triazine + 2-phenyl-4,6-dichloro- <i>s</i> -triazine	50	200	45	88	Orange, brittle resin
12		Polymer 9 + 2,4-diphenyl-6-chloro- <i>s</i> -triazine	75 160 25	200 250 300	76	82	Green-yellow powder
13		2,4-Diphenoxy-6-anilido- <i>s</i> -triazine	120	300		60	Dark brown powder
14		2-Chloro-4,6-dianilido- <i>s</i> -triazine	190	250	85	77	Yellow, clear, brittle resin
15		2,4-Dichloro-6-amino- <i>s</i> -triazine	540	250	77*		Yellow, clear, brittle resin
16		2,4-Dichloro-6-anilido- <i>s</i> -triazine	490	200	52*	84	Yellow, hard, tough resin
17		Cyanuric chloride + 2,4,6-tri-anilido- <i>s</i> -triazine	670	250	98	50	Yellow, clear resin

^a From hydrogen chloride evolved.

^b From amount of reaction product calculated.

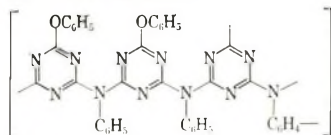
^c Inversion point of softening curve under a load of 45 psi and a rate of temperature increase of 150°C./hr.

^d Calculated for structure:

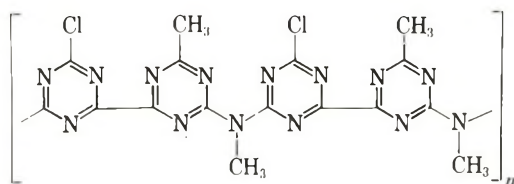


(continued)

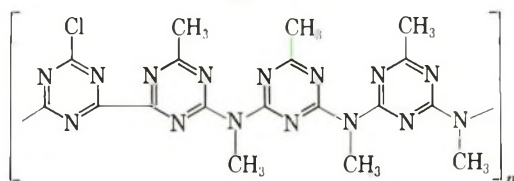
Soluble in	Analyses								η_{inh} (% in solvent)	Heat soften- ing temp., °C. ^e
	Calc. for DP = ∞				Found					
	C, %	H, %	N, %	Cl, %	C, %	H, %	N, %	Cl, %		
Phenol <i>m</i> -cresol	58.8	4.6	36.6	0	57.1	4.5	32.4	6.1	0.06 (0.5% in phenol)	310
<i>m</i> -Cresol	71.8	3.7	24.5	0	73.4	4.6	22.6	—	0.04 (0.5% in <i>m</i> -cresol)	150
Insoluble	67.6 ^f	3.5 ^f	24.3 ^f	4.6 ^f	67.8	4.1	23.5	3.9	—	155
<i>m</i> -Cresol	69.0	4.2	26.8	0	67.9	4.2	27.1	0.5	0.03 (0.5% in <i>m</i> -cresol)	205
Insoluble	28.1	0.8	43.5	27.6	32.5	2.3	56.6	5.6	—	440
<i>m</i> -Cresol	52.8	2.5	27.3	17.4	53.8	2.7	27.3	16.4	0.15 (0.5% in <i>m</i> -cresol)	175 (460)
Insoluble	61.9	3.4	27.1	7.6	58.4	3.1	25.4	8.5	—	355

^e Bromine content.^f Calculated for structure:^g 100% = both chlorine reacted.

spectra point to rigid structures with partial conjugation and pendant chlorine groups on about every third ring. Since the molecular weight of at least one of the polymers is fairly high, the halogens cannot be end-groups. Since it has been observed³ that 2-chloro-4,6-dimethylamino-*s*-triazine forms basic condensation by-products above 250°C., possibly methylamine or dimethylamine, the structures III or IV could have formed.



III



IV

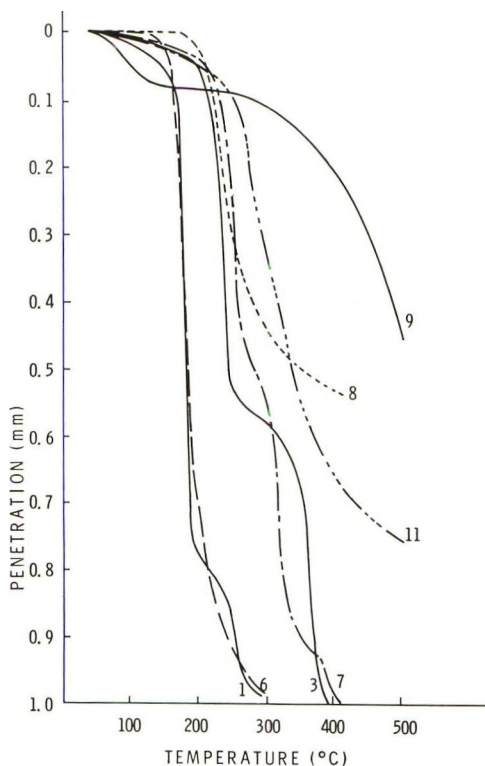


Fig. 1. Heat softening of poly-*s*-triazinyleneimides. Polymer numbers as in Table I.

Mixtures of structures III and IV would fit rather well to the analytical data found. One of the polymers has also been prepared in diphenyl ether at 200°C. The resulting product, however, was insoluble and contained 4.4% oxygen, probably from hydrolysis of some of the pending chlorine groups. The mixed polymer 11 (Table I), also shows the coloration and chlorine content typical for the polymers with the methyl group on the triazine ring.

Melt reaction of poly-2-phenyl-4,6-*s*-triazinyleneimide with 2,4-diphenyl-6-chloro-*s*-triazine resulted in a soluble polymer (V) of low inherent viscosity (the inherent viscosity of the original polymer could not be determined, since it was insoluble):

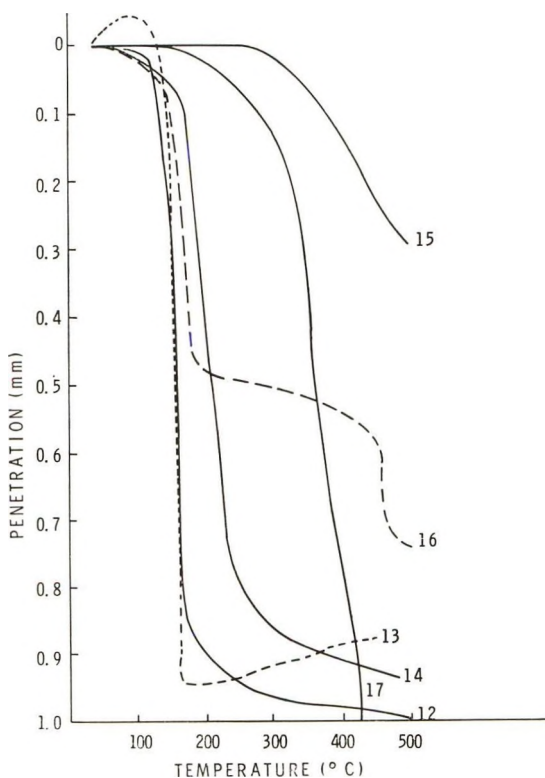
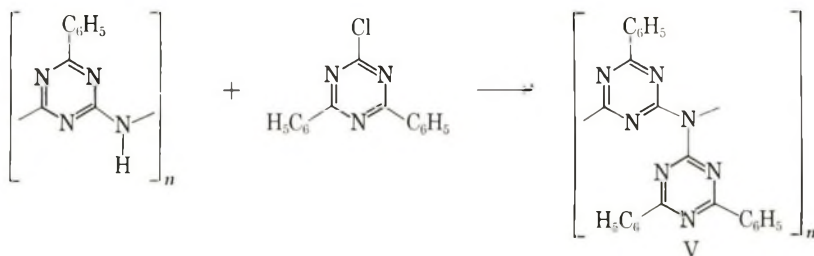


Fig. 2. Heat softening of poly-*s*-triazinyleneimides. Polymer numbers as in Table I

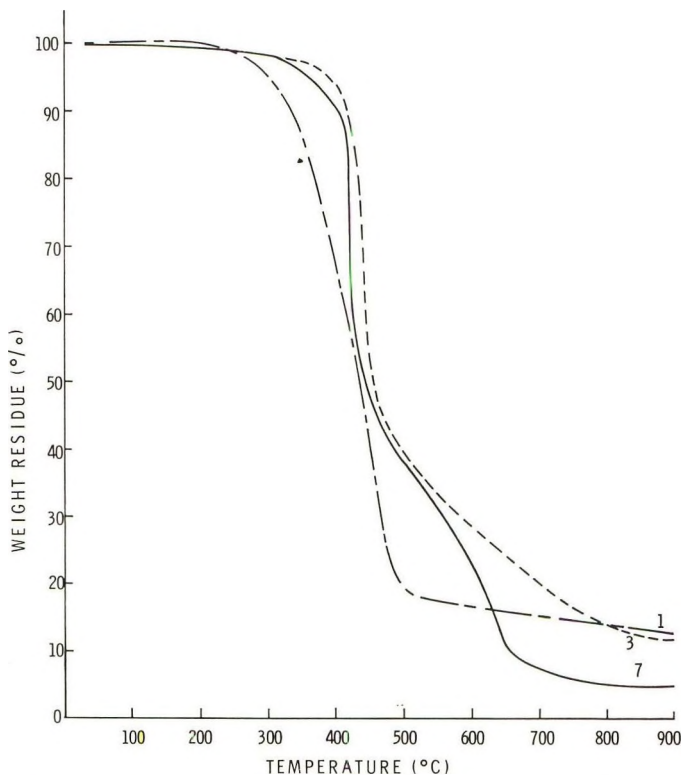
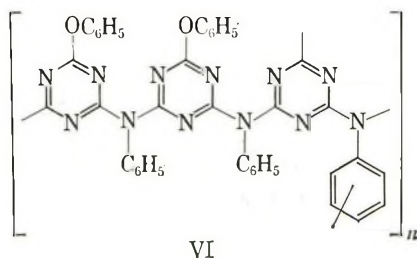


Fig. 3. Thermogravimetric analysis of poly-*s*-triazinyleneimides under nitrogen; $\Delta T = 150^\circ\text{C./hr.}$ Polymer numbers as in Table I.

This polymer is interesting because of its bulky, pending groups. While its softening point is low, the thermal stability is the highest of all of the poly-*s*-triazinyleneimides; it has also the highest phenyl/triazinyl ratio of all of the polymers. Introduction of an even bulkier group, bis[*N*-phenyl-*N*-(4',6'-diphenyl-*s*-triazinyl-2')] - 2,4-diamino-6-chloro-*s*-triazine into poly-2-phenyl-4,6-*s*-triazinyleneimide did not succeed; the reaction was incomplete, and poorly defined reaction products were obtained. A molecular model suggests that steric hindrance is the limiting factor.

A number of trials have been made to synthesize polymers with functional groups on the triazine ring. The polymer from 2,4-diphenoxy-6-anilido-*s*-triazine melts fairly low, but is insoluble, and results of analysis point to the structure VI:



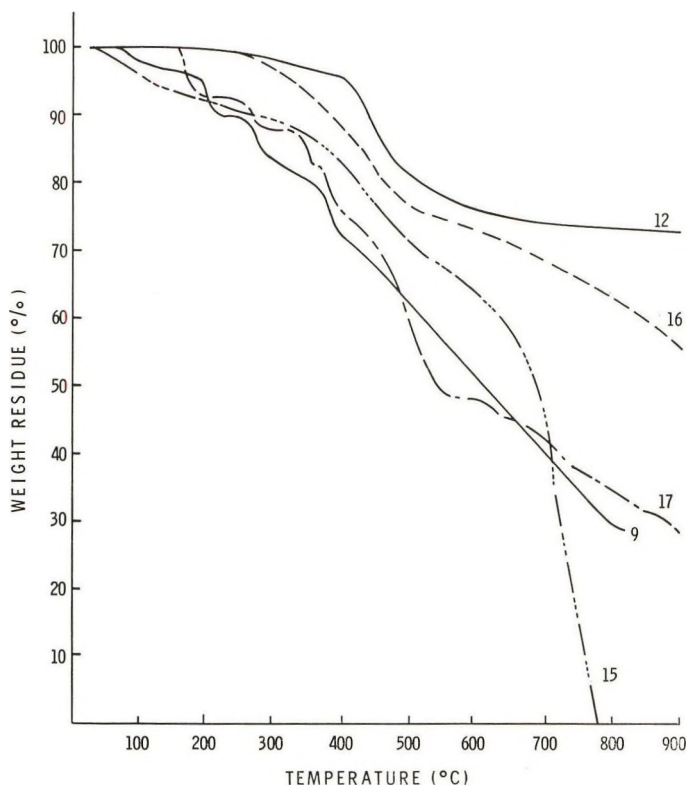
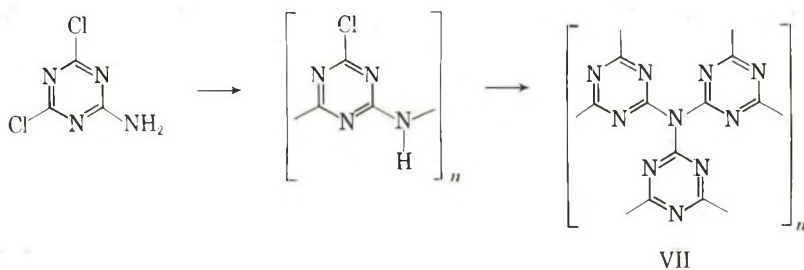


Fig. 4. Thermogravimetric analysis of poly-*s*-triazinyleneimides under nitrogen; $\Delta T = 150^\circ\text{C./hr.}$ Polymer numbers as in Table I.

with crosslinks through hydrogen abstraction from a benzene ring. This seems to be feasible at the reaction temperature of 300°C.

Preparation of poly-2-chloro-4,6-*s*-triazinyleneimide from 2,4-dichloro-6-amino-*s*-triazine was attempted. However, this compound reacted below its melting point and also tended to sublime. It was therefore virtually impossible to control the reaction to the extent that only one chlorine reacted:



The polymer actually obtained in this reaction (VII) approaches the crosslinked structure. It shows only a limited degree of softening.

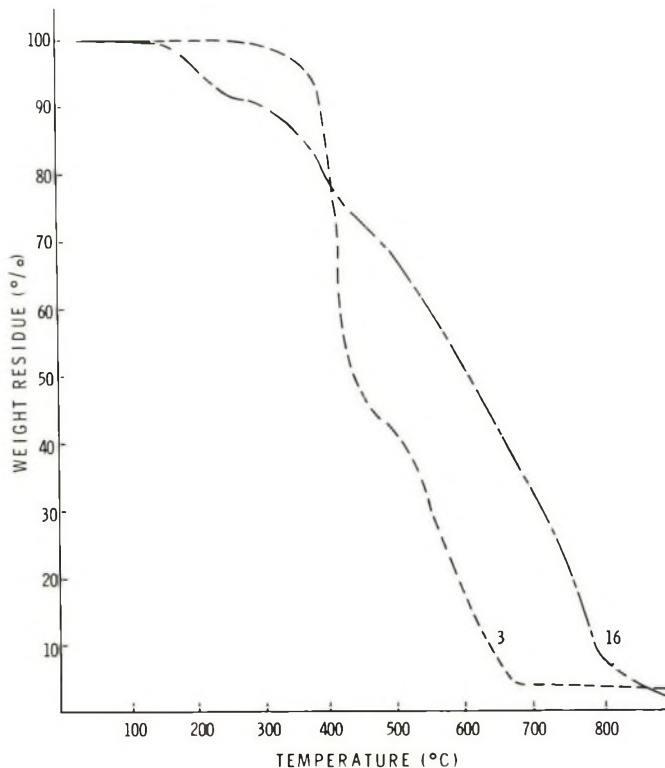
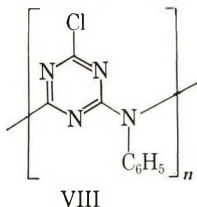


Fig. 5. Thermogravimetric analysis of poly-*s*-triazinyleneimides in air; $\Delta T = 150^\circ\text{C./hr.}$ Polymer numbers as in Table I.

Poly-2-chloro-4,6-*N*-phenyl-*s*-triazinyleneimide (VIII)



exhibits considerable toughness and cannot be ground to a fine powder. Tough, strong pellets can be formed under heat and pressure. The polymer softens only to a certain extent around 175°C. [the second dip in the softening curve (see Fig. 2) can be explained by thermal decomposition] and is of high thermal stability. Since the molecular weight of the polymer is not extremely high, the mechanical strength probably has to be attributed to secondary bonding forces involving the chlorine atom. When the polymer is exposed to the open atmosphere, the chlorine slowly hydrolyzes, the polymer loses its strength and becomes brittle and insoluble. An attempt was made to convert the pendant chlorine to phenoxy groups by treatment with phenol; however this cleaves the polymer, 2,4,6-triphenoxy-*s*-

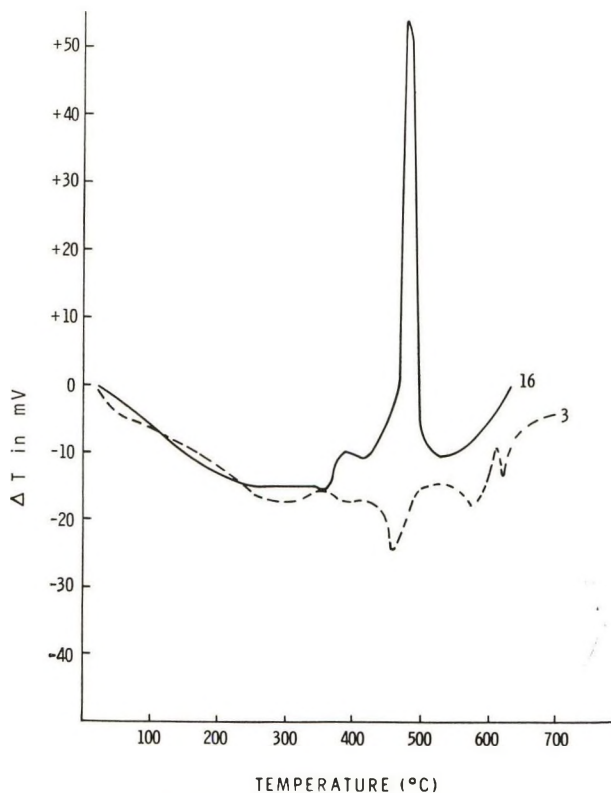
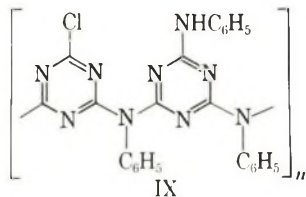


Fig. 6. Differential thermal analysis of poly-*s*-triazinyleneimides under nitrogen; $\Delta T' = 180^\circ\text{C./hr.}$

triazine and 2,4-diphenoxy-6-anilido-*s*-triazine were isolated. *m*-Cresol dissolves the polymer without appreciable decomposition for a certain length of time; refluxing in *m*-cresol yields unidentified cleavage products. Various trials to crosslink the polymer with difunctional compounds gave non-uniform reaction products, which often retained considerable amounts of chlorine. It is likely that this polymer is of randomly branched rather than of linear structure.

In another crosslinking trial, cyanuric chloride was reacted with 2,4,6-trianilido-*s*-triazine. The insoluble reaction product retained a considerable amount of chlorine. Results of analysis suggest a linear structure (IX)



rather than a crosslinked structure.

Figures 1 and 2 show the softening under load in temperature dependence of the majority of the poly-*s*-triazinyleneimides, Figures 3-5 the thermograms from thermogravimetric analysis. The major thermal breakdown of most of these polymers under nitrogen (inversion point of the TGA curve) occurs around 450°C. The chlorine-containing polymers lose some weight at fairly low temperatures, but retain more weight at high temperatures. The high stability of polymer 12 may have to do with the high content of phenyl groups. Differential thermal analysis (Fig. 6) reveals a high decomposition exotherm at 480°C. for polymer 16. The softening curve (Fig. 2) indicates this decomposition at 460°C., while the TGA curve shows a maximum rate of decomposition, but only a minor weight loss, around the same temperature under nitrogen (around 400°C. in air). Polymer 3, however, has a low endotherm connected with a high weight loss. Unless the decomposition pattern of the two polymers is completely different, it seems to be possible that the evolution of decomposition products of polymer 3 caused a cooling effect and reversed the direction of the DTA peak.

Most of the infrared spectra of the polytriazinyleneimides have a rather diffuse pattern without sharp bands. It can be noted that this is particularly true for the polymers with high softening ranges, less distinct for lower melting polymers.

EXPERIMENTAL

The following example of preparation of poly-6-phenyl-*N*-ethyl-2,4-*s*-triazinyleneimide (polymer 6) is typical of the polymer preparations. A mixture of 0.81 g. of 2-phenyl-4,6-diethylamino-*s*-triazine and 0.75 g. of 2-phenyl-4,6-dichloro-*s*-triazine was heated to $200 \pm 1^\circ\text{C}$. for 43 hr. under a slow stream of nitrogen. The nitrogen stream was directed into an absorption flask with water and the solution titrated at intervals with 0.1*N* sodium hydroxide solution. The reaction was considered terminated when no hydrogen chloride was detected after a period of 8 hr. Total titration was 50.4 ml. of 0.1*N* sodium hydroxide, equivalent to a conversion of 76%. The crude product, a clear, light yellow, brittle resin, was crushed, and extracted for 2 hr. with diethyl ether. The polymer did not seem to melt in a capillary, but decomposed at around 400°C.; $\eta_{inh} = 0.07$ (0.5% in phenol).

ANAL. Calcd. for $(\text{C}_{11}\text{H}_{16}\text{N}_4)_n$: C, 66.7%; H, 5.1%; N, 28.2%; Cl, 0.0%. Found: C, 66.0%; H, 4.7%; N, 28.9%; Cl, 0.5%.

Heat softening curves were obtained in an experimental, automatic recording instrument, to be described elsewhere.⁴ The polymer powder was packed into a mold of $5/16$ in. diameter and 1 mm. depth. A load of 1000 g. was applied through a disk of 0.25 in. diameter, and the temperature was raised at a rate of 150°C./hr. The penetration of the load into the sample was measured.

Thermogravimetric analysis was performed in a Chevenard thermobalance under nitrogen at a heating rate of 150°C./hr.

Differential thermal analysis plots were obtained by use of an experimental unit attached to an Aminco thermobalance. The heating rate was 180°C./hr., the atmosphere nitrogen.

References

1. Reimschuessel, H. K., A. M. Lovelace, and E. M. Hagerman, *J. Polymer Sci.*, **40**, 270 (1959).
2. Ehlers, G. F. L., G. A. Loughran, J. D. Ray, and E. M. Hagerman, *J. Chem. Eng. Data*, **9**, 110 (1964).
3. Ehlers, G. F. L., and J. D. Ray, unpublished results.
4. Ehlers, G. F. L., and W. M. Powers, *Materials Res. Stds.*, **4**, 298 (1964).

Résumé

Des poly-*s*-triazinyl-èn-imides ont été préparés à partir de réactions à l'état fondu entre des dérivés d'amino-triazine-*s* et chloro-triazines. Les polymères qui ont été caractérisés par des domaines de fusion, viscosité intrinsèque, solubilité, analyse élémentaire et analyse thermogravimétrique, sont des résines fragiles de poids moléculaire relativement bas. Le poly-6-phényl-*N*-méthyl-2,4-*s*-triazinyl-èn-imide, de viscosité intrinsèque 0.35, possède le poids moléculaire de plus élevé des polymères synthétisés. Le poly-6-chloro-*N*-phényl-2,4-*s*-triazinyl-èn-imide présente une résistance mécanique considérable à température de chambre, apparemment due à des forces de liaisons secondaires élevées.

Zusammenfassung

Poly-*s*-triazinylenimide wurden durch Reaktion zwischen amino- und chlosubstituierten *s*-Triazinderivaten in geschmolzener Phase hergestellt. Diese durch Schmelzbereich, Viskositätszahl, Löslichkeit, Elementar- und thermogravimetrische Analyse charakterisierten Polymeren sind spröde Harze mit relativ geringen Molekulargewichten. Poly-6-phenyl-*N*-methyl-2,4-*s*-triazinylenimid hatte von den synthetisierten Polymeren bei einer Viskositätszahl von 0,35 das höchste Molekulargewicht. Poly-6-chlor-*N*-phenyl-2,4-*s*-triazinylenimid zeigte bei Zimmertemperatur beträchtliche mechanische Festigkeit, was offensichtlich durch die starken sekundären Bindungskräfte bedingt ist.

Received February 18, 1964

2,7-Disubstituted 1,3,6,8-Tetraazopyrene and Related Polymers

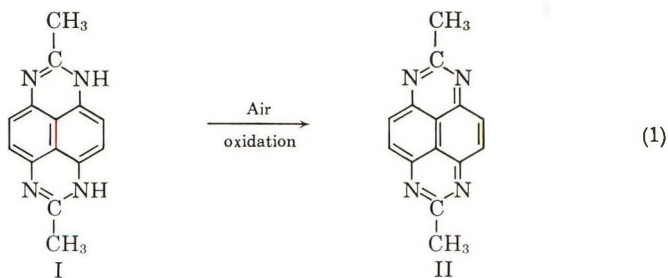
F. DAWANS,* B. REICHEL,† and C. S. MARVEL, *Department of
Chemistry, University of Arizona, Tucson, Arizona*

Synopsis

2,7-Disubstituted derivatives of 1,3,6,8-tetraazopyrene were synthesized as model compounds for some polymers of similar structure. Conjugated and high molecular weight polymers were obtained by polycondensation of 1,4,5,8-tetraaminonaphthalene with various diphenyl esters of bifunctional aromatic acids. The inherent viscosities of a number of polymers ranged from approximately 0.15 to 0.70. Most of the polymers are infusible and some of them are insoluble in the usual organic solvents. The thermal stability properties of the polymers were very good.

Many years ago, Dimroth and Roos¹ observed the formation of a tetraazopyrene compound by the reduction of tetranitronaphthalene in formic acid solution by the use of stannous chloride followed by oxidation with ferric chloride.

By catalytic reduction of 1,4,5,8-tetranitronaphthalene in a mixture of acetic acid and acetic anhydride, we obtained a product which presumably has structure (I) which on isolation in air was oxidized to the interesting condensed heterocyclic compound (II).

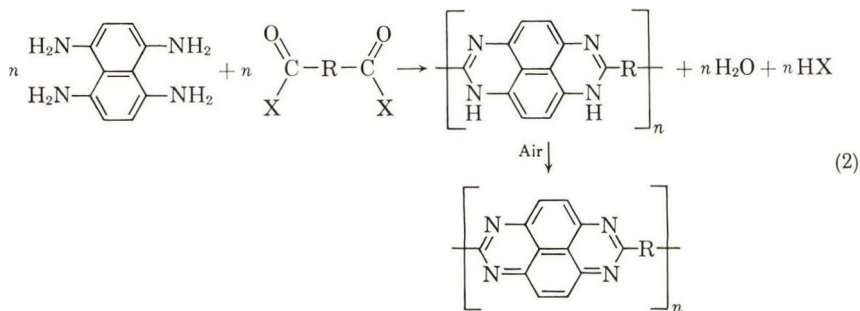


* Postdoctoral Research Associate supported by Plastics Department, E. I. du Pont de Nemours and Company, 1963-64. Present address: Institut Francais du Pétrole, Rueil-Malmaison, France.

† Postdoctoral Research Associate supported by Textile Fibers Department, E. I. du Pont de Nemours and Company, 1961-62. Present address: Badische Anilin und Soda Fabrik, Ludwigshafen, Germany.

We were able to synthesize the dimethyl- and diphenyl-tetraazopyrene by interaction of the reduction product of 1,4,5,8-tetranitronaphthalene with the phenyl esters of acetic and benzoic acids.

In order to prepare a conjugated and thermally stable polymer, we investigated this condensation reaction with some bifunctional aromatic reagents:



where X is Cl or OC₆H₅ and R is the aromatic nucleus.

DISCUSSION

2,7-Dimethyl-1,3,6,8-Tetraazopyrene

Catalytic reduction of 1,4,5,8-tetranitronaphthalene in a mixture of acetic acid and acetic anhydride yielded a brownish compound (I), melting at 260°C. with decomposition. This product oxidized spontaneously when recrystallized from alcohol in the air to yield 2,7-dimethyl-1,3,6,8-tetraazopyrene (II).

The same reaction products were obtained by interaction of a solution of 1,4,5,8-tetraaminonaphthalene with phenyl acetate, but all attempts to employ acetyl chloride in this condensation reaction failed because of some side reactions of the amino groups with the acid chloride functions.

The 2,7-dimethyl-1,3,6,8-tetraazopyrene was obtained as yellow needles subliming without decomposition at a temperature above 280°C. The compound is very slightly soluble in diethyl ether and cold ethanol; it is slightly soluble in acetone, chloroform, carbon tetrachloride, sulfuric acid, boiling ethanol and dimethylsulfoxide; it can be recrystallized from the latter solvents. It is soluble to the extent of 6% by weight in cold formic acid.

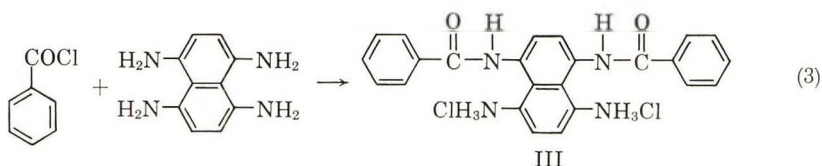
The infrared spectrum showed aromatic C—H stretching vibration at 3050 cm.⁻¹, bands associated with aromatic C=C and C=N at 1570, 1550, 1500, and 1490 cm.⁻¹, methyl group hydrogen atoms at 1355 and 1345 cm.⁻¹, and C—H out-of-plane deformation vibration associated with two adjacent free hydrogen atoms in an aromatic system at 855 cm.⁻¹.

In concentrated sulfuric acid solution the ultraviolet absorption was as follows: 400 mμ (ε = 9,360), 335 mμ (ε = 9,360), 330 mμ (ε = 5,610), 320 mμ (ε = 4,910), and 227 mμ (ε = 25,100).

Without success, we tried to show by nuclear magnetic resonance spectrometry the presence of the quinone cycle due presumably to the oxidation of the compound in air as the solubility of 2,7-dimethyl-1,3,6,8-tetraazopyrene in carbon tetrachloride or in deuterated dimethylsulfoxide is too low.

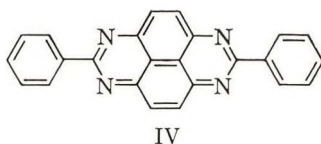
2,7-Diphenyl-1,3,6,8-Tetraazopyrene

When the reaction is carried out with benzoyl chloride, only a partial condensation seems to occur, probably due to salt formation on the adjacent amino groups.



Indeed, the elementary analysis of the reaction product agrees with the structure (III); further, the infrared spectra show an absorption band at 1755 cm.^{-1} , frequency characteristic of carbonyl groups.

By condensation of 1,4,5,8-tetraaminonaphthalene with phenyl benzoate, we were able to synthesize the model compound, 2,7-diphenyl-1,3,6,8-tetraazopyrene (IV):



This compound is a brown powder not melting below 300°C. and having about the same solubility characteristics as the dimethyl derivative; however, its purification was more difficult because the diphenyl derivative does not sublime. The infrared spectra showed absorption at 3050 cm.^{-1} (aromatic C-H), 1570 , 1550 , 1500 , and 1490 cm.^{-1} (aromatic C=C and C=N), 855 cm.^{-1} (aromatic C—H; 2 adjacent free H) and 765 and 635 cm.^{-1} (aromatic C—H; 5 adjacent free H).

In concentrated sulfuric acid, the ultraviolet absorption was as follows: $400\text{ m}\mu$ ($\epsilon = 7,160$), $337\text{ m}\mu$ ($\epsilon = 15,400$), $315\text{ m}\mu$ ($\epsilon = 16,700$), $263\text{ m}\mu$ ($\epsilon = 31,100$), $235\text{ m}\mu$ ($\epsilon = 30,000$), and $220\text{ m}\mu$ ($\epsilon = 50,800$).

Polytetraazopyrenes with Mixed Aromatic Units

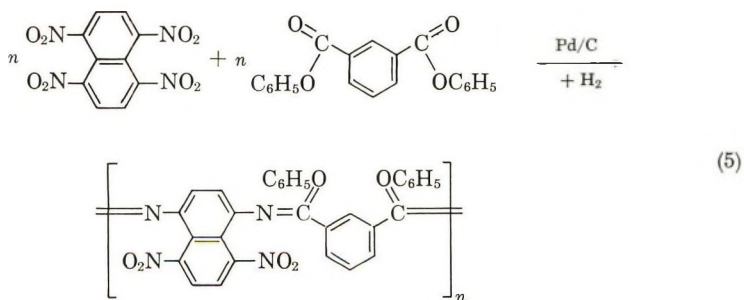
Several attempts to synthesize polymers from tetraaminonaphthalene and isophthaloyl chloride, in solution or in melt, failed to yield the expected polymers; indeed, as previously reported for the reaction with benzoyl chloride, only a partial polycondensation with the tetraamino compound occurred to yield a low molecular weight (intrinsic viscosity $0.020\text{--}0.025$) polymer which appeared to be the amide hydrochloride (V).

cyclization reaction occurred only at higher temperatures; for example, the reaction carried out at a temperature below 200°C. yielded a polymer containing a great amount of oxygen and the infrared spectrometry showed the presence of some primary NH_2 groups (absorption at 3450 and 3300 cm^{-1}).

However, the oxygen content of the polymers was much lower and the inherent viscosity was higher when the condensation reaction was carried out at a temperature over 250°C. or when the polymer synthesized at low temperature was reheated over 300°C. under vacuum.

The decrease of oxygen content due to the intramolecular condensation involves a diminution of solubility of the polymers. We observed that the polymers containing more than 6% oxygen are slightly soluble in diglyme, benzene, and chloroform and completely soluble in dimethylformamide, acetamide, and sulfoxide; also it is possible to get some brittle films by evaporation of the solutions. When the oxygen content is lower than 6%, the polymers are insoluble in the usual organic solvents, but soluble in concentrated sulfuric acid. Sometimes only a partial solubility of these polymers in concentrated sulfuric acid was observed, probably due to the formation of some crosslinks by intermolecular elimination of phenol.

Further, it was observed that it is better to carry out the reaction in two parts: first, the reduction of 1,4,5,8-tetranitronaphthalene; and second, the polycondensation of the unstable tetraamino compound with the diester. When the reduction of the tetranitro compound is carried out in the presence of the ester, we obtained primarily a polymer having a higher oxygen content than that of the samples prepared in two steps at the same reaction temperature. Presumably, when the reduction is carried out in the presence of the diester component there is some partial condensation of the ester with the amino groups before the reduction of the tetranitro compound, and then the steric hindrance of the preformed chain prevents the completion of the reduction and condensation.



In some samples, infrared absorptions at 1550 and 1350 cm^{-1} , frequencies due to the valence vibration of $\text{R}_3\text{C}-\text{NO}_2$ bonds, were observed.

We have also noted that whatever the experimental conditions, a polymer sample free of oxygen was never obtained; the oxygen content is too high to be ascribed to the presence of ester groups only at the end of the chain.

From the viscosity data we can estimate a molecular weight of 10,000 as a minimum, and in this case the oxygen percentage due to the presence of two terminal ester groups should be equal only to 0.64%, whereas the found average content of oxygen is 2.5%. There seem to be some failures in the ring closure along the chain due to small amounts of trinitro compound in the starting material or of a tetranitro isomer other than the 1,4,5,8.

The thermal stability of the polymers has been studied by thermogravimetric analysis (TGA).

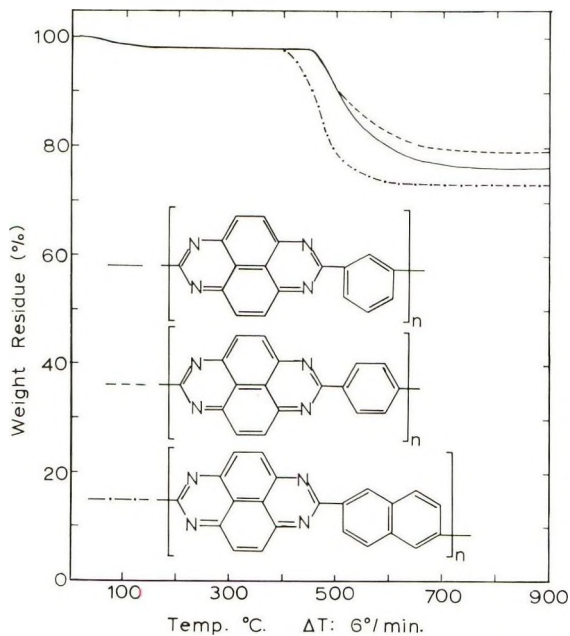


Fig. 1. TGA in nitrogen.

TGA was performed in a commercial Stanton thermobalance; a flowing nitrogen or air atmosphere was used. As it appears from the TGA curves presented in Figure 1 and 2, the polymers synthesized from diphenyl isophthalate or terephthalate have almost identical TGA curves; they showed a similar initial loss of about 2% in weight up to 410°C., followed by 22% loss up to 840°C. in a nitrogen atmosphere. TGA in air showed an initial loss of 1% from room temperature up to 340°C. and a rapid loss of 98% between 340°C. and 710°C. The polymer synthesized from diphenyl-2,6-naphthalenedicarboxylate showed an initial weight loss of less than 1% from room temperature up to 170°C. It lost 26% between 390° and 850° C. in nitrogen and 99.5% between 360 and 780°C. in air.

Seemingly, these new polymers are slightly less thermally stable than aromatic polybenzimidazoles in either nitrogen or air,² when we consider the starting temperatures of decomposition.

Electron spins resonance studies of the solid polymers or solutions in dimethylacetamide of the soluble fractions have shown that these high conjugated polymers contained from 1.9 to 9.7×10^{19} spins/g. The radicals are not trapped in the solid but are present on the polymer chains as is shown by the fact that a signal was observed in the polymer solutions. However, it was not possible to get information about the location of the free electrons on the carbon or nitrogen atoms from the structure of the observed ESR signals because of the low resolution of these signals due to some interactions through the polymer chains.

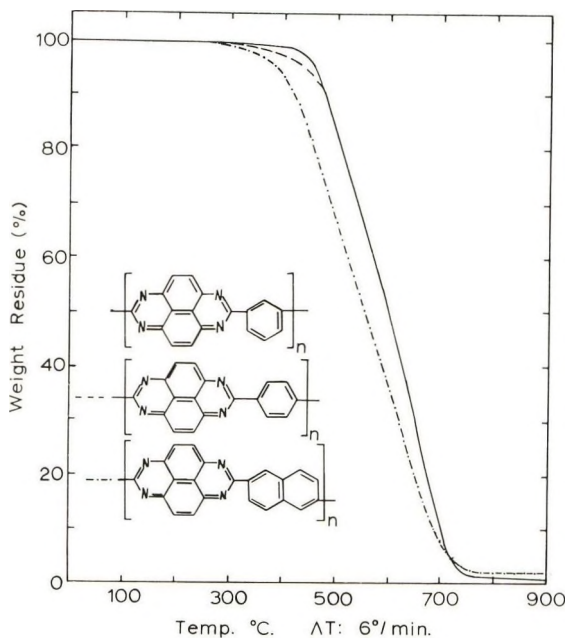


Fig. 2. TGA in air.

An ESR signal was also observed in dimethylacetamide solutions of the model compound, the 2,7-diphenyl-1,3,6,8-tetraazopyrene.

Room temperature resistivities and dielectric constants were determined on the polymers prepared from isophthalic, terephthalic, and 2,6-naphthalene dicarboxylic acids. The results (Table I) are typical of insulating organic polymers.

TABLE I

Polymer	Resistivity, ohm-cm.	Dielectric constant
Isophthalic derivative (flake)	1×10^{16}	3 (100 Mcycles)
Terephthalic derivative (flake)	5×10^{13}	4 (100 Mcycles)
2,6-Naphthalene nucleus (flake)	2×10^{14}	3 (100 Mcycles)

EXPERIMENTAL

Monomers

1,4,5,8-Tetranitronaphthalene. The tetranitronaphthalene was synthesized by nitration of 1-nitronaphthalene⁴ in 52% yield. The 1,4,5,8-isomer was isolated from the mixture by extraction with boiling acetone (16 ml./g.) in a total yield of 18.4%. The product does not melt below 350°C. but partially decomposes at about 315–320°C.

ANAL. Calcd. for $C_{10}H_4N_4O_8$: C, 39.00%; H, 1.30%; N, 18.10%; O, 41.60%. Found: C, 39.24%; H, 1.35%; N, 17.05%.

Phenyl Acetate, Phenyl Benzoate, Diphenyl Isophthalate and Terephthalate. The commercial esters (Eastman Kodak Company) were recrystallized twice from methanol with application of decolorizing Darco.

Diphenyl Naphthalene-2,6-dicarboxylate. 2,6-Naphthalenedicarboxylic acid chloride was synthesized by heating 2,6-naphthalenedicarboxylic acid with a mixture of phosphorus pentachloride and phosphorus oxychloride, and recrystallized from benzene (70% yield).

The diphenyl ester was obtained by heating the acid chloride with phenol; the reaction product was recrystallized twice from methanol with application of decolorizing Darco. The overall yield of diphenyl naphthalene 2,6-dicarboxylate was 35%; m.p. 215–216°C.

ANAL. Calcd. for $C_{24}H_{18}O_4$: C, 78.33%; H, 4.38%; O, 7.09%. Found: C, 78.18%; H, 4.51%.

Diphenyl Oxybisbenzoate. The diphenyl oxybisbenzoate was synthesized by Burdick and Jackson Laboratories by oxidation of the dimethyl derivative, followed by esterification of the diacid. The compound (m.p. 185–187°C.) was used without further purification.

Model Compounds

2,7-Dimethyl-1,3,6,8-tetraazopyrene. To a suspension of 800 mg. of 1,4,5,8-tetranitronaphthalene in 100 ml. of a mixture of equal parts of glacial acetic acid and acetic anhydride were added 200 mg. of palladium catalyst on charcoal and this mixture was shaken in a pressure flask for about 40 hr. at 50°C. with hydrogen under a pressure of 50 psi. The mixture was filtered and the solution was evaporated to dryness under reduced pressure. The brown residue was sublimed twice under reduced pressure and then recrystallized several times from ethanol. After recrystallization, the product was again sublimed at 280°C. without melting or decomposition. The yield of yellow needles was 40% of the theoretical amount.

ANAL. Calcd. for $C_{14}H_{10}N_4$: C, 71.78%; H, 4.30%; N, 23.92%. Found: C, 72.03%; H, 4.33%; N, 23.66%.

The same tetraazopyrene derivative was also synthesized from phenyl acetate.

A suspension of 616 mg. of 1,4,5,8-tetranitronaphthalene and 100 mg. of palladium catalyst on charcoal in 20 ml. of diglyme (bis-2-methoxy ethyl ether, purified by distillation on lithium aluminum hydride, b.p. 160–163° C.) was shaken for 45 hr. at 50°C. with hydrogen under a pressure of 50 psi. The reaction mixture was then filtered through a sintered glass, avoiding any contact with the atmosphere, and the filtrate was added, under nitrogen, to a solution of 544 mg. of phenyl acetate in 10 ml. of diglyme (molar ratio ester/nitro = 2). This mixture was heated at about 110°C. under an inert atmosphere for 2 hr. and then the diglyme was removed by distillation. The residue was heated at 200°C., under reduced pressure, for 1 hr., and then recrystallized from ethanol and purified as previously reported.

The yield of yellow needles was 36% of the theoretical amount.

ANAL. Found: C, 71.50%; H, 4.29%; N, 23.55%.

2,7-Diphenyl-1,3,6,8-tetraazopyrene. A suspension of 616 mg. of 1,4,5,8-tetranitronaphthalene and 100 mg. of palladium catalyst on charcoal in 20 ml. of diglyme was shaken for 45 hr. at 50°C. with hydrogen under a pressure of 50 psi. The reaction mixture was then filtered under inert atmosphere and the filtrate added to a solution of 793 mg. of phenyl benzoate in 10 ml. of diglyme (molar ratio ester/nitro = 2). This mixture was heated at about 110°C., under nitrogen for 2 hr., the solvent was removed by distillation and the brown residue heated at 300°C. under reduced pressure for 1 hr. The reaction product was purified by dissolution in dimethyl sulfoxide and precipitation in ice cold methanol. It was then washed several times with diethyl ether and dried at 0.1 mm. Hg to a constant weight to give a 40% yield. The product did not melt below 350°C.

ANAL. Calcd. for $C_{21}H_{14}N_4$: C, 80.44%; H, 3.91; N, 15.50%. Found: C, 79.14%; H, 5.14%; N, 13.77%.

Polycondensations

Polymers from Diphenyl Isophthalate. (a) In a pressure flask 616 mg. of 1,4,5,8-tetranitronaphthalene and 100 mg. of palladium catalyst on charcoal in 30 ml. of diglyme were shaken with 632 mg. of diphenyl isophthalate (molar ratio ester/nitro = 1) under 50 psi of hydrogen.

The polymer was isolated by distillation of the solvent, dissolution of the residue in dimethylacetamide or dimethyl sulfoxide, filtration to separate the reduction catalyst and precipitation of the filtrate in a alcohol-water mixture or in benzene. The polymer was then washed several times with methanol and diethyl ether and dried at 0.1 mm. Hg to a constant weight.

The reaction carried out at 130°C. for 65 hr. yields a polymer fractionated in two parts: (1) a fraction soluble in diglyme (71% yield; inherent viscosity in dimethylacetamide = 0.15. Anal: C, 65.38%; H, 4.83%; N, 11.68%; O, 13.53%); and (2) a fraction insoluble in diglyme

but soluble in dimethylacetamide (11% yield; inherent viscosity in dimethylacetamide = 0.28. Anal.: C, 59.09%; H, 4.26%; N, 16.40%).

When the reduction was carried out at 130°C. for 28 hr., and the reaction mixture was heated under reduced pressure at 280°C. for 3 hr., there was obtained a 60% yield of a polymer soluble in dimethylsulfoxide (inherent viscosity in DMSO = 0.47; Anal.: C, 71.66%; H, 3.25%; N, 16.40%) and a 21% yield of insoluble material.

Finally, at the same reduction temperature for 50 hr. and an additional heating of the reaction mixture under nitrogen at about 350°C. for 5 hr., the yield was 32% of polymer soluble in DMSO (inherent viscosity in DMSO = 0.70. Anal.: C, 73.20%; H, 4.07%; N, 15.33%; O, 8.78%) and 48% of insoluble polymer (Anal.: C, 73.26%; H, 3.84%; N, 18.00%; O, 7.57%).

ANAL. Calcd. for $(C_{18}H_{10}N_4)_n$: C, 77.14%; H, 2.86%; N, 20.00%.

The yields were calculated on the basis of the theoretical structure $(C_{18}H_{10}N_4)_n$, and several values are probably too high on account of the presence of some residual oxygen in the polymers as it was shown by the elementary analysis.

(b) A suspension of 1.232 g. of 1,4,5,8-tetranitronaphthalene and 200 mg. of palladium catalyst on charcoal in 20 ml. of diglyme was shaken with hydrogen under a pressure of 50 psi at 50°C. for 46 hr. The reaction mixture was then filtered under an inert atmosphere and the filtrate was added to a solution of 1.264 g. of diphenyl isophthalate in 10 ml. of diglyme (molar ratio ester/nitro = 1). This solution was heated at 180°C. under nitrogen for 3 hr.; then, the diglyme was distilled. The black residue was then heated at 300°C. under reduced pressure for an additional 2 hr. Under such experimental conditions there was obtained 12% of polymer soluble in DMSO (inherent viscosity in DMSO = 0.52 and in concentrated sulfuric acid 0.50. Anal.: C, 73.00%; H, 3.84%; N, 16.71%; O, 5.40%) and 60% of polymer insoluble in DMSO (inherent viscosity in concentrated H_2SO_4 = 0.66. Anal.: C, 75.22%; H, 3.10%; N, 18.63%; O, 2.40%).

Polymers from Diphenyl Terephthalate. (a) 1,4,5,8-Tetranitronaphthalene (616 mg.) and 100 mg. of palladium catalyst on charcoal in 40 ml. of diglyme were shaken with 632 mg. of diphenyl terephthalate at 60°C. for 48 hr. under 50 psi hydrogen pressure. The diglyme was then distilled off under nitrogen and the residue heated at 200°C. for 1 hr. under reduced pressure. This experimental procedure yields 73% of polymer soluble in DMSO with an inherent viscosity in DMSO of 0.24.

(b) A suspension of 1.232 g. of 1,4,5,8-tetranitronaphthalene and 200 mg. of palladium catalyst on charcoal in 30 ml. of diglyme was shaken at 50°C. for 40 hr. with hydrogen under a pressure of 50 psi. The reaction mixture was then filtered under an inert atmosphere and the filtrate added to a solution of 1.264 g. of diphenyl terephthalate in 10 ml. of diglyme and heated at 170°C. under nitrogen for 3 hr. The diglyme was distilled off and the residue was heated at 300°C. under reduced pressure for 2 hr.

to yield 31% of soluble polymer (inherent viscosity in DMSO = 0.46. Anal.: C, 72.63%; H, 3.96%; N, 11.12%; O, 9.72%) and 62% polymer insoluble in DMSO, but soluble in concentrated sulfuric acid (inherent viscosity in concentrated H₂SO₄ = 0.60. Anal.: C, 75.33%; H, 3.94%; N, 18.20%; O, 2.55%).

ANAL. Calcd. for (C₁₈H₁₀N₄)_n: C, 77.14%; H, 2.86%; N, 20.00%.

(c) An attempt to promote the intramolecular cyclization at a lower temperature by carrying out the polycondensation in the presence of an organic base was unsuccessful. For example, the reduction product of 1,4,5,8-tetranitronaphthalene in diglyme solution was heated at 120°C. for 25 hr. with diphenyl terephthalate in the presence of pyridine, but almost all of the starting material was recovered.

Polymers from Diphenyl 2,6-Naphthalenedicarboxylate. A solution of 1.432 g. of diphenyl 2,6-naphthalenedicarboxylate in 20 ml. of diglyme was added to a solution of the reduction product of 1.232 g. of 1,4,5,8-tetranitronaphthalene in 40 ml. of diglyme (molar ratio ester/nitro = 1). The mixture was heated at 250°C. under nitrogen for 3 hr. and the solvent removed by distillation. The residue was then heated at 300°C. under reduced pressure for 2 hr. to give a yield of insoluble, black polymer of 73%.

ANAL. Calcd. for (C₂₂H₁₂N₄)_n: C, 79.50%; H, 3.70%; N, 16.80%. Found: C, 77.04%; H, 4.63%; N, 15.56%.

Polymers from Diphenyl 4,4-Oxybisbenzoate. A solution of 820 mg. of diphenyl oxybisbenzoate in 10 ml. of diglyme was added to a solution of the reduction product of 616 mg. of 1,4,5,8-tetranitronaphthalene in 25 ml. of diglyme (molar ratio ester/nitro = 1). The mixture was heated at 250°C. under nitrogen for 3 hr. and the solvent was distilled off. The residue was then heated at 300°C. under reduced pressure for 2 hr. A low melting (186°C.) and easily soluble polymer was obtained in a 13% yield (inherent viscosity in DMSO = 0.13. Anal.: C, 73.42%; H, 4.75%; N, 10.08%; O, 9.24%).

The yield of polymer not melting below 350°C. and insoluble in usual solvents, but slightly soluble in concentrated sulfuric acid was 50%. The inherent viscosity of this polymer in concentrated H₂SO₄ was 0.34.

ANAL. Calcd. for (C₂₄H₁₄O)_n: C, 77.00%; H, 3.70%; N, 15.00%; O, 4.30%. Found: C, 76.14%; H, 4.26%; N, 11.98%; O, 6.77%.

The authors wish to express their thanks to Dr. Gordon Tollin, University of Arizona, for help in obtaining and interpreting the electron spins resonance diagram.

For the TGA curves, we wish to thank Dr. W. F. Gresham, Plastics Department, E. I. du Pont de Nemours and Company, Inc.

We are grateful to Mr. J. L. Gillson, Central Research Department, E. I. du Pont de Nemours and Company for determining the resistivities and dielectric constants of our polymers.

One of us (F. Dawans) is indebted for a travel grant from the French Petroleum Institute (Rueil-Malmaison, France).

The financial support of the Plastics and Textile Fibers Departments of E. I. du Pont de Nemours and Company, Inc., is gratefully acknowledged.

References

1. Dimroth, O., H. Roos, *Ann.*, **456**, 178 (1927).
2. Vogel, H., and C. S. Marvel, *J. Polymer Sci.*, **50**, 511 (1961).
3. Wrasidlo, W., and H. H. Levine, paper presented at 145th Meeting, American Chemical Society, New York, Sept. 1963; *Preprints*, **4**, No. 2, 15 (1963).
4. Wood, E. R., C. D. Johnson, and C. A. Day, *J. Chem. Soc.*, **1959**, 491.

Résumé

Des dérivés 2,7-disubstitués du tétraazopyrène 1,3,6,8 ont été synthétisés comme composés modèles pour des polymères de structure similaire. Des polymères entièrement conjugués et de poids moléculaires élevés ont été obtenus par polycondensation du naphthalène 1,4,5,8-tetraaminé avec divers esters phényles d'acides aromatiques bifonctionnels. Les viscosités inhérentes de ces polymères sont de l'ordre de 0.15 à 0.70. La plupart de ces polymères sont infusibles et certains d'entre eux sont insolubles dans les solvants classiques. La stabilité thermique de ces polymères s'est révélée être bonne.

Zusammenfassung

2,7-Disubstituierte Derivate von 1,3,6,8-Tetraazopyren wurde als Modellverbindung für einige Polymere mit ähnlicher Struktur synthetisiert. Konjugierte Polymere mit hohem Molekulargewicht wurden durch Polykondensation von 1,4,5,8-Tetraaminonaphthalin mit verschiedenen Diphenylestern von bifunktionellen aromatischen Säuren erhalten. Die Viskositätszahl einer Reihe von Polymeren bewegte sich etwa zwischen 0,15 bis 0,70. Die meisten Polymeren sind nicht schmelzbar, und einige sind in den gebräuchlichen organischen Lösungsmitteln unlöslich. Die thermische Stabilität der Polymeren ist sehr gut.

Received February 16, 1964

Revised March 9, 1964

Glass Transitions of Polyoxyetanes

J. J. STRATTA, F. P. REDING, and J. A. FAUCHER,
Chemicals Division, Research and Development Department, Union Carbide Corporation, South Charleston, West Virginia

Synopsis

Glass transition data of polyoxyetanes suggest that the responsible segmental chain motions are rather short range in nature. The incorporation of three different structural features within the repeat unit of a polyoxyetane results in three separate and independent transition temperatures. The temperature positions of the transitions arising from different structures within the chain are essentially the same as observed in other polymers with a similar structural element. Structural groups and their corresponding transitions which were studied in combination are: $-\text{CH}_2-\text{CH}_2-\text{CH}_2-$ at -125°C ., $-\text{CH}_2-\text{O}-\text{CH}_2-$ at -50 to -70°C ., and $-\text{CH}_2\text{CHCH}_3-\text{CH}_2-$ or $-\text{O}-\text{CHCH}_3-\text{CH}_2-$ at -20 to -30°C .

INTRODUCTION

Many polymers exhibit several transitions which appear to arise from the separate motion of different structural elements within the chain. For example, the transition in polyethylene at -125°C . has been attributed to segmental skeletal motion involving three to five methylene units in sequence.¹⁻³ The incorporation of a branch point³ on an aliphatic chain yields another transition at -40 to -10°C . Polyethers possess a transition in the range -70 to -50° which is believed due to carbon-oxygen-carbon motion.

In the present study polyoxyetanes have been investigated, since these polymers incorporate more than one of the above mentioned structural groups per repeat unit. Hence, they present an opportunity to study the resulting transition effects of combining functional groups close together.

EXPERIMENTAL

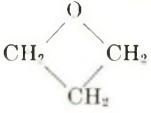
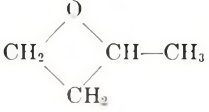
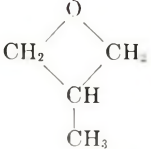
Synthesis of Oxyetane Monomers

Three monomers were prepared: oxyetane (*syn*-trimethylene oxide, oxacyclobutane), 2-methyloxyetane and 3-methyloxyetane. All three were synthesized in about 40% yields from appropriate γ -chloroacetate esters via Noller's⁴ molten KOH cyclization reaction. Depending upon availability, either diols or allyl halides were used to prepare the ester inter-

mediates. Oxetane and 2-methyloxetane were prepared from the cyclization of 1,3-propanediol and 1,3-butanediol respectively by the method of Bogert and Slocum⁵ and Rose.⁶ The preparation of 3-methyloxetane involved the cyclization of 2-methyl-3-chloropropyl acetate. This ester intermediate was synthesized in a three-step reaction starting with methyl chloride ($\text{CH}_2=\text{CCH}_3-\text{CH}_2\text{Cl}$). First, the allyl halide was transformed to the trialkyl boron compound, $\text{B}(-\text{CH}_2-\text{CHCH}_3-\text{CH}_2\text{Cl})_3$ via Brown's⁸ diborane hydrobromination reaction. Secondly, the boride was oxidized to the corresponding chlorohydrin, $\text{HO}-\text{CH}_2-\text{CHCH}_3-\text{CH}_2\text{Cl}$, with basic peroxide. Finally, the ester intermediate was formed by esterifying the chlorohydrin with acetic anhydride.

The monomers were purified by redistillation from potassium hydroxide. Table I presents the boiling points of the purified monomers.

TABLE I
List of Monomers Synthesized

Monomer	Structure	Boiling point, °C./mm. Hg.	
		Reported ^a	Found
Oxetane		48/770	47.0-47.5/750
2-Methyl-oxetane		59.7-59.8/760	59.0-60.0/755
3-Methyl-oxetane		67/760	67.0-67.8/755

^a Data of Rose⁶ and Searles et al.⁷

Polymerization of Oxetanes

Three polymers were synthesized: polyoxetane, $[-\text{CH}_2-\text{CH}_2-\text{CH}_2-\text{O}-]_n$; poly-2-methyloxetane, $[-\text{CH}_2-\text{CH}_2-\text{CHCH}_3-\text{O}-]_n$; and poly-3-methyloxetane, $[-\text{CH}_2-\text{CHCH}_3-\text{CH}_2-\text{O}-]_n$.

Oxetane readily polymerized from methyl chloride solution at -80°C . with the use of boron trifluoride etherate catalyst as described by Rose.⁶ The polymer had a reduced viscosity of 0.18 in benzene solution at 0.200 g./dl. concentration and a melting point of 35°C .

Both methyloxetanes were extremely difficult to polymerize, and their resulting polymers were viscous oils. (Rose⁶ reported a viscous oil resulting from the polymerization of 2-methyloxetane.) By using monomers redistilled to 99+ % purity, together with reaction times of one week

and Phosfluogen A⁹ (*p*-chlorobenzenediazonium hexafluorophosphate) catalyst at -60°C . both methyloxetanes were polymerized. Reduced viscosities of 0.17 and 0.18 were obtained for poly-2-methyloxetane) and poly-3-methyloxetane, respectively. The carbon-hydrogen elemental analysis of the polymers corresponded closely to that expected by theory. No evidence of crystallinity was found for either methyl oxetane polymer, even at liquid nitrogen temperature.

Dynamic Measurements

The mechanical loss (Q^{-1}) of each polymer was determined from -180°C . up to room temperature. Measurements were made with a recording torsion pendulum¹⁰ operating at a frequency of about 3-7 cycles/sec.

Considerable effort was required to obtain these mechanical loss spectra due to the low molecular weight of the polymer samples. Initially the test specimens were prepared in the form of aluminum foil sandwiches, the inner layer being the polymer to be tested. Specimens prepared this way were 0.030-0.050 in. thick, and the low temperature transition at -125°C ., if present, could be easily seen. This method of sample preparation was inadequate at higher temperatures since good recovery was hard to obtain after the -60° transition. To obtain more precise data for this transition, a blotter technique was used. For this method a sample of pressed cellulose sheet pulp $1 \times 0.25 \times 0.030$ in., was impregnated with the test polymer, frozen at -180°C ., and mounted on the torsion pendulum. With this method of sample preparation, it was possible to obtain mechanical loss measurements up to room temperature.

RESULTS AND DISCUSSION

Mechanical loss spectra of cellulose and of cellulose impregnated with polyoxetane are shown in Figure 1. The logarithmic decrement for the cellulose blank is nearly constant over the temperature range studied. For the polymer-impregnated cellulose, the spectrum is characteristic of the polymer below room temperature and characteristic of cellulose above room temperature. From -180°C . to room temperature the polymer is more rigid than the blotter and the resultant spectrum is due to the polymer. Around room temperature the polymer becomes so soft that it drains away from the blotter and spectrum becomes characteristic of the remaining cellulose. Figure 2 presents the spectra of poly-2-methyloxetane and poly-3-methyloxetane obtained by the blotter technique.

To study the -125°C . transitions, aluminum foil sandwich specimens were used, and the spectra obtained are shown in Figure 3. A summary of the transitions observed for the three polymers is shown in Table II.

The data presented in Table II are in accord with previous structure-transition correlations and suggest strongly that the segmental chain motions involved are independent in nature. Each structural unit appears

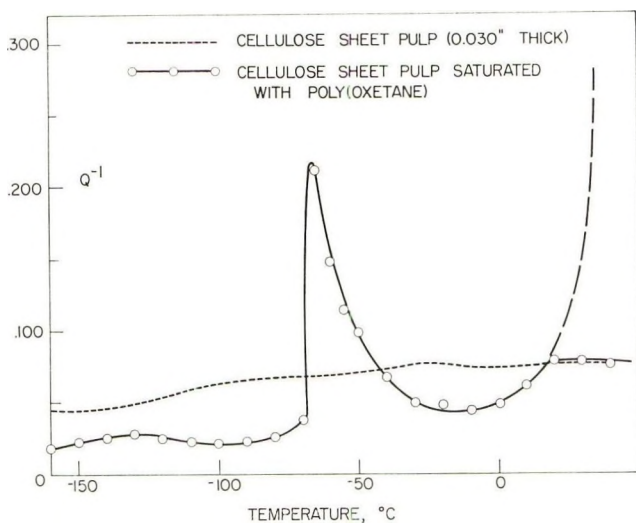


Fig. 1. Mechanical loss of polyoxetane.

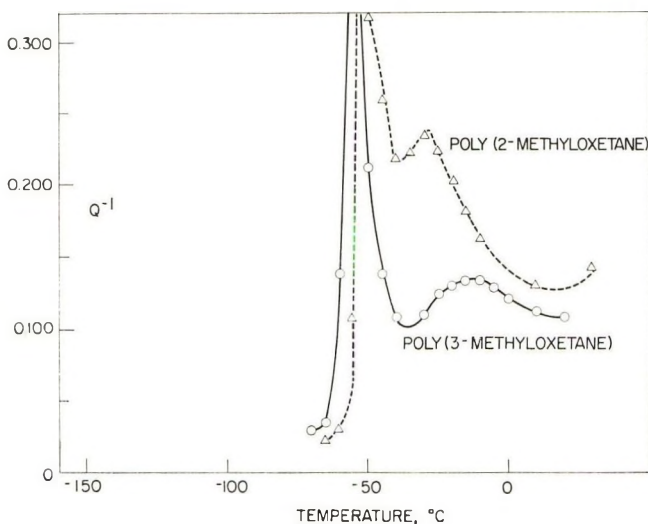


Fig. 2. Mechanical loss of poly-2-methyloxetane and poly-3-methyloxetane. Data were obtained by saturated blotter method.

to have its own characteristic transition, regardless of the identity of its close neighbors.

It has previously been postulated^{1-2,3} that three to five methylene units in sequence are responsible for the $-125^{\circ}\text{C}.$ transition. Hence, the $-128^{\circ}\text{C}.$ value observed for polyoxetane is entirely expected. Willbourn² has found this same transition for polyoxetane and for poly(tetramethylene oxide). When the main chain of the polyether contains only three carbons in sequence, this $-125^{\circ}\text{C}.$ transition can be influenced by a

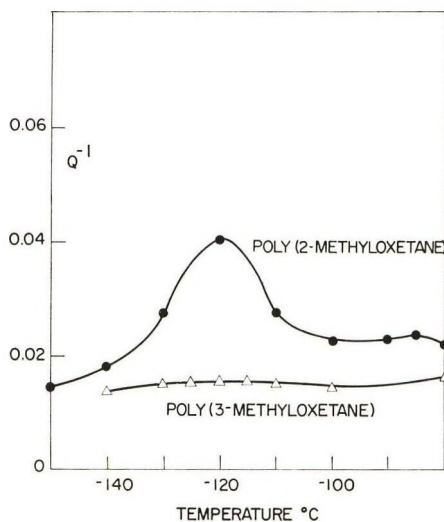


Fig. 3. Low temperature mechanical loss for poly-2-methyloxetane and poly-3-methyloxetane. Data were obtained with aluminum foil sandwich specimens.

methyl pendant group. Poly-2-methyloxetane, $[-\text{CH}_2-\text{CH}_2-\text{CHCH}_3-\text{O}-]_n$, exhibits this transition. Poly-3-methyl oxetane, $[-\text{CH}_2-\text{CHCH}_3-\text{CH}_2-\text{O}-]_n$, does not. This finding is explained in the following way. The -125°C . transition is attributed to a skeletal motion resulting from limited rotation about the carbon-carbon bond. When a methyl group is situated on the central carbon, the motion is restricted and no transition is seen. The above postulate also explains why no -125°C . transition is exhibited by polypropylene. However, if the methyl pendant group is located on the terminal carbon, the adjacent oxygen atom does not interfere too severely with the motion and the transition is seen.

For all three polymers studied, the main transition was found in the range -50 to -65°C ., characteristic of the $-\text{C}-\text{O}-\text{C}-$ transition.

TABLE II

Monomer	Polymer repeat unit	Transition temp., $^\circ\text{C}$.		
		$-(\text{CH}_2)_3-$	$-\text{CH}_2-\text{O}-\text{CH}_2-$	$\begin{array}{c} \text{R} \\ \\ -\text{CH}- \end{array}$
Oxetane	$[-\text{C}-\text{C}-\text{C}-\text{O}-]$	-128^a	-64^a	None ^a
2-Methyloxetane	$\left[\begin{array}{c} \text{C} \\ \\ -\text{C}-\text{C}-\text{C}-\text{O}- \end{array} \right]$	-120^b	-50^a	-30^a
3-Methyloxetane	$\left[\begin{array}{c} \text{C} \\ \\ -\text{C}-\text{C}-\text{C}-\text{O}- \end{array} \right]$	None ^b	-55^a	-18^a

^a Values obtained with "Blotter" sample.

^b Values obtained with "Aluminum Sandwich" sample.

The value of -64°C . observed for polyoxetane is in accord with current transition studies for poly(ethylene oxide).¹¹ Such a value (-64°C .) would be predicted for a polyether having a low molecular weight of 500–800. The reduced viscosity of only 0.18 suggests that the molecular weight is this low. The analogous transitions for poly-3-methyl oxetane, $[-\text{CH}_2-\text{CHCH}_3-\text{CH}_2-\text{O}-]_n$, and for poly-2-methyloxetane, $[-\text{CH}_2-\text{CH}_2-\text{CHCH}_3-\text{O}-]_n$, appear at -55 and -50°C . respectively. This shift is attributed to interference to the motion by the methyl group. As the pendant group is situated closer to the oxygen atom, the interference becomes more pronounced and the subsequent transition shift becomes greater.

A third transition was observed in the range of -16 to -30°C . for polymers of both methyloxetanes, coinciding well with the -25°C . value previously attributed to the $-\text{CH}_2-\text{CHR}-\text{CH}_2-$ branch juncture.³ This juncture is not present in polyoxetane and no transition for it was found in that polymer.

In view of the rather low molecular weights of the polymers studied one might well wonder whether the corresponding high polymers would have significantly different transition temperatures. The authors' feeling is that such a change is unlikely. The -125°C . peak associated with methylene groups has very little dependence on molecular weight. In fact, it has been found to occur in hydrocarbon waxes.¹² Similarly, the -60°C . peak assigned to the $\text{C}-\text{O}-\text{C}$ group is little affected by molecular weight, at least in amorphous polymers. Thus we have found in the polypropylene oxide series that all members from dipropylene glycol on up have a main glass transition at -60°C .¹² There is as yet no corresponding evidence for the -25°C . transition, but if its assignment is correct it ought to be also rather independent of molecular weight.

The authors wish to acknowledge advice on the polymerization procedure from Drs. N. L. Zutty and A. Turner. In addition, we are indebted to Mr. J. E. Patrick for the measurements of mechanical loss.

References

1. Schmieder, K., and K. Wolf, *Kolloid-Z.*, **134**, 149 (1953).
2. Willbourn, A. H., *Trans. Faraday Soc.*, **54**, 717 (1958).
3. Reding, F. P., J. A. Faucher, and R. D. Whitman, *J. Polymer Sci.*, **57**, 483 (1962).
4. Noller, C. R., *Organic Synthesis*, **1949**, 92.
5. Bogert, M. T., and E. M. Slocum, *J. Am. Chem. Soc.*, **46**, 763 (1924).
6. Rose, J. B., *J. Chem. Soc.*, **1956**, 542.
7. Searles, S., K. A. Pollart, and E. F. Lutz, *J. Am. Chem. Soc.*, **79**, 948 (1957).
8. Brown, H. C., *J. Org. Chem.*, **22**, 1136 (1957); *J. Am. Chem. Soc.*, **81**, 1010 (1959).
9. Campbell, T. W., and V. S. Foldi, *J. Org. Chem.*, **26**, 4654 (1961).
10. Nielsen, L. E., *Rev. Sci. Instr.*, **22**, 690 (1951).
11. Read, B. E., *Polymer*, **3**, 529 (1963).
12. Stratta, J. J., F. P. Reding, and J. A. Faucher, unpublished data.

Résumé

Les résultats obtenus pour les points de transition vitreuse des polyoxétanes suggèrent que les mouvements des segments de chaîne responsables de la transition sont de faible amplitude. L'incorporation de trois caractéristiques structurelles différentes dans chaque unité d'un polyoxétane a comme résultat trois températures de transition, séparées et indépendantes. La position des températures de transition provenant des structures différentes dans la chaîne sont essentiellement les mêmes que celles observées dans d'autres polymères contenant un élément structurel similaire. Les groupements structuraux et leurs transitions correspondantes qui ont été étudiés sont: $-\text{CH}_2-\text{CH}_2-\text{CH}_2-$ à -125° ; $-\text{CH}_2-\text{O}-\text{CH}_2-$ de -50° à -70° et $-\text{CH}_2-\text{CHCH}_3-\text{CH}_2-$ ou $-\text{O}-\text{CHCH}_3-\text{CH}_2-$ de -20° à -30°C .

Zusammenfassung

Ergebnisse über die Glasumwandlung von Poly(oxetanen) legen nahe, dass die verantwortlichen Kettensegmentsbewegungen verhältnismässig kurze Reichweite besitzen. Die Zusammenfassung von drei verschiedenen Struktureigenschaften in einer Poly(oxetan)-Grundeinheit ergibt drei verschiedene und unabhängige Umwandlungstemperaturen. Die durch verschiedene Struktur innerhalb der Kette bedingte Lage der Umwandlungstemperaturen ist im wesentlichen dieselbe wie die bei anderen Polymeren mit einem ähnlichen Strukturelement beobachtete. Folgende strukturelle Gruppen und die ihnen entsprechenden Umwandlungen wurden kombiniert untersucht: $-\text{CH}_2-\text{CH}_2-\text{CH}_2-$ bei -125° ; $-\text{CH}_2-\text{O}-\text{CH}_2-$ bei -50° bis -70° und $-\text{CH}_2\text{CHCH}_3-\text{CH}_2-$ oder $-\text{O}-\text{CHCH}_3-\text{CH}_2-$ bei -20° bis -30° .

Received December 26, 1963

Revised March 5, 1963

BOOK REVIEW

N. G. GAYLORD, Editor

Foreign-Language and English Dictionaries in the Physical Sciences and Engineering, a Selected Bibliography 1952 to 1963, TIBOR W. MARTON, National Bureau of Standards Miscellaneous Publication 258, July 24, 1964, 189 pp., \$1.25. (Order from the Superintendent of Documents, U. S. Department of Commerce Field Offices.)

This is a comprehensive bibliography providing sources for up-to-date foreign language and standardized English terminology in the physical sciences and engineering. It is processed by punched-card, machine-sorting, and photo-offset techniques, and lists over 2800 unilingual, bilingual, and polyglot dictionaries, glossaries, and encyclopedias published during the past 12 years. The majority of the titles cited have English as the source or target language, or are English defining dictionaries. The entries are arranged in 49 subject classes; within each subject the entries are listed alphabetically by language and within each language group, by author. Forty-seven foreign languages are represented in the compilation.

Dictionaries and encyclopedias covering polymer science and related areas, are listed under three headings: Chemistry and Chemical Engineering, Materials Testing and Industrial Products, Plastics and Polymers.

This bibliography should prove very valuable to anyone working with the polymer literature and especially those concerned with the translation, abstracting and indexing of journal articles, books or other scientific publications.

The reviewer was very much impressed by the broad coverage of this work and the fact that the bibliography even lists works in preparation, such as the Mark-Gaylord-Bikales *Encyclopedia of Polymer Science and Technology* which had not appeared at the time the bibliography was issued.

E. H. Immergut

Interscience Publishers (John Wiley & Sons)
New York, New York
and Polytechnic Institute of Brooklyn
Brooklyn, New York

ERRATA

Poly(bicyclo[2.1.1]heptadiene-2,5)

(article in *J. Polymer Sci.*, **61**, S38-S40, 1962)

By RICHARD H. WILEY, W. H. RIVERA, T. H. CRAWFORD,
and N. F. BRAY

*Department of Chemistry, College of Arts and Sciences,
University of Louisville, Louisville, Kentucky*

On page S39, line 7 from the top of the page, read 9.03-9.07 instead of 9.03-8.07.
On page S39, line 9 from the top of the page, the reference cited should be 9 instead of 8.

Determination of Halogen in Copolymers by Dye-Partition Technique and Calculation of r_1 Therefrom

(article in *J. Polymer Sci.*, **A2**, 1365-1372, 1964)

By MIHIR KUMAR SAHA, PREMAMOY GHOSH, and SANTI R. PALIT
Indian Association for the Cultivation of Science, Calcutta, India

On page 1369, the seventh column of Table I, for "Corresponding LPC concn., $10^{-4} N$ "
read "Corresponding LPC concn., $10^{-6} N$."

Evaluation of Rate constants from Thermogravimetric Data

(article in *J. Polymer Sci.*, **A2**, 3147-3151, 1964)

By RAYMOND M. FUOSS

Yale University, New Haven, Connecticut

IVAL O. SALYER and HARRY S. WILSON

Monsanto Research Corporation, Dayton, Ohio

On page 3148 replace eq. (6') by

$$E = -(nRT_i^2/w_i)(dw/dT)_i \quad (6')$$

and delete the last line on the page.

General Conclusions about the Copolymerization of Ethylene with Other Monomers by Free Radical Catalysis

(article in *J. Polymer Sci.*, A2, 3623-3632, 1964)

By FRANCIS E. BROWN and GEORGE E. HAM

Research Center, Spencer Chemical Company, Merriam, Kansas

On page 3627 in the third column of Table IV, the third line in the heading should read $r_1' = 0.10$. Similarly, in the fourth column the third line should read $r_1' = 0.15$.

On page 3629, lines 19 and 20 should read:

$$\begin{aligned} P_{ab}P_{bc}P_{ca} &= P_{ac}P_{cb}P_{ba} \\ 0.00511 &= 0.00815 \end{aligned}$$

On page 3630 in the second column of Table VI, K^{bb}/K^{ba} should equal 10